Evaluation of water management strategies for sustainable land use of acid sulphate soils in coastal low lands in the tropics

H. Van den Bosch (DLO Winand Staring Centre),
Ho Long Phi (Ho Chi Minh University of Technology),
J. Michaelsen (University of Kiel) and
Kusumo Nugroho (Centre for Soil and Agroclimate Research)

sc-dlo HCUT IWL AARD/ CSAR

REPORT 157
Wageningen (The Netherlands), 1998

Evaluation of water management strategies for sustainable land use of acid sulphate soils in coastal low lands in the tropics

H. Van den Bosch (DLO Winand Staring Centre)
Ho Long Phi (Ho Chi Minh University of Technology)
J. Michaelsen (University of Kiel)
Kusumo Nugroho (Centre for Soil and Agroclimate Research)

Report 157

DLO-Staring Centrum, Wageningen, 1998

ABSTRACT

H. van den Bosch, Ho Long Phi, J. Michaelsen and Kusumo Nugroho, 19998 *Evaluation of water management strategies for sustainable land use of acid sulphate soils in coastal low lands in the tropics*. Wageningen (The Netherlands), DLO Winand Staring Centre. Report 157 177 pp.; 64 Figs; 15 Tables; 74 Refs; 1 Annex.

A two-dimensional model was developed to simulate the effects of water management strategies in acid sulphate soil areas. Two field experiments were carried out under typical land uses (a rice field in Indonesia and a fish pond in Vietnam) to calibrate and validate the model. The model could reasonably well simulate the processes and their interactions occurring within a pyritic soil profile, both in the rice field and in the mound related to the fish pond. The calibrated model was used to evaluate different water management strategies in the two countries.

Keywords: acid sulphate soils, acidification, Vietnam, Indonesia, pyrite, rice, fish pond, modelling.

ISSN 0927-4537

P.O. Box 125, NL-6700 AC Wageningen (The Netherlands)
Phone: 31 (317) 474200; fax: 31 (317) 424812; e-mail: postkamer@sc.dlo.nl

Project 8614 [REP157.EVR - 06/98]

Contents

Preface

This study was carried out in the framework of the EU program 'Life Sciences and Technologies for Developing Countries (STD3)', contract number ERBTS3*CT940338 for account of the EU program and the Dutch Ministry of Agriculture, Fisheries and Nature Management. The study was a joint effort of the DLO Staring Centre for Integrated Land, Soil and Water Research (SC-DLO), Wageningen, The Netherlands (project management), the Centre for Soil and Agroclimate Research (AARD/CSAR), Bogor, Indonesia, the Institute for Water Management and Landscape Ecology (IWL), University of Kiel, Germany, and the Ho Chi Minh City University of Technology (HCUT), Ho Chi Minh City, Vietnam.

The authors like to thank Ir. Ngo Dang Phong, Ms. Huynh Thi Thuy Trang, Ir. Nguyen Duy Nang and Le Van Du (MSc) from the Department of Water Management, University of Agriculture and Forestry, Vietnam, for its efficient participation in the project. Gratefully acknowledged are Dr. Chr. Samtleben and his team who enabled and supported the Scanning Electron Microscopical investigations at the Geologisch-Palaeontologisches Institut at Kiel University, Germany. From the same institute we thank Dr. J. Scholten and Dipl.geol. O. Krueger for soil sample analyses by X-ray diffraction and interpretation of the results. We also thank Ir. J. Wesseling, Ir. J. Huygen and Ir. J.G. Kroes from the DLO Staring Centre for helping us patiently and promptly with water balance simulations.

Summary

Introduction

Upon drainage acid sulphate soils generate sulphuric acid that brings their pH below 4, sometimes as low as 2. The acid leaks into drainage and floodwaters, corrodes steel and concrete, and attacks clay liberating soluble aluminium. Drainage waters may also be enriched in heavy metals and arsenic - a toxic cocktail endangering aquatic life and public health. The weathering of sulphitic mine spoil and overburden presents the same problems, so acid sulphate soils are not the concern of soil science alone: agronomy, fisheries and environmental management, land and property development, civil and mining and water engineering, and public health all have an acute interest.

Most recent estimates of the extent of acid sulphate soils indicate an area of some 24 million ha worldwide where the topsoil is severely acid or will become so if drained. In addition, there may be as much again thinly covered by peat and non-sulphitic alluvium. However, estimates of the extent and distribution of acid sulphate soils suffer more than most from scanty field surveys, even fewer reliable laboratory data and, also, variable definition.

More significant than their absolute area is their location. They are concentrated in otherwise closely-settled coastal and flood plains, mostly in the tropics, where development pressures are intense and there is little suitable alternative land for expansion of farming or urban and industrial development. Two thirds of the known extent is in Vietnam, Thailand, Indonesia, Malaysia and northern Australia.

In Indonesia, acid sulphate soils cover about 4 million ha, which is c.10 percent of the Indonesian wetlands or about c.1 percent of the Indonesian archipello. The exact location and the extent of Indonesian acid sulphate soils is not yet known. Generally they occur in young marine deposits along the coasts of Sumatra, Kalimantan and Irian Jaya. Because of the ever growing population, the restricted productivity in many of the transmigration areas, and the wish of the Indonesian government to be self sufficient with respect to rice production, more and more land has to be taken into production for rice cultivation. Further, large scale creation of oil palm plantations claims huge areas of land. Often reclamation is preceded by forest clearing. Most of these activities take place in wetland areas, often with acid sulphate soils. Tremendous distortions of the ecological environment have been reported, such as erosion, acidification, peat subsidence, changes in microclimate, and disappearance of complete habitats. Toxic compounds are released into public water schemes during reclamation processes, resulting in decreased biological quality, destruction of natural fauna and flora, decrease of bio-diversity and decline of agricultural productivity.

In most of the areas pyrite is present in the very top layer of the mineral soil. In many cases the mineral soil is covered with a peat layer, varying in depth between 0.2 and 1 metre. Reclamation of these areas is expected to lead to subsidence of

the peat layer, making deeper drainage necessary. Once the water table drops into the sulphitic layer, severe acidification will take place. These developments make the problem of acid sulphate soils in Indonesia important.

In Vietnam, areas with acid sulphate soil cover about 1.8 million hectares, mostly in the Mekong Delta. The complicated hydrological conditions in the delta, characterized by interactions between river flow and sea intrusion have favoured acid sulphate soils formation in inland back swamps such as the Long Xuyen Quadrangle and the Plain of Reeds and coastal wetland like Camau Peninsula and Can Gio district. The coastal areas with acid sulphate soils of about 400.000 ha undergo saline intrusion during 4 to 9 months per year. Despite unfavourable conditions, acid sulphate soils in the Mekong delta are exploited extensively for various farming systems. Many local farmers have successes with different management techniques, resulted from numerous trials and errors, however their experiences are just suitable to the specific conditions in which they live. It is difficult to transfer such experiences to other areas without judging them scientifically. On large scale, traditional rice systems have been replaced by other crops which can bring more benefit. In many remote areas, where fresh water conveyance systems were installed recently, the farmers can even expand to multi-cropping systems. On severe actual acid sulphate soils, with suitable managements and fresh water availability, diversified plants such as cashew, melaleuca, pineapple, sugar cane and yam can be grown well. In saline intruded areas, shrimp farming has increased since 1990, due to their promised benefit. Large areas with acid sulphate soils were intensively disturbed by canals and ponds whose dikes are mounded by pyritic material. Despite increasing profit, sustainable land use in such area is still questionable. In the period of 1994-1996, water pollution resulted in extensive shrimp pests in Camau Peninsula where the shrimp ponds population is the highest in Vietnam. A damage cost of hundreds million dollars was estimated.

Common subject of the above mentioned research project is to concentrate the investigation mostly on agricultural uses of acid sulphate soil. The land exploitation situation, however, also requires knowledge of environmental impacts of acid sulphate soil reclamation, sustainable land use and preservation of fragile coastal ecosystems. The knowledge is specially important for saline intruded acid zones with acid sulphate soils. Some saline prevention systems have been abandoned due to intensive acidification occurring in the related areas afterwards. Fresh water conveyance systems are polluting downstream regions by acid propagation. Increase of acidity in aquatic environments caused by leached acidity from mounded pyritic soils may not only reduce fish population but also damage mangrove ecosystem located downstream.

Objectives

The main objectives of the project are:

— to develop a field scale model, that enables to predict the consequences of various water management strategies on soil and water quality in acid sulphate soil areas in coastal lands in the tropics;

— to increase knowledge on physical and chemical processes and to validate the model by collection and interpretation of field data on soil and water quality in coastal areas;
— to help formulating water management strategies for sustainable development on the scale of farmers fields.

Materials and methods

In order to be able to evaluate future water management strategies for acid sulphate soils areas, a simulation model had to be developed and tested for a range of varying circumstances. For calibration and validation (and later application) of the model, datasets of field experiments were required, with at least one complete dataset for the humid tropics of Indonesia and one for the sub-humid tropics of Vietnam. A review was carried out to inventory all previously conducted field experiments in both Indonesia and Vietnam and the datasets they yielded. Based on this, it was decided that additional field experiments were required for model validation.

The field experiments were carried out on a two-dimensional scale, i.e. chemical and physical parameters were measured on various locations along rows perpendicular to the drainage means. Parameters measured were soil parameters (such as water content, oxygen concentration, temperature, redox potential, composition of soil solution, hydraulic characteristics, groundwater levels), level and chemical composition of water in canals and climate data (precipitation, potential evapotranspiration, temperature and air humidity). The exact methodology followed in the field experiments is described in the chapters 3 and 4.

The existing one-dimensional Simulation Model for Acid Sulphate Soils (SMASS) was extended to a field scale model, applicable on the scale of a farmer field. This was done by linking the chemical part of the model to a pseudo two-dimensional water flow model. The pseudo two-dimensional approach was chosen (above a real two-dimensional water flow model), because of lesser input requirements. Especially for applications in low data environments this is an important criterion. The newly developed model was calibrated and validated using the datasets from the experiments carried out in Indonesia and Vietnam.

After validation the two-dimension model was used to evaluate currently applied and alternative water management strategies for both Indonesian and Vietnamese circumstances.

Results of the field experiments

In Indonesia a field was selected in a tidal area with actual acid sulphate soils (tidal land class (TLC) B). The land class covers a relatively high percentage of the acid sulphate soils in Indonesia. The site was formerly overlain by a peat layer, locally with a depth of 1.5 m. The area was reclaimed in 1981 with the construction of a fork system, and due to drainage and subsequent oxidation the peat topsoil disappeared. Transmigration from Java and surrounding areas in South Kalimantan took place after the drainage system was finalized in 1982/1983. A one-way flow system in combination with shallow drainage is a newly developed watermanagement strategy, and is now actively applied in the Tarantang area by the farmers.

Groundwater and surface water quality under this water management were monitored over time.

In general chloride (Cl-) concentrations increase with depth. Throughout the whole period chloride concentrations in the top layer were lower than those in deeper layers. For all layers, chloride concentrations declined rapidly with time; after 1.5 year chloride concentrations in the profile reached a level of less then 1 meq.l-1. Like chloride, iron (Fe2+) concentrations increase with depth. For all layers, iron concentrations declined with time, but more or less stable concentrations were observed in the period May-July. Concentration decline was faster in the topsoil than in deeper layers. In the lower layer iron was constant between 3-6 meq.l-1. Sulphate (SO42-) concentrations ranged between 1 to 22 meq.l-1. Again, in general the concentrations increase with depth and decrease with time. Decrease of concentrations with time is more pronounced in the top layer than in the lower layers. Values for pH ranged between 3 and 6. In all layers, values increased after one year. The top layer showed slightly lower values than the underlying layers.

In Vietnam the investigations focused on problems related to the construction and operation of a shrimp pond. These aquacultural activities are possibly very beneficial to farmers. On the other hand they resulted in large, unpredictable and, in some cases, irreversible changes in the ecological system in large areas of the coastal zone in Vietnam. The acidification upon disturbance of the acid sulphate soil plays a key role in these processes. If the water in the ponds is not refreshed periodically, its quality turns very poor because of the leached acidity from the dike. Obviously with negative effects on shrimp production. However, refreshing the ponds may result in pollution of the surrounding mangrove areas. Therefore a tool is required to predict the effects of shrimp pond management.

The experimental farm is located at the border of Vam Sat river at Ly Nhon in Can Gio district, about 50 km far away from Ho Chi Minh city. The site is characterised by typically tropical monsoon climate (1600 mm per year) and by serious saline intrusion. An 'E' shaped shrimp pond of 1400 m2 water surface was built. The pond was 1 m deep and surrounded by dikes, 10 m broad and 1 m high. The dikes were constructed in a way it is usually done in the area: while digging the pond the pyrite containing material from the lower soil horizons was deposited on top of the dike.

The pyrite crystals, observed by electron-microscope, showed various forms, sizes and oxidation grades. Single euhedral octahedra, framboids mainly composed of octohedra, big aggregates of framboids (diameter >100 mm) and thousands of small crystals (diameter < 0.1 mm) were observed. Jarosite was not detected in any sample of the undisturbed soil profiles. In contradiction to pyrite jarosite content decreased with depth in the mound. Immediately after excavation oxidation occurred in the topsoil of the dike. Already after two weeks jarosite mottles could be observed in the upper horizons. The rain water leached the topsoil and this resulted in the transformation of jarosite to ferric iron hydroxide. The oxidation status in deeper horizons remained constant, even during the rainy season. Oxidation is boosted because of aeration of the profile through macropores. The spatial variation of chemical properties in the dike was high, but the chemical parameters showed similar

trends in all locations. Leaching was not effective enough to remove toxics quickly from the dike.

Model development

The computer simulation model SMASS consists of a number of mutually linked submodels in which the various physical and chemical processes occurring in acid sulphate soils are described with mathematical equations. To solve these equations, the soil profile is divided into compartments of variable size. The initial physical and chemical conditions in each compartment must be given as model input. For the complete simulation period, values for the boundary conditions are required as input. The physical and chemical conditions in each compartment, together with the water and solute fluxes at the boundary of the soil system are computed on a daily basis. The sequence in which the various physical and chemical processes are computed are:

1. The *water transport submodel* computes vertical and lateral water transport. This yields water fluxes and the water content profile in the soil. The air contents in the soil are complementary to the water contents.
2. In the *oxygen transport and pyrite oxidation submodel*, air contents are used to compute oxygen diffusion coefficients in the air-filled soil macropores. Oxygen consumption values in the soil are calculated from pyrite and organic matter contents. Subsequently, the oxygen content profile in the soil macropores is computed. The rate of pyrite oxidation at each depth is calculated depending on the local oxygen concentration. For each depth, the oxidized amount of pyrite is converted into amounts of produced H^+, Fe^{3+}, SO_4^{2-}. The remaining amount of pyrite in the soil is used for calculations in the next time step.
3. The *solute transport submodel* computes vertical solute fluxes between soil compartments and lateral solute fluxes to and from the surface water, both based on the water fluxes calculated in step 1.
4. In the *chemical submodel*, first the production/consumption terms for the non-equilibrium processes (such as precipitation/dissolution of precipitates) are calculated. Then the total concentration of each chemical component is calculated in the soil compartments by summing for each component the production/consumption terms, the inflow/outflow (from step 3), and the total amounts at the end of the previous time-step. From these total concentrations, the equilibrium concentrations in the soil solution, the composition of the exchange complex, and the amount of minerals and precipitates are computed for each compartment.

Time steps for computations of the water and solute transport submodels are in the order of hours. Pyrite oxidation, oxygen profiles and chemical equilibria are computed once every day. The output of the model SMASS and its submodels is given on a daily basis. Model predictions can be carried out for one or more decades, so that the long-term effects of various water management strategies can be evaluated quantitatively.

Model validation

The rapid leaching of conservative ions such as sulphate and chloride in the Indonesian field was well simulated by the model. The development of Fe^{2+} concentrations in the top soil could be simulated reasonably well, whereas in deeper layers the model predicts considerably higher concentrations than was measured. Vertical, downward fluxes of Fe^{2+} produced in the topsoil during oxidation causes these high concentrations in the subsoil. Al^{3+} concentrations showed similar patterns. The pH values (both measured and simulated) where relatively stable and could be simulated reasonably well.

The comparisons of measured data and simulated data from the Vietnamese site showed good results. The model could simulate the various processes and their interactions occurring within a pyritic soil profile of the mound. However, some elements are still poor simulated like Mg^{2+}, Al^{3+}, and Fe^{2+}. Because many of the technical difficulties to get reliable data in the case of unsaturated soil of a mound, it is not easy to judge whether the differences between measured data and calculated data are due to inaccuracy of measurements or inaccuracy of simulations. Generally, the major processes and elements in soil solution were well simulated.

Evaluation of water management strategies

Indonesia

Indonesian scenarios were evaluated for tidal land class B, a land class under high reclamation pressure in Indonesia. The most frequently applied land management in this area is the so-called Sawitdupa system. Sawitdupa is an idiom for 'once planting and twice harvesting'. The technique is developed in view of Indonesia's wish to be self supporting in rice production. The system combines high-yielding and local rice varieties. During the growth of the short-duration high- yielding variety, the local variety is in nursery and in first transplanting stages, located at the outer fringes of the field. Harvest of the high-yielding coincides with the last transplanting (to full field) of the local variety. The system is efficient in water use and yields on yearly basis and economic returns are high. Research carried out in Tarantang showed that rice yields increased from about 2 to 3 ton.ha-1.a-1 under the Sawitdupa system. The method has been recognized as the best system for rice cultivation in acid sulphate soils in Indonesia. Farmers' adoption of the technology is good. Further development and finetuning of Sawitdupa is high priority.

In view of the importance of the Sawitdupa system, the scenarios tested all have the same type of water management, namely the one required for implemention of this system. The tendency in Indonesia is to promote Sawitdupa irrespective of soil type, whereas it is recognised that the impact of the system on soil and water quality largely depends on soil type. Therefore in scenarios 1 and 2 the effects of Sawitdupa in different soil types is studied (actual and a potential acid sulphate soil). Further, major concern exists on the effects of El Nino on the acidification processes in acid sulphate soils. Therefore the effects of climate on oxidation and leaching is studied in scenarios 3 and 4.

Table S.1 Scenarios tested for Indonesian reference sites

Scenario	Water/crop management	Soil	Climate
1	Sawitdupa	actual ASS	average rainfall (2300 mm.a^{-1})
2	Sawitdupa	potential ASS	average rainfall (2300 mm.a^{-1})
3	Sawitdupa	actual ASS	typical dry year (1100 mm.a^{-1})
4	Sawitdupa	potential ASS	typical dry year (1100 mm.a^{-1})

Under scenario 1, i.e. Sawitdupa system on actual acid sulphate soils with normal climatic circumstances, the soil profile is reacidified every year due to in-situ oxidation of pyrite, in periods with a low water table. This situation occurs during ripening and directly after harvest of the second crop. In these periods SO42- and Fe2+ rapidly increase to levels of 6 and 4 meq.l-1. The pH is rather well buffered, but the values show a similar tendency. After 6 years the initially available pyrite is depleted, and a more or less stable situation develops, with a pH value of around 6. Conservative ions, such as chloride, are leached out effectively, with low concentration after one year.

Under scenario 2, i.e. Sawitdupa system on potential acid sulphate soils with normal climatic circumstances, acidification in periods with lower groundwater tables is much more severe as compared to scenario 1. SO42-, Fe2+ and Al3+ concentrations in the topsoil rapidly increase to levels of 60, 20 and 25 meq.l-1. pH is buffering is not sufficient and on the long run it drops to values between 2 and 3.5. Similar patterns are observed for the subsoil.

Under scenario 3 (Sawitdupa system on actual acid sulphate soils with dry climatic circumstances) and under scenario 4 (Sawitdupa system on potential acid sulphate soils with dry climatic circumstances) the tendencies in the solute concentrations are to a large extend comparable to scenario 1 and 3 respectively. However, yearly re-acidification is slightly more severe than under average climatic conditions (scenario 1), due to dryer soil conditions. Leaching is also less effective, confirmed by the higher residual concentrations after 10 years, especially in the subsoil.

Vietnam

In Vietnam shrimp farming is a quickly expanding enterprise, with high potential profits, but also with high risks for both the farm enterprise and the vulnerable coastal mangrove systems. Therefore different ways of fish pond construction/management were evaluated. In scenario 1 ('normal scenario') the dikes bordering the fish pond are constructed in the same as farmers usually do it. The removed topsoil is deposited at the bottom of the dike and the removed subsoil, usually pyrite containing, is deposited on top of the dike. Dikes constructed like this have a very high potential for acidification. In scenario 2 farmers build small dikes (10-20 cm) on top of the dike to minimize run-off and maximise infiltration ('forced leaching scenario'). This could accelerate leaching of acidic elements from the dikes and may reduce the minimum time span between pond preparation and the start of shrimp farming. Scenario 3 ('reversed construction scenario') evaluated a situation were farmers cover the pyritic material taken from the subsoil by non-pyritic material from the topsoil. Therefore farmers have to move aside the non-pyritic topsoil material before

constructing the base of the dike from pyritic material from the subsoil. The non-pyritic soil, then, is deposited on the top of mound. This method may reduce oxidation intensity since the pyritic soil is buried inside the dike. For scenario 4 ('fresh water scenario') reference is made to some coastal areas where fresh water is conveyed to rainfed areas by canal systems for irrigation and drainage. Excavated pyritic soil is used to built dikes. Unlike in the 'normal scenario', in this case the water environment around the dikes is not saline. The characteristics of the soil profile applied in this scenario are the same with that in the 'normal scenario' (initial saline soil, with pyritic material on the top), but the quality of surface water is assumed to be similar to that of fresh river water.

Table S.2 Scenarios tested for Vietnam

Scenario	Land management	Characteristic
1	Shrimp farming	normal dike construction
2	Shrimp farming	forced leaching through dike
3	Shrimp farming	reversed dike construction
4	Shrimp farming	fresh water

Under scenario 1 (the 'normal scenario') the topsoil (0-30 cm) reached its lowest pH value (pH=2) after three years. The products of pyrite oxidation, such as Fe2+, SO42-, showed large variation within a year during the first stage and smaller changes during the last stages. Pyrite in the topsoil is almost completely oxidised after 3 years. However, the acidic elements such as H+, Fe2+, SO42-, Al3+, were still produced in the lower horizon and transported to upper layers through capillary rise during the dry season. This process continued over a long period after construction. After 10 years, the acidification of the mounded soil still continued.

Under scenario 2 ('forced leaching') leaching increased remarkably; acidic elements were transported downwards to the subsoil resulting in higher concentrations of H+, Fe2+, Al3+ and SO42- in lower horizon (50 and 90 cm). After 7 years, when the pyrite of the upper soil horizons is oxidised totally, pH start to increase gradually and Al3+ and SO42- show almost negligible concentrations in the upper horizons. In this scenario the total pyrite oxidation per year is less as compared to the normal scenario and therefore the total oxidation period is extended. After 10 years of oxidation, the acidification of the mounded soil still occurs within horizons below 50 cm. Generally, the construction of small dikes on top of the large dike accelerated leaching in the topsoil and decreased oxidation at deeper horizons.

Under scenario 3 ('reversed construction') the pH of the topsoil remained around 3 to 4 during the first 5 years of simulation, which is about 1 unit higher than in scenario 1. During the rainy seasons of the next 5 years the pH of the topsoil reached values of up to 5. The differences between the two scenarios disappeared gradually over time. This method of dike construction can reduce the concentration of acidic elements such as Fe2+, SO42- and Al3+ in the topsoil during the first years considerably. The concentration in soil solution of these elements is reduced by a factor 100 to 1000 as compared to that in the normal scenario, and ranged in

acceptable limits of toxicity. Generally, this treatment suggests a suitable method to keep the oxidation rate low in raised soil material.

Under scenario 4 ('fresh water') pH values in all horizons during the first 5 years were about 1 unit higher than in the normal scenario. Fe2+ concentrations were lower than in the normal scenario during the first 2 years, but reached similar levels after 5 years. SO42--concentration in all horizons were lower as compared to the normal scenarios. The fresh water quality decreased salinity in the mound significantly.

Conclusions and recommendations

Indonesia
Sawitdupa systems on a actual acid sulphate soil effectively leach out toxic elements from the top soil. However, this only holds true if groundwater tables do not drop into the pyritic layer and therefore in-situ oxidation of pyrite does not occur.

Sawitdupa systems on potential acid sulphate soils, with pyrite high in the profile, results in severe acidification and concentrations of Fe2+ and Al3+ far above their toxic levels. Also high loads of toxic elements to the environment were predicted.

Typical dry circumstances have a limited impact on acidification: slightly more pyrite oxidation and slightly less leaching of toxic elements was predicted under these circumstances.

Vietnam
All scenarios predicted long term acidification of raised soil material related to the soil construction of canals or ponds. The pyrite oxidation may continue at least 5 years after construction. Considerable amounts of toxic elements will be released into the environment. Therefore disturbance of acid sulphate soils should be done with great care.

Construction of small dikes on top of the mounds to stimulate infiltration and leaching is effective and reduces the minimum time span between construction of the pond and the start of shrimp production. However, this method can only be applied if the pyrite content in the soil is less then <5%.

The method of reverse construction of a dike or mound yields the best results. However, this method requires more labour and financial means. The method can be applied only if the pyritic soil is covered by at least 50 cm of the non-pyritic soil. For setting up irrigation systems to reclaim potential acid sulphate soil, numerous canals have to be constructed and soil material will be exposed to the air, favouring pyrite oxidation. The method of reverse building of dikes will help to reduce environmental risks trough acidic water propagation in the surface water.

1 Introduction

1.1 General problem description

Upon drainage acid sulphate soils generate sulphuric acid that brings their pH below 4, sometimes as low as 2. The acid leaks into drainage and floodwaters, corrodes steel and concrete, and attacks clay liberating soluble aluminium. Drainage waters may also be enriched in heavy metals and arsenic - a toxic cocktail endangering aquatic life and public health. The weathering of sulphitic mine spoil and overburden presents the same problems, so acid sulphate soils are not the concern of soil science alone: agronomy, fisheries and environmental management, land and property development, civil and mining and water engineering, and public health all have an acute interest.

Most recent estimates of the extent of acid sulphate soils indicate an area of some 24 million ha worldwide where the topsoil is severely acid or will become so if drained. In addition, there may be as much again thinly covered by peat and non-sulphitic alluvium (Van Mensvoort and Dent, 1997). However, estimates of the extent and distribution of acid sulphate soils suffer more than most from scanty field surveys, even fewer reliable laboratory data and, also, variable definition.

More significant than their absolute area is their location. They are concentrated in otherwise closely-settled coastal and floodplain, mostly in the tropics, where development pressures are intense and there is little suitable alternative land for expansion of farming or urban and industrial development. Two thirds of the known extent is in Vietnam, Thailand, Indonesia, Malaysia and northern Australia.

Acid sulphate soils have an enormous spatial variation in their characteristics, but they also exhibit very significant temporal variability, not least in their defining characteristics of acidity and its related toxicities. Almost uniquely, acid sulphate soils export their problems in drainage and floodwaters so, to provide useful information for soil and environmental management, both reliable static soil survey and dynamic chemical/hydrological modelling are required.

The high degree of acidity (or potential acidity) of acid sulphate soils makes liming to neutralize the acid, impracticable in most cases. The only practical way to manage these soils is by adequate soil and water management (Dent, 1986). Maintaining high water tables controls the oxidation of pyrite and the rate of acid production. Drainage and leaching can be applied to remove acidity. Adequate water management and controlled drainage could minimize the acid production and maximize the leaching of oxidation products (Dost and Van Breemen, 1982).

Acid sulphate soils cause on-site and off-site problems. Nowadays the off-site problems are attracting more attention than on-site soil problems. On-site problems

have been extensively reviewed (e.g. Dent, 1986). They include aluminium toxicity in drained soils, iron and H_2S toxicity in flooded soils, salinity and nutrient deficiencies. Most of our agronomic data are from pot experiments and, more recently, growth chamber experiments (e.g. Moore and Patrick, 1993) which may be far removed from the uncontrolled situation in the field. Engineering problems include corrosion of steel and concrete; uneven subsidence, low bearing strength and fissuring leading to excessive permeability of unripe soils; blockage of drains and filters by ochre; and the difficulties of establishing vegetation cover on earthworks and restored land.

Off-site problems are carried by effluent from drainage schemes, earthworks, excavations and mines. The acid drainage water carries aluminium released by acid weathering of soil minerals, and heavy metals released by oxidation of sulphide minerals. Toxic drainage waters may be released only episodically, for example at the onset of the wet season after a period of low water table during which oxidation has taken place. This makes it difficult sometimes to pinpoint the source of the problem; acid drainage and floodwaters may travel for many kilometres before they are neutralised. Acid sulphate drainage can have disastrous effects on freshwater and estuarine fisheries, especially on invertebrates that are unable to escape. Massive fish kills and ulcerative disease have often been reported in estuarine waters but these have only recently been linked to acid sulphate soils (Callinan et al., 1993; Sammut et al., 1996). The effects on aquatic vegetation are more variable since many species rooting in the reduced mud are little affected - *Nyphar* and *Phragmites* often come to dominate freshwater subject to acid flushes.

Even very low concentrations of aluminium can be hazardous. Concentrations of 1000 to 2000 $\mu g.l^{-1}$ Al are toxic to most crops; fish are more susceptible, the few data available indicate fish kills at >500 $\mu g.l^{-1}$ and increased mortality from exposure to concentrations of only 100 $\mu g.l^{-1}$. Standards for potable water mostly range between 50 and 1450 $\mu g.l^{-1}$ but are being tightened, e.g. Canada, Australia and New Zealand specify 5 $\mu g.l^{-1}$ for water of pH <6.5. 5 $\mu g.l^{-1}$ is equivalent to 2×10^{-4} $mol.m^{-3}$. In acid sulphate soils concentrations of dissolved Al reach from 4 to 80 $mol.m^{-3}$ in soil water and from 3 to 10 $mol.m^{-3}$ in drainage waters.

1.2 Main chemical processes in acid sulphate soils

1.2.1 Oxidation

If a soil layer, which contains pyrite is drained, oxidation will occur, according to the reaction (Van Breemen, 1976):

$$FeS_2 + 3\ 3/4\ O_2 + ½\ H_20 \rightarrow Fe^{3+} + 2SO_4^{2-} + H^+ \qquad (1.1)$$

The ferric iron released in this reaction may precipitate as amorphous hydroxide, which is ultimately transformed into goethite and hematite. Under acid and oxidized conditions, jarosite is usually formed:

$$FeS_2 + 15/4\ O_2 + 5/2\ H_20 + 1/3\ K^+ \rightarrow 1/3KFe_3(SO_4)_2(OH)_6 + 4/3SO_4^{2-} + 3H^+ \quad (1.2)$$

Jarosite is stable under oxidized and acid conditions. The acid released by these reactions will be partly neutralized by various buffer mechanisms. If present calcite and/or dolomite will neutralize the produced acidity. In non calcareous soils or if the amount of sulphuric acid produced exceeds the content of these minerals, exchange of hydrogen and aluminum ions against basic cations at the exchange complex will buffer the pH. In most acid sulphate soils the pH will drop below 4. At this pH aluminum minerals will buffer the pH and dissolve into the soil solution. It may reach concentrations which are toxic to plants. High iron and aluminum concentrations will reduce the availability of phosphate. Also, aluminum will replace basic cations on the cation exchange complex, upon which these basic cations will be leached from the soil. Not only will the K^+ supply for plant growth become restricted, but also Mg^{2+} and Ca^{2+} deficiencies may be the result (Moore and Patrick, 1993). Low concentrations of basic cations also increase the plants susceptibility to iron toxicity. Finally at very low pH (around 3) iron oxides will dissolve and buffer the pH of the soil solution.

1.2.2 Reduction

Flooding of an already acidified acid sulphate soil may alleviate the high concentrations of acid substances and their related toxicities, but some new problems are introduced. Upon flooding the supply of oxygen is stopped and after the oxygen already present has been consumed other substances will act as the electron acceptor in the oxidation of organic matter. Nitrate is after oxygen the strongest oxidator found in soils and is the first to be reduced. After that manganese oxides, iron (hydr)oxides and sulphate are reduced successively although some overlap may occur. With the reduction of ferric (hydr)oxides the concentration of ferrous iron increases and hydrogen ions are consumed:

$$Fe(OH)_3 + 1/4\ CH_20 + 2H^+ \rightarrow Fe^{2+} + 1/4\ CO_2 + 11/4\ H_20 \quad (1.3)$$

The reduction of iron may lead to toxic concentrations of ferrous iron. After the reduction of iron has stopped sulphate reduction may start during which the sulphate concentration decreases and H^+ is consumed. H_2S, which accompanies sulphate reduction, is highly toxic to plants.

1.3 Problem description Indonesia

The Republic of Indonesia counts about 43 million ha of swamp land, of which 10.5 million hectare are considered as potential arable land. 7 Million ha is located in the tidal zone. Nugroho et al. (1991) reported that most of the swamp lands are situated in Sumatra (9 million ha), Kalimantan (11 million ha) and Irian Jaya (12 million ha). According to Nugroho et al. (1991) swamp areas can be divided up into

acid sulphate soils (both potential and actual depending on the depth of the sulphitic layer and the water management applied), peat lands (subdivided into deep, moderately deep and shallow peat soils), inland swamps (with seasonal water logging) and saline soils.

In Indonesia, acid sulphate soils cover about 4 million ha, which is c.10 percent of the Indonesian wetlands or about c.1 percent of the Indonesian archipello.The exact location and the extent of Indonesian acid sulphate soils is not yet known. Generally they occur in young marine deposits along the coasts of Sumatra, Kalimantan and Irian Jaya.

Because of the ever growing population, the restricted productivity in many of the transmigration areas, and the wish of the Indonesian government to be self sufficient with respect to rice, more and more land has to be taken into production for rice cultivation. Further, large scale creation of oil palm plantations claims huge areas of land. Often reclamation is preceded by forest clearing. Most of these activities take place in wetland areas, often with acid sulphate soils. Tremendous distortions of the ecological environment have been reported, such as erosion, acidification, peat subsidence, changes in microclimate, and disappearance of complete habitats. Toxic compounds are released into public water schemes during reclamation processes, resulting in decreased biological quality, destruction of natural fauna and flora, decrease of bio-diversivity and decline of agricultural productivity.

In most of the areas pyrite is present in the very top layer of the mineral soil. In many cases the mineral soil is covered with a peat layer, varying in depth between 0.2 and 1 meter. Reclamation of these areas is expected to lead to subsidence of the peat layer, making deeper drainage necessary. Once the water table drops into the sulphitic layer, severe acidification will take place. These developments make the problem of acid sulphate soils in Indonesia important.

Swamp ecosystems are important fresh water resources, and their utilisation and conservation were regulated in the Indonesian Government Rule No. 27/1991 and Indonesian President decree No. 57/1989. For acid sulphate soil in coastal plains they official policy in Indonesia is based on the following priorities: (i) keep conditions as natural as possible, (ii) reclaim the land with as small as possible destruction, and use it for rice production or shrimp ponds.

In Indonesia many research projects yielded a wealth of information on the occurrence of ASS, the chemical and physical processes and the different water management strategies applied. Integration of this information is required. Spatial variation is high and field experiments can not be carried out for each farmers field. Therefore a model is required to be able to estimate the future effects of reclamation and drainage. A model that integrates both hydrological and chemical aspects is not yet available.

Other problems related to acidification in ASS areas are salt formation at the soil surface, iron suspension in surface water, excessive growth of swamp grasses,

resulting in blockage of drainage systems. In certain areas the soil and water quality has worsened to such an extent that they areas have been abandoned, and farmers moved into upstream areas, often protected forests.

1.4 Problem description Vietnam

In Vietnam, areas with acid sulphate soil cover about 1.8 million hectares, mostly in the Mekong Delta. The complicated hydrological conditions in the delta, characterized by interactions between river flow and sea intrusion, have favoured acid sulphate soils formation in inland back swamps such as the Long Xuyen Quadrangle and the Plain of Reeds and coastal wetland like Camau Peninsula and Can Gio district. The coastal areas with acid sulphate soils of about 400 000 ha undergo saline intrusion during 4 to 9 months per year. Despite unfavourable conditions, acid sulphate soils in the Mekong Delta are exploited extensively for various farming systems. Many local farmers have successes with different management techniques, resulted from numerous trials and errors, however their experiences are just suitable to the specific conditions in which they live. It is difficult to transfer these experiences to other areas without judging them scientifically. On large scale, traditional rice systems have been replaced by other crops which can bring more benefit. In many remote areas, where fresh water conveyance systems were installed recently, the farmers can even expand to multi-cropping systems. On severe actual acid sulphate soils, with suitable managements and fresh water availability, diversified plants such as cashew, melaleuca, pineapple, sugar cane and yam can be grown well (Xuan, 1993; Xuan, 1995). In saline intruded areas, shrimp farming has increased since 1990, due to their promised benefit. Large areas with acid sulphate soils were intensively disturbed by canals and ponds whose dikes are mounded by pyritic material. Despite increasing profit, sustainable land use in such area is still questionable. In the period of 1994-1996, water pollution resulted in extensive shrimp pests in Camau Peninsula where the shrimp ponds population is the highest in Vietnam. A damage cost of hundreds million dollars was estimated.

Research on acid sulphate soils in Vietnam has been carried out for some decades. In 1980 a co-operation project (named VH-10) between University of Can Tho (Vietnam) and the Agricultural University Wageningen (the Netherlands) was started. The project has contributed significantly to training of researchers, bridging gaps in knowledge on acid sulphate soils and strengthening interaction between experts and farmers to improve agricultural systems in the Mekong Delta. Soil survey works were also done under the national project 60-02, 60-B supplying a soil map, a hydrological map and a geological sedimentation map of the Mekong Delta.

In the early nineties a project (Problem Soils Project) funded by SAREC (The Swedish Agency for Research Co-operation with Developing Countries) conducted soil surveys in order to update the present soil map and to transfer the Vietnamese classification system into the FAO system. After the project,12 zones were distinguished in acid sulphate soil areas in the Mekong Delta (Tin and Tri, 1991).

An international funded project has been conducted in the period of 1990-1994 (Project on Management of Acid Sulphate Soils) under supervision of the Interim Committee for Co-ordination of Investigations of the Lower Mekong Basin. This project carried out field and laboratory measurements in order to establish a simple model for predictions of chemical processes of dissolved substances within already oxidised acid sulphate soils (Eriksson, 1993).

Common subject of the above mentioned research projects is to concentrate the investigation on agricultural uses of acid sulphate soils. The land exploitation situation, however, also requires knowledge on environmental impacts of acid sulphate soil reclamation, sustainable land use and preservation of fragile coastal ecosystems. The knowledge is specially important for saline intruded acid zones with acid sulphate soils. Some saline prevention systems have been abandoned due to intensive acidification occurring in the related areas afterwards. Fresh water conveyance systems are polluting downstream regions by acidic propagation. Increase of acidity in aquatic environments caused by leached acidity from mounded pyritic soils may not only reduce fish population but also damage mangrove ecosystem located downstream.

1.5 Objectives of the project

Chemical processes occurring in ASS have been studied and described by many authors (e.g. Van Breemen, 1976; Moore and Patrick, 1989). The integration of these processes in a quantitative simulation model was done by AARD/LAWOO (1992). A one-dimensional simulation model was developed and tested, describing pyrite oxidation, water and solute transport, reduction, dissolution and precipitation of secondary minerals. To be able to evaluate water management strategies on field level, one-dimensional model was extended to a field level model, taking into account mutual lateral influences of field and surface water. The model was tested in two field experiments and later applied to evaluate a series of relevant water management strategies for both Indonesia and Vietnam.

The main objectives of the project are:
- to develop a field scale model, that enables to predict the consequences of various water management strategies on soil and water quality in acid sulphate soil areas in coastal lands in the tropics;
- to increase knowledge on physical and chemical processes and to validate the model by collection and interpretation of field data on soil and water quality in coastal areas;
- to help formulating water management strategies for sustainable development on the scale of farmers fields;
- to introduce and train junior project staff in computer modelling, field and laboratory techniques, data processing and reporting.

Crop yields are determined by many different factors such as climate, soils, water availability, water quality, economic factors (e.g. distance to markets, quality of

infrastructure, labour and cash availability) and social factors (e.g. crop selection by farmers, cultural factors determining land management etc.). This research focuses on the relation between water management and soil and water chemistry. The simulation model presented can be used to predict these relations. As to crop yields no predictions can be made. In order to be able to predict crop yields as a function of soil and water management, quantitative relations should be established between water availability and the chemical quality of the soil on the one hand and crop yields on the other hand. This is however, not the scope of this project.

1.6 Reading guide

In this report the results of this work is presented. Chapter 2 describes the methodology applied, chapter 3 and 4 describe the field experiments carried out in South Kalimantan, Indonesia and the Mekong Delta, Vietnam, respectively. In chapter 5 and 6 the principles and the calibration and validation of the field scale model is described. Chapter 7 gives the characteristics of selected ASS areas (reference sites) in both Indonesia and Vietnam. In chapter 8 land use scenarios for the selected reference sites are evaluated. Chapter 9 gives general conclusions and recommendations.

2 General research methodology

In order to be able to evaluate future water management strategies for acid sulphate soils areas, a simulation model had to be developed and tested for a range of varying circumstances. For calibration and validation (and later application) of the model, datasets of field experiments were required, with at least one complete dataset for the humid tropics of Indonesia and one for the sub-humid tropics of Vietnam. A review was carried out to inventory all previously conducted field experiments in both Indonesia and Vietnam and the datasets they yielded. Based on this, it was decided that additional field experiments were required for model validation.

The field experiments were carried out on a two-dimensional scale, i.e. chemical and physical parameters were measured on various locations along rows perpendicular to the drainage means. Parameters measured were soil parameters (such as water content, oxygen concentration, temperature, redox potential, composition of soil solution, hydraulic characteristics, groundwater levels), level and chemical composition of water in canals and climate data (precipitation, potential evapotranspiration, temperature and air humidity). The exact methodology followed in the field experiments is described in the chapters 3 and 4.

The existing one-dimensional Simulation Model for Acid Sulphate Soils (SMASS) was extended to a field scale model, applicable on the scale of a farmer field. This was done by linking the chemical part of the model to a pseudo two-dimensional water flow model. The pseudo two-dimensional approach was chosen (above a real two-dimensional water flow model), because of lesser input requirements. Especially for applications in low data environments this is an important criterion.

The newly developed model was calibrated and validated using the datasets from the experiments carried out in Indonesia and Vietnam.

For each country reference sites were selected. Reference sites are typical acid sulphate soils situations for the country with a characteristic soil profile, water regime and climate. Different possible water management strategies for the reference sites were defined and tested with the model.

3 Field experiment in South Kalimantan

3.1 Evaluation of the available dataset

The accuracy of the model computation is largely depending on the accuracy of model input. Since a validation study aims at testing the model's concept, the influence of inaccurate model input should be eliminated. Therefore a complete and accurate set of data is required for model validation. A division of all input parameters of SMASS is made as follows:

a. input data that need to be measured in the field;
b. input data that can be obtained from previous model calibration in similar areas;
c. input data that can be obtained from literature;
d. data for which assumptions can be used.

All input data required for model validation are listed below. The data are marked with a, b, c or d and are divided into two main groups:

I Data to be determined only once. These data serve to characterise the experimental site and are input to the model.

II Data to be determined as a function of time (process monitoring). These data partly serve as model input and are partly so-called target quantities for model validation. The latter are measured and later compared with model calculations to determine the predicting accuracy of the model.

Group I. Data be determined once

Crop:

— leaf area index (LAI) as a function of soil cover (SC) (c),
— interception as a function of SC (c),
— sink variables (c).

Soil (all as a function of depth!):

— bulk density (a),
— total CEC (a),
— K(h) and h(θ) (a),
— organic matter content (a),
— initial conditions (a),
  — composition of the soil solution (a),
  — concentration of pyrite (a),
  — concentration of precipitates (b),
  — average diameter of pyrite crystals (b),
  — initial water content (a/d),
  — soil redox potential (a/d),
  — O_2-concentration in soil air (a/d),
— aggregate radius (b),

— tortuosity factor (b/c/d).

Hydrology:
— distance between drains (a),
— wet diameter of drains (a),
— an-isotropy of waterflow in saturated zone (a/c),
— chemical composition of the soil water at the bottom boundary (a/d).

Others:
— oxygen consumption by decomposition of organic matter (d),
— average soil temperature (c),
— oxygen diffusion coefficients in liquid and air (c),
— Henry coefficient of O_2 (c).

Group II. Data to be determined as a function of time (process monitoring)
Climate:
— daily precipitation data (a),
— chemical composition of precipitation (a),
— daily temperature, radiation, humidity and wind dependant on the submodel chosen for calculation of the potential evapotranspiration. See appendix II for an exact summary of required input per submodel (a).

Crop:
— soil cover (SC) as a function of time (a),
— root depth as a function of time (a),
— development of an inactive root layer as a function of time (a).

Hydrology:
— water level and chemical composition in drains (a),
— amount and quality of irrigation water (a),
— level of the groundwater table (a).

Target quantities for validation:
— soil moisture content as a function of depth and time,
— redox potential as a function of depth and time,
— O_2 concentration in soil air as a function of depth and time,
— soil moisture composition as a function of depth and time,
— final concentration of pyrite and/or other precipitates as a function of depth.

During the period November 1992 to July 1994 field experiments were carried out by CSAR/BARIF on three different sites aiming at the collection of data to be used in the validation of SMASS. The datasets were evaluated using the criteria above. All sites, being Tabunganen, Barambai Dalam and Tarantang, Pulau Petak, South Kalimantan, covered a tertiary unit and all had a similar lay out, consisting of one transect of monitoring points between the two tertiary canals and one transect perpendicular to the first, ranging from the secondary canal to the end of the unit,

marked by a ditch. Comparing the measurements carried out during the experiments and the data requirements for model validation, it was concluded that the dataset is rather complete, except for daily precipitation (to be purchased from three meteo stations close to the experimental fields) and daily radiation and temperature (both to be gathered from the Banjarmasin meteo station). Also crop data were not gathered (root depth and soil cover as a function of time). A few other constraints are identified.

— Water management on the tertiary unit was not uniform; farmers were allowed to manage their water on field level.
— Liming and fertilizer experiments were carried out on the tertiary unit during the monitoring period. Although these experiments were not coinciding with the monitoring cross-sections, a lateral influence of individual monitoring sites is expected.
— No measurements were carried out for validation of water balance calculations.
— The monitoring period was interrupted twice in the period from July to November.

Given these constraints it was decided to carry out one additional comprehensive field experiment.

3.2 Site selection

For this experiment it was important to select a site where it is possible to measure oxidation and reduction processes, and horizontal and vertical leaching of toxic elements. Therefore, a field was selected with fluctuating groundwater, periodically above and below the top of the pyritic layer, and with the possibility to control and manipulated water management in the field. Further, the site had to be easily accessible for fortnightly measurements.

A system of tidal land classes (TLC) was introduced by Noorsyamsi (1976) and later finetuned by AARD/LAWOO (1992). The classification is based on the degree of influence of the tidal movement on the hydrology of the area. The classification is summarised as follows:

TLC A: Daily flooding due to tidal influence.
TLC B: Fortnightly flooding, and daily fluctuation of the groundwater under tidal influence.
TLC C: No flooding, but fortnightly fluctuation of the groundwater under tidal influence.
TLC D: No tidal influence.

A field was selected in an area with tidal lands with actual acid sulphate soils TLC B, a land class covering a relatively high percentage of the area in Pulau Petak (Fig. 3.1). Hydro-topography conditions in TLC B show more variability than in TLC A. Because of this high spatial variability of the soils and hydrology generalisation and recommending land management is difficult.

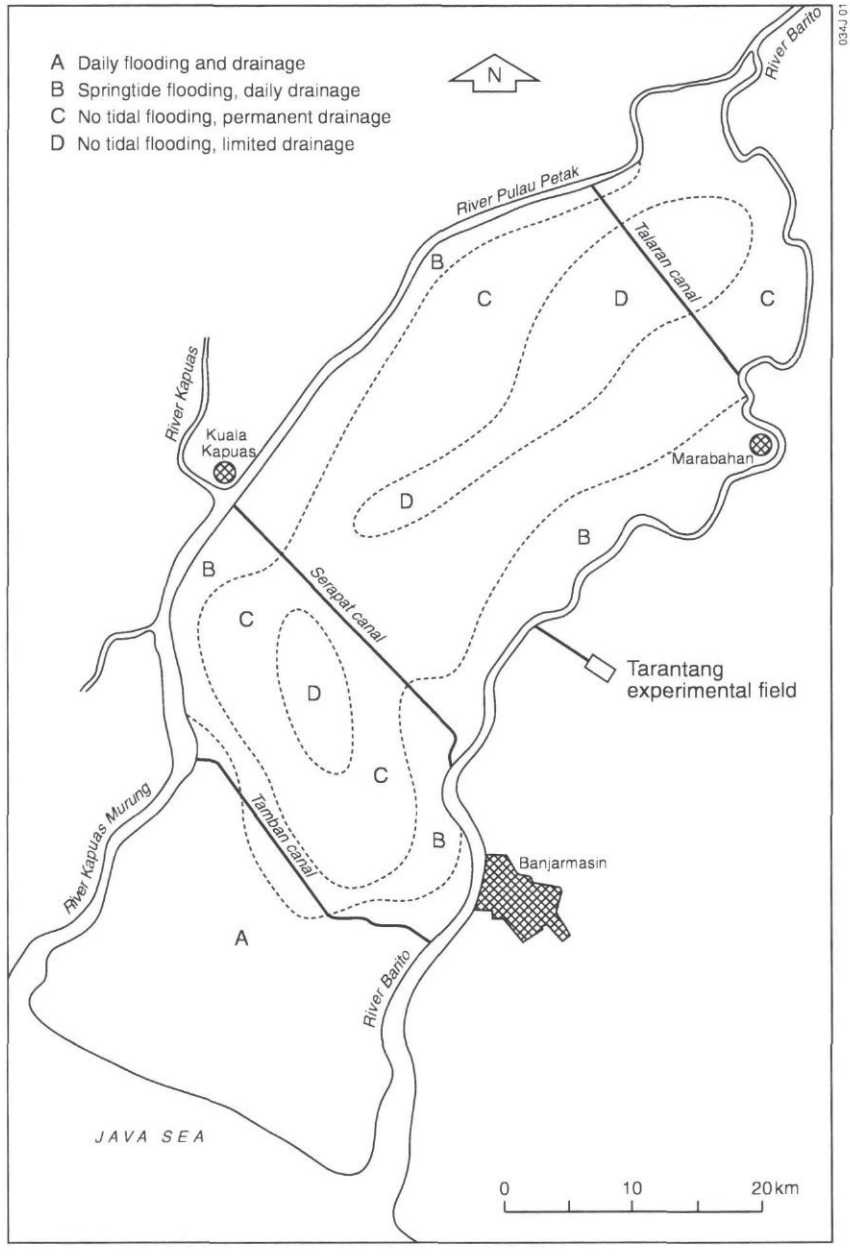

Fig. 3.1 Tidal land classes of Pulau Petak and its surroundings (after AARD/LAWOO, 1992)

3.3 General description of the field site

The site is located in Tarantang (desa Karang Buah, Kecamatan Belawang, Kabupaten Barito Kuala, South Kalimantan Province, see Fig. 3.1), and was classified as actual acid sulphate soil which was formerly overlain by a peat top soil, locally with a depth of 1.5 m. The area was reclaimed in 1981 with the construction of a fork system (Fig 3.2), and due to drainage and subsequent oxidation the peat top soil disappeared. Transmigration from Java and surrounding areas in South Kalimantan took place

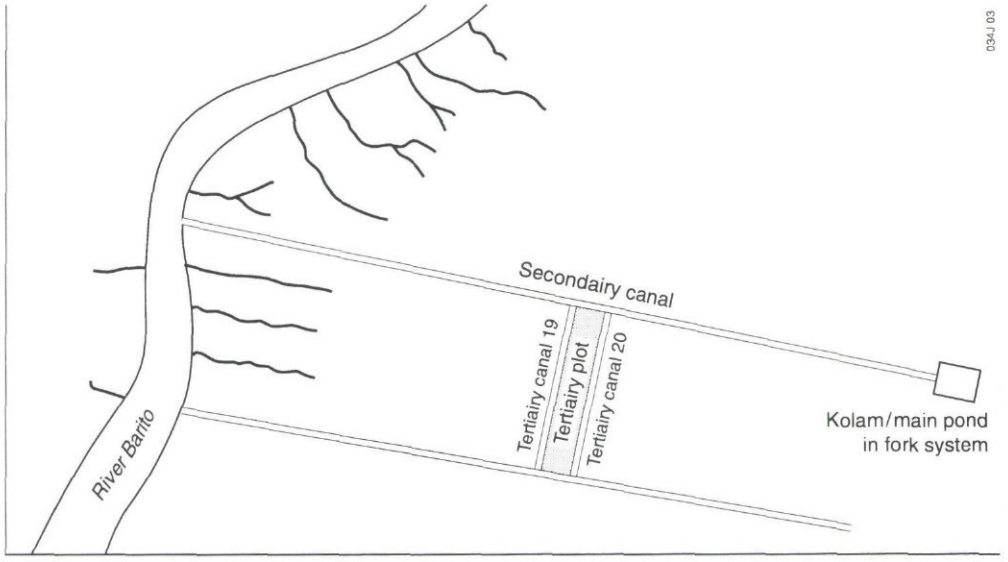

Fig. 3.2 The Tarantang fork system and the location of tertiary canals 19 and 20

after the drainage system was finalized in 1982/'83 (Euroconsult & Biec International, 1991).

From previous experiments, it is known that Tarantang has severe limitations for agricultural uses. Acidification and the limited availability of fresh irrigation water to leach the toxic elements from the fields are the most pronounced problems.

A one-way flow system in combination with shallow drainage is a newly developed strategy, and is now actively applied in the Tarantang area by the farmers. The basic principles of the system is a deliberate flushing of toxics and preventing or reducing acidification during drainage. Previous research in the area showed that under this type of water management, soil and water quality near the secondary and tertiary canals improved due to frequent flushing by water movement in the canals (Subagyono et al., 1994). The strategy is more and more applied in Indonesia in acid sulphate soils areas with similar characteristics. It is considered to be a promising and suitable strategy for further finetuning.

The water management in tertiary level is executed between an irrigation canal and a drainage canal (in this case canals no. 19 and 20, see Fig. 3.2), with a spacing of 150 m.

The water level in the irrigation canal is kept high by allowing in water during high tide and closing a stoplock at the beginning of the canal during low tide. The water level in the drainage canal is kept lower, by closing the stoplock during high tide and episodically opening of the stoplock during low tide. A lateral hydraulic gradient is established this way, resulting in a one way flow of water through the field. During neap tide, the water in the irrigation canals is high enough for irrigation. This is done with a so-called 'gorong-gorong', which is a pipe through the small dikes bordering the fields. The pipe is locked with a flapgate that allows water in but not out (Fig.

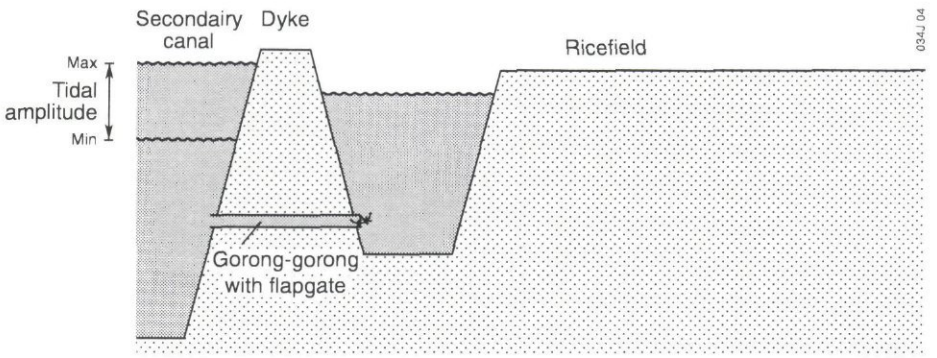

Fig. 3.3 The flapgates in the gorong-gorong system

3.3). Drainage occurs when the stoplock in the drainage canal is opened, which is usually decided upon by the farmers' group when they perceive that the quality of the water in the fields is unacceptable. After drainage, water from the irrigation canal is allowed into the fields when available, which usually is of better quality. However, in the dry season fresh water availability is limited, and in this case the water level in the field may drop for a longer period upon drainage, resulting in acidification and water stress for the crop. The farmers have to strike a balance between drainage and water conservation.

3.4 Setup of the field experiments

Since this project is particularly aiming at the lateral processes in the field, suction cups, piezometers and airchambers were installed in the field along two transects between the tertiary canals (Fig. 3.4). The transects covered an area of about 40 ha, meaning that a group of farmers was involved in the experiment.

Flap gates were installed in both canals with different flow direction, and operation during the experiment was according to the one-way flow water management system as described above. The measurement of water levels in the field and in the canals were carried out manually and on a daily basis. Benchmarks from earlier irrigation/drainage projects by the Minister of Public Works were used.

Precipitation was measured daily at 7.00 a.m. by using a simple ombrometer. Precipitation data were also retrieved from a local weather station, together with daily values of temperature (minimum, maximum and average). Evaporation was measured by a small calibrated 'E' type evaporation pan. To be able to calculate transpiration using the leaf area index, plant growth, plant leafs, plant stem, and plant shoots characteristics were measured monthly.

Soil samples were taken on three depths (25, 65, 105 cm, see Fig. 3.5) and CEC, occupation of the exchange complex, bulk density, and hydraulic properties including soil permeability were determined. Pyrite analyses were executed both in Wageningen (wet analysis) and in Bogor (wet analysis using a static function of iron and sulphur, Sudjadi and Widjik, 1974). Bulk density and permeability were determined at

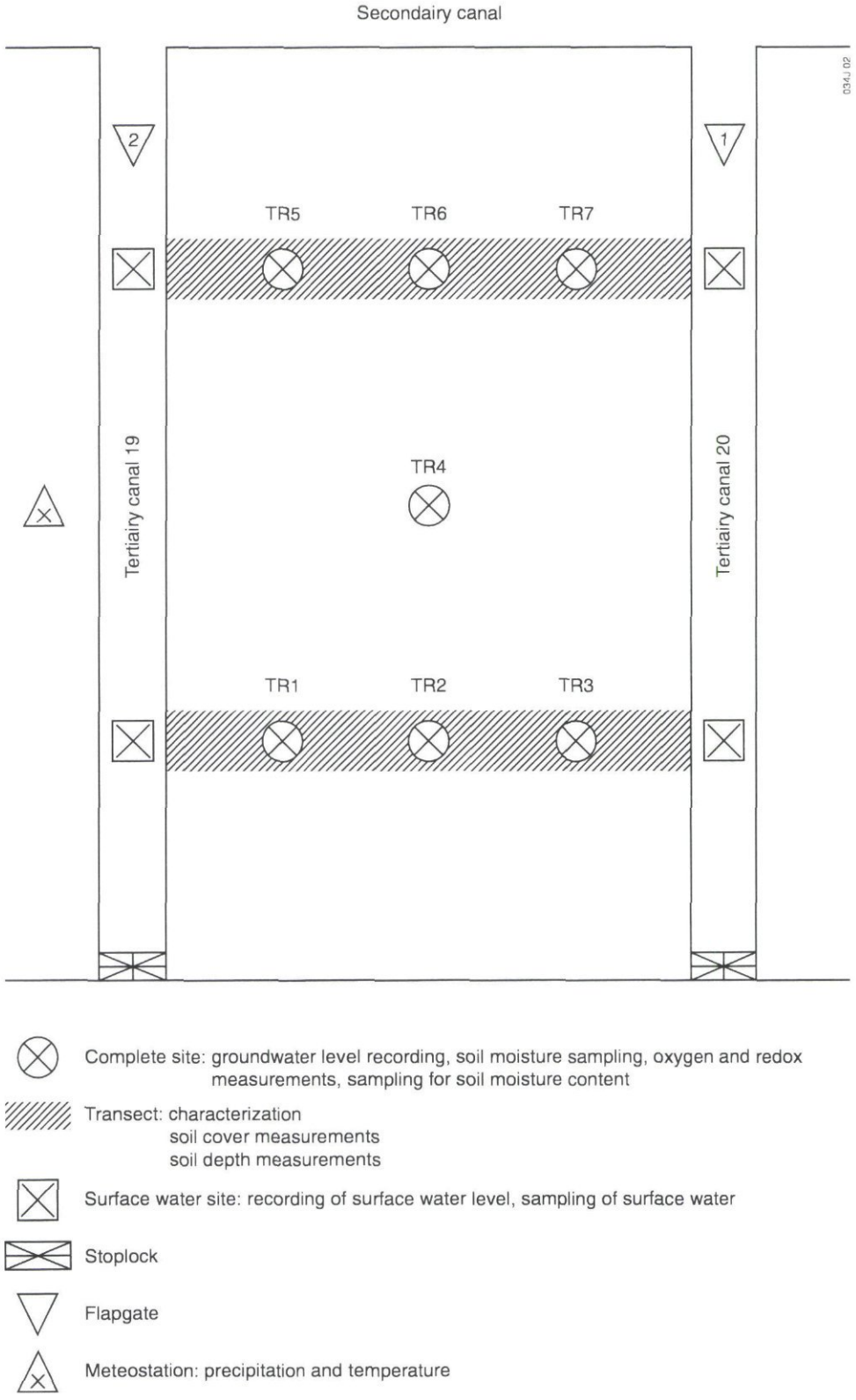

Fig. 3.4 Layout of the experimental field

BALITRA, Banjarbaru, South Kalimantan. The rest of the measurements were carried out by the Centre for Soil and Agroclimate Research laboratory in Bogor. Organic matter was determined by dry combustion 16 hours at 375 ° C, and water contents on different depths by drying 24 hours at 105 °C.

Soil water and surface water samples were taken fortnightly and analyzed using methods described by Van den Toorn et al. (1987). Since the quality of the water is under tidal influence, sampling was always carried out on the same time (starting from 10.00 a.m.).

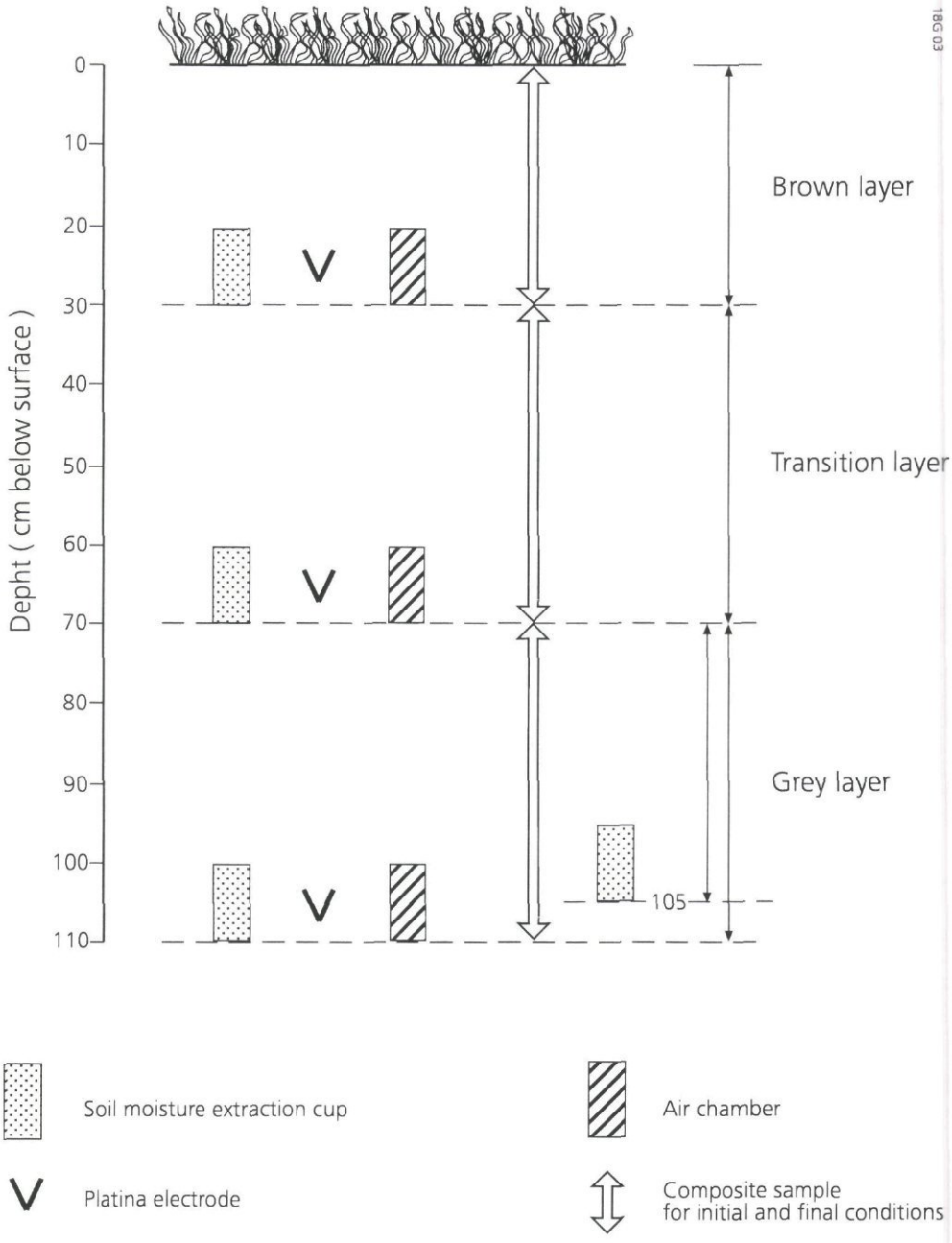

Fig. 3.5 Soil layers and situation of measuring devices

A detailed description of the setup is given by Van den Bosch and Nugroho (1996). The total duration of the experiment was 700 days, from 1-5-96 to 1-10-97.

3.5 Results

3.5.1 Hydrology

Figure 3.6 gives the measured daily precipitation and water levels, both in the fields and in the canals. The level in the irrigation canal (T20) is consequently higher than the water in the drainage canal (T19). When the fortnightly peaks of the irrigation canal touch the soil surface, the fields can be irrigated through the gorong-gorongs. During the growing season, the groundwater level is always above soil level (ponding), but after harvesting the farmers do not deliberately irrigate any more and the groundwater level slowly decreases and drops into the field.

Total precipitation in the period of May 1995 to December 1995 amounted to 750 mm; whereas in the period of January 1996 to November 1996 reached 1200 mm. These totals are relatively low, but both years are known as dry years. A clear fortnightly tidal influence on the canal water levels is observed. In the dryer period, from April to July, canal water levels are relatively due to higher tidal influence in this time of the year.

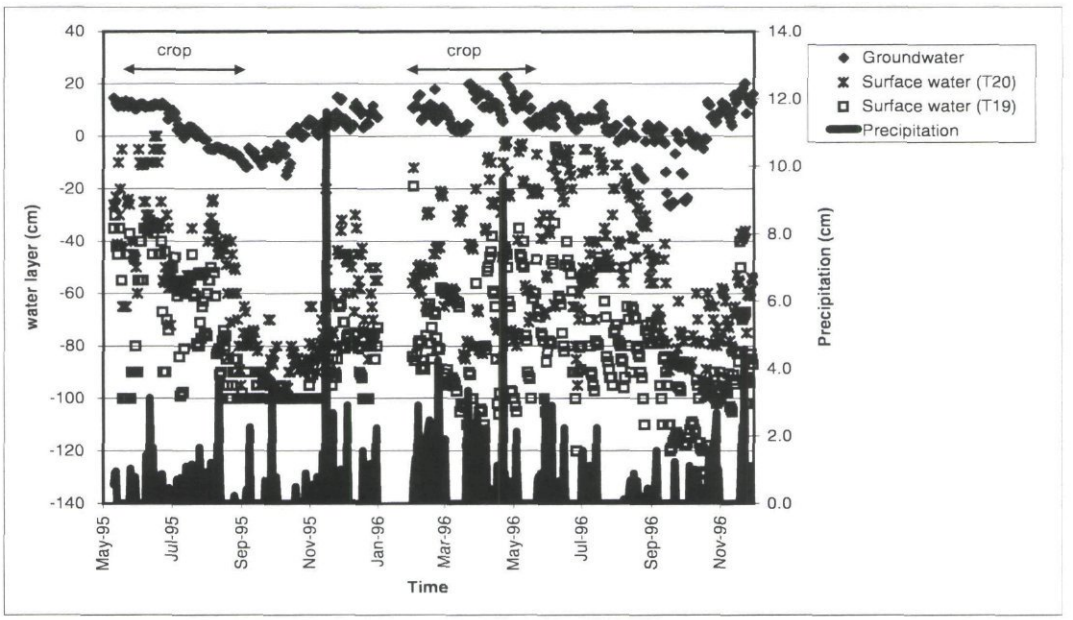

Fig. 3.6 Measured groundwater level, surface water level and precipitation as a function of time, Tarantang, Pulau Petak, South Kalimantan

3.5.2 Soil analysis

The bulk density of the soil was relatively low, and ranged between 0.52 $g.cm^{-3}$ up to 0.95 $g.cm^{-3}$, which corresponds with the high organic contents (Tabel 3.1). Soil permeability in the top layers ranged between 0.34-1.59 $cm.h^{-1}$, which is considered slow. Apparently, due to puddling of the soil, the soil structure is destroyed, resulting in a compacted, rather impermeable layer. The data are supported by previous observations in the same field (AARD/LAWOO, 1992). Pores drained relatively slow, resulting in a slow aeration of the soil. Also according to previous observation, the air diffusion/aeration in this kind of soils is low. Quick drainage of the soil is therefore not possible, making the area less suitable for other crops than paddy rice. Pyrite content was low in the top soil, but increased rapidly with depth.

Table 3.1 Soil physical characteristics of Tarantang before the experiment

Point code	Depth	Volume density	Total porosity	Drainage pores		Available water	Permeability
				Fast	Slow		
	(cm)	($g.cm^{-3}$)	(% vol)	(% vol)	(%vol)	(% vol)	($cm.h^{-1}$)
T I	0-20	0.76	71.3	7.1	5.0	32.1	0.93
T II	0-20	0.52	80.4	17.2	5.7	36.9	1.40
T III	0-20	0.85	67.5	8.3	4.7	28.1	0.34
T IV	0-20	0.95	64.2	6.2	4.4	24.5	0.84
T V	0-20	0.77	70.9	6.8	5.2	32.3	1.59
T VI	0-20	0.52	80.4	28.8	5.1	32.6	0.42

3.5.3 Chemical composition of the soil water and surface water

In this report, graphs are presented for Cl^-, Fe^{2+}, SO_4^{2-} concentrations and pH for both transect and three different depths.

For all chemical parameters the measurements along the two different transects (TR1-TR3 and TR5-TR7) show similar trends.

In general chloride (Cl^-)concentrations increase with depth. Throughout the whole period chloride concentrations in the top layer are lower than the concentrations in the lower layers. For all layers, chloride concentrations decline rapidly with time; after 1.5 years chloride in the top layer has reached a level of less then 1 $meg.l^{-1}$. In the second layer it reaches this level after 2 years (Fig. 3.8).

Like chloride, iron (Fe^{2+}) concentrations increase with depth. The concentrations in the top layer are higher than those in the intermediate layer, which are again higher than those in the lower layer. For all layers, iron concentrations decline with time, but more or less stable concentrations were observed in the period May-July. Decline is faster in the top layer; in the second layer concentrations are more constant. In the lower layer iron remains between 3-6 $meq.l^{-1}$ (Fig 3.9).

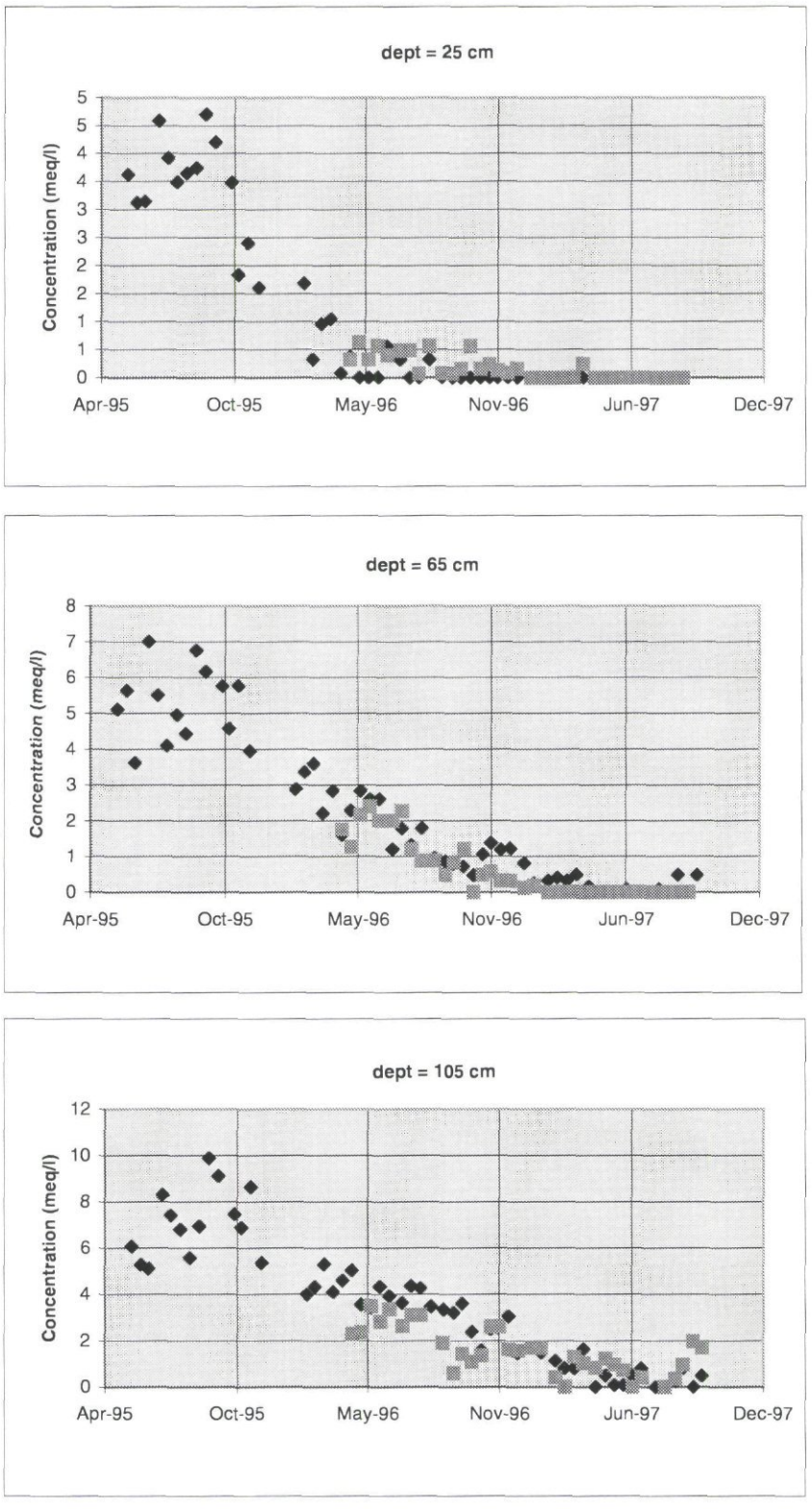

Fig. 3.7 Chloride (Cl^-) concentrations as a function of time on different depths in the Tarantang experimental field

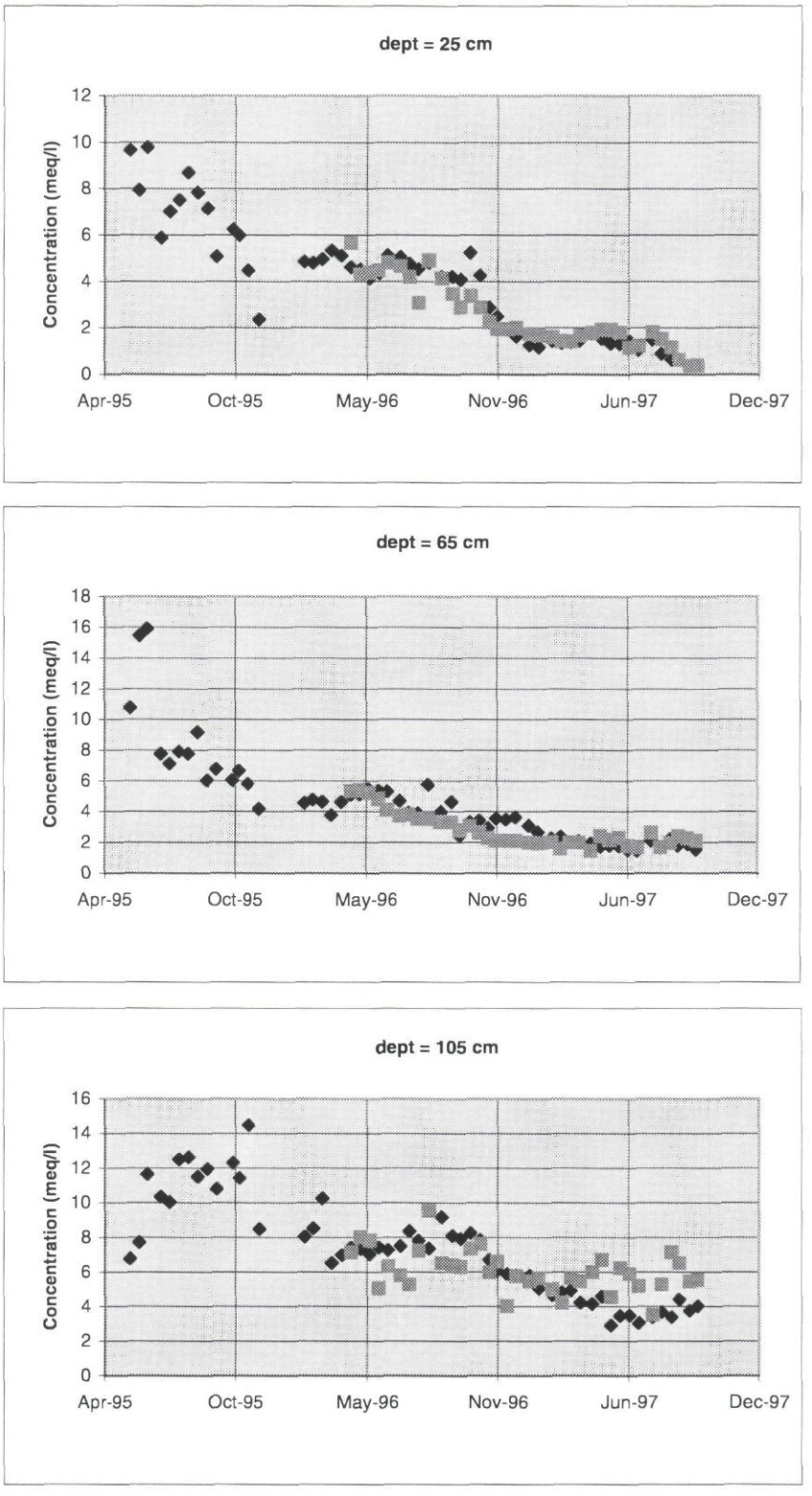

Fig. 3.8 Iron (Fe^{2+}) concentrations as a function of time on different depths in the Tarantang experimental field

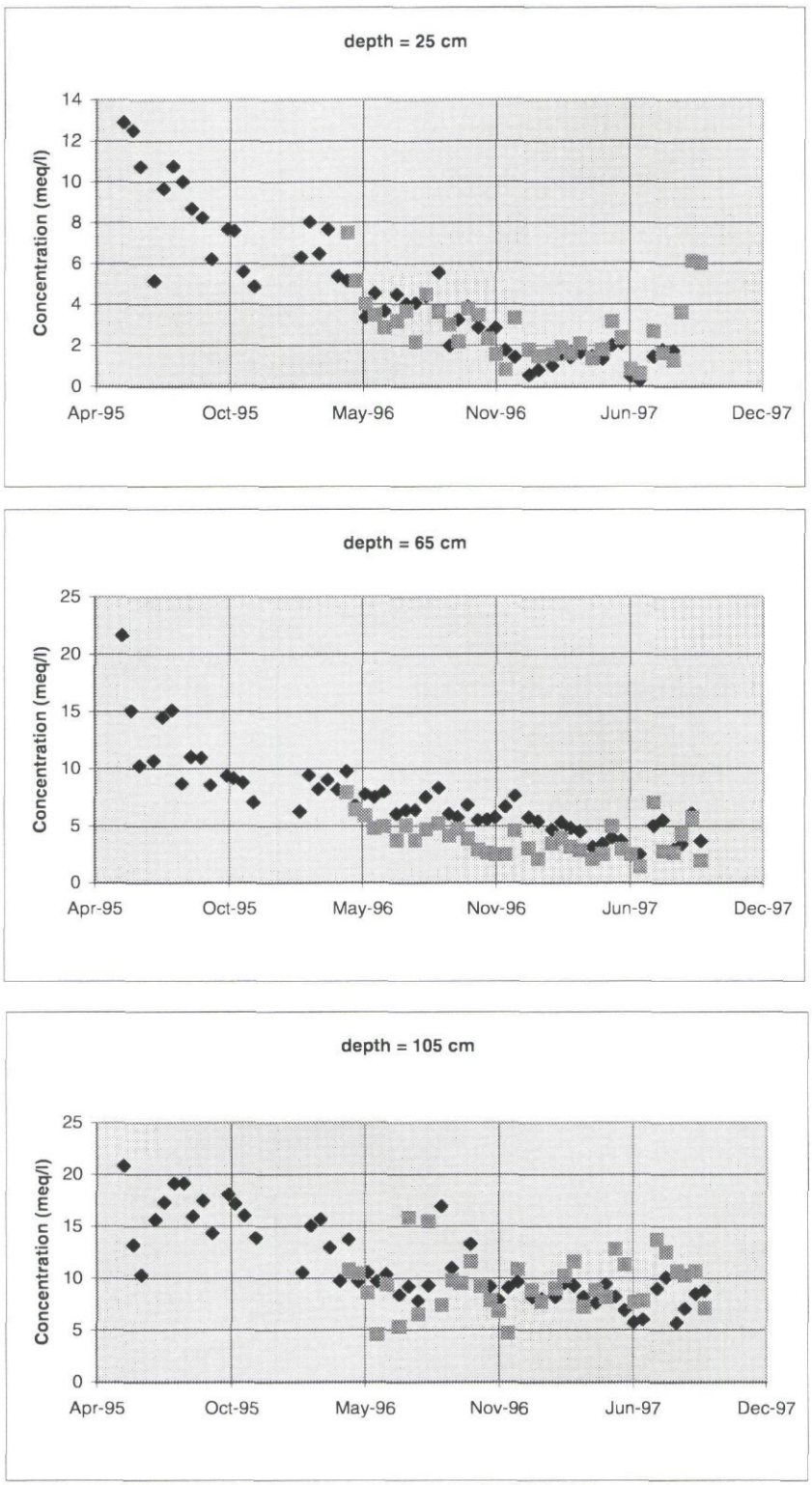

Fig. 3.9 Sulphate (SO_4^{2-}) concentrations as a function of time on different depths in the Tarantang experimental field

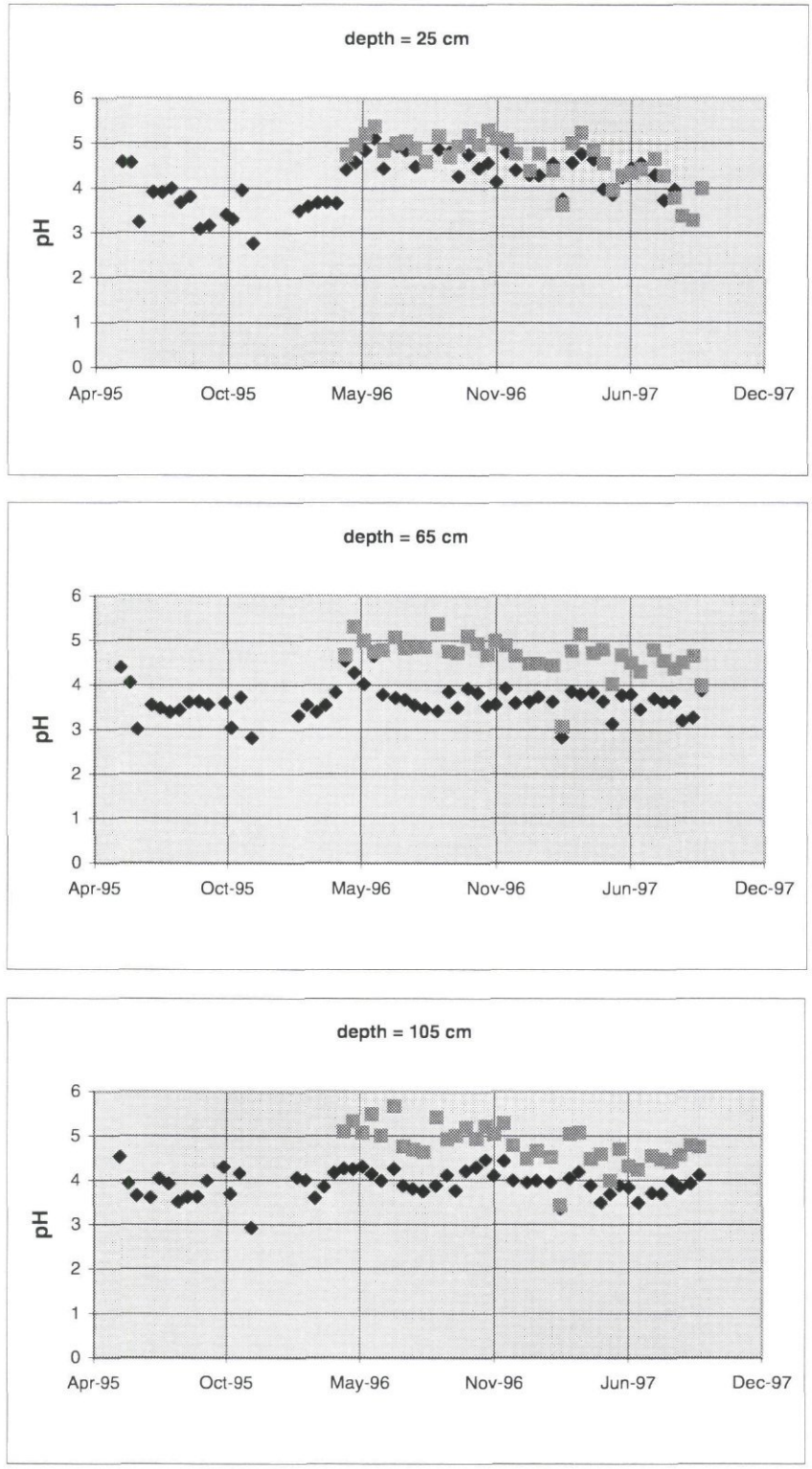

Fig. 3.10 pH values as a function of time on different depths in the Tarantang experimental field

Sulphate (SO_4^{2-}) concentrations range between 1 to 22 meq.l^{-1}. Again, in general the concentrations increase with depth and decrease with time. Decrease of concentrations with time is more pronounced in the top layer than in the lower layers (Fig. 3.10). Values for pH ranged between 3 and 6. In all layers, values increase after one year. The top layer showed slightly lower values than the underlying layers (Fig. 3.11). On basis of the measurements it is concluded that leaching of the top soil was quite efficient.

4 Field experiments in Ly Nhon

4.1 Objectives

In order to supply data for calibration and validation of a two-dimensional model, which simulates chemico-physical processes in acid sulphate soils, a new field experimental site was set up in Vietnam. The investigations were conducted under various land use patterns, including undisturbed acid sulphate soil as well on agricultural- and aquacultural uses (rice and shrimp production).

While for the Indonesian part we concentrate on acid sulphate soil under rice production, in Vietnam the investigations focus on problems related to the construction and operation of a shrimp pond. Therefore, below, emphasis is given on presenting and discussing results obtained from the field research on processes in disturbed acid sulphate soils related to aquacultural activities. Such activities have increased at high intensities and large scale in many regions of the Mekong delta. Those coastal areas in the Mekong delta that are favourable to shrimp production are covered by potential acid sulphate soils. Thousands of shrimp farms have been built since recent years in the coastal part of the delta. Aquacultural activities, that promise attractive income to farmers, have resulted in large, unpredictable and, in some cases, irreversible changes in the ecological system of large areas.

Decreasing productivity and distinct disasters like the shrimp pest 1995/96 are closely related to the degradation of the natural environment. Obviously, the acidification of the disturbed acid sulphate soil play a key role in these processes. There are gaps of knowledge on these processes and its governing parameters. Our works aim to examine these processes and use long term simulation as a tool to develop strategies for sustainable aquaculture. Results may be extrapolated for example to canal construction in areas with acid sulphate soils. The outcome may be helpful in other coastal zones in the tropics, e.g. Indonesia and Malaysia, which face similar problems.

4.2 The experimental field site

In April and May 1995, a team of experts investigated many sites in the coastal zones of South Vietnam. The choice of the experimental field site is based on the following criteria:

— representative soil type,
— representative land use,
— short distance to the laboratory,
— agreement with the local authorities and land owners (farmer).

4.2.1 Location

The experiment farm is located at Ly Nhon, a small village in Can Gio district, about 50 km away from Ho Chi Minh city (Fig. 4.1). Can Gio district represents a coastal flat area, covering about 50,000 ha of acid sulphate soils. Most of them are only used for rainfed cultivation due to lack of fresh water. Soil maps 1/25000 are available, although this scale is not adequate for the research purposes.

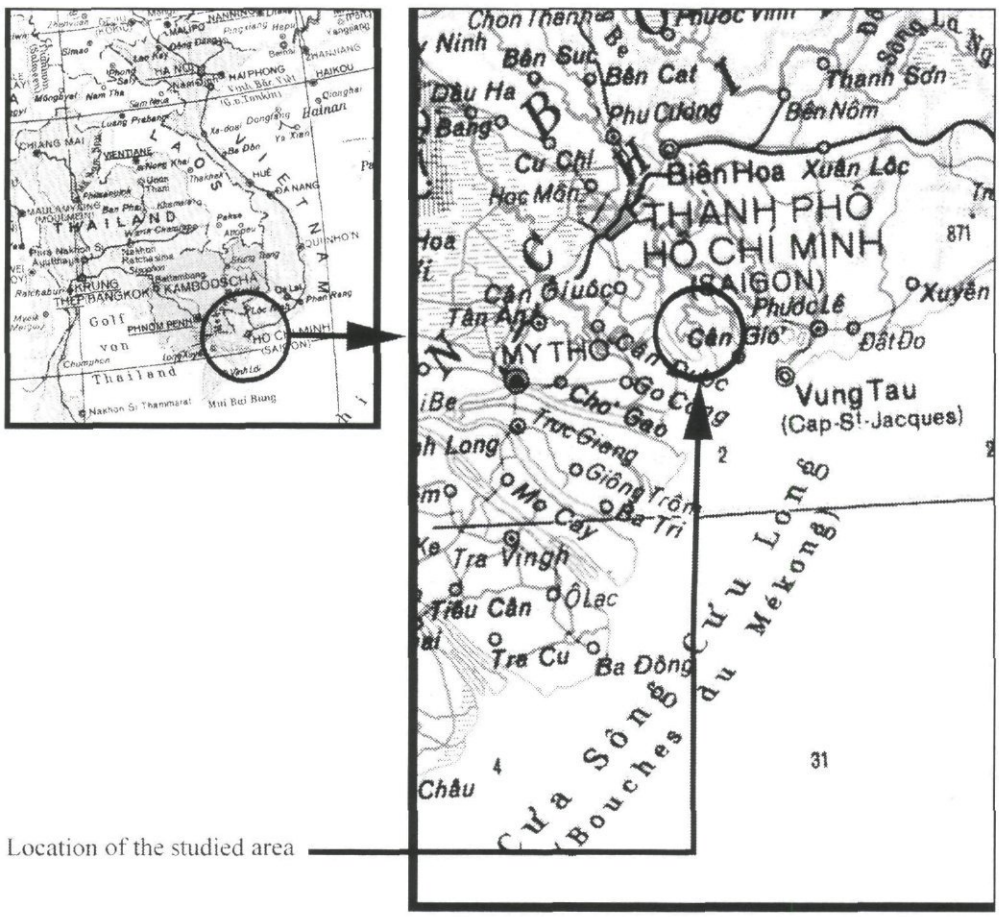

Fig. 4.1: Location of experimental farm at Ly Nhon, Vietnam (RV,1987).

The area that was selected for the field studies is Ly Nhon because of some advantages.

— Soils represent undisturbed potential acid sulphate clay soils with high potential acidity. Other investigated locations were characterised by either more or less disturbance related to agricultural activities.
— The location is representative for coastal areas with strong tidal and saline influences.
— The area is relatively close to the laboratory where the analysis will be conducted. The sample transport from the experiment site to the laboratory may take two

hours. This condition is favourable for the case of soil solution, that may react very sensitively to outside environment and should be analyzed as quick as possible after being collected.
— The experiment site is next to the Vam Sat river. This is suitable for water management and supplies favourable conditions to shrimp farming.
— The transportation and the accessibility are in acceptable condition.
— Local authority gives a good support to the experiment farm.

However, disadvantages can be seen are:
— There is no electricity there, hence the operation of the farm may be difficult in that place. We installed there a small wind energy equipment 1500 VA for charging batteries and for lighting. Besides, a gasoline generator 1400 VA will be used to operate a vacuum pump.
— The logistic and communication conditions are bad. The management and operation activities would face more obstacles.
— Permanent presence of researchers is impossible due to many difficulties. It is required to train and employ local farmers in some activities such as control and watching the site. Besides, security aspects about construction of the field site and installation of field equipment must be taken into account.

4.2.2 Geography

Cangio district that covers an area of 69 061 ha represents the delta of Saigon river and its tribunes. It is located south-eastern of Ho Chi Minh city and stretches from latitude 10°22'14" to 10°40'09" and from longitude 106°46'12" to 107°00'59" (Fig. 4.1).

4.2.3 Climate

With typically tropical monsoon, temperature is constantly high around the year, mean daily temperature: 27 °C, daily variation of temperature: 5-7 °C (Fig. 4.3). Daily sunshine duration reaches highest value in March (9.1 $h.d^{-1}$), monthly amount of sunshine is 240 h/month for dry season and 170 $h.month^{-1}$ for rainy season. Net radiation is rich with a maximum value of 14.2 $Kcal.cm^{-2}$ per day in March and a minimum value of 10.2 $Kcal.cm^{-2}$ per day in June. Relative humidity is always high over the year: 81% in September and 75% in April. More than 90% of the annual rainfall amount (around 1600 mm per year) occurs during the period of June-October. Long-term dry spells occurring annually during early period of monsoon cause severe damage to rainfed rice of the area (Fig. 4.3).

4.2.4 Soil

The two main soil groups can be recognised: alluvial plain with saline and potential acid sulphate soils and mangrove marsh with saline soils and acid sulphate soils. The west-northern part of the region, where the saline intrusion duration is shorter, arable

lands were reclaimed for rice with one cropping per year. Mangrove areas that were destroyed during the last war are now partly rehabilitated. Since recent years, aquatic farming in brackish water have been promoted due to economical reasons. The land reclamation in acid sulphate soil areas for shrimp ponds resulted in environmental impacts.

4.2.4.1 General soil profile description

a/ Profile name: Ly Nhon
b/ Soil name: Potential acid sulphate soil.
c/ Higher category classification:
— FAO: Thionic Fluvisol
— USDA: Sulfidic Tropaquepts
d/ Date of examination: 22 April, 1995
e/ Authors of description: Dang Hong Hai
f/ Location (Fig.4.2): Ly Nhon, Can Gio district, Ho Chi Minh city, Vietnam
g/ Elevation: 2.00
h/ Landform:
— Physiographic position of the site: plain
— Surrounding landform: flat
— Microtopography:
i/ Slope on which profile is sited: class 1 (flat)
j/ Land use or vegetation:
— Uncultivated
— Scirpus glossus, Pluchea indica, Acrostichum aureum
k/ Climate: tropical monsoon
General information the soil
a/ Parent material: Alluvio-marine sediment
b/ Drainage: Class 4 (well drained soil)
c/ Moisture condition in the soil: wet from 1 to 100 cm
d/ Depth of the groundwater table: 50 cm
e/ Presence of surface stones or rock outcrops: none
f/ Evidence of erosion: none
g/ Presence of salt or alkali: class 1
h/ Human influence: none

4.2.4.2 Description individual soil horizons

Ahg: 0-30 cm: Mixed reddish brown (5YR 4/3) and reddish gray (5YR 4/2), many coarse prominent diffuse strong brown (7.5YR 4/6) mottles, clay, weak coarse sub angular blocky, half ripe, slightly sticky, slightly plastic, firm, continuous thick strong brown (7.5YR 5/6) iron cutains on wall of root channels, very frequent very fine and fine roots, many fine pores and interstitial, pH=7.5.

Bg: 30-50 cm: dark gray (2.5YR 4/0), peaty clay, weak coarse sub angular blocky, half ripe, slightly sticky, slightly plastic, friable, abundant organic matter and coarse nympa roots remnant, frequently very fine and fine roots, thick brown cutains in old root channels probably of clay with iron, pH=7.5.

Br1: 50-80 cm: dark grey (2.5YR 4/0) peaty clay, weak, slightly sticky, slightly plastic, friable, abundant organic matter and coarse nympa roots remnant.

Br2: 80-120 cm: Mixed grey (2.5YR 5/0) and light grey (2.5YR 7/0), silty clay, practically unripe, sticky, lightly plastic, frequently fine and very fine roots remnants.

C: > 120 cm: grey (2.5YR 5/0), silty clay, structureless, non sticky, non plastic, few fine and very fine roots remnants, frequently very fine and fine debris of oyster-shell.

4.2.4.3 Characteristics of soil profile

Salinity soil: EC (ratio of soil :water 1:3) > 4 $mS.cm^{-1}$.
Total actual acidity (TAA) is low: 4-13 mol H^+ per 100 g soil
Total sulphidic acidity (TSA): > 100 mol H^+ per 100 g soil. This is a strong potential acid sulphate soil, especially TSA is very high in the layer 30-90 cm.

In exchangeable bases, Ca^{2+} and Mg^{2+} take part a large amount of quantity in each layer, with Ca^{2+} dominance (% total of cation), due to product of disintegration and deposition of mollusk .

Analysis of soil layers in 11 nests of soil solution sampling (R1-R4, S1-S7) (Fig. 4.2):
Layer 0-15 cm: pH decreased strongly from 5.30 down to 3.0, especially at S3, S6, S7. The difference of pH among nests can be explained by the redistribution of excavated soil in building shrimp pond.

At observed time, soil surface was formed by deep excavated soil, hence EC of surface layers were higher than those of subsoil. In layer of 90 cm, results of analysis were the same with those of the surface layer of undisturbed soil (natural soil).

In exchangeable bases, Ca^{2+} and Mg^{2+} dominated in quantity in each layer.

Exchangeable K^+ varied remarkably and could be categorised in two groups:
— R2, R3, R4, S1, S6 and S7 : high amount of K^+.
— S2, S3, S4, S5 : low amount of K^+.
Amount of SO_4^{2-} showed the distinction between excavated soil (S3, S4, S5, S6, S7) and undisturbed soil (R1 to R4). Fe total was usually higher in the top layers (0-15 and 15-30). Al^{3+} varied from depth to depth and nest to nest, and was very difficult to discriminate. Detailed data of initial compositions of horizons (undisturbed soil) are given in tables 4.1 to 4.3.

Table 4.1 Salinity and acidity of soil at selected horizons (undisturbed soil)

Layer (cm)	pH	EC (mS.cm^{-1})	Salinity (ppm CaCO3)	Humidity (%)	TAA (mmol H+ per 100g)	TPA	TSA	SO_4^{2-} (%)	Cl^- (%)
0-30	5.30	11.90	3.60	37.00	4.14	16.20	12.06	0.36	0.75
30-50	5.40	16.01	9.24	41.00	4.06	126.61	22.55	1.09	0.51
50-80	4.75	19.35	8.95	50.00	5.63	121.80	116.17	1.80	0.76
80-120	3.85	18.45	9.02	52.00	13.85	110.78	96.92	1.60	0.53
>120	7.13	12.20	10.52	63.00	80.67	80.67	0.95	0.52	

Table 4.2 Chemical composition of soil at selected horizons (undisturbed soil)

Layer	CEC	Ca^{2+}	Mg^{2+}	K^+	Na^+	Fe^{2+}	Fe^{3+}	Al^{3+}	Fe^{3+}	Al^{3+}
(cm)	(meq per 100g)									
column no.		1	2	3	4	5	6	7	8	9
0-30	25.8	5.9	6.8	3.4	8.7	0.11	0.54	0.15	22.3	2.7
30-50	29.7	7.7	8.3	2.4	10.9	0.11	0.00	0.22	21.3	2.4
50-80	35.5	8.3	11.0	0.3	15.0	0.18	0.00	0.69	13.1	1.2
80-120	37.3	9.1	12.0	0.7	15.1	0.07	0.00	0.20	19.0	5.5

Remarks:
Column 1-7: Percolation with 1 molair CH_3COONH_4, pH=7.
Column 8 and 9: Extraction with 1 molair CH_3COONa, pH=2.8.

Table 4.3 Physical properties of soil at selected horizons (undisturbed soil)

Layer (cm)	Soil particle (%)			Density (g.cm^{-3})	Bulk density (g.cm^{-3})	
	Sand	Silt	Clay		Wet	Dry
0-30	5.6	18.4	75.9	2.60	1.73	1.15
30-50	2.8	18.0	78.2	2.65	1.63	0.96
50-80	2.8	60.4	36.7	2.63	1.51	0.78
80-120	10.7	49.4	39.9	2.63	1.47	0.96

4.2.5 Hydrology

The region is influenced by the semi-diurnal tidal regime of the East Sea (South China Sea). The tidal fluctuation results in daily submergence of maximal 80 cm in the investigated area and, therefore, in serious saline intrusion during 9-10 months per year.

4.3 Methodology

4.3.1 The layout of the experimental site

The farm covers an area of approximately 10 000 m^2, naturally divided by a channel 4 m in width. An E-shape pond of 1400 m^2 water surface was built (Fig. 4.2). The pond is 1 m deep below the soil surface and surrounded by dikes of 10 m width and

1 m height. The dikes were constructed by earth material taken up from pond digging. A water gate of 1 m width, which connects pond and the Vam Sat river, serves for management of pond water and other operations of the pond following technical procedure for shrimp production.

On the opposite of the channel, the rice field of 1000 m^2 was established (Fig. 4.2). It is surrounded by small dikes of 1 m in height in order to prevent daily floods. However, the water management was restricted by biological activities. Macropores up to 20 cm width were observed.

The meteo-station, equipped with instruments for measurements of daily rainfall, potential evapotranspiration (E-pan class A), wind velocity and direction, relative air humidity, air temperature and sunshine duration, was built nearby.

4.3.2 Monitored parameters

The main purpose of the field experiment includes:
— Observation of processes (acidification, salination/desalination, water and solute transport).
— Observation on effects on aqua-environment (biological and physico-chemical parameters).
— Establishment of data sets for input of the models
— Establishment of data sets for calibration and validation of the models
Monitored parameters are given in Table 4.4.

Table 4.4 Monitored parameters at the Ly Nhon experimental farm

Environment	Parameters
Soil :	
Chemical	Fe^{2+}, Fe^{3+}, SO_4^{2-}, Al^{3+}, Cl^-, K^+, Na^+, Ca^{2+}, Mg^{2+}, pH, EC, TAA, TPA, TSA
Physical	Water content, water head, temperature, oxygen content, redox potential, groundwater level
Water:	
Chemical	Fe^{2+} ,Fe^{3+}, SO_4^{2-}, Al^{3+}, Cl^-, K^+, Na^+, Ca^{2+}, Mg^{2+}, pH, EC, COD, BOD, S%, SiO_2, NH_4, NO_3, NO_2, H_3PO_4, H_2S, $CaCO_3$,
Physical	DO, turbidity, surface water level
Biological	Phytoplankton, zooplankton, zoobenthos, shrimp population
Climate:	Rainfall, temperature, wind, air relative humidity, sunshine duration, Epan class A

4.3.3 Parameters determined in laboratory

Basic input parameters were measured in the laboratory. Undisturbed and disturbed soil samples were taken from representative soil profiles, including undisturbed soil as well as from rice field and mound of shrimp pond. The soil physical characteristics (pF-curve and unsaturated hydraulic conductivity curve), bulk density and texture

were determined by standard methods. In situ experiments, using e.g. tension-infiltrometer and tracer techniques, confirmed and completed the data sets. For the single soil horizons CEC was determined once and pyrite content twice.

4.3.4 Chemical analysis methods

SO_4^{2-} was measured by turbidimetric method in spectrophotometer Spectronics 21D. Cl^- was measured by titration method with digital burette. Exchangeable cations (Ca^{2+}, K^+, Mg^{2+}, Na^{2+}, Al^{3+}, Fe^{2+}, Fe^{3+}) were determined by atomic absorbtion spectrophotometer. For this purpose a SPECTRA AA Varian-600 was purchased.

4.3.5 Installation and operation of field instruments

Two transects, one for the rice field with 4 monitoring positions (R1-R4) and one for shrimp pond with 7 monitoring positions (S1-S7) were installed (Fig. 4.2). At each position, instruments were implemented at depths of 15 cm, 30 cm, 50 cm and 90 cm. In some nests measurements were also performed at 120 cm or 150 cm depth. The instruments installed in each nest comprised suction cups, tensiometers, air chambers, redox electrodes, temperature sensors PT-100 and groundwater monitoring tube.

The instruments for the measurement of the above mentioned parameters had to meet the following requirements:
— sufficient accuracy,
— reliability and wear resistance,
— suitable for the South-East Asia climate,
— resistant to aggressive media – salinity and acidity of the soil,
— low maintenance,
— possibility for construction and repair on-site (Vietnam),
— low costs in purchase and maintenance.

Datalogger do not represent adapted technology for the in-situ experiments. Besides high costs and technical requirements, monthly measurements would be an adequate temporal resolution. The regular measurements were conducted monthly, and from hourly up to daily during intensive campaigns.

Below follows a brief description of the instruments used within the monitoring programme as given.

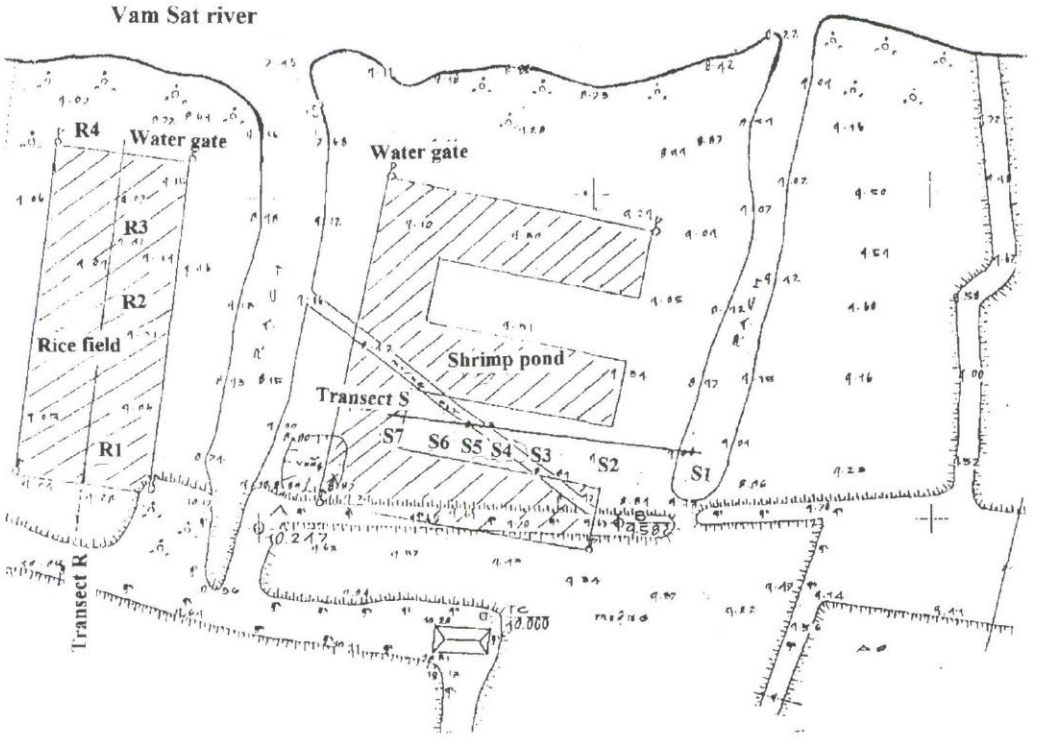

Fig. 4.2 Layout of the experimental site Ly Nhon

4.3.5.1 Suction cups

Suction cups are improved from the prototype suggested by Bronswijk et al. (1988). Moreover, the thickness of wall of cups is optimised and tested carefully so that they can extract sufficient soil solution, and are durable for a long time. This synthetic material (polyester acrylate) is quite neutral against strongly aggressive medium of oxidized acid sulphate soils. Suction cups were operated at an initially vacuum pressure of 0.7 bar. The pressure reduced gradually during extraction period, but not below 0.4 bar at finishing. In order to keep the extracted solution undisturbed, suction period always started at evening of a day and finished at 6 a.m. of the next day. The soil solution bottles were kept together with ice cubes in a box, and transported quickly to the lab, where they were analyzed as soon as possible.

4.3.5.2 Tensiometers

Tensiometer is one of most important device installed in field site. The tensiometer type used at the experimental farm is the same with that applied in Indonesia as described in Bronswijk et al. (1988). In some tensiometers, copper tubes were replaced by PE tube of 2 mm in diameter. This improvement enabled more convenience in construction and installation. After two years of operation, almost no difference between the different tensiometers was recognised. Measurements were conducted by a single handy pressure transducer, characterised by high accuracy and

temperature compensation. Soil water tension was measured manually once every month at various depths (15 cm, 30 cm, 50 cm, 90 cm and 120 cm).

4.3.5.3 Redox potential electrodes

Redox electrodes used are the separated type with one Ag/AgCl electrode as reference and one electrode made of platina. The platina electrode was constructed by soldering a small piece of platina to a copper wire with gold. This connection was embedded in a ceramic or plastic coat and fixed in tube (diameter 5 mm) with special glue. Good contact between the two electrodes was guaranteed by a tube filled with a mixture of KCL (3 M) and agar-agar. The contact-tubes of 2 m length were constructed with PVC tube of 34 mm in diameter with many holes drilled in the tube-walls. The holes were sealed with sticky tape and filled with the boiled liquid mixture of KCl and agar-agar. The liquid mixture became solid during cooling. The sticky tape was removed and the tubes were ready to be installed nearby the position where redox potentials were monitored. During a measurement, reference electrode was inserted in the gelatine of contact tube and connected to COM-port of a multimeter, the other port (mV) was connected to the platina electrode.

Redox potential was measured at depths of 15, 30, 50 and 90 cm in mounded dike of the pond, and at depths 5, 10, 15 and 20 cm in the case of the field.

4.3.5.4 Air chamber

Air chambers were made by using PVC tube of 21 mm in diameter. They were closed inside 4 cm up from the lower end by a rubber stopcock. A copper tube (diameter 2 mm) connects air chamber with measurement device above soil surface. Air chambers were installed only in dike at various depths: 15, 30, 50 and 90 cm. Oxygen content of soil air was measured by an oxygen indicator (Eijkelkamp).

4.3.5.5 Temperature sensor PT-100

Temperature sensors were installed at desired depths by using PVC tubes for extension. The combination of sensor and the tube was enabled by PVC adapter, mounted with epoxy glue. Temperatures were measured manually by a digital thermometer model GTH 601 (Greisinger Electronic). The low cost device was reliable and includes constant current supply, Voltmeter and converting unit.

4.3.5.6 Meteorological instrumentation

Standard devices were used to measure meteorological parameters. Readings were performed by a local farmer twice a day.

4.4 Chemico-physical processes in transects

The mounds of the shrimp pond were built as the custom way of farmers. Earth material was dug from soil horizons including pyritic soils and mounded around the pond in order to prevent flooding and to minimize area needed for deposition of excavated soil. The shrimp pond was constructed from May to August 1995. Monitoring started in August. Data presented below start from October 1995.

Below, soil quality of the mounds and soil under agriculture use are characterised by pH, sulphate, aluminium and iron concentration of soil solution and redox potential with respect to acidity as well as pH and concentrations of sodium with respect to salinity. These exemplary measurements over time and depth should display the ongoing processes (Fig. 4.3-4.13).

4.4.1 Meteorological measurements

The local weather conditions have crucial impacts on the processes in the soil. It determines periods of leaching and high water content (low oxygen content) as well as periods dominated by upward flux of water and solute in the unsaturated soil. At Ly Nhon rainfall data show distinct phases of monsoon interrupted by dry spells of 5 months (Fig. 4.3). Rainy season begins in May 1995, 1996 and 1997 and lasts up to November. Reference evapotranspiration, ET_0, was calculated by the Penman equation. Mean daily temperature ranges from 27 °C to 35 °C (Fig. 4.3).

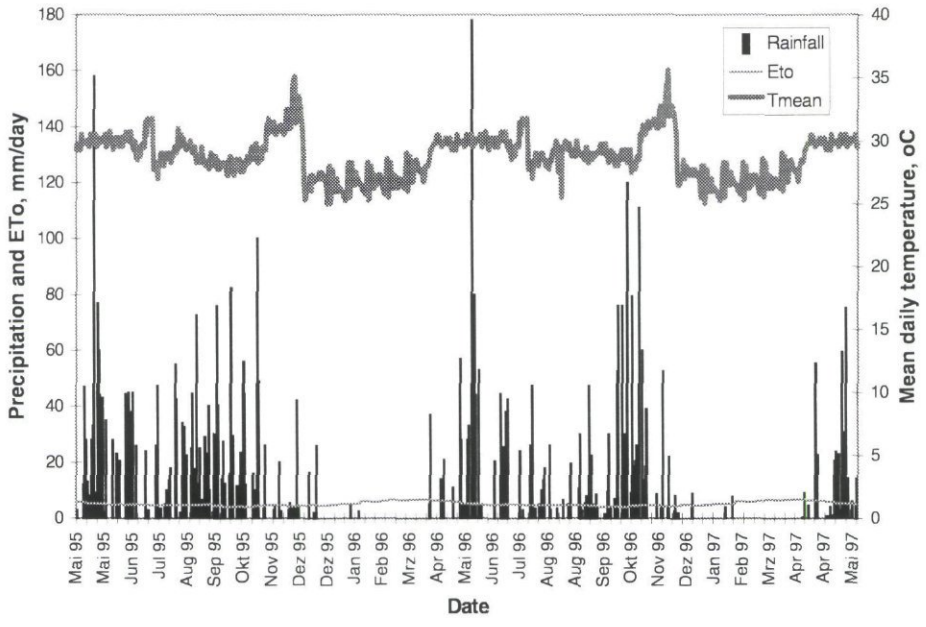

Fig. 4.3 Daily meteorological data at Ly Nhon experimental farm, Vietnam

4.4.2 Temporal and spatial variation of soil quality

4.4.2.1 Temporal variation

In disturbed soil of the dikes

Since groundwater level (GWL), effected strongly by tide, was always at -1.0 m or lower, the soils in the dikes of shrimp pond were permanently aerated and unsaturated. Otherwise the soils under GWL were submerged and saturated. The following results were observed at nests S1-S6 (Fig. 4.2, Fig. 4.4 to 4.8).

pH reduced rapidly at upper horizons at beginning of dry season, December 1995, and reached lowest value at the end of dry season in May 1996 (Fig. 4.4). pH values of 2.5 to 3 were observed in horizons above GWL. At the horizon -90 cm (S90), acidification was not observed. In general the pH-value of soil solution (groundwater) was controlled by surface water quality (Fig. 4.4).

Sulphate concentration was high in dry season (up to 200 meq.l^{-1}) in the unsaturated horizons, down to 50 cm (Fig. 4.5). It showed a close relation to the water balance (negative correlation). In the rainy season SO_4^{2-} decreased strongly due to leaching. Concentration peaks were observed at the ends of dry spells (April and August-September). In the depths below 50 cm, sulphate concentrations were lower in both seasons (rainy and dry season) and characterised effect of surface water quality (Fig. 4.5).

Even the water level in the pond changed twice per day due to the tidal effect. GWL fluctuated slightly; it alternated between depth of 70 cm and 100 cm below soil surface, keeping the lower horizons saturated permanently. Fe^{2+} concentrations increased downwards during dry season. However, in the unsaturated zone concentration peaks were observed during the beginning and the end of rainy season 1996 (Fig. 4.6). In upper horizons, 15, 30 and 50 cm, aluminium concentration in soil solution was high (mean value of 150 meq.l^{-1}). Two peaks were observed during rainy season. While in saturated layer, 90 cm, it was low (mean value of 1 meq.l^{-1}, Fig. 4.7).

Over the whole profiles Na^+ concentrations show the same behaviour at the same concentration levels (Fig. 4.8). In dry season Na^+ content in soil solution increases. In August-October 1996, four months after beginning of monsoon, salt concentration decreased significantly. It rises again with beginning of the following dry period. The same tendency was observed for other exchangeable cations such as Ca^{2+}, Mg^{2+} and Cl^-. The described patterns are similar to that of surface water quality (in shrimp pond). This showed that leaching was not effective enough to remove dissolved substances. The processes were determined by the driving forces: leaching and capillary rise (Fig. 4.8).

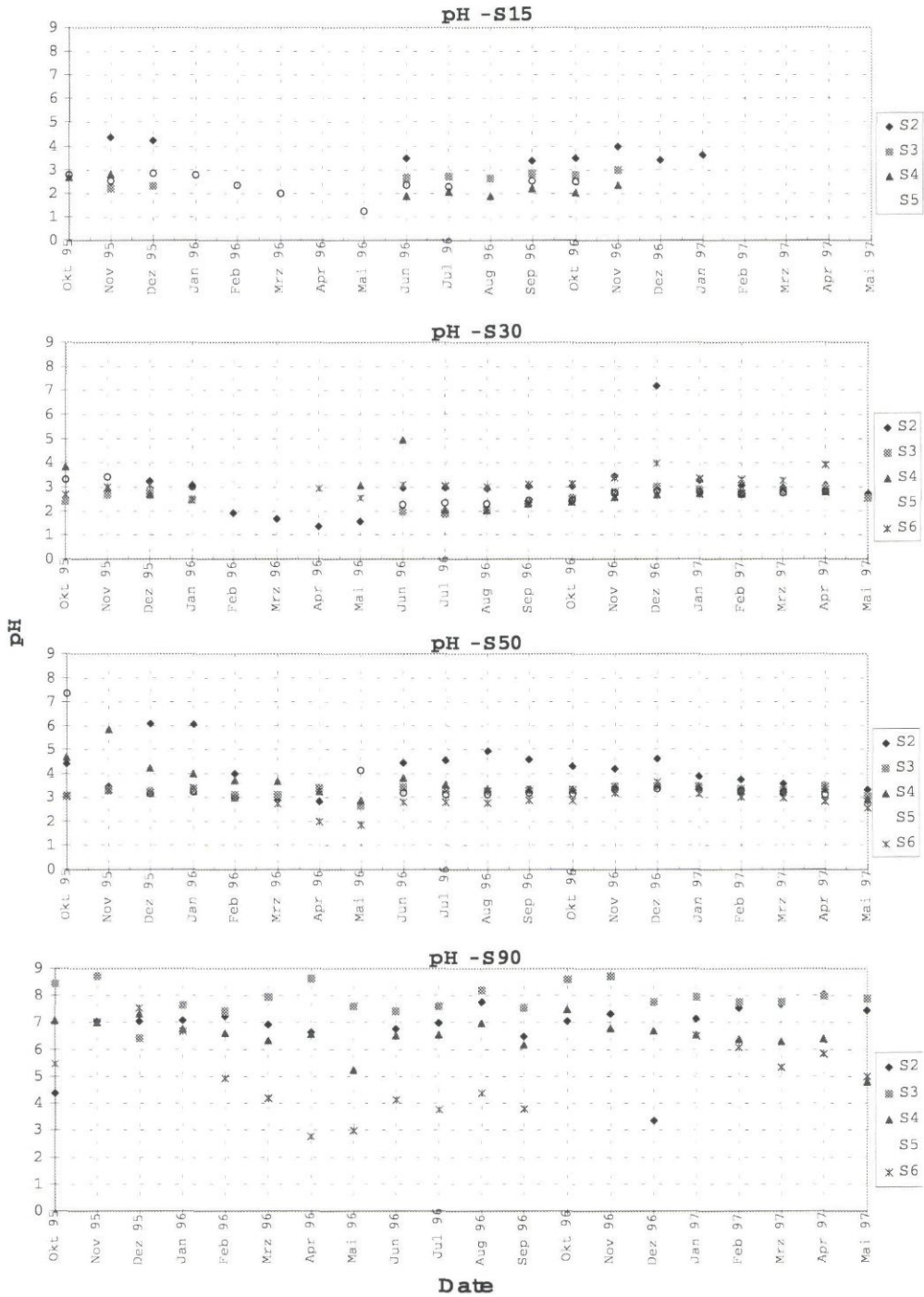

Fig. 4.4 Measured pH of soil solution over time and depth (15, 30, 50 and 90 cm) in mound at nest S2-S6

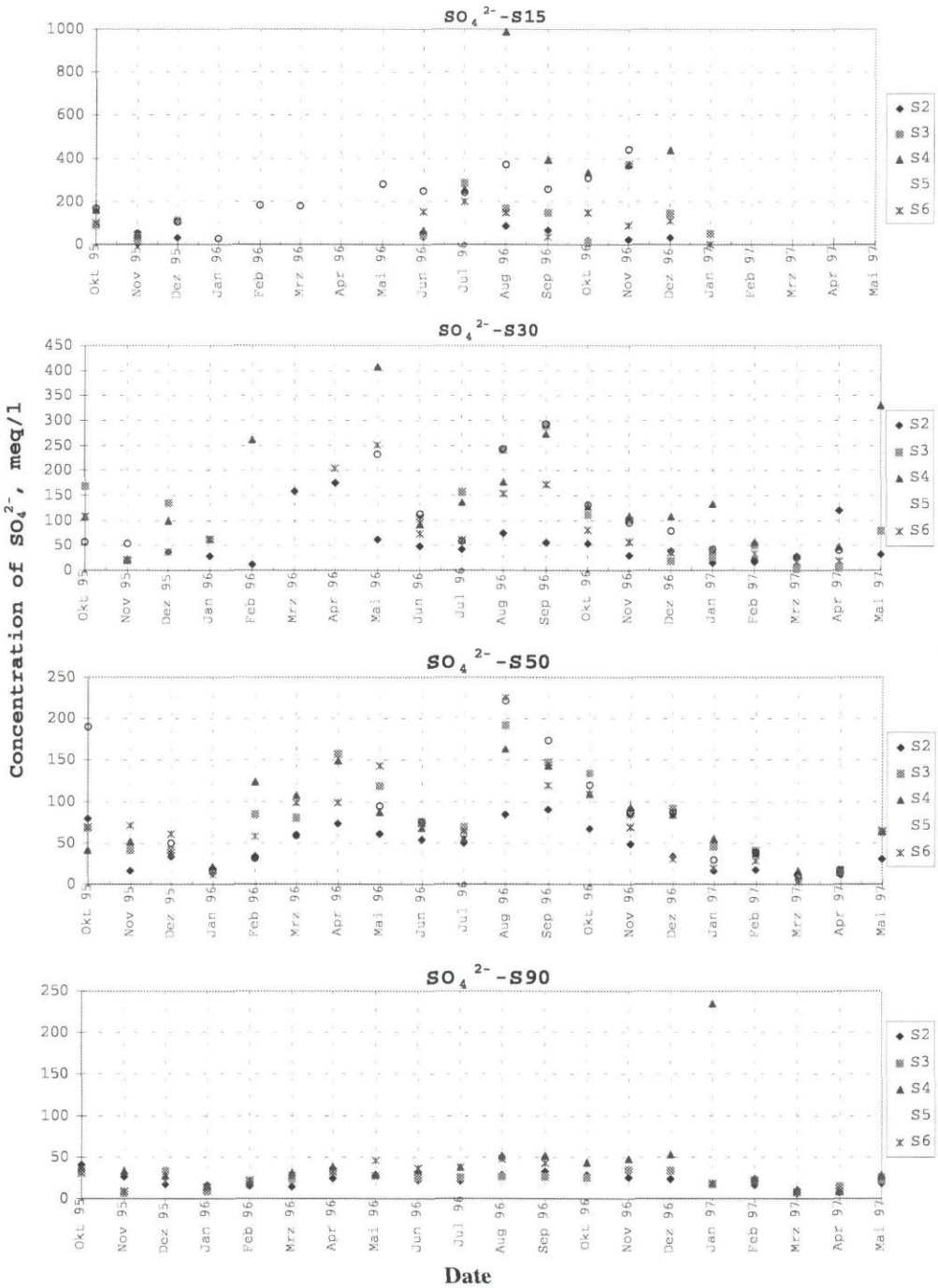

Fig. 4.5 Measured SO_4^{2-} concentration in soil solution over time and depth (15, 30, 50 and 90 cm) in mound at nests S2-S6

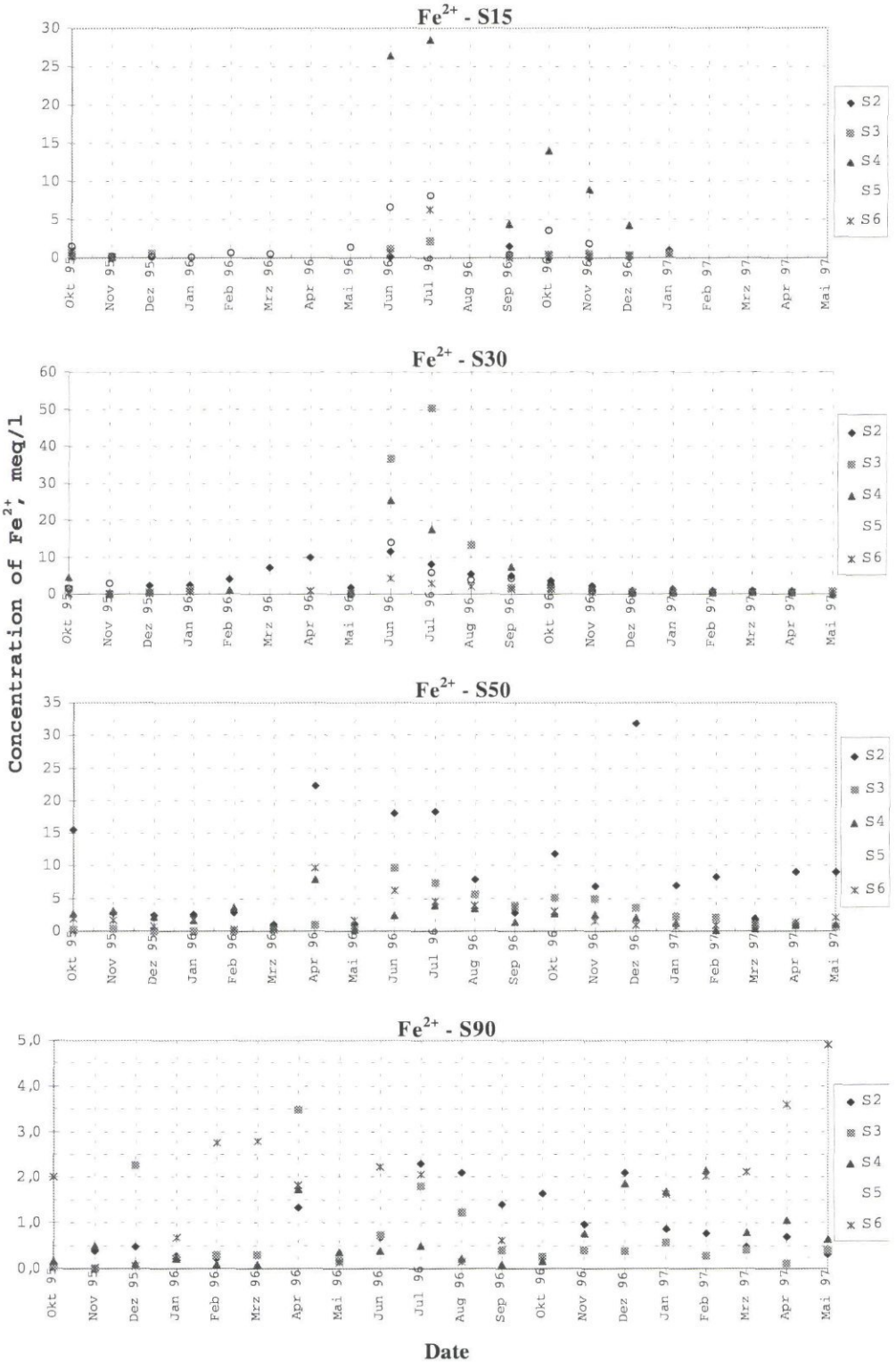

Fig. 4.6 Measured Fe^{2+} concentration in soil solution over time and depth (15, 30, 50 and 90 cm) in mound at nest S2-S6

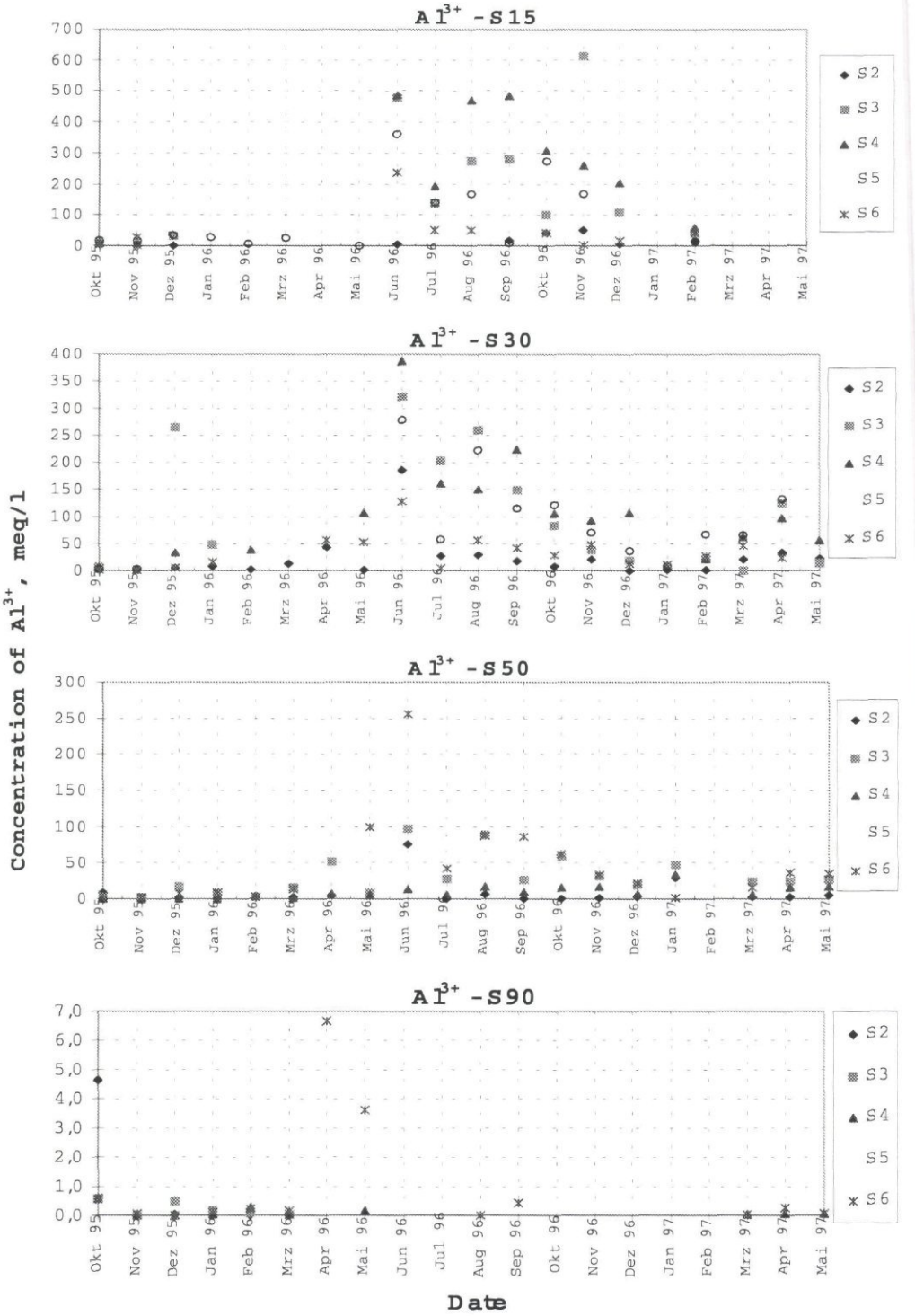

Fig. 4.7 Measured Al^{3+} concentration in soil solution over time and depth (15, 30,50 and 90 cm) in mound at nest S2-S6

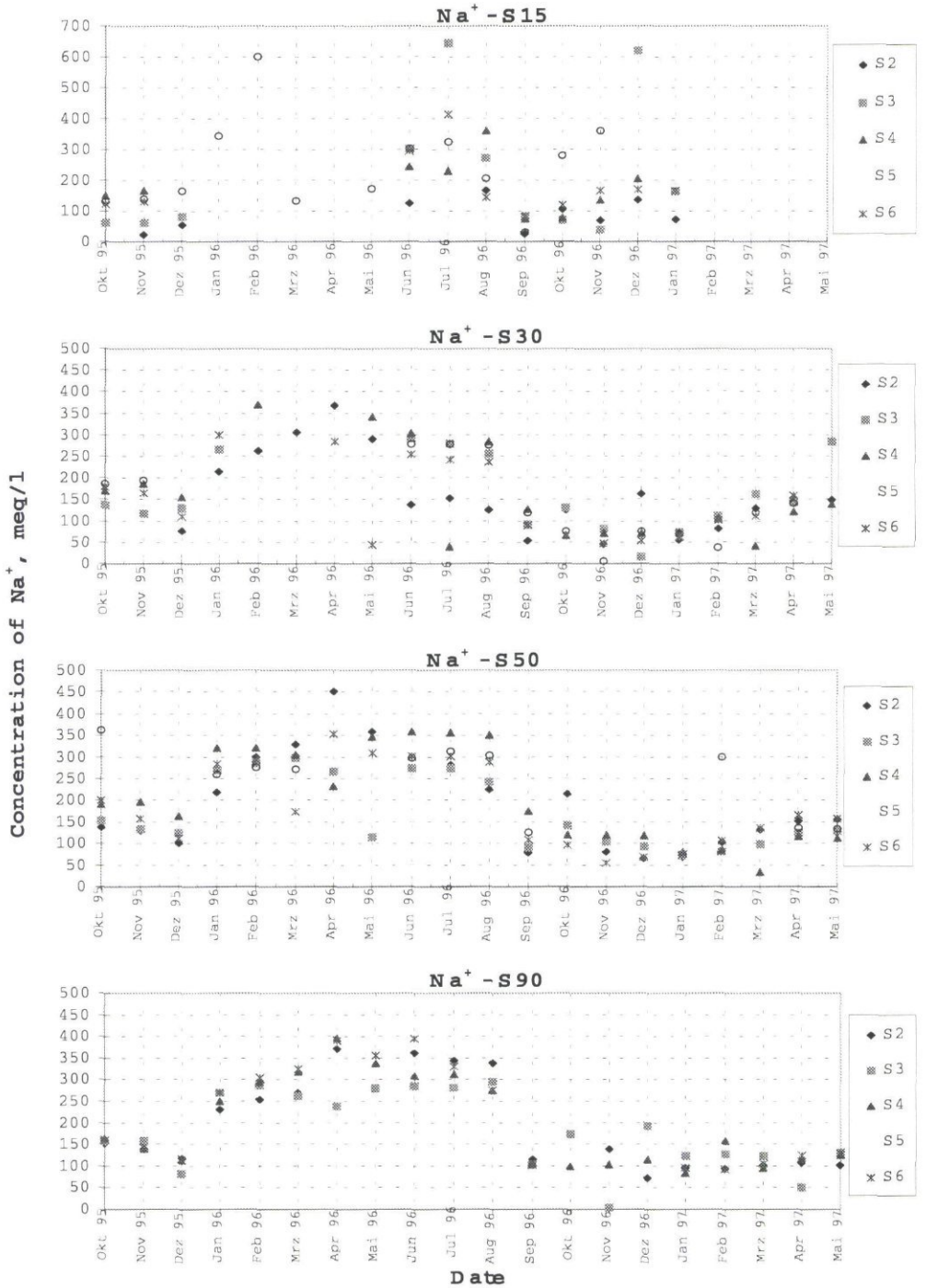

Fig. 4.8 Measured Na^+ concentration in soil solution over time and depth (15, 30, 50 and 90 cm) in mound at nests S2-S6

Chemical processes in unsaturated horizons were determined by oxidation, which was governed by rainfall distribution. In the saturated zone, where reduced condition controlled the chemical processes, concentrations were determined by surface water quality.

Undisturbed soil (frequently flooded)

The experimental site locates in a low land coastal area, effected directly by semi-diurnal tide. It was very difficult to control water management in the new reclaimed field, due to horizontal seepage. Fresh water is available only during 4 months of the rainy seasons (September to December). During the rest of the year salinity dominates whole area. Rice was hardly cultivated under such conditions. Some of these features are discussed below (Fig. 4.3, 4.9-4.13).

pH values of all horizons were controlled by surface water quality (river) and reflect saline dominance (pH=7 to 8, Fig. 4.9).

Sulphate concentration in soil solution increased during the dry period and decreased during the monsoon within the overall range from 5 to 35 meq.l^{-1}. The concentration as well as their changes during the seasons coincided with that of river water quality (Fig. 4.10).

In the upper horizon Fe^{2+} concentration is low from August 1995 up to November 1995. In the beginning of dry season a peak of concentration was observed. With increasing depth Fe^{2+} content in soil solution approaches that of surface water. Concentrations did not exceed 1 meq.l^{-1}. Both concentrations of Fe^{2+} and Al^{3+} stay below level of toxicity for rice plants (Fig. 4.11, 4.12).

Na^{+} concentration in soil solution as well as in river water increased during the dry season and decreased during monsoon. In the soil concentrations are higher during dry period and lower in rainy season. In general Na^{+} content alternated from 50 to 500 meq.l^{-1} (Fig. 4.13).

In undisturbed soil the observations show negligible effects of oxidation; chemical characteristics were controlled by surface water quality.

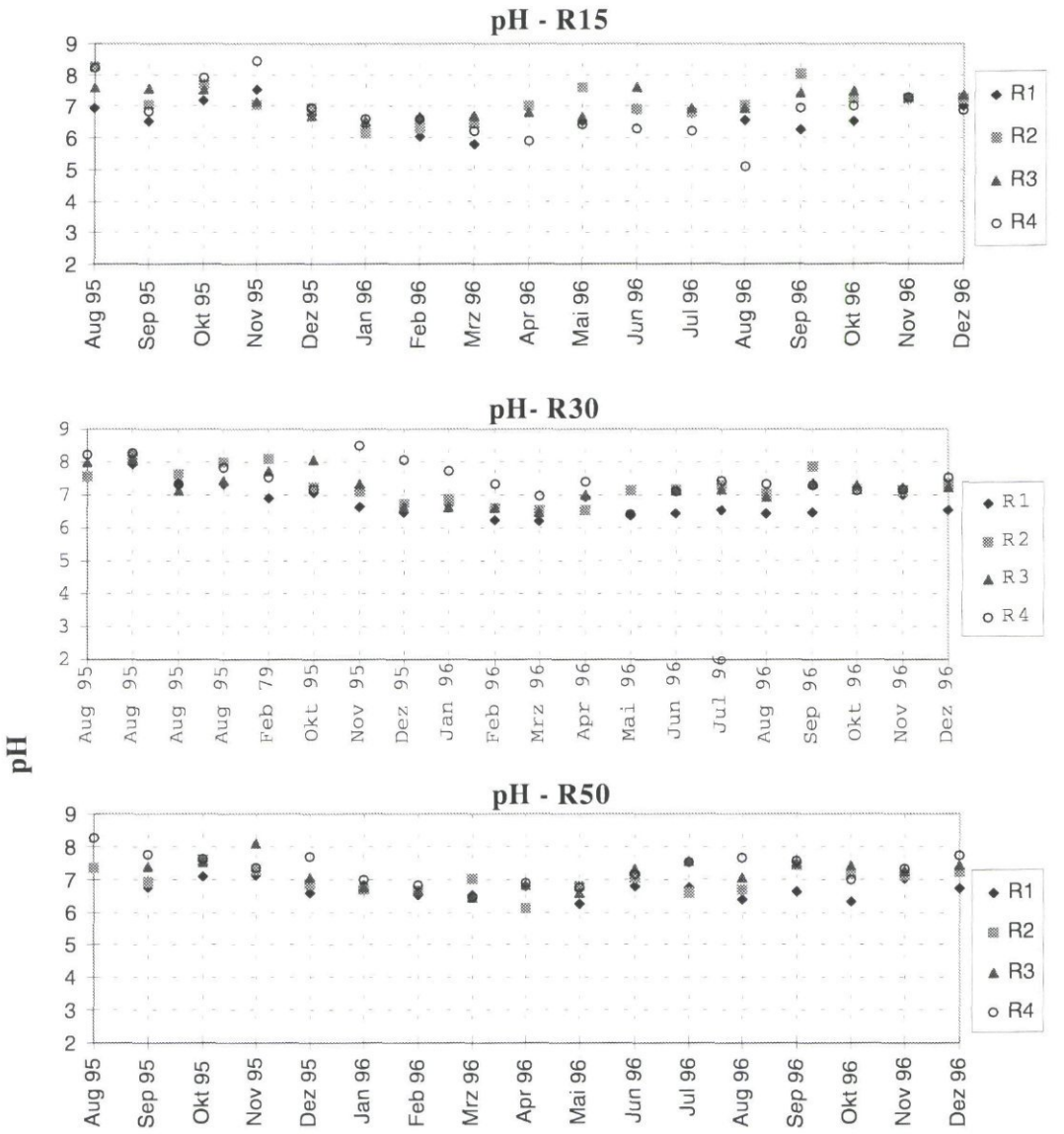

Fig. 4.9: Measured pH of soil solution over time and depth (15, 30, 50 and 90 cm) in rice field at nests R1-R4

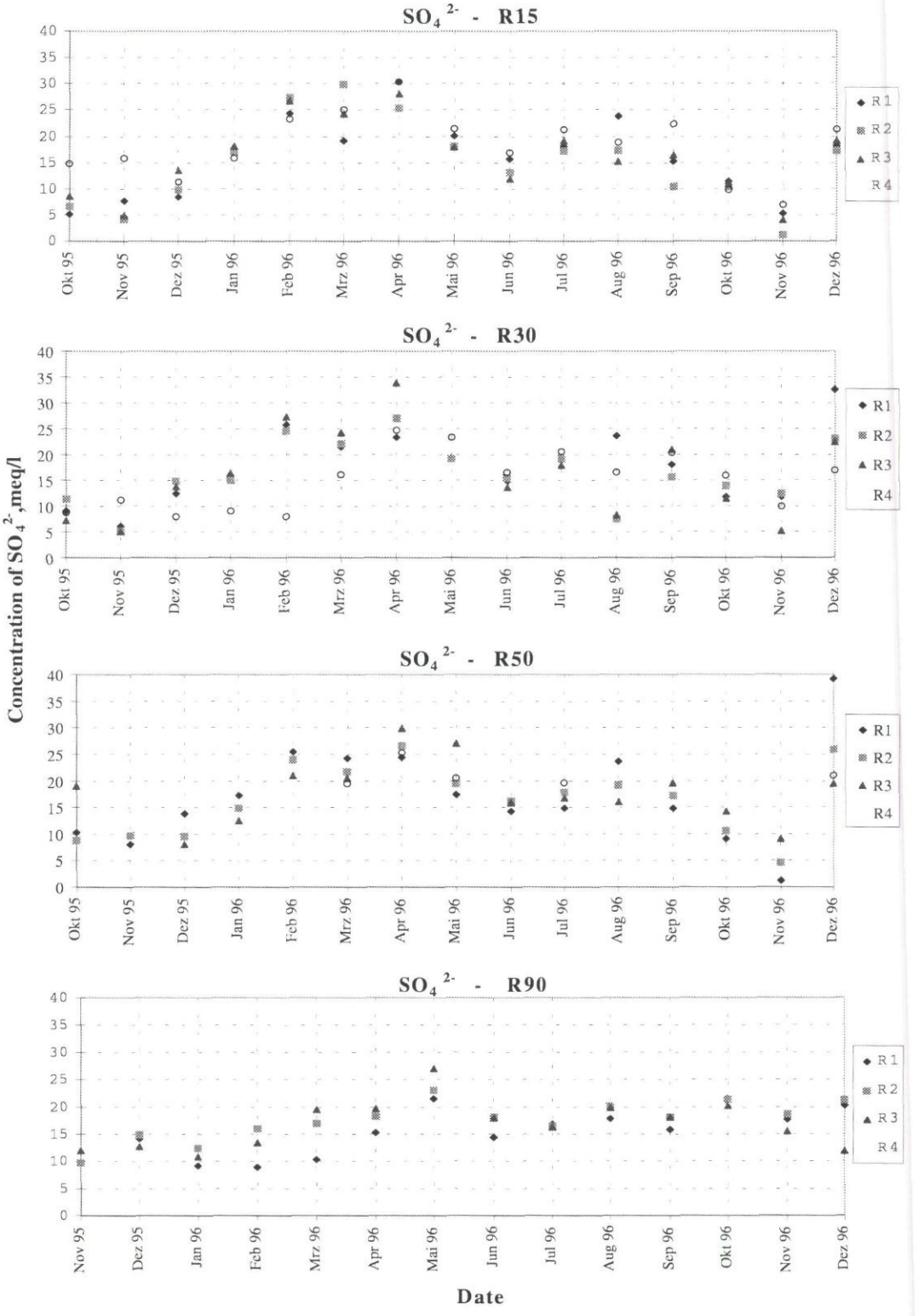

Fig. 4.10: Measured SO_4^{2-} concentration of soil solution over time and depth (15, 30, 50 and 90 cm) in rice field at nests R1-R2

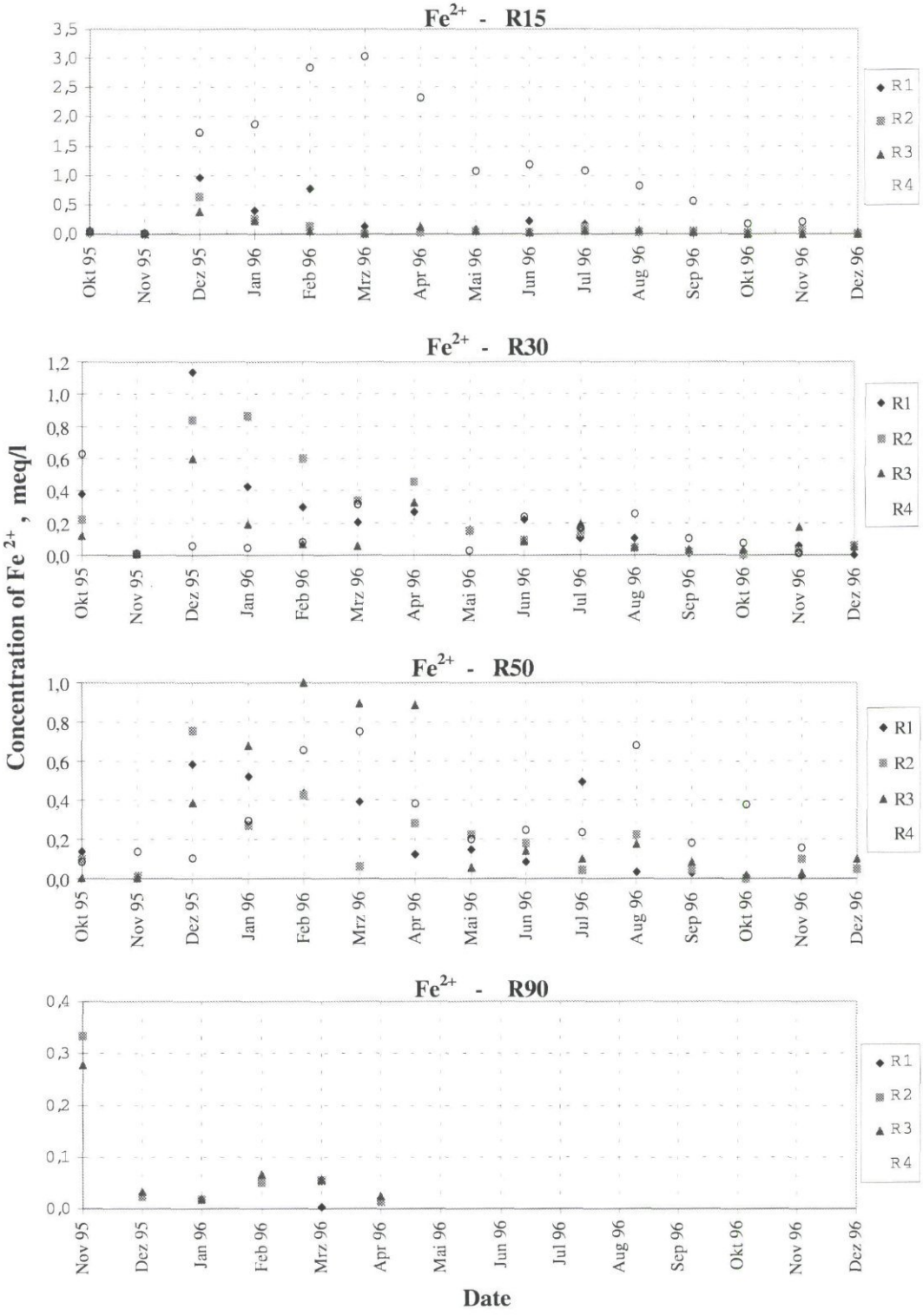

Fig. 4.11: Measured Fe^{2+} concentration of soil solution over time and depth (15, 30, 50 and 90 cm) in rice field at nests R1-R4

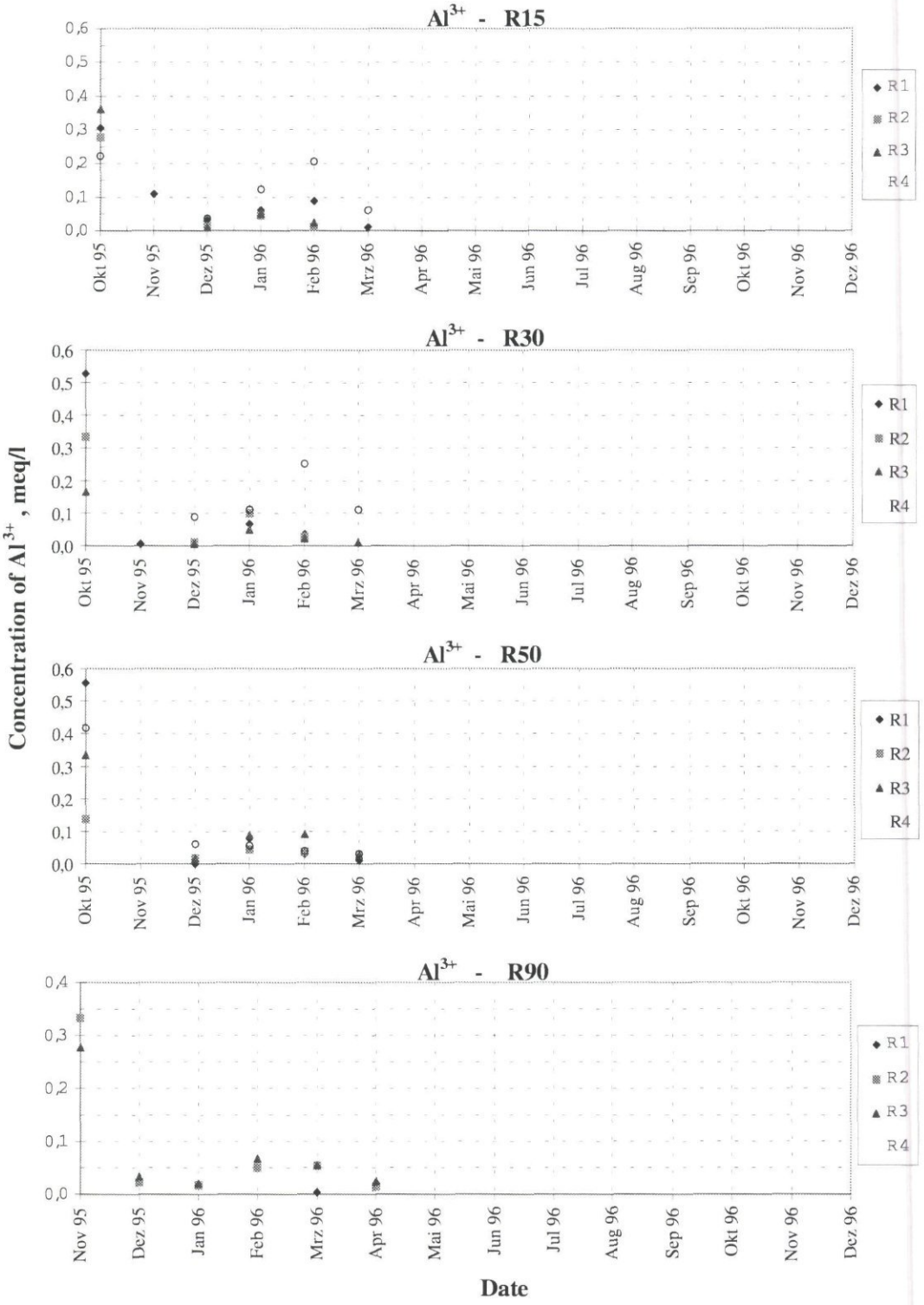

Fig. 4.12: Measured Al^{3+} concentration of soil solution over time and depth (15, 30, 50 and 90 cm) in rice field at nests R1-R4

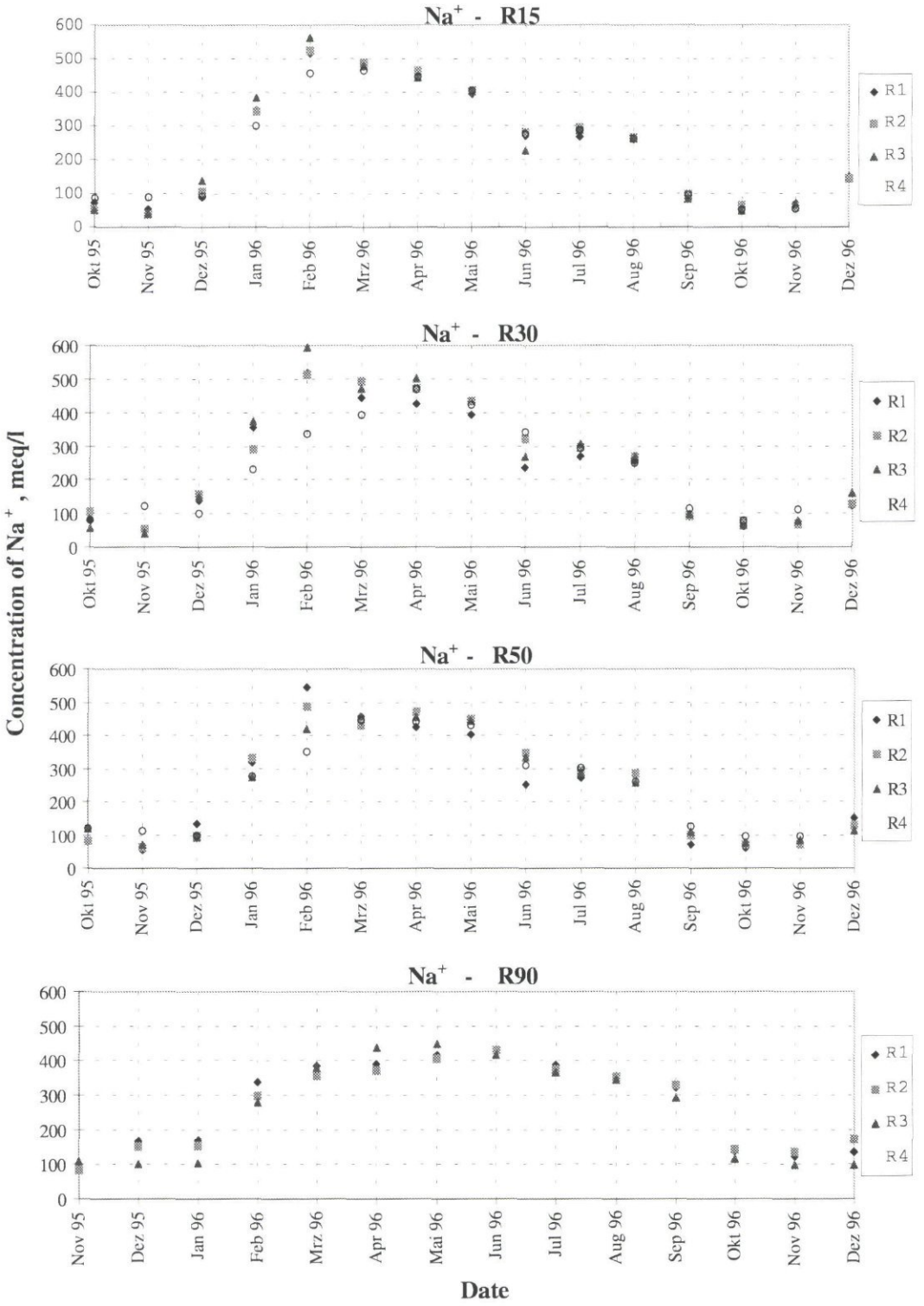

Fig. 4.13: Measured Na^+ concentration of soil solution over time and depth (15, 30, 50 and 90 cm) in rice field at nests R1-R4

4.4.2.2 Spatial variation

Disturbed soil of the dikes

Measurements at nests S2-S6 might be considered as repetition. The spatial variations among nests was high (Fig. 4.4-4.8). Within the 5 nests of the transect, variation of chemical parameters showed the same pattern. However their value scattered widely. Lowest and highest values differed up to factor 10. At a distinct depth Na^+ concentration varied less than those concentrations of ions related to oxidation process. Difference of pH-value was up to 1-2 units in the upper layers and 2-3 units in 90 cm depth. These observations may be related to network of macropores in the mound (section 4.4.4). The macropores divided the soil into regions with high oxygen content and regions characterised by low oxygen content. In addition the macropores lead to a pronounced preferential flow during rainfall events of high intensities.

Distinct differences within the single profiles were recognised as comparing between unsaturated and saturated zone. In upper zones where oxidation process was dominant, pyrite oxidation consequent substances such as Fe^{2+}, SO_4^{2-}, H^+ and Al^{3+} showed remarkable concentrations. In lower horizon, always low redox potential, soil concentrations were controlled by water qualities of shrimp pond. (Fig. 4.4-4.8).

Undisturbed soil

The processes in undisturbed soil showed dominant control of surface water quality over all soil horizons. However, leaching by horizontal seepage to the river contributed in variation of some chemical concentrations in locations towards riverside. In the rainy season, as effect of leaching of top horizons, Fe^{2+} concentration decreased gradually towards the riverside. In contrary SO_4^{2-} and Cl^- concentration increased. Changes of pH are not considerable in distance (Fig. 4.9-4.13).

4.4.2.3 Comparison of the concentrations in disturbed and undisturbed soil

- pH of soil solution in undisturbed soil was always higher than that in disturbed soil (Fig. 4.4, 4.9).
- In both soils sulphate concentrations followed the same pattern (Fig. 4.5, 4.10). However in unsaturated layers of disturbed soil the level of concentration and its variability was higher than that in undisturbed soil (about 10 times).
- Especially during rainy season Fe^{2+} concentrations in the disturbed soil were significantly higher than those in the undisturbed soil (Fig. 4.6, 4.11). In contrast to disturbed soil no peak of Fe^{2+} concentration in soil solution was observed at any nest of rice field.
- During the rainy season in the horizons above the groundwater level Na^+ concentrations decreased below the level of concentration in the saturated horizon. This may be caused by leaching. In general Na^+ concentrations decreased below those of the saturated zone during dry season (Fig. 4.8, 4.13).

4.4.3 Pyrite in soil profiles

4.4.3.1 General

Pyrite content and the size of pyrite crystals represent important input parameters of the simulation model SMASS. Within the model the rate of oxidation is governed by number and surface area of pyrite crystals per unit weight of soil.

The model assumes pyrite crystals as spheres. By given (input) amount and diameter of pyrite firstly number of crystals and secondly surface area is calculated. Then the oxidation process by itself is governed by the concentration of oxygen and expressed by a time dependent equation. During the oxidation spheres decrease in size. No distinct biological activity is implemented.

Therefore these soil characteristics (amount pyrite and size of crystals) should be determined independently. Soil samples were taken from different profiles at the experimental field site Ly Nhon. Chemical analysis and ray diffraction (XRD) were chosen for determination of total pyrite content. The mean size of pyrite crystals should be measured by Scanning Electron Microscopy (SEM). Especially XRD and SEM offer the possibility for further information on mineralogical and morphological aspects.

4.4.3.2 Formation and oxidation of pyrite

Iron sulphides play an important role in the sulphur and iron cycle of the earth (Berner and Raiswell, 1983). In Table 4.5 examples are given for different minerals involved in the formation and oxidation process of pyrite (Schwertmann and Fitzpatrick, 1992).

Pyrite contains 46,55% by weight Fe and 53,45% S. It appears as striated, cubic, octahedral and pyritohedral crystals (isometric system). Single crystals, loose aggregates as well as densely packed elliptical and spherical aggregates (framboids) are common. While pyrite is characterised by paramagnetism, greigite shows a ferromagnetic behaviour.

Pyrite form in modern anoxic environments, like in argillous marine, lacustrine and salt marsh sediments. Its often preserved in ancient sedimentary rocks e.g. in shales, carbonate and coal since Proterozoic (Love and Amstutz, 1965). Pyrite is abundant also in hydrothermal veins and other ore deposits and types. So pyrite can be formed in many different geological processes. Its type of origin includes hydratogenesis, sedimentary metamorphism and contact metasomation.

Different theories for the formation of pyrite in anoxic sedimentary environments have been proposed. They range from biogenic to inorganic processes. Based on laboratory experiments it is evident that pyrite formation does not depend directly on biological activity (Wilkin, 1996). Due to the biological production of HS, it has at least to be described as biological induced.

Table 4.5 Examples of iron minerals involved in the formation and oxidation process and their chemical formula

Mineral	Chemical formula
Amorphous iron Sulphide	FeS
Mackinawite	FeS_{x-1}
Pyrrhotite	Fe_4S_5
Greigite	Fe_3S_4
Pyrite	FeS_2
Marcasite	FeS_2
Jarosite	Na (K) $Fe_3(OH)_6$ $(SO_4)_2$
Goethite	α-FeOOH
Lepidocrocite	γ-FeOOH
Ferrihydrite	$Fe_5HO_8*4H_2O$ (and others)
Siderite	$FeCO_3$

The following factors govern the formation of pyrite:
— sulphate reducing bacteria;
— organic matter;
— low redox potential;
— sulphate;
— reactive iron.
Each of the above mentioned factors may limit the degree or rate of pyrite formation (Berner, 1984).

Within the formation process of pyrite the precursors amorphous iron sulphide, mackinawite and greigite are often observed. Framboidal habit of pyrite is proposed to be formed in the stage of ferromagnetic greigite (Wilkin, 1996). The small magnets attract each other and create the densely packed spherical. A more rapid chemical reaction of Fe^{2+} with polysulphide ion immediately lead to pyrite. Small single crystals will be formed (Raiswell, 1982; Fig. 4.14).

In recent years the bio-mineralisation of greigite and pyrite, within magnetotactic bacteria has been proven (Heywood et al., 1990; Farina et al., 1990; Bazylinski et al., 1993; Mann et al., 1990). Mann et al. (1990) observed a mean size of individual crystals of about 75 μm. Magnetotactic bacteria are common in sulphide rich water, sediment and soil (Fassbinder et al., 1990).

Pyrite might be oxidized by oxygen, Fe^{3+} and by bacteria. Different bacteria are capable to oxidize pyrite. For example, the chemolitotrophic, acidophile gram-negative bacterium thiobacillus ferrooxidans oxidizes ferrous iron, elemental sulphur and sulphide containing minerals. The bacterium, as observed by Bennett and Tributsch (1976), is about 1-1,5 μm long and 0,5 μm in diameter. Wakao et al. (1984) observed enhanced dissolution of pyrite after release of bacteria from mineral surface. However there is evidence that Thiobacillus f. dissolves a sulphide surface by means of contact with its cell surface (Rodriguez-Leiva and Tributsch, 1988). Crystalline imperfections

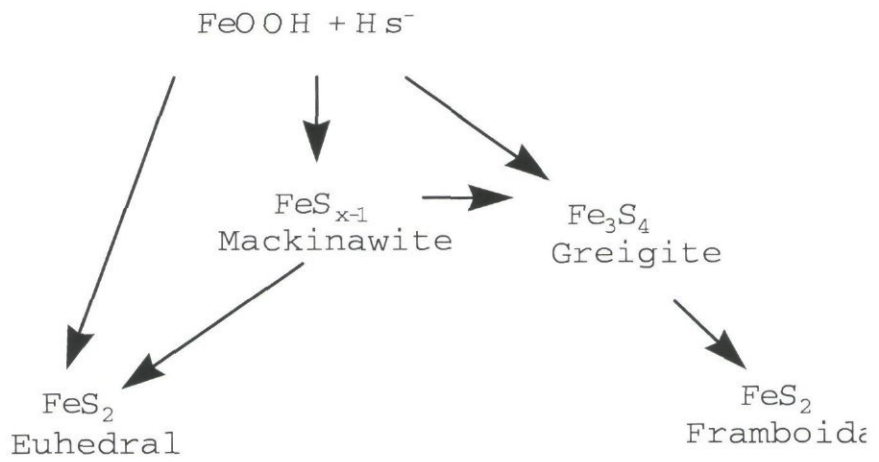

Fig. 4.14: Possible reaction pathways to framboidal and euhedral pyrite

(e.g. fracture lines) influence the distribution of Thiobacillus f. on the crystal surface and consequently their corrosion pits (Tributsch, 1976). After transformation of ferrous iron to ferric iron Fe^{3+} might again oxidize pyrite. Pyrite oxidation by oxygen represents a rather slow process.

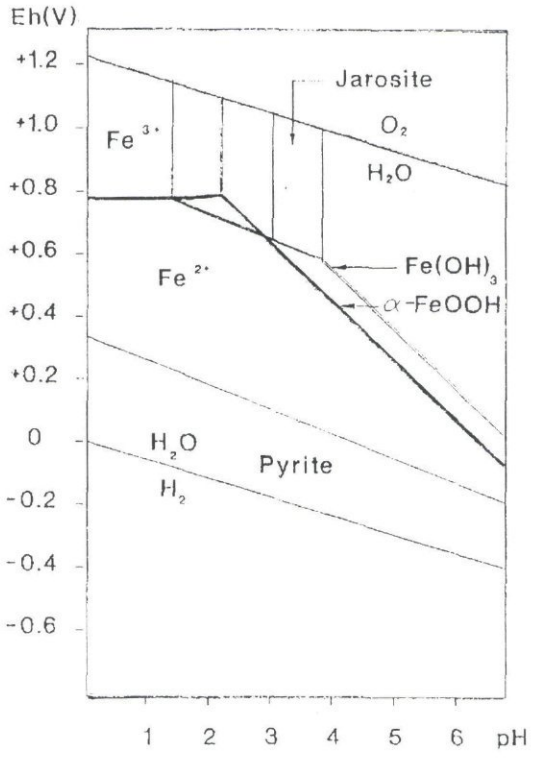

Fig. 4.15 Eh-pH diagram for the Fe-S-O-H system

Table 4.6 Soil samples taken at Ly Nhon experimental field site: time, location and depth of sampling, kind of laboratory investigation - XRD = x-ray diffraction, SEM = scanning electron microscopy

May 1996 Hydrological characterization	Depth of sampling	Type of investigation	July 1997 Hydrological characterization	Depth of sampling	Type of investigation
monthly flooded, new reclaimed rice field			Daily flooding, rice field		
RMA	15	XRD	RDC	15	XRD
RMA	30	XRD	RDC	30	SEM, XRD
RMA	50	XRD	RDC	50	XRD
RMA	90	XRD	RDC	90	SEM, XRD
			monthly flooded, new reclaimed rice field		
RMB	15	XRD	RM	15	SEM, XRD
RMB	30	XRD	RM	30	SEM, XRD
RMB	50	XRD	RM	50	SEM, XRD
RMB	90	XRD	RM	90	SEM, XRD
daily flooded, undisturbed soil			daily flooded, undisturbed soil		
RA	15	XRD	R	15	SEM, XRD
RA	30	XRD	R	30	SEM, XRD
RA	50	XRD	R	50	SEM, XRD
RA	90	SEM, XRD	R	90	SEM, XRD
RB	15	XRD			
RB	30				
RB	50	XRD			
RB	90				
no flooding, disturbed soil from the dike of the shrimp pond			no flooding, disturbed soil from the dike of the shrimp pond		
SA	15	XDR	SA	15	XDR
SA	30	XDR	SA	30	SEM, XRD
SA	50	XDR	SA	50	SEM, XRD
SB	15	XDR	SB	15	XRD
SB	30	XDR	SB	30	XRD
SB	50	XDR	SB	50	XRD

The stability fields for different iron species are characterised by the Eh-pH diagram for the Fe-S-O-H system (Miller, 1980) (Fig. 4.15). With respect to the mineral species the diagram seems to be suitable for describing conditions in the acid sulphate soils at the experimental field site in Vietnam.

4.4.3.3 Soil samples

Soil samples were taken from profiles at different sites. Soil cores from 15, 30, 50 and 90 cm depth were excavated for the case of undisturbed soil. Depths of specimen from the mound of the shrimp pond were 15, 30 and 50 cm. Detailed information of selected sites is given in Table 4.6. The elevation of profile-sites increases with distance to the river RA<R, RB< RMA, RMB, RM, RDC.

Undisturbed soil samples, 100 cm^3 per depth and profile, were taken and covered immediately thereafter with cotton mesh and wax. The samples then had been transported to Kiel University where they were analyzed by using X-ray diffractor and by electron microscope.

The sampling was conducted 1 and 2 years after construction of shrimp pond.

4.4.3.4 Methods

X-ray diffraction
Roentgen diffraction analysis, XRD, represents a nondestructive method for qualitative and quantitative determination of mineral content. Intensities and angles of incidence (here given in °2θ) of a roentgen beam are measured. The angles of incidence are determined by the distances of planes of atoms within a crystal. Minerals are characterised by a typical set of angles with different relative intensities. Peak height was chosen as a measure of intensity because it was less disturbed than peak area. The baseline of the diffractogram (angle over intensity) showed low noise and the variability in height was small. Measurements were carried out by a PW1710 based diffractometer (Philips) a Cu tube anode was used (wavelength=0.154060 µm) a generator tension of 40 kV and a current of 30 MA. One time step lasted 1 s at a step size of 0.020 °2θ. Soil samples were dry freezed and grinded in a agate mortar. The homogenized samples were filled in the measuring frame and compacted.

For calibration purpose standard samples were prepared by adding to a sample of the top soil of the rice field defined amounts of pyrite. Sample with a weight percentage of 0, 2.5, 5 and 10 were obtained. The top soil did not show any peak at the angles characteristic for pyrite during repeated measurements of several samples. As reference substance a single euhedral cubic pyrite crystal of 1 cm in width was crushed by a mechanical hammer and homogenised in a mill as well as by manual grinding in a quartz mortar.

Scanning electron microscopy
Some of the soil samples were chosen for morphological investigations (Tab. 4.6), They were examined with a scanning electron microscope (SEM) of the type CamScan44. Dry freezed and air dried soil was carefully broken into small piece, 1-5 mm in size. The samples were mounted on SEM stubs and coated either with carbon or gold/palladium. Analysis of element composition by EDX could only be performed qualitatively. Completely plain (polished) surfaces are needed for exact quantitative information. Consequently different iron sulfides could not be

distinguished. Taken into account the results of the various applied methods, the minerals (iron sulphides) described below, are pyrite.

4.4.3.5 Results

X-ray diffraction

For the determination of pyrite content the peak at an angle of 56.2 °2θ was the most sensitive. At 47.5 °2θ the base line was smoother but the peak for 10% pyrite was less than half as high as at 56.2 °2θ. Pyrite content determined by a regression function obtained at 47.5 °2θ was a little higher than those derived by a calibration done at 56.2 °2θ. All data presented here are based on measurements at 56.2 °2θ.

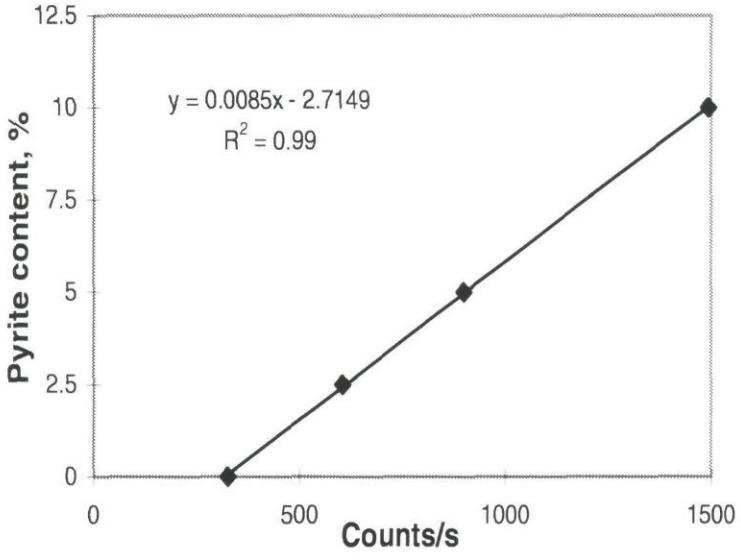

Fig. 4.16 Calibration of diffractometer; counts/s over pyrite content (0, 2.5, 5 and 10% by weight) and regression line; measurements at an angle of 56.2°2θ.

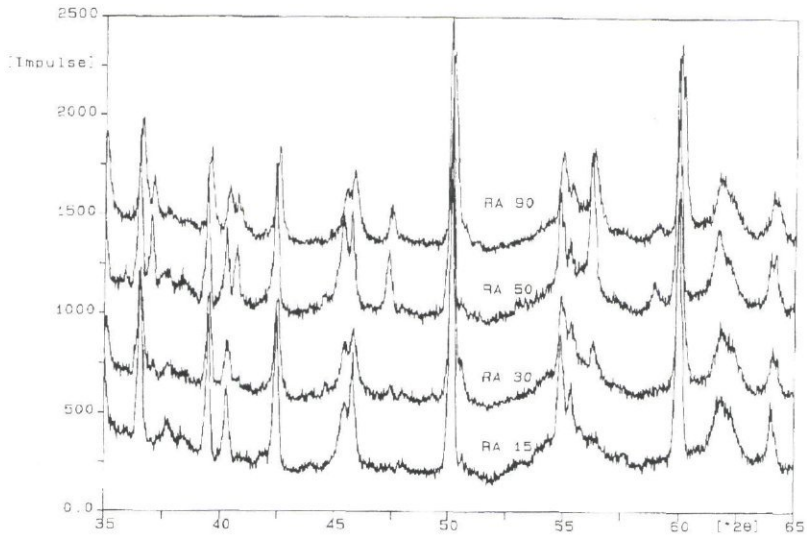

Fig. 4.17 Diffractograms of from soil samples taken from profile RA; for comparison reasons the single curves were separated by shifting upwards.

In Figure 4.16 the data set for calibration of XRD are presented. Each standard sample was repeatedly measured. The linear regression seem to be a good fit. Figure 4.17 show diffractograms for profile RA.

Pyrite content increases with depth. Profile RA, located right next to the river, contains most pyrite. In general, results show that the thickness of oxidized horizon (no pyrite) increases with distance of profile from the river (Tab. 4.7). In the mound of the dike pyrite content is characterized by a high variability. The mean value show a decrease of iron sulphide downwards from soil surface.

Results of XRD show a maximal pyrite content of 6%. In general the real pyrite content might be a little higher because a single euhedral cubic crystal was used as reference substance. In the soil there might be also amorphous pyrite present as well as imperfect crystals.

Table 4.7 Pyrite content, measured by XRD, of the soil samples taken at Ly Nhon experimental field site

1996			1997		
location	depth (cm)	pyrite content (% by weight)	location	depth (cm)	pyrite content (% by weight)
RMA	15	0	RDC	15	0
	50	0		50	0
	90	5,5		90	3,8
RMB	15	0	RM	15	0
	30	1,1		30	0,7
	50	2,4		50	0,9
	90	4,9		90	3,1
RA	15	0	R	15	0
	30	1,2		30	0,4
	50	2,7		50	2,4
	90	6		90	3,3
RB	15	0	SA	15	0
	30			30	2,1
	50	3,2		50	3,5
	90				
SA	15	0,2	SB	15	0
	30	0		30	0
	50	0		50	2,8
SB	15	0			
	30	0,6			
	50	1,4			

In addition to pyrite, jarosite content was determined. Intensity of peak at 28.9°2θ was used as measure for relative jarosite content. Due to the fact that no pure jarosite standard was available, data are given in relative content, counts/s (Fig. 4.18). In comparison to pyrite jarosite show a reverse distribution along the profiles of the mound of the pond. Its content decreases with depth. Jarosite was not detected in any sample of the undisturbed soil profiles. Jarosite forms as a result of the oxidation of Fe^{2+}. Results give evidence of a pronounced oxidation of pyrite during the first year after construction of shrimp pond. These observations are confirmed by results of monitoring program (Section 4.4.2) and scanning electron microscopy. In the soil of the rice field oxidation of pyrite seems to be a long term process at rather low intensities.

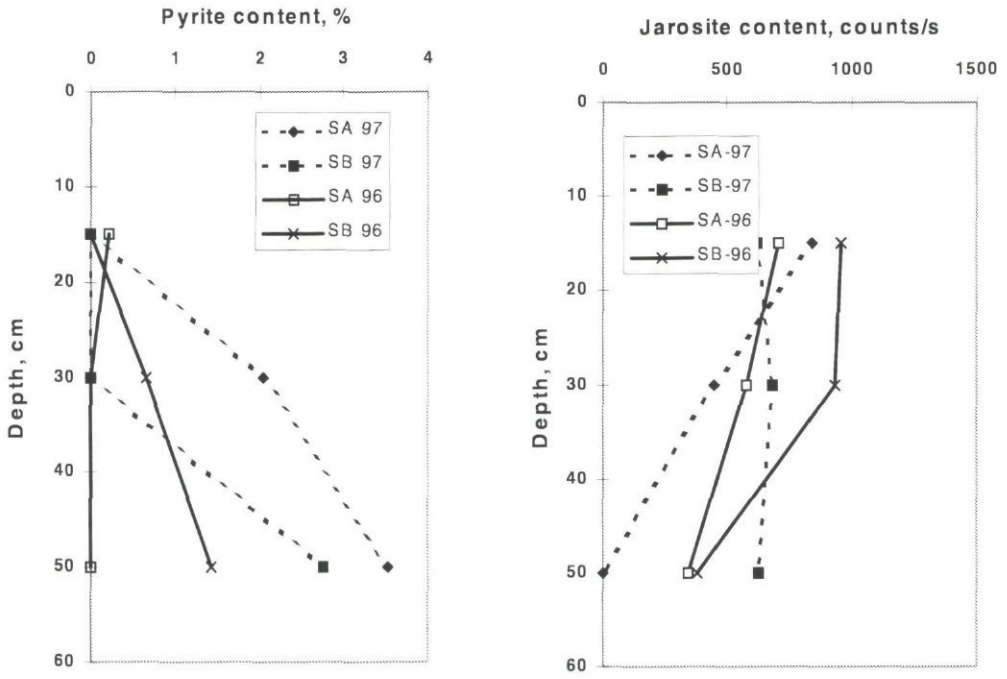

Fig. 4.18 Pyrite content and jarosite content of soil samples taken from mound of shrimp pond

Electron scanning microscopy

The pyrite crystals as observed by electron microscope showed various forms, sizes and oxidation grades (Fig. 4.19-4.21). Single euhedral octahedra are observed within the clay matrix (Fig. 4.19a). Figure 4.19c shows a nest of pyrite crystals, with rounded edges. The larger crystals in Figure 4.19b appear in a habit which represents a mixture of different habits of the cubic system. The framboid in Figure 4.19b consists of pyritohedral crystals. Most observed framboids are composed of octohedra (4.20b). Big framboids consist of big single crystals whereas small framboidal pyrites are formed by small crystals (Fig. 4.19b, d). Beyond a certain state of growth framboids start to close their surface (Fig. 4.19f).

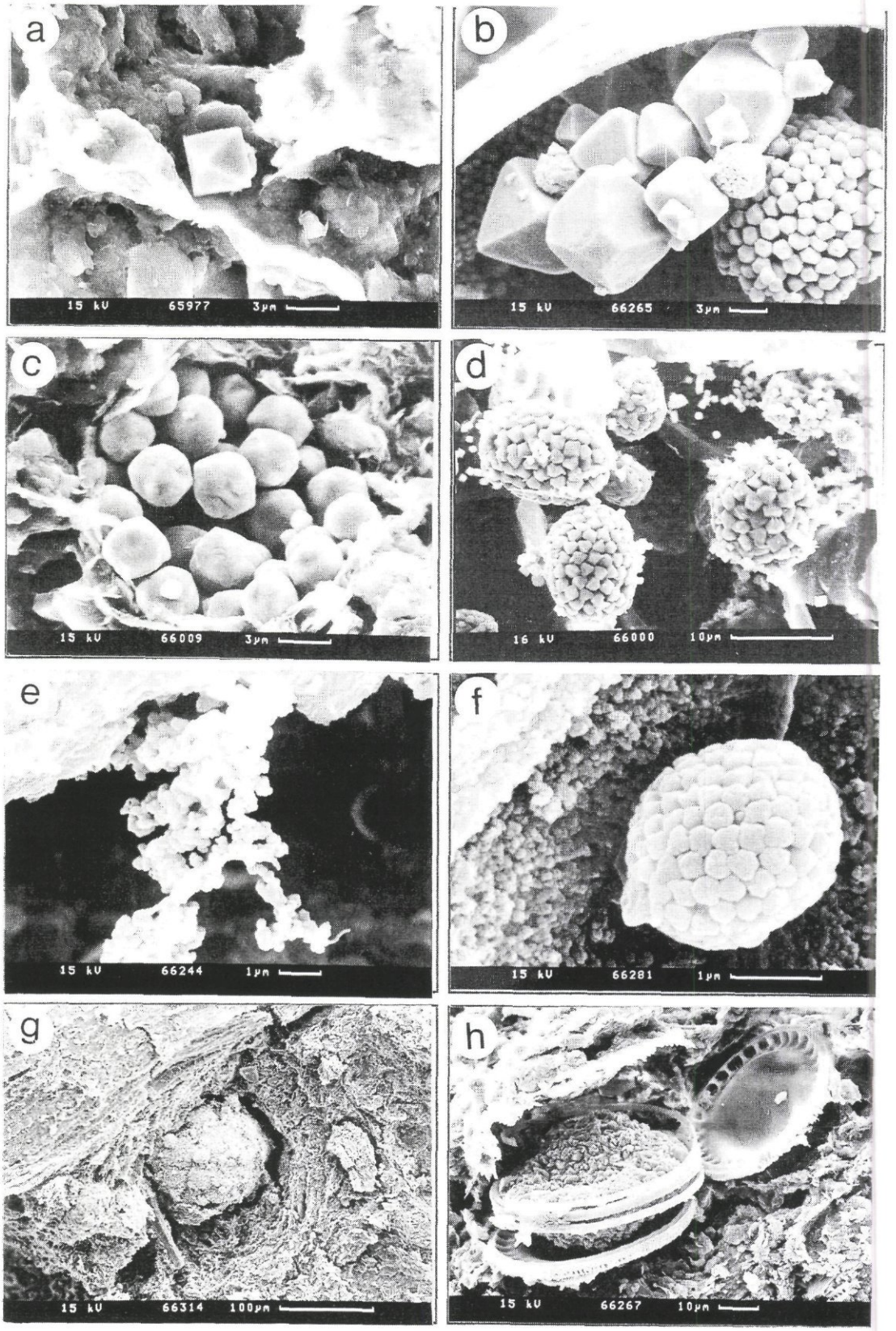

Fig. 4.19 SEM photographs of pyrite (a-h) from Ly Nhon, Vietnam

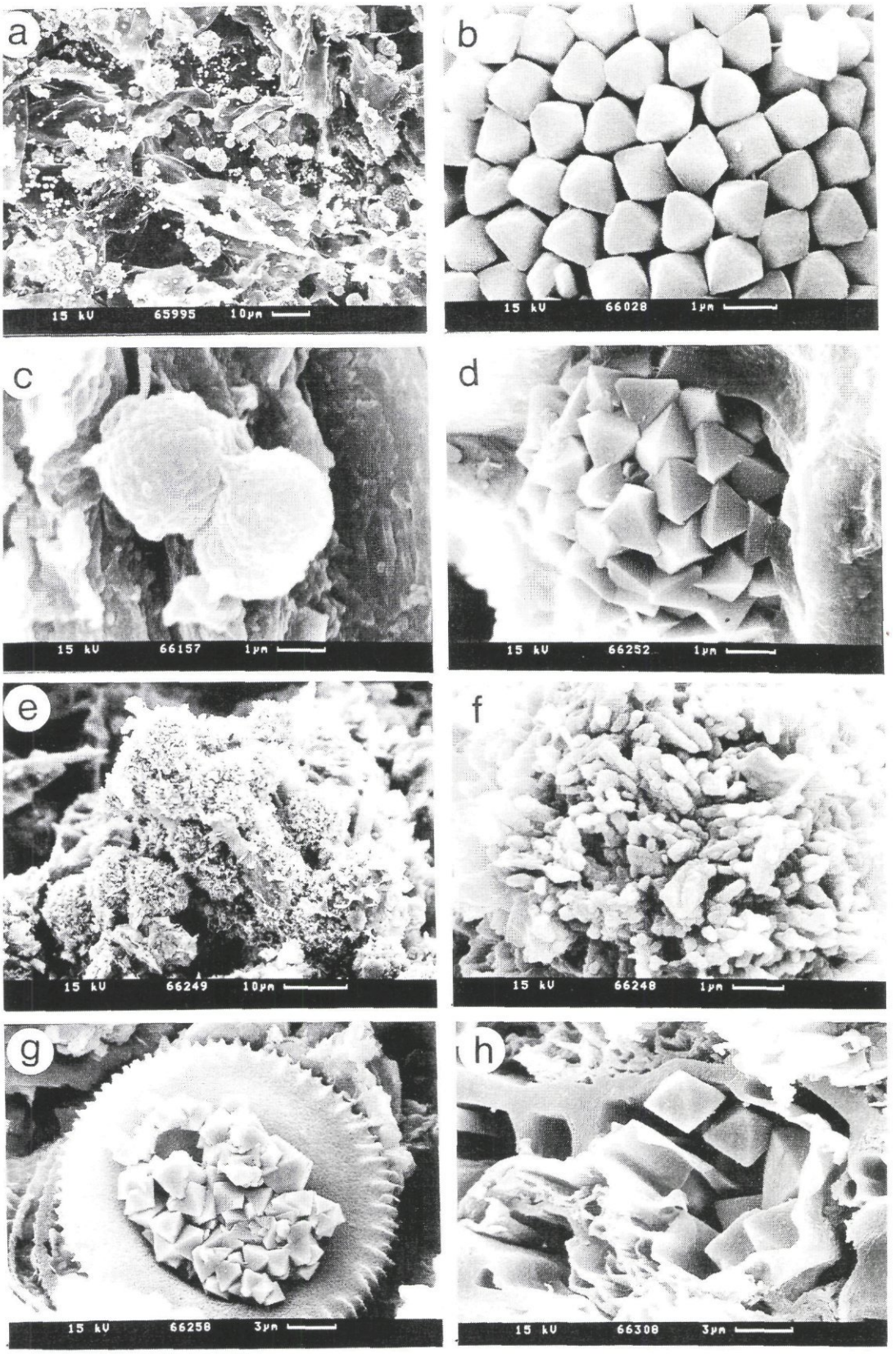

Fig. 4.20 SEM photographs of pyrite (a-h) from Ly Nhon, Vietnam

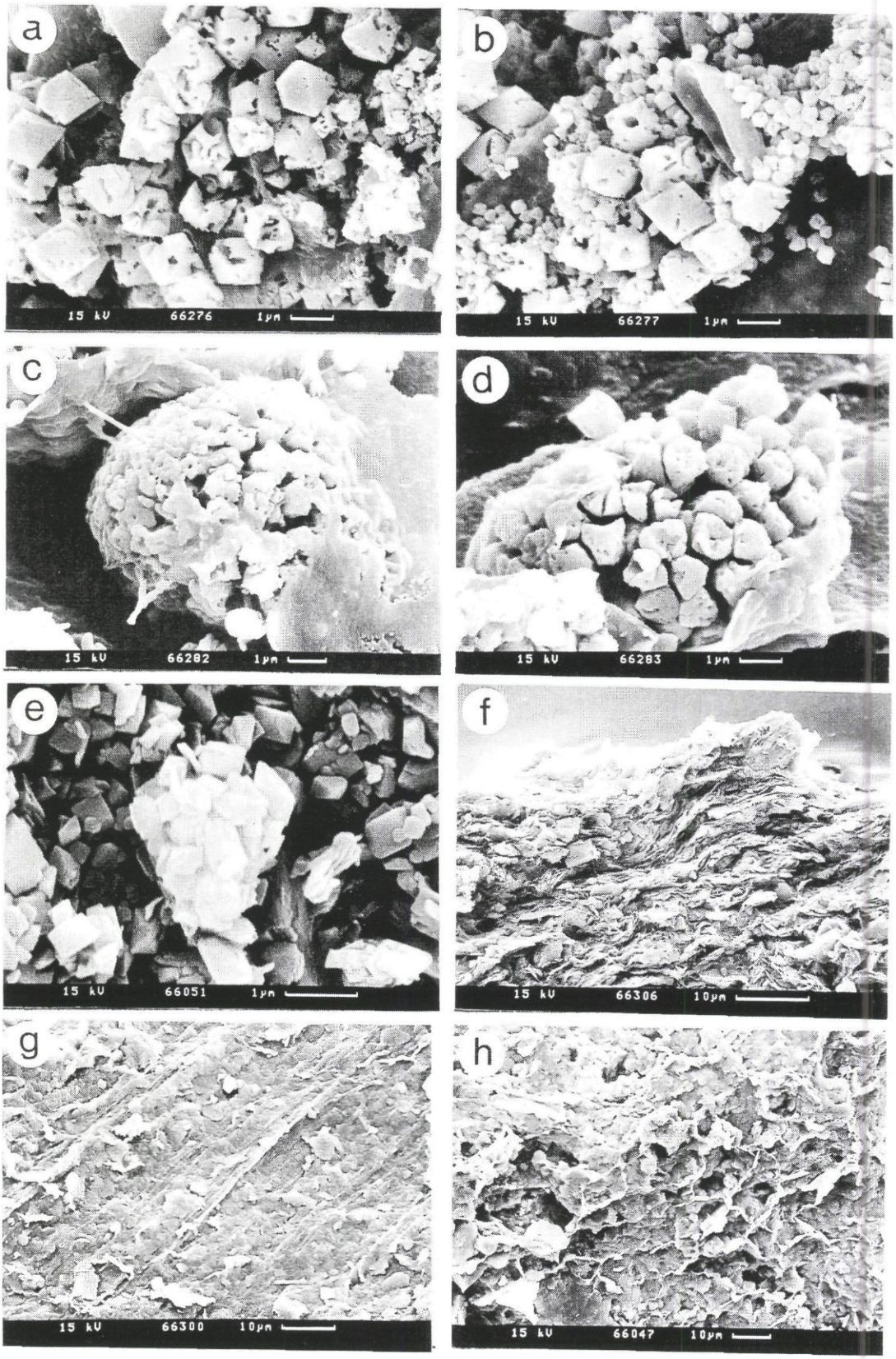

Fig. 4.21: SEM photographs of pyrite (a-d), jarosite (e) and clay matrix (f-h) from Ly Nhon, Vietnam

During infilling the surface will become either smooth (Fig. 4.19f, 4.20c) or rough. For the rough case, crystals of the framboid stand out of the surface (see small framboid in middle left part of Figure 4.18b, Fig. 4.20d). Big aggregates (diameter up to >100 μm) of framboids may fill larger cavities like pores (Fig. 4.18g). The accumulation of spheres presented in Figure 4.20e show a somehow radiated surface (Fig 4.20f). EDX indicates a content of 52-53% by weight S and 40-43% Fe. Taken into account the inaccuracy of the determination due to the rough surface the mineral should be pyrite (46,55% by weight Fe and 53,45% S). Pyrite appears also as complete infilling of diatomee (Fig. 4.18h). The crystalline overgrowth of single crystals may lead to aggregates (Fig. 4.20g). Organic substance, like decayed roots or wood represent obviously favourable locations of pyrite formation (Fig. 4.20a,h).

Thousands of small crystals (width down to <0,1μm) were observed covering the surface of organic material or appearing in loose accumulations (Fig. 4.19e,f, 4.21b, 4.22). Their abundance bear the potential risk of quick oxidation accompanied by severe acidification.

Crystals in the state of oxidation are shown in Figure 4.21a,b,c and d. The surface of crystals is covered by pits and deeper holes. Holes are often arranged in a chain or bigger ones represent elongated 'canyon' like structure. Their main axis seem to be orientated parallel to the edges of the crystal (Fig. 4.21a,b). In the state of oxidation the framboid show larger space between the single crystals and corrosion starts from the outside (Fig. 4.21c, d). Pyrite in the state of decomposition and euhedral pyrite with perfect surfaces were observed less than 1 mm far from each other.

Accumulations of jarosite appeared only in soil samples of the mound (Fig. 4.21e). In Figure 4.21f the clay shows a well developed preferred orientation. No pores are visible. Clay may also form a completely closed plane surface (Fig. 4.21g). Those structures may separate soil into isolated regions. Exchange of gas and solute may be inhibited. The micro fabric, shown in Fig. 4.21h, builds a porous structure. The size of pyrite was determined by measuring diameter of framboids and length of mid crystal edge of octahedra (Fig. 4.22).

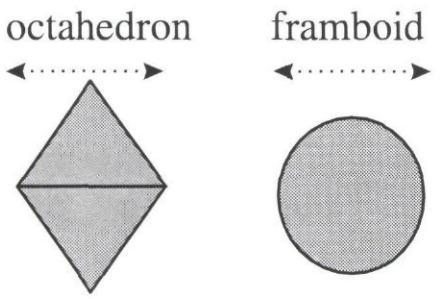

Fig. 4.22 Determination of size of octahedra and framboids

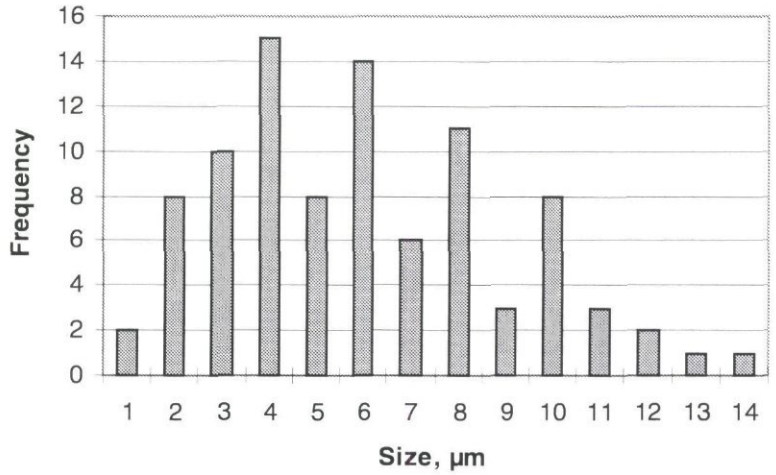

Fig. 4.23 Size distribution of pyrite framboids

Size of framboidal pyrite ranges from 1 to 14 µm (Fig. 4.23). 29 of 92 framboids were infilled, including all pyrite larger than 11 µm in diameter. The average size of 6 µm coincides with results of Wilkin et al. (1996) and Love and Amstutz (1963). Three aggregates of framboids were observed (diameter up to 100µm).

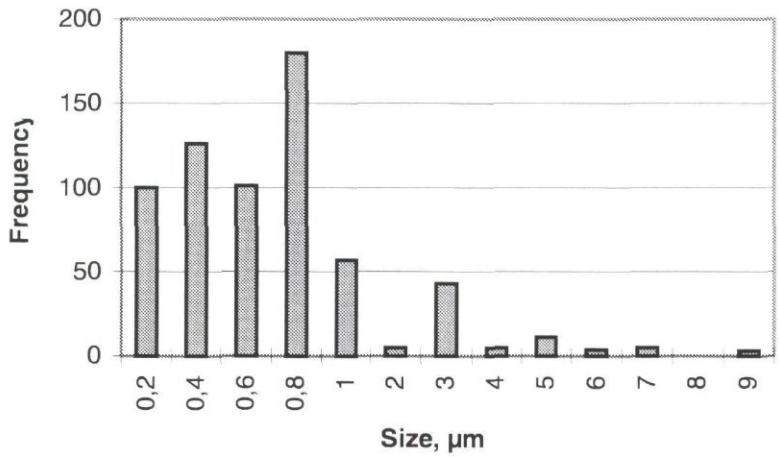

Fig. 4.24 Size distribution of single pyrite crystals

The single crystals show a different size distribution (Fig. 4.24). Most pyrites are smaller than 1 µm in width. The smallest crystals are difficult to count and their size is difficult to measure. The question whether framboidal pyrite or single crystals represent the biggest portion of mass of pyrite is not yet answered

The oxidation process lead to a distinct higher increase of surface of pyrite in comparison to the decrease of surface of spheres calculated by SMASS. Based on the morphological investigations, described above, the input parameter diameter of

pyrite crystals has to be adjusted during calibration procedure. Especially for the horizons, where oxidation is expected, the size should be fixed at a lower value than the average of measurements.

4.4.4 Macroporous structures of acid sulphate soils

Macropores play an important role in physical and chemical processes in acid sulphate soil. Therefore, tracer experiments were conducted in summer 1996. A dye solution was applied at different sites at the experiment farm. Results should provide information on the nature, structure and behaviour of the macropore system.

4.4.4.1 Dye tracer experiment

Four different factors might influence the macropore system in soil: land use pattern, soil structure, soil type and hydrology. These factors are closely related to each other. Taken into account the four parameters, four experimental sites were chosen (Tab. 4.9).

Table 4.8 Selected experimental sites

site	soil type	land use / soil cover	hydrological condition
1	Potential acid sulphate soil	Bare, tillage	Monthly flooded
2	Potential acid sulphate soil	Uncultivated, bushes	Daily flooded
3	Saline-acid sulphate soil	Rice field, bare	Daily flooded
4	Actual, disturbed acid sulphate soil	Mounds of shrimp pond	Dry, never flooded

Under natural conditions a solution of dye should infiltrate into the soil. Stepwise the soil below the infiltration area will be excavated. The description of the stained surface on horizontal cross sections should deliver qualitative and quantitative information concerning their distribution, shape, number and covered area. The observations should be related to soil properties/structure. The parameter should be extrapolated from two-dimensional (cross section-profile) to three dimensional features (soil bulk-volume). Brilliant Blue (Food Blue 2, Acid Blue 9, Colour Index Number: 42090) was chosen for the dye tracer.

At the experimental field infiltration occurs during flooding due to tidal influence and after rainfall. Both processes should be considered for the experimental layout.

Before flooding a metal frame (side length 60 cm, height 40 cm) is pressed several cm into the soil. When water level of the flood reaches it's highest level a solution of dye (final concentration 3 $g.l^{-1}$) is added to the water within the frame. Time for excavation is limited by tide.

In order to simulate natural rainfall defined amounts of water were applied by a watering can. Before starting the experiment intensity and area of application were defined.

After the application of dye solution a frame net (50 cm x 50 cm), which was divided into 25 squares of 10 cm x 10 cm; was placed on the stained soil surface. Steel rods were rammed in two opposite corners of the main frame in order to provide a reference for the excavated horizontal profiles. The stained patterns of each horizontal plane were described. For further investigations photos were taken and pictures were drawn.

The soil nearby the river (daily flooding) was characterised by macropores due to high biological activity. The soil at larger distances from river (monthly flooding) was more developed and was also characterised by preferential pathways (cracks).

Examples of stained pattern on horizontal planes from mound are given in Figure 4.25. The soil of the mound showed same pore structure as undisturbed soil nearby the river. In addition a distinct system of cracks developed due to shrinkage of blocks which were formed during excavation of shrimp pond. The continuity of macropores was partly interrupted; only part of these pores were stained blue. This pore structure seemed to remain stable after 10 years as evidenced by the stained pattern of a soil profile of a artificial pond dug out in the 1980's.

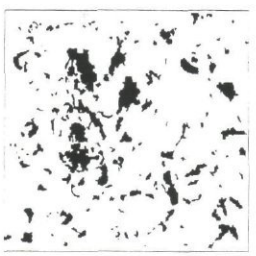

a) Macropores pattern at depth of 10 cm

b) Macropores pattern at depth of 20 cm

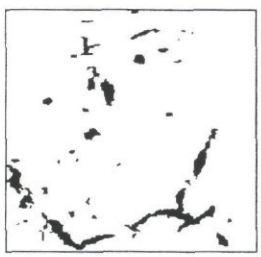

c) Macropores pattern at depth of 40 cm

d) Macropores pattern at depth of 60 cm

Fig. 4.25 Macropore system in mound as displayed by stained pattern of horizontal planes (50 cm x 50 cm) depths of 10 (a), 20 (b), 40 (c) and 60 cm (d)

The photos of cross sections were digitized by scanner and analyzed by the program PORA. The program lays the pictures of two adjacent planes over each other. It calculates the area of pores (set equal to stained area) which have at least one point (pixel) of intersection. Then the determined area is divided by total area of pores. The results are shown in Table 4.9.

Table 4.9: Distribution of macropore systems inside the mound

Depth (cm)	Relative area macropores (%)	Arrival time of tracer (min)	Interconnection ratio of 2 adjacent horizons (%)
0	100	0	12.69
10	3.25		8.78
20	9.94	1	4.39
30	8.68		3.67
40	6.09	2	1.7
50	3.49		1.5
60	10.48	18	

4.4.4.2 Flow pattern and efficiency of leaching in macroporous soil of the mound

Infiltration tests conducted on the soil surface of the mound shows that the infiltration rate is rather low. The mean value of three replications (mesured by tension-infiltrometer) on the mound is 0.0008 $cm.s^{-1}$. This fact shows that effective rainfall amount may be low if rainfall intensity excesses 30 $mm.h^{-1}$. On the soil surface one can observe hard-layer compacted by heavy rainfall.

Otherwise, soil structure inside the mound as described by stained pattern show a distinct macropore system. The geometry of macroporous structure as shown above plays an magnificent role in leaching of the mounds. Despite the sealed surface of the mound high amounts of tracer solution were observed short time after start of tracer application (Table 4.9). The macropore system represents the mobile region of the mound. Bypass flow contributes just a little to leaching of the immobile regions inside the matrix. In 10 cm depth the density of macropores in the mound was high and leaching might be efficient. (Fig. 4.25). At a depth of 20 cm macropore density already decreased significantly and consequently leaching of matrix by preferential flow became inefficient. Substances located nearby macropores will be leached quickly. The described processes will lead to a high variation of the spatial distribution of various substances in the soil of the mound.

4.4.5 Oxygen concentration, redox potential and pyrite oxidation in the mound

In the mound oxygen was found at high concentration even at depths of 30 and 50 cm (Fig. 4.26). The values remain high through the year.

Profile observations carried out during the dye-tracer experiment recognised the existence of jarosite mottles, which surround the macropores. The yellow structures stretched from topsoil to the bottom of the mound. This evidence, once again, proves the important role of macroporous structure in pyrite oxidation process inside a mound.

The presence of oxygen in the soil was reflected by redox potential (Fig. 4.27).

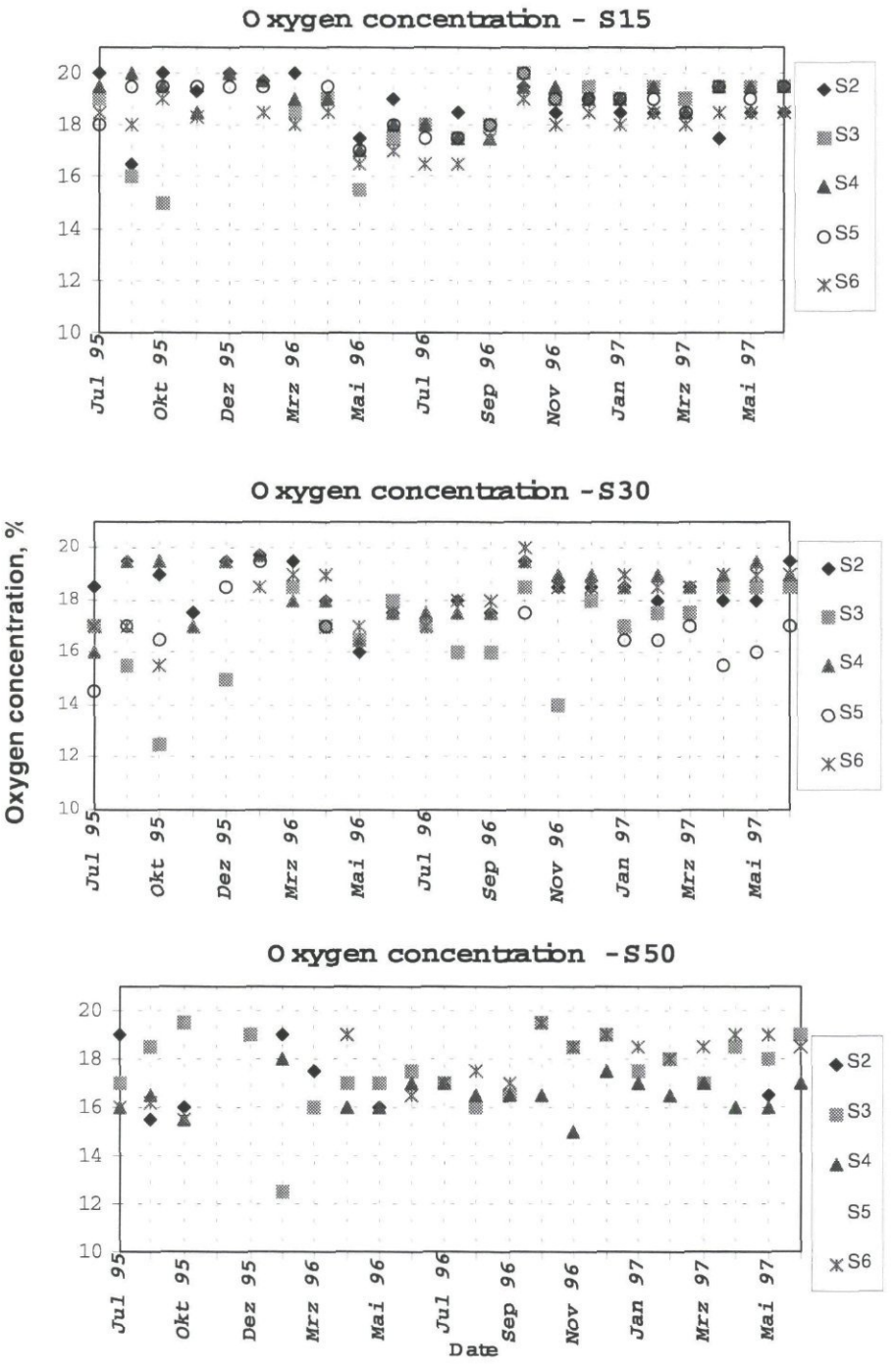

Fig. 4.26 Oxygen concentration in mounded soils versus depth and time in mound at nest S2-S6

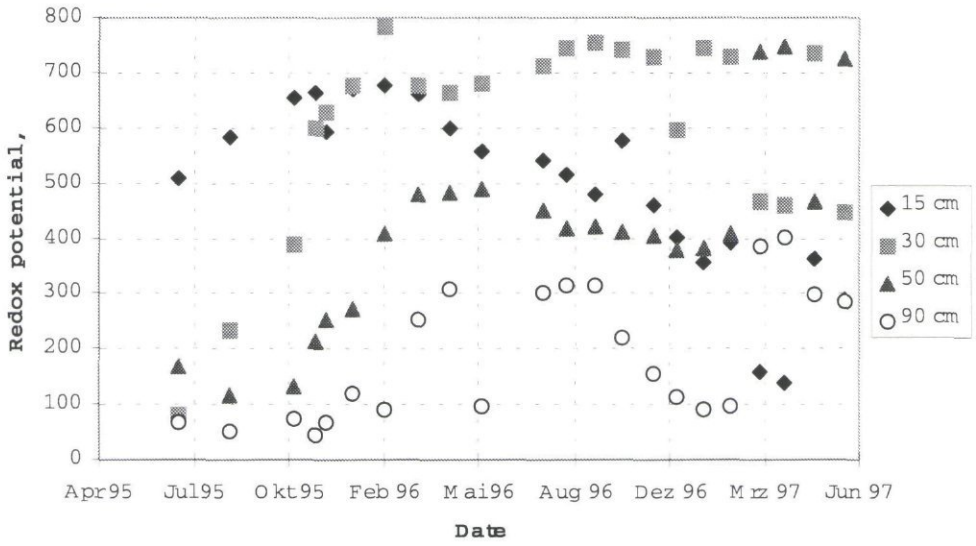

Fig. 4.27 Measured redox potential over time and depth in mound

During the process of drying the redox potential increased stepwise, first in the top of the mound and at last at its base. Redox potential and pH indicated a continuous oxidation of pyrite at depths of 15, 30 and 50 cm (Fig. 4.4, 4.15, 4.27). At a depth of 90 cm redox conditions showed a temporal and spatial variability with respect to stability field of pyrite.

In the upper layers of the mound Eh exceeds 600 mV and the pH value ranged from 3 to 4. According to Eh-pH diagram (Fig. 4.15) jarosite might be formed. Field observations, laboratory investigations, results from monitoring program and theoretical considerations seem to confirm each other.

4.5 The interactions between soil and water qualities in a new built shrimp pond

Soil characteristics change strongly after mounding. Immediately after excavation oxidation occurs at top of the soil. Jarosite mottles can be observed in upper horizons just after 2 weeks. The rain water can leach the topsoil and results in the transform of jarosite to ferric hydroxide. The oxidation status in deeper horizons, however, remains even during rainy period as shown by oxygen concentration and redox potential of the soils. Oxidation rate is promoted through aeration of whole profile caused by the overall existence of macropores.

The pollution mechanism of a pond with acidified material can be categorised: by-pass flow transports acidic ions (sulphate, aluminium, iron) directly to groundwater in ponds, whereas run-off flow washes out acidic products from topsoil to the pond. Due to high acidity of soil in mound, the water quality of pond will change remarkably, if the pond can not be drained effectively. On other hand, the effective

drainage of the ponds may result in pollution of mangrove environment, especially if the density of pond is large.

The role of river water is very important in dilution and buffering acidic pollutant in pond water. The refreshing of pond water required good operation of ponds and good hydraulic condition. In order to maintain a sustainable development in the coastal area with acid sulphate soils, it is required that planners must be able to forecast the situation qualitatively or quantitatively.

5 Simulation Model for Acid Sulphate Soils (SMASS)

5.1 Introduction

The computer simulation model SMASS consists of a number of mutually linked submodels in which the various physical and chemical processes occurring in acid sulphate soils are described with mathematical equations (Fig. 5.1). To solve these equations, the soil profile is divided into compartments of variable size (Fig. 5.2). The initial physical and chemical conditions in each compartment must be given as model input. For the complete simulation period, values for the boundary conditions, as given in Fig. 5.1, are required as input. The physical and chemical conditions in each compartment, together with the water and solute fluxes at the boundary of the soil system are computed on a daily basis.

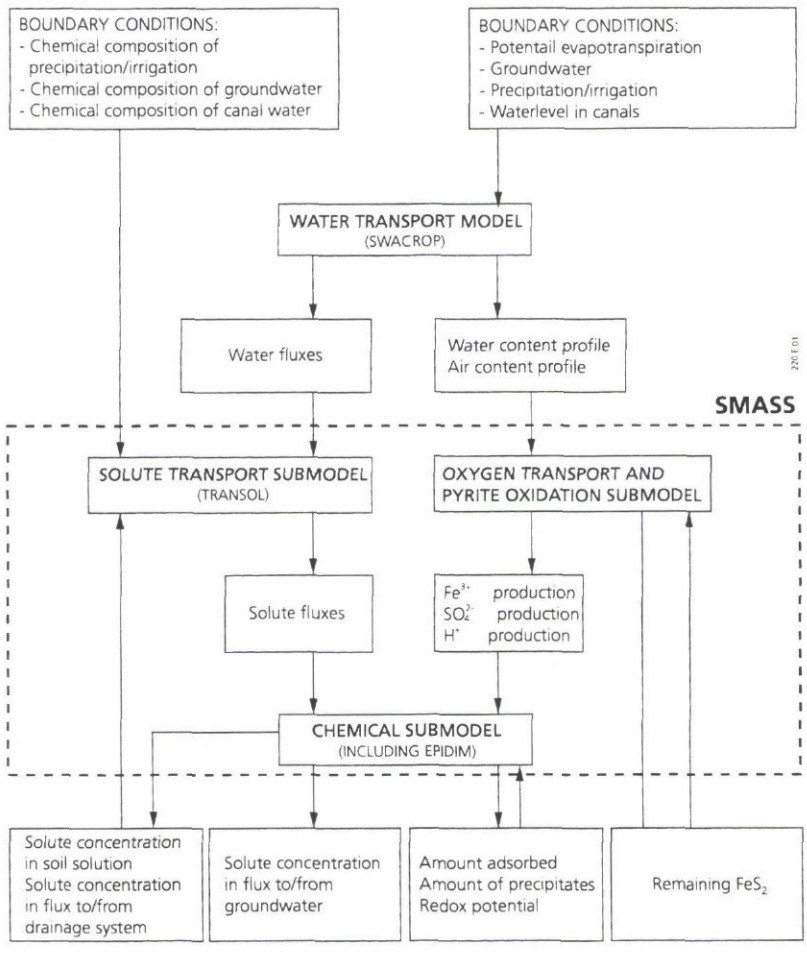

Fig. 5.1 Structure of SMASS: Simulation Model for Acid Sulphate Soils

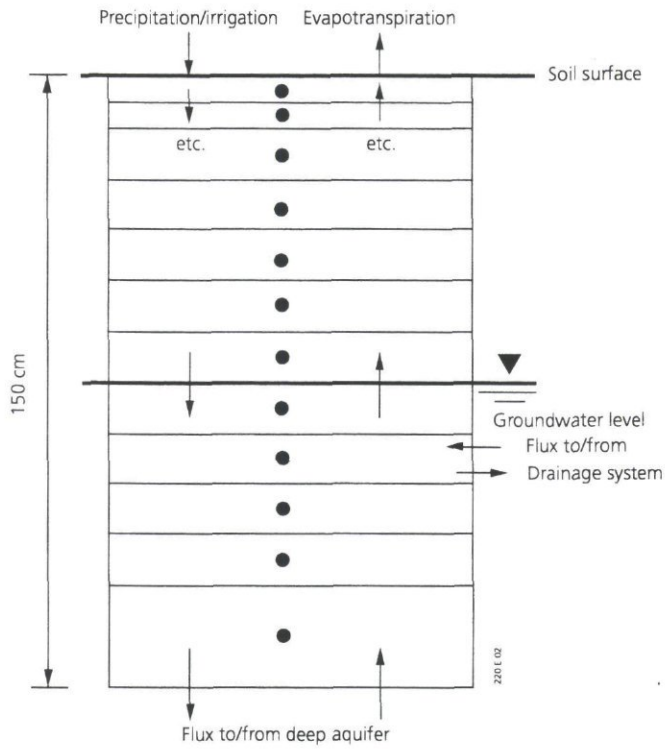

Fig. 5.2 Schematization of a soil profile, as applied in SMASS. Arrows indicate water and solute fluxes

Fig. 5.1 illustrates the sequence in which the various physical and chemical processes are computed:

1. The *water transport submodel* computes vertical and lateral water transport. This yields water fluxes and the water content profile in the soil. The air contents in the soil are complementary to the water contents.
2. In the *oxygen transport and pyrite oxidation submodel*, air contents are used to compute oxygen diffusion coefficients in the air-filled soil macropores. Oxygen consumption values in the soil are calculated from pyrite and organic matter contents. Subsequently, the oxygen content profile in the soil macropores is computed. The rate of pyrite oxidation at each depth is calculated depending on the local oxygen concentration. For each depth, the oxidized amount of pyrite is converted into amounts of produced H^+, Fe^{3+}, SO_4^{2-}. The remaining amount of pyrite in the soil is used for calculations in the next time step.
3. The *solute transport submodel* computes vertical solute fluxes between soil compartments and lateral solute fluxes to and from the surface water, both based on the water fluxes calculated in step 1.
4. In the *chemical submodel*, first the production/consumption terms for the non-equilibrium processes (such as precipitation/dissolution of precipitates) are calculated. Then the total concentration of each chemical component is calculated in the soil compartments by summing for each component the production/consumption terms, the inflow/outflow (from step 3), and the total

amounts at the end of the previous time-step. From these total concentrations, the equilibrium concentrations in the soil solution, the composition of the exchange complex, and the amount of minerals and precipitates are computed for each compartment.

Time steps for computations of the water and solute transport submodels are in the order of hours. Pyrite oxidation, oxygen profiles and chemical equilibria are computed once every day. The output of the model SMASS and its submodels is given on a daily basis. Model predictions can be carried out for one or more decades, so that the long-term effects of various water management strategies can be evaluated quantitatively. The one-dimensional is described in detail in AARD/LAWOO (1993a,b) and Bronswijk and Groenenberg (1993). Below a brief description of the submodels is given.

5.2 Water transport submodel (SWAP)

5.2.1 General

SWAP employs the Richard s' equation for soil water movement in the soil matrix:

$$\frac{\partial h}{\partial t} = \frac{1}{C(h)} \frac{\partial}{\partial z} [K(h) (\frac{\partial h}{\partial z} + 1)] - \frac{S(h)}{C(h)} \qquad (5.1)$$

in which: h = soil water pressure head (cm), t = time (d), C = differential moisture capacity $d\theta/dh$ (cm^{-1}), z = vertical coordinate (positive upwards) (cm), $K(h)$ = hydraulic conductivity (cm d^{-1}), and S = water uptake by roots (d^{-1}).

The soil hydraulic functions are described by the analytical expressions of Van Genuchten and Mualem or by tabular values. Hysteresis of the retention function can be taken into account. Root water extraction at various depths in the root zone is calculated from potential transpiration, root length density and possible reductions due to wet, dry, or saline conditions. The numerical solution of the Richards' equation is described by Belmans et al. (1983). At the lower boundary of the soil profile, which may be either in the saturated or in the unsaturated part of the soil, the user can specify the soil water flux, flux as function of groundwater level, free drainage, or lysimeter with free drainage. A complete description of the model is given by Van Dam et al., 1997.

Solving Equation (5.1) yields the flux of water through the upper and lower boundary of each soil compartment (Fig. 5.2). For the top and bottom compartment boundary conditions determine the flux at the upper and lower boundary of the soil profile. With respect to the boundary conditions at the top (precipitation/irrigation, evaporation, evapotranspiration) and the bottom of the soil system (groundwater level, pressure heads, free drainage, fluxes) various options are possible, which makes the model flexible and generally applicable.

SWAP has options to simulate an extended water balance. Such a complete water balance for a soil-water-crop system can be formulated as:

$$\frac{\Delta V}{\Delta t} = q_p + q_s - q_{e,s} - q_{e,p} - q_{e,i} - q_t - q_r - q_l - q_{d,1} - q_{d,2} - q_{d,3} \qquad (m^3.m^{-2}.d^{-1}) \quad (5.2)$$

where: ΔV is the change in areic water volume during a time step ($m^3\ m^{-2}$), Δt is the length of the time step (d), q is a water flux ($m^3\ m^{-2}\ d^{-1}$) with q_p is precipitation, q_s is seepage, $q_{e,s}$ is the soil evaporation, $q_{e,p}$ is the ponding evaporation, $q_{e,i}$ is the interception evaporation, q_t is the transpiration, q_r is the surface run-off, q_l is the leaching across the bottom boundary, $q_{d,1}$ $q_{d,2}$ $q_{d,3}$ is the drainage to or from (positive or negative) the first, second and third order drainage systems.

The net incoming flux across the top boundary of a one-dimensional schematized profile results from the precipitation minus the evaporation by interception, bare soil and a ponding layer, and minus part of the surface run-off. The net incoming flux across the lateral boundary of the profile results from the difference between infiltration from and drainage towards surface water system(s). The net incoming flux across the lower boundary results from the difference in seepage from and leaching towards deeper soil layers below the profile. All water fluxes across boundaries of the model system and across the boundaries of compartments may be incoming or outgoing.

SWAP has an option to simulate water flow to/from surface water systems. This option is based on a regional approach for the surface water system(s). Since the two-dimensional approach plays an important role within the framework of this project, this approach will be discussed more in detail in the next section.

5.2.2 A regional approach for lateral flow towards surface waters

In regions with water discharge towards drainage systems, the residence time of soil water is strongly influenced by the size and depth of the drainage systems. For solute transport it is essential to take this discharge into account because it reduces the discharge towards groundwater and it may contribute considerably to the solute balance of a soil system.

5.2.2.1 Lower boundary

Groundwater flow can be divided into a local and a regional flow (Fig. 5.3). The regional flow is mostly not important for the transport of substances from the soil surface to a neighbouring surface water system. The local flow however is the essential transport route towards the surface water system. To catch this local flow the position of the model profile should be such that it accounts for most of the streamlines that describe the local flow. In the model this is achieved by using an approach formulated by Ernst (1973, p. 26-27), who related the depth of the local flow to the distance between drainage systems or ditches. He proved for homogeneous soil profiles, that the depth of the local flow occurs for 85% within a depth which is equal to 1/4 of the drain distance.

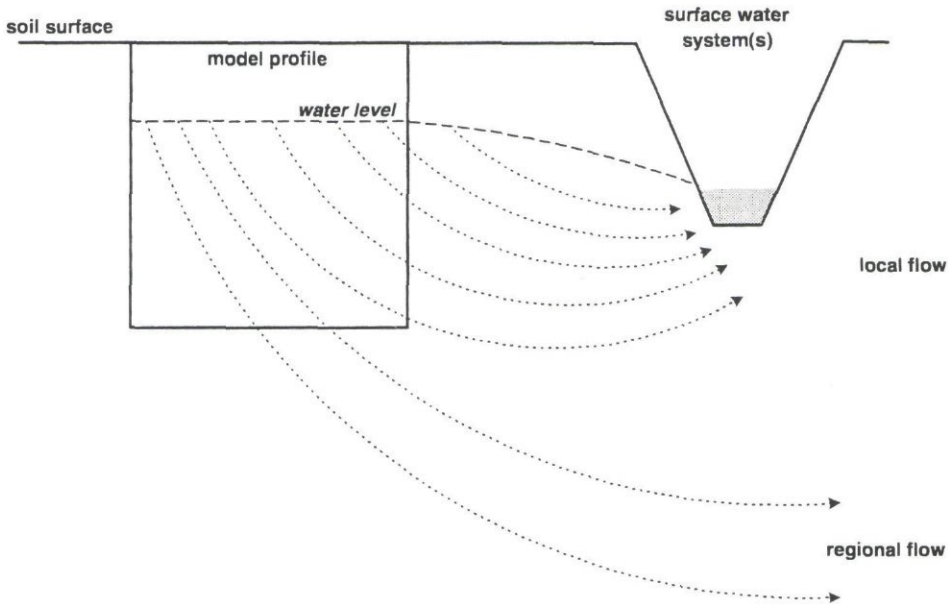

Fig. 5.3 A groundwater system with local and regional flow and the position of a one-dimensional model profile to simulate lateral flow to surface water system(s)

Once the regional and local flow have been segregated by the position of the lower boundary, the lateral boundary can be used to simulate discharge to drainage systems. Given water discharges and drain distances are used to simulate residence times of water and solute in the saturated part of the soil profile. The next two paragraphs will explain how the lateral boundary can be used to simulate fluxes to and from surface water systems.

5.2.2.2 Lateral boundary with one surface water system

In humid climates, most drainage problems can be solved by using approaches valid for steady flow between parallel drains with equal distance, size and drainage level. A general equation to quantify a drainage flux in such a situation is:

$$q_d = \frac{h - h_d}{Y_d} \tag{5.3}$$

where: q_d is the drainage flux ($m^3.m^{-2}.d^{-1}$), Y_d is the drainage resistance of an open field drain or a tile drainage system (d), h_d is the drainage level (m), h is the phreatic groundwater level (m).

With the assumption that the given drainage flux q_d is determined by the precipitation excess, it will now be explained how this drainage flux can be appointed to the lateral boundary of a one-dimensional model profile.

In a homogenous layer of constant thickness where radial flow in the surroundings of the drains can be neglected, drainage water flow can be described with a stream function. Ernst (1973) describes the transport of water particles along streamlines

using a streamfunction. For a two-dimensional transect between parallel perfect drains the stream function can be given as a function of depth and distance:

$$\psi(x,z) = -\frac{N}{D}x(D-z) \qquad (m^3.m^{-1}.d^{-1}) \quad (5.4)$$

where: $\psi(x,z)$ is the stream function ψ which is a function of depth z and distance x ($m^3.m^{-1}.d^{-1}$), N is the precipitation excess ($m^3.m^{-2}.d^{-1}$), z is the depth below the soil surface (m), x is the distance from a reference point in the middle of 2 drains towards the drain (m), D is the thickness of the homogeneous soil layer (m).

The water fluxes q_z in the z-direction and q_x in the x-direction can be found by taking partial derivatives of the streamfunction ψ.
The flux q_z can be found by differentiating ψ to x, keeping z constant:

$$q_z = \psi_x(x,z) = -\frac{\partial\psi}{\partial x}(x,z) = \frac{N}{D}(D-z) \qquad (m^3.m^{-2}.d^{-1}) \quad (5.5)$$

where q_z is the water flux in the z-direction ($m^3.m^{-2}.d^{-1}$).

The lateral flux q_x can be found by differentiating ψ to z, keeping x constant:

$$q_x = \psi_z(x,z) = -\frac{\partial\psi}{\partial z}(x,z) = \frac{N}{D}x \qquad (m^3.m^{-2}.d^{-1}) \quad (5.6)$$

where q_x is the water flux in the x-direction ($m^3.m^{-2}.d^{-1}$). In the one-dimensional model system the water flux q_x becomes the lateral drainage flux q_d, which can now be written as:

$$q_d = k_d\, x \quad \text{with} \quad q_d = q_x, \quad k_d = \frac{N}{D} \qquad (5.7)$$

where q_d is the drainage flux ($m^3\ m^{-2}\ d^{-1}$), k_d is the drainage rate ($m^3\ m^{-3}\ d^{-1}$).

This formulation is introduced in the general mass balance equation by means of the sink term R_x. The vertical flux q_z in the one-dimensional model system can be formulated as a linear relation with depth according to:

$$q_z = q_d\,(1 - \frac{z}{D}) \qquad (5.8)$$

By means of the approach given above for saturated flow towards drainage systems a pseudo two-dimensional transport is considered. In the one-dimensional model system the water flux q_d is divided proportional to the thickness of the model compartments between the phreatic groundwater level and the lower boundary of the model profile. The sum of model compartments from which water fluxes to and from a drainage system are simulated is called a 'model discharge layer'. The effect of pseudo two-dimensional transport on the residence time of water particles discharging to a drainage system will be explained by looking at a 'model discharge layer' into more detail. A 'model discharge layer' and its water fluxes in a discharging situation

are shown in Fig. 5.4a. For a system with one surface water system the vertical water flux is given as a linear function with depth (Fig. 5.4b).

The residence time of water particles in the one-dimensional profile is achieved by integrating the vertical water flux over depth:

$$\tau = \int_{z_1}^{z_2} \frac{\varepsilon \, dz}{q_z} \tag{5.9}$$

where τ is residence time (d) within one simulated time step for water particles moving from depth z_1 (m) to depth z_2 (m), ε is porosity ($m^3.m^{-3}$).

A combination of the previous 2 equations results in the following formulation for the residence time:

$$\tau = \frac{\varepsilon D}{q_d} \ln \frac{q_{z,2}}{q_{z,1}} \tag{5.10}$$

where $q_{z,1}$ and $q_{z,2}$ are the water fluxes in the vertical z-direction ($m^3\ m^{-2}\ d^{-1}$) at depths z_1 and z_2, D is the thickness of a model discharge layer (m). This solution implies that the residence time of the water particles flowing vertically downward increases logarithmic with depth (Fig. 5.4c).

The hydrological model schematization results in a similar expression for the relation between residence time variation and depth in the soil profile as given by Ernst (1973).

Summarizing the following assumptions have been made:
— Dupuit-assumption: pressure head, groundwater level and equivalent thickness of 'model discharge layer' , in the horizontal plane, are assumed to be equal.
— Symmetric groundwater flow.
— Equivalent thickness of 'model discharge layer' should be less than 25% of the distance between the drains. If the equivalent thickness is larger than 25% of the drain distance, than the lower boundary of the 'model discharge layer' is adjusted untill this conditions is met.
— Radial flow near the drains is neglected.

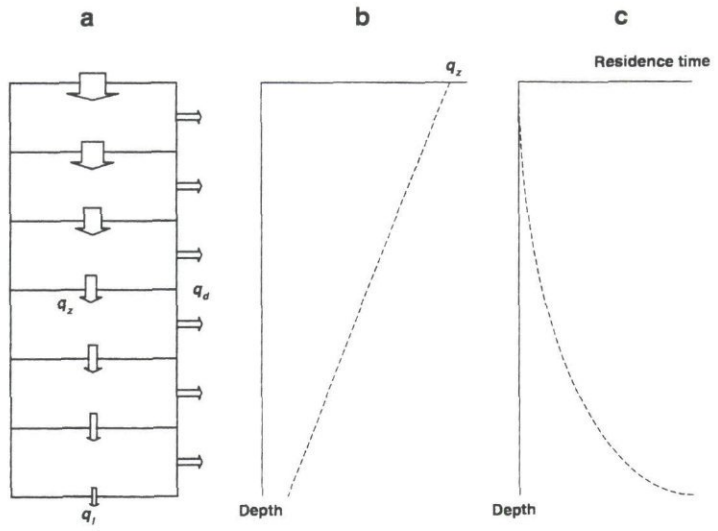

Fig. 5.4 A model discharge layer and water fluxes in a discharging situation.
a. Model discharge layer with vertical flux q_z , leaching flux q_l and drainage flux q_d
b. Vertical flux q_z as function of depth
c. Residence time as function of depth

5.2.2.3 Lateral boundary with more than one surface water system

Regional water discharges generally give a non-linear relation between measured discharges and groundwater tables. The general shape of such a so-called q/h-relation is given in Fig. 5.5a, from which it appears that a distinction can be made between discharges with a low and discharges with a high intensity. High discharge intensities with shallow groundwater tables are mainly caused by shallow drains, as open field drains and tile drains, with relatively short residence times, whereas low discharge intensities with deep groundwater tables are the result of drainage canals at larger distance, resulting in large residence times.

In the model schematization the q/h-relation is subdivided into a number of linear relations (Fig. 5.5b), each of them representing a certain type of drainage system. From these schematized q/h-relations drainage resistances are derived and they are used as input for the calculation of the drainage quantities per time step and per surface water system, as depending on the depth of the groundwater table and the surface water level.

Total regional discharge is calculated by the expression:

$$q_{d,r} = \sum_{i=1}^{n} q_{d,i} = \sum_{i=1}^{n} \frac{h - h_{d,i}}{\Upsilon_i} \qquad (5.11)$$

where: $q_{d,r}$ is the regional drainage flux ($m^3\ m^{-2}\ d^{-1}$), i is the number of drain system (-), n is the total number of drain systems present (-), Υ_i is the drainage resistance of system i (d), where: $q_{d,i}$ is the drainage water flux ($m^3\ m^{-2}\ d^{-1}$), h is the height of

the phreatic groundwater level at half of the drain distance (m), $h_{d,i}$ is the height of the water level in drain system i (m).

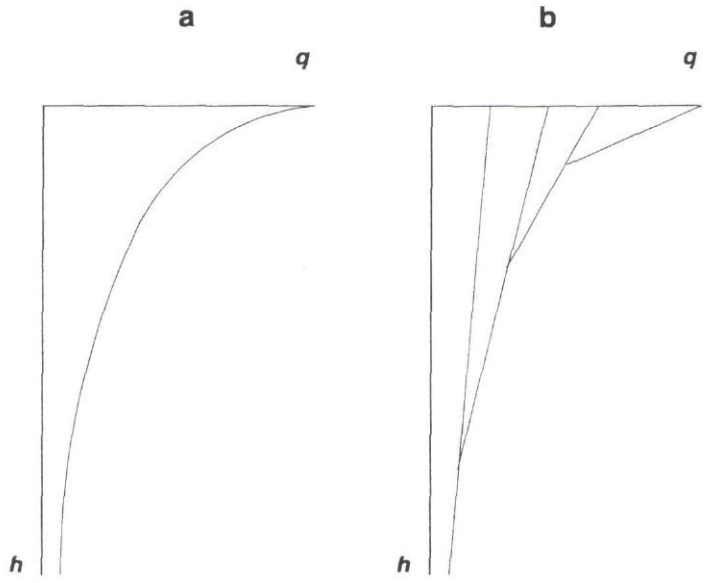

Fig. 5.5 Relations between groundwater level (h) and regional discharge (q)
a. Measured q/h-relation (after: Ernst, 1978)
b. Schematized q/h-relation with 4 drainage systems

Drains continuously containing water will have an infiltration function when the phreatic groundwater level becomes lower than the water level in the drainage system under consideration. When the phreatic groundwater level falls below the pressure head of the aquifer, leaching conditions are changing into seepage conditions.

Analogue to the situation with only one surface water or drainage system, so-called 'model discharge layers' are identified from which water is discharged to corresponding drainage systems.

The differences in residence time of the water particles discharging to the corresponding drainage systems can taken into account by assuming the thickness of the discharging layers ('model discharge layers') proportional to the drainage flux towards the corresponding drains, or:

$$D_1 : D_2 : D_3 = q_1 : q_2 : q_3 \qquad (5.12)$$

where D_i is the thickness of the 'model discharge layer' of drainage system i (m), q_i is the drainage flux towards drainage system i ($m^3.m^{-2}.d^{-1}$)

The size of the discharging soil layers or 'model discharge layers' can now be determined, since the sum of the thicknesses of the 'model discharge layers' is fixed by groundwater level and lower boundary of the model profile. For each 'model discharge layers' the thickness (D_i) can be calculated with:

$$D_i = \frac{L_i}{L_{prof} - h} q_i \qquad \text{(m)} \quad (5.13)$$

The position of the 'model discharge layers' is now fixed by their sizes and the upper and lower boundary which is respectively groundwater level and lower boundary of the model profile.

Dependent on the hydraulic conductivity of the soil layers, the residence time of water particles can be reduced or increased. In the model this is simulated by adjusting the thickness of the 'model discharge layer' in correspondence to the conductivity of the soil layers that belong to it.

5.3 The solute transport submodel (TRANSOL)

By combining the continuity equation and the flux density equation a general convec-tion-dispersion equation (CD-equation) is obtained:

$$\frac{\partial(\theta c)}{\partial t} = \frac{\partial}{\partial z}(qc - \theta D_{dd}\frac{\partial c}{\partial z}) + R_x \qquad (5.14)$$

where c is the mass concentration of a substance in the liquid phase (kg m-3),q is the volume fraction of liquid (m3 m-3), t is time (d), z is depth in the soil (m), q is the water flux (m3 m-2 d-1, or m d-1), Ddd is the apparant dispersion coefficient (m2 d-1), which is the sum of the coefficients for dispersion and diffusion of a solute in the liquid phase, Rx is the lateral discharge to surface water as a sink (drainage) or source (infiltratoin) term expressed as a volumic mass rate of the substance (kg m-3 d-1).

From this equation the concentration c is solved in the submodel TRANSOL. The second order partial differential equation is simplified to a first order equation by eliminating the dispersion/diffusion term. The remaining first order differential equation is solved analytically. Diffusion/dispersion is introduced by the selection of an appro-priate numerical solution scheme. A complete description is given by Kroes and Rijtema (1996).

5.4 Oxygen transport and pyrite oxidation sub-model

The principles of the oxygen transport and pyrite oxidation submodel have been outlined by Bronswijk et al. (1993). In the model, it is assumed that in natural soils with pH-values of about 3 and higher, pyrite is mainly oxidized by oxygen via the following reaction:

$$FeS_2 + 3\frac{3}{4}O_2 + \tfrac{1}{2}H_2O \rightarrow Fe^{3+} + 2SO_4^{2-} + H^+ \qquad (5.15)$$

The fate of the produced Fe^{3+}, SO_4^{2-} and H^+ is considered in the chemical submodel. Neglecting oxidation by ferric iron is justifiable because above pH 3 ferric iron has

a low solubility. Furthermore, oxidation of pyrite by ferric iron in natural soils will be inhibited by complexation of ferric iron by organic substances, as was found for sewage sludge (Pitchel et al., 1989). Finally, in the case of pyrite oxidation by ferric iron, the concentration of ferric iron must be sustained by the oxidation of ferrous iron by oxygen, and thus oxygen is still the driving force for pyrite oxidation. In the model approach two main processes were distinguished: vertical diffusion of gaseous oxygen through air-filled macropores and lateral diffusion of dissolved oxygen from macropores into the saturated soil matrix (Fig. 5.6). The two processes interact at the walls of the macropores where gaseous oxygen dissolves into the matrix soil solution. The equilibrium between gaseous and dissolved oxygen at the walls of the macropores is described by Henry's law: $[O_2]_{air} = K_H * [O_2]_{water}$, in which K_H is Henry's constant. This constant is temperature dependent. At 20 °C, $K_H = 29.7$, at 30 °C, $K_H = 52$.

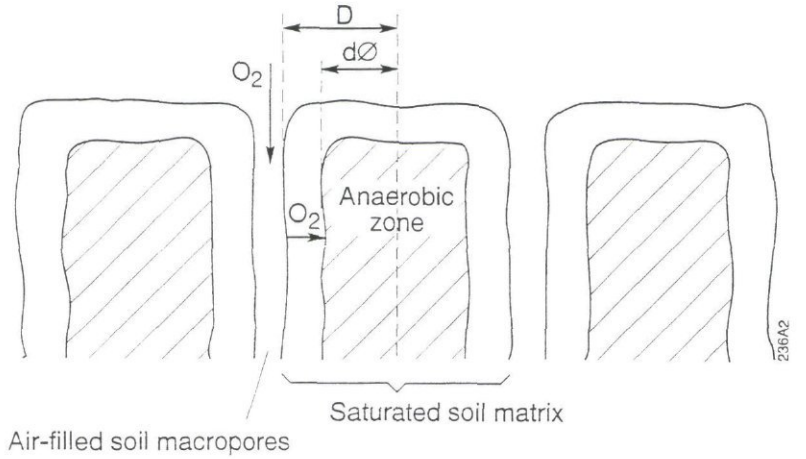

Fig. 5.6 Model approach for the distribution of oxygen in a structured acid sulphate soil, as applied in SMASS. Pyrite is still present in the anaerobic zones. D is the radius of the soil aggregates (m), d_0 is the radius of the anaerobic zone (m)

In SMASS, the gaseous oxygen concentration profile in the air-filled pores is calculated by:

$$\frac{\partial}{\partial x}\left(D_s(\varepsilon_g)\,\frac{\partial C_a(x)}{\partial x}\right) = \alpha_v \qquad (5.16)$$

where $C_a(x)$ = concentration of O_2 in air-filled macropores (m^3 O_2 per m^3 air), $D_s(\varepsilon_g)$ = diffusion coefficient of oxygen in air-filled pores (m^2 d^{-1}), x = distance (m), α_v = oxygen consumption rate in the soil (m^3 oxygen per m^3 soil per day), and ε_g = air-filled porosity. The relation between diffusion coefficient D_s, and air content, ε_g, is described in the model by:

$$D_s(\varepsilon_g) = F(1 - (1-\varepsilon_g)^{2/3})D_o \qquad (5.17)$$

where D_s = diffusion coefficient of O_2 in the atmosphere ($m^2\ d^{-1}$), F = an empirical tortuosity factor (dimensionless) and D_o = oxygen diffusion coefficient in air ($m^2\ d^{-1}$). To solve differential Equation (5.16), the oxygen consumption term α must be quantified. In the model, oxygen is consumed by two processes inside the soil matrix: decomposition of organic matter and oxidation of pyrite. According to Bronswijk and Groenenberg (1993) and Bronswijk et al. (1993) the steady state diffusion equation for the aerobic part of the soil matrix can be written as:

$$D_w \frac{d^2 C_w(x)}{dx^2} = \frac{0.311262 X_{Fe_{S2}}}{\rho d} \sqrt{C_w(x)} + Q \qquad (5.18)$$

where D_w = diffusion coefficient of O_2 in the soil matrix ($m^2\ d^{-1}$), C_w = concentration of dissolved oxygen ($kg.m^{-3}$), X_{FeS2} is the pyrite content ($kg.m^{-3}$), ρ = density of pyrite ($kg.m^{-3}$), d = average diameter of the pyrite crystals (m), and Q = oxygen consumption rate by organic matter ($kg.m^{-3}.d^{-1}$). According to Christensen et al. (1986) Q is taken constant. The first part of the right hand side of this equation expresses the disappearance of pyrite crystals by oxidation and is derived by combining the equal diameter reduction model with the McKibben and Barnes rate law for pyrite oxidation (McKibben and Barnes, 1986). Solving this equation with appropriate boundary conditions yields expressions for the steady state oxygen concentration profile in the aerobic part of the soil matrix, for the radius of the (an)aerobic zone, and for the total oxygen consumption per volume of soil. Subsequently this oxygen consumption is used to solve Equation (5.16) numerically.

The steady state oxygen consumption by pyrite oxidation is then computed as the difference between the total oxygen consumption and the (constant) oxygen consumption by organic matter. Next, from the stoichiometry of Equation (5.15) the amount of oxidized pyrite is computed, together with the produced quantities of Fe^{3+}, H^+, and SO_4^{2-}.

5.5 Chemical submodel (EPIDIM)

The important chemical processes occurring in acid sulphate soils are listed in Table 5.1. Pyrite oxidation is computed in the oxygen transport and pyrite oxidation submodel. All other chemical processes are modeled in the chemical submodel. This submodel is based on the existing EPIDIM model (Groenendijk, 1991). In the chemical submodel, changes in solution concentration, changes in adsorbed amounts, and changes in amounts of minerals and precipitates as a result of cation exchange and precipitation/dissolution reactions are calculated. Because cation exchange and precipitation/dissolution reactions are related to ion activities, ion association is considered as well. Each time-step, for each compartment, total amounts for each chemical component in solution and at the exchange complex are calculated from the amounts at the end of the previous time-step, the amounts released into the soil solution due to pyrite oxidation, and the net amounts transported to or from that compartment. From these total amounts, new concentrations, new adsorbed amounts and new amounts of minerals and precipitates are calculated.

Ion association and cation exchange are modeled as equilibrium processes, while precipitation and dissolution of minerals and precipitates are modeled as a kinetic process. The equations describing these different processes, are solved simultaneously. In various application of the SMASS model precipitation/dissolution has been modeled for $Al(OH)SO_4$ (jurbanite), $Al(OH)_3$ (gibbsite), $Fe(OH)_3$ (goethite), $CaCO_3$ (calcite), $CaMg(CO_3)_2$ (dolomite), and $CaSO_4$ (gypsum). If neccessary for a specific situation, other minerals can easily be included as well. It has been assumed that

Table 5.1 Chemical processes and their effects in acid sulphate soils. Processes included in SMASS are indicated with +.

Process	Effects	Included in SMASS
Rate limited		
Pyrite oxidation	acidification, produces Fe^{3+} and SO_4^{2-}	+
Iron oxidation	acidification, lowers Fe^{2+}-concentration	-
Iron reduction	de-acidification, raises concentration of Fe^{2+}	+
Sulphate reduction	de-acidification, raises sulphide concentration	-
Weathering of primary minerals	produces base cations, consumes protons	-
Weathering of secondary minerals	consumes protons, regulates Fe and Al^{3+} concentrations	+
Instantaneous		
Cation exchange	buffers pH and determines concentrations of Ca^{2+} and Mg^{2+}	+
Ion association	raises equilibrium concentrations, especially of Al^{3+}	+

the dissolution/precipitation rate of these minerals and precipitates is proportional to the difference between the actual activity product (Q_i) and its particular solubility product (K_i) (e.g. Kachanoski et al., 1992). The rate expression is formulated as follows:

$$\frac{dB_i}{dt} = K(Q_i - K_i) - \frac{\theta}{\rho} \qquad (5.19)$$

where B_i = amount of a precipitate ($mol.kg^{-1}$), K = a rate constant, ρ = dry bulk density of the soil ($kg.m^{-3}$) and θ = volumetric water content. This differential equation is approximated with finite differences.

Because the concentrations of NO_3^- in acid sulphate soils are often small and amounts of Mn(III/IV)-oxides are generally negligible, the most likely electron acceptor in redox reactions is Fe^{3+}. Reduction of ferric oxide is described by:

$$Fe(OH)_3 + \frac{1}{4}CH_2O + 2H^+ \rightarrow Fe^2 + \frac{1}{4}CO_2 + \frac{11}{4}H_2O \qquad (5.20)$$

in which $Fe(OH)_3$ represents any reducible ferric oxide and CH_2O represents organic matter. In SMASS iron reduction starts when a soil layer is saturated with water. The model distinguishes two forms of ferric oxides: reducible ferric oxide and non reducible ferric oxide. Reducible ferric oxide is formed when Fe^{3+} precipitates. The

transformation of reducible ferric oxide into non-reducible ferric oxide is described according to:

$$\Delta[Fe(OH)_3^R] = -k_1(pH)\ [Fe(OH)_3^R]\delta t \qquad (5.21)$$

in which $[Fe(OH)_3{}^R]$ = amount of reducible ferric oxide ($mol.kg^{-1}$) and $k_1(pH)$ = rate constant (h^{-1}). In the model the pH dependency of the rate constant $k_1(pH)$ is described with an exponential function which fits the data of Schwertmann and Murad (1983). If reducible ferric oxide is present in a soil layer and this compartment is saturated with water, the reduction of reducible ferric oxide is described by:

$$\Delta[FE(OH)_3^R] = -k_2\Delta t \qquad (5.22)$$

in which k_2 = rate constant ($mol.k^{-1}\ h^{-1}$). New amounts of reducible ferric oxide are calculated by combining Equations (5.21) and (5.22) and adding the amount of precipitated $Fe(OH)_3$ calculated in the precipitation/dissolution subroutine. From the amount of ferric oxide reduced, the produced amounts of Fe^{2+}, OH^- and HCO_3^- are calculated using the stoichiometry of Equation (5.20). Cation exchange is modeled according to the Gaines-Thomas expression (see Bolt, 1967).

6 Calibration and validation of SMASS

6.1 Calibration and validation using data from the Tarantang experimental field

6.1.1 Calibration of the waterflow model SWAP

Since an important focus of this project is to study and simulate the mutual lateral influence between the soil and the adjacent surface water (both hydrological and chemical), the lateral flows of water and solutes between the field and the surface water are of particular interest during the calibration. The aim of calibrating the waterflow model is to ensure simulation of the water balance as accurate as possible, especially the lateral water fluxes, being the main driving force behind the chemical fluxes.

A calibration procedure was followed in which the measured groundwater table was the target quantity for calibration. This means that measured and calculated groundwater level were compared for calibration of the model. Another possible target quantity would have been the volumetric water content (theta) as a function of depth, but since the profile was saturated for almost nine months per year, this quantity was regarded less suitable in this situation.

The top boundary condition was the combination of a measured potential pan evaporation, a measured daily precipitation and an estimated irrigation gift. The lateral boundary condition was the measured surface water level in the ditches adjacent to the experimental field. The bottom boundary condition was zero-flux at a depth of -140 cm below soil surface, implicitly assuming that the layer below 140 cm with unripe clay has a very low hydraulic conductivity and hardly plays any role in the hydraulic system.

The year 1996 was used for calibration of SWAP. The day of planting of the local rice variety was taking as staring point. During the crop period the farmers applied surface irrigation by allowing in water from the ditches into their fields during high tide. In this period the field was pounded and the soil profile saturated. The rice crop was harvested after 4 months, and the field was left bare for the remaining period. Irrigation was stopped. The field drained to a level of about 50 cm depth.

Two input parameters which were not measured in the field, were obtained through calibration: the drainage resistance and the irrigation gifts. Firstly, the drainage resistance was obtained using data from the period between harvest (May 31) and the day on which unsaturated conditions occur for the first time after the growing season (August 1). In this period no irrigation was given. A drainage resistance of 300 days yielded the best correspondence between measured and calculated groundwater levels.

Secondly, the data covering the growing season (February 2 - June 1) and the found drainage resistance, were used to obtain the approximate surface irrigation gifts. It turned out to be impossible to measure irrigation quantities on a daily basis under given water management (see Section 3.3). Furthermore, farmers individually determine the water management for their own fields, by operating the gorong-gorongs (flapgates). Monitoring of this process was not easy and it required the permanent presence of a researcher in the field. Further, it was hard to estimate the precise amount of water that entered the field under this type of surface irrigation. Due to these difficulties, no accurate data were collected on the irrigation quantities. Therefore it was decided to get hold of these quantities through calibration of the waterflow model. A total irrigation gift of 250 mm.a^{-1} yielded the best correspondence between measured and calculated groundwater levels during the growing season.

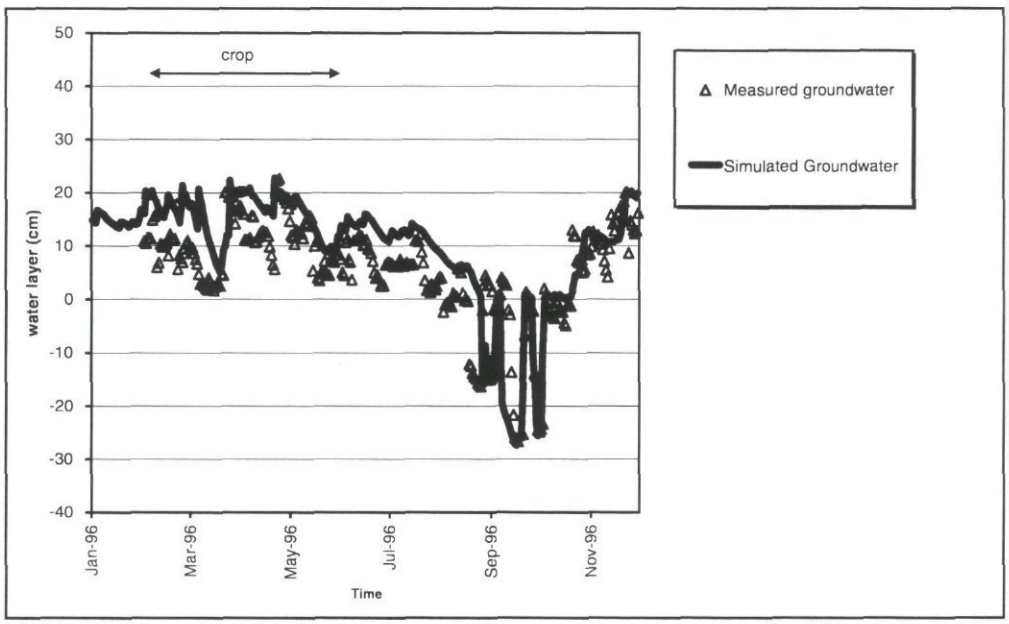

Fig. 6.1a Measured and simulated groundwater levels, Tarantang experimental field

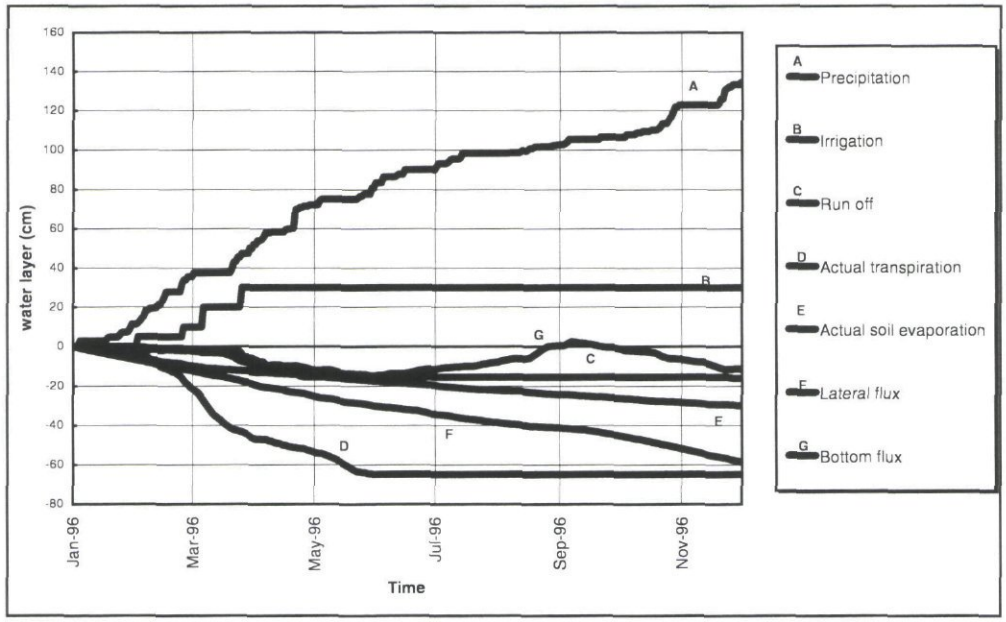

Fig. 6.1b Calculated waterbalance, Tarantang experimental field

Fig 6.1 shows the results of the calibration. Over the year the groundwater table could be simulated reasonably well. The cumulative evaporation and transpiration are 30 and 60 cm respectively. Over a period of 299 days the calculated cumulative net lateral drainage of the field was 60 cm. No subirrigation was calculated.

For calibration of SMASS, values for input parameters not measured in the field, were taken from AARD/LAWOO (1992), a study in which the 1 dimensional model was applied to similar fields in Pulau Petak, South Kalimatan. Further, data from Tarantang experimental field (period April 1, 1995 to December 31, 1995) were used. Presence and initial concentrations of secondary minerals, such as amorphous ferric iron hydroxide ($Fe(OH)_3$) and jurbanite ($AlOHSO_4$) were obtained through calibration.

6.1.2 Validation of SMASS

The Figures 6.2 tot 6.6 show the results of the validation experiment. The rapid leaching of conservative ions like sulphate and chloride is well simulated by the model (Fig. 6.2 and 6.3). The development of Fe^{2+} concentrations in the top soil could be simulated reasonably well (Fig 6.4), whereas in deeper layers the model predicts considerably higher concentrations than was measured. Vertical, downward fluxes of Fe^{2+} produced in the topsoil during oxidation causes these high concentrations in the subsoil. Al^{3+} concentrations showed similar patterns. The pH values (both measured and simulated) where relatively stable and could be simulated reasonably well.

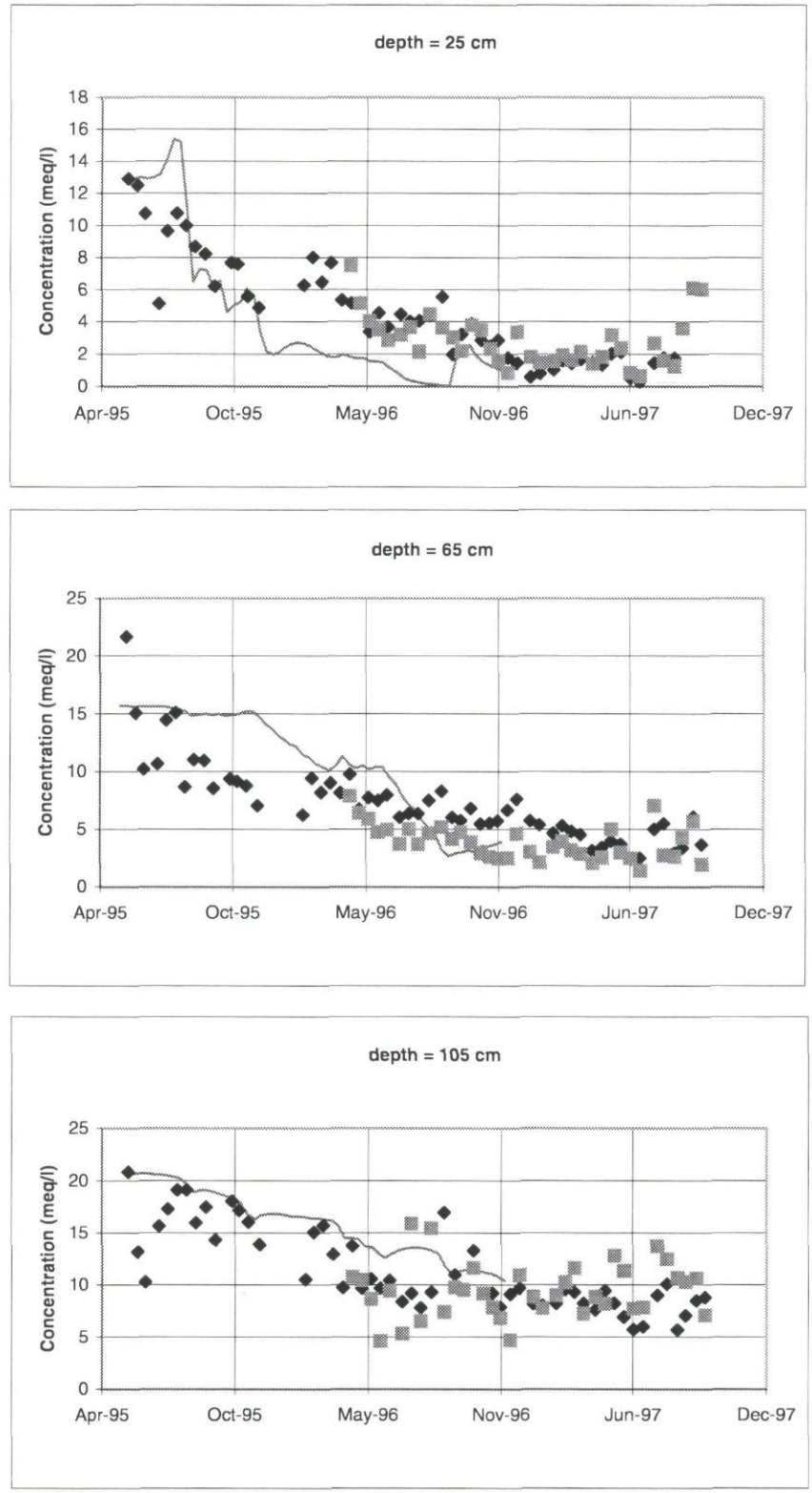

Fig. 6.2 Measured and simulated SO_4^{2-} concentrations as a function of time in the Tarantang experimental field

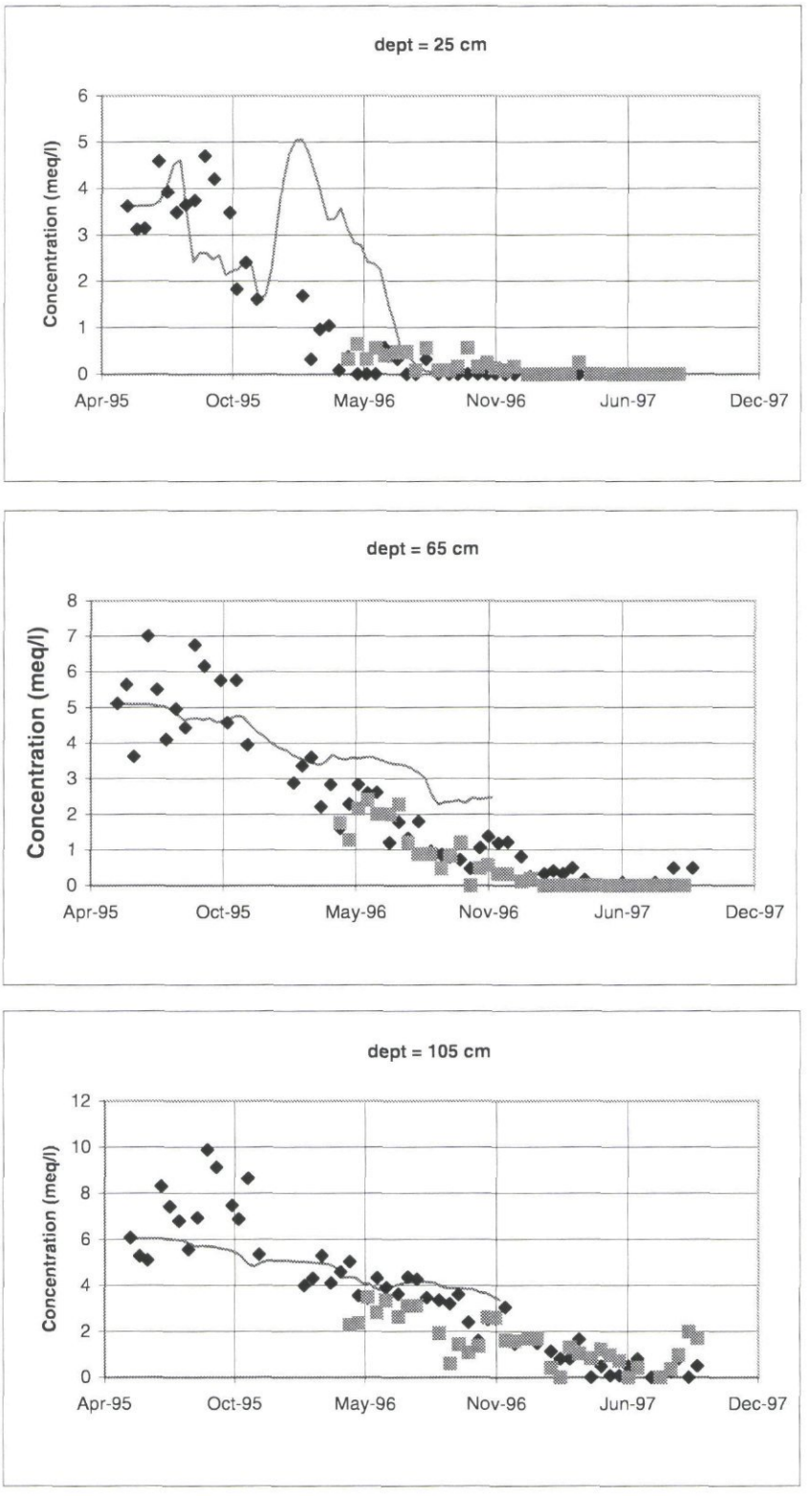

Fig. 6.3 Measured and simulated Cl^- concentrations as a function of time in the Tarantang experimental field

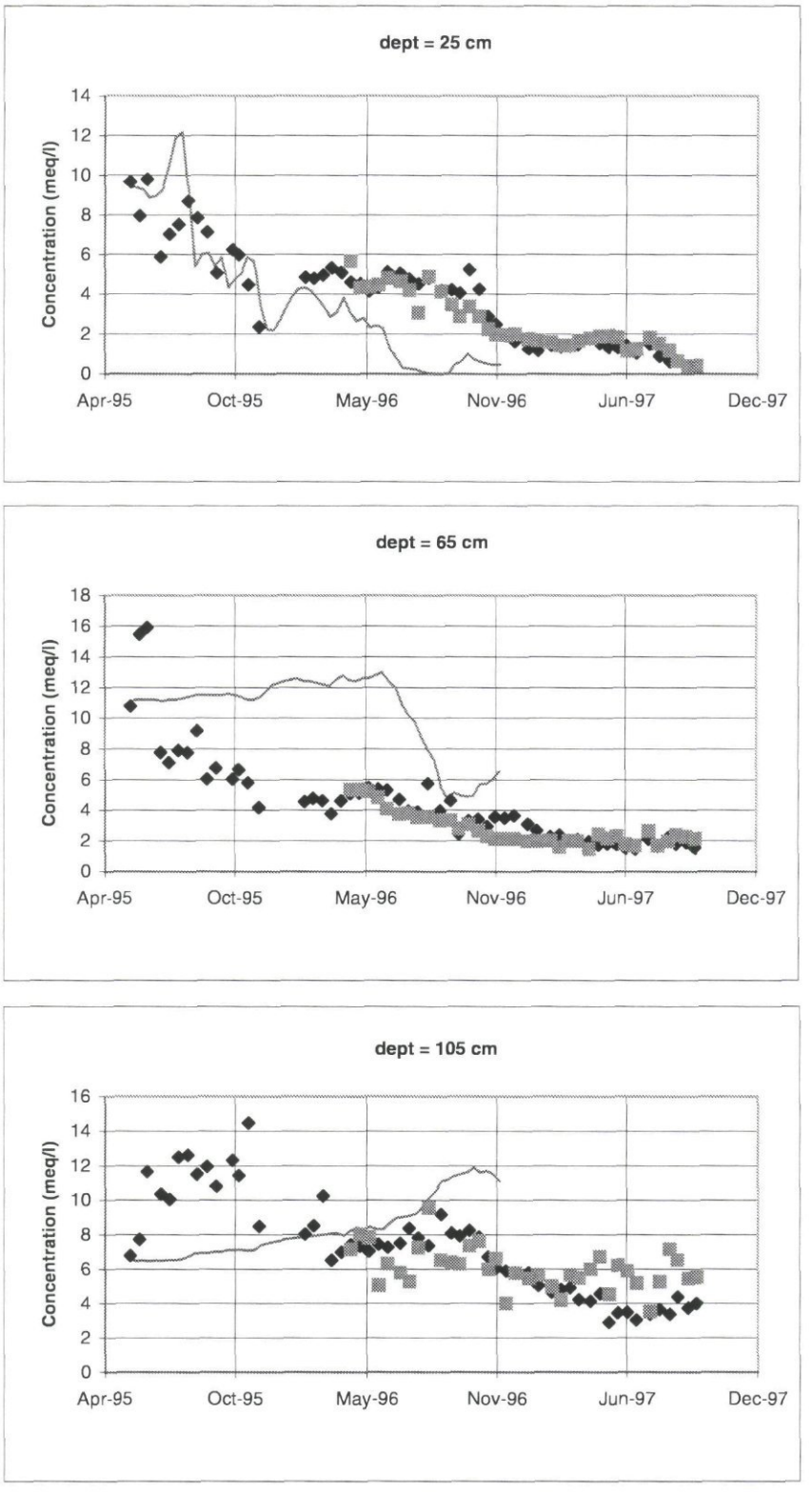

Fig. 6.4 Measured and simulated Fe^{2+} concentrations as a function of time in the Tarantang experimental field

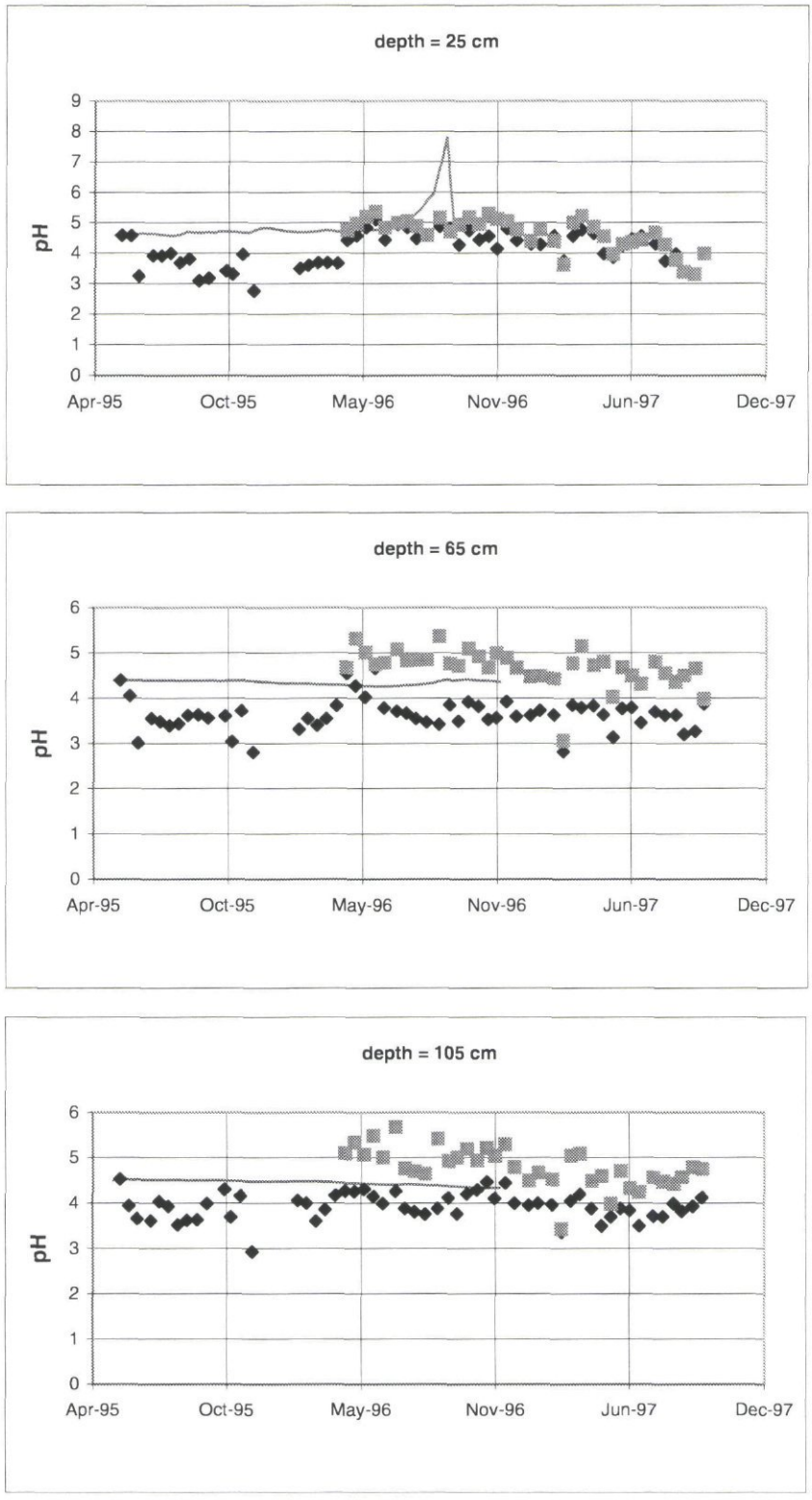

Fig. 6.5 Measured and simulated pH values as a function of time in the Tarantang experimental field

6.2 Calibration and validation using data of a disturbed acid sulphate soil, Ly Nhon

6.2.1 Calibration

Calibration of SMASS consists of two steps: calibration of physical parameters used within SWAP and calibration of physico-chemical parameters used within SMASS submodels. For the calibration of SWAP, drainage resistance values were the most important parameters. These values comprise resistant coefficients of soil media and of canal wall where water flow occurs in either directions. Due to unripe structure of the soil under investigation, the resistances were found relatively small; in the order of 10^{-2} days. For the chemical part of the model, pyrite characteristics were used to calibrate SMASS. These characteristics consists of size of soil structural elements and mean diameter of pyrite crystal. The pyrite content determined by different methods was fixed in input file.

Initial conditions were taken from data set of the nest S4 where data quality is the best. Therefore, calibration results are also compared to this data set. Soil tension was used as a main criterium for judging the calibration. Besides, oxygen concentration of soil horizons are also used. For chemical calibration, pH and Na were used during the calibration: calibrated parameters were adjudged until these controlled criteria met measured values.

6.2.2 Validation

The whole process occurring within a mound (dike) constructed in coastal areas is controlled by two main phenomena: oxidation process in upper horizons and leaching downwards for acidification and horizontal flow and upward capillary for salinisation. The distinct characteristics between acidified horizons (15, 30 and 50 cm from soil surface) and saline horizons (below 80 cm) are observed and simulated very good by SMASS. Some validation results are shown in Figures 6.6 - 6.10

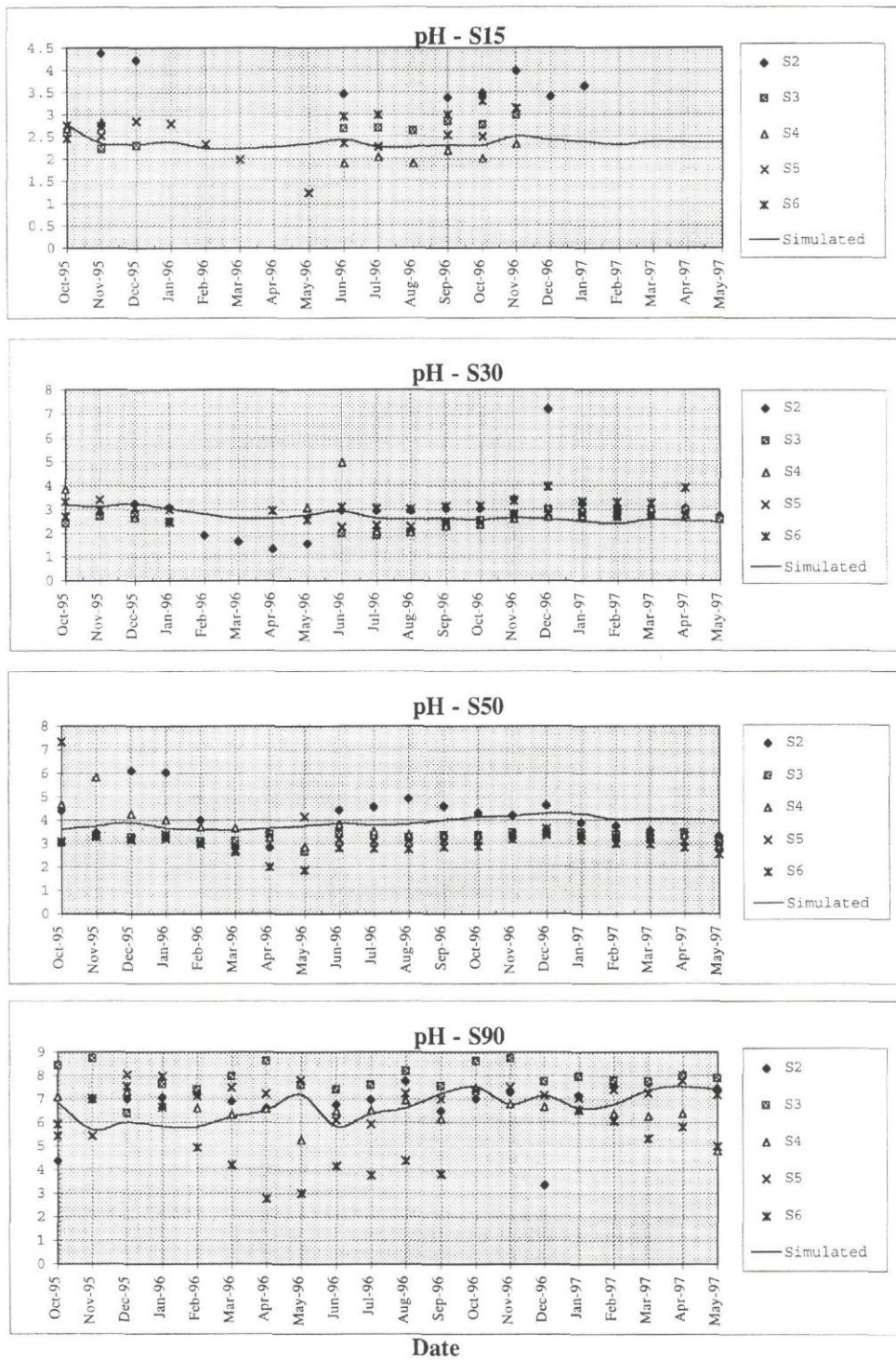

Fig. 6.6 Calibration result: pH of soil solution in the mound

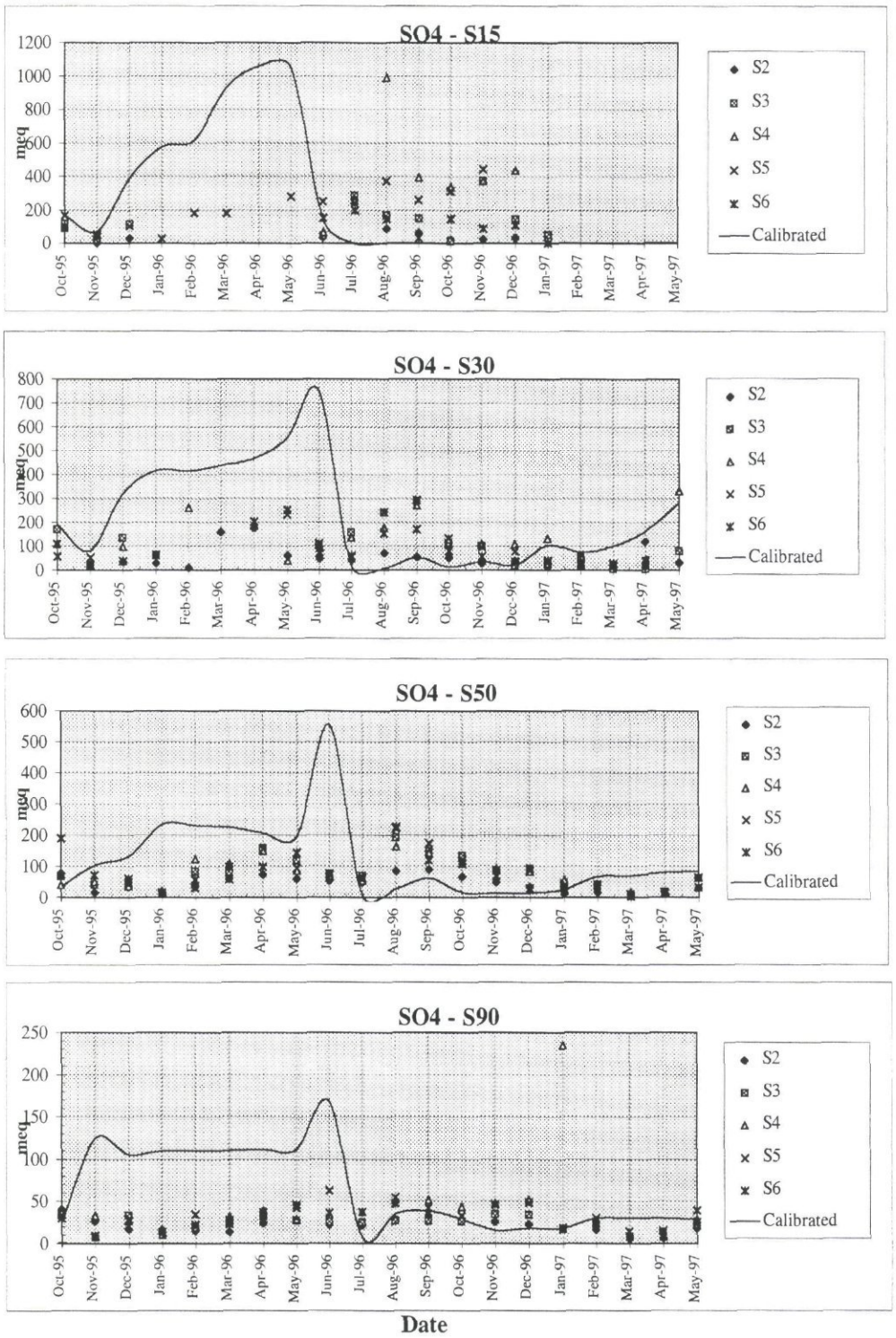

Fig. 6.7 Calibration result: SO_4^{2-} concentration in the mound

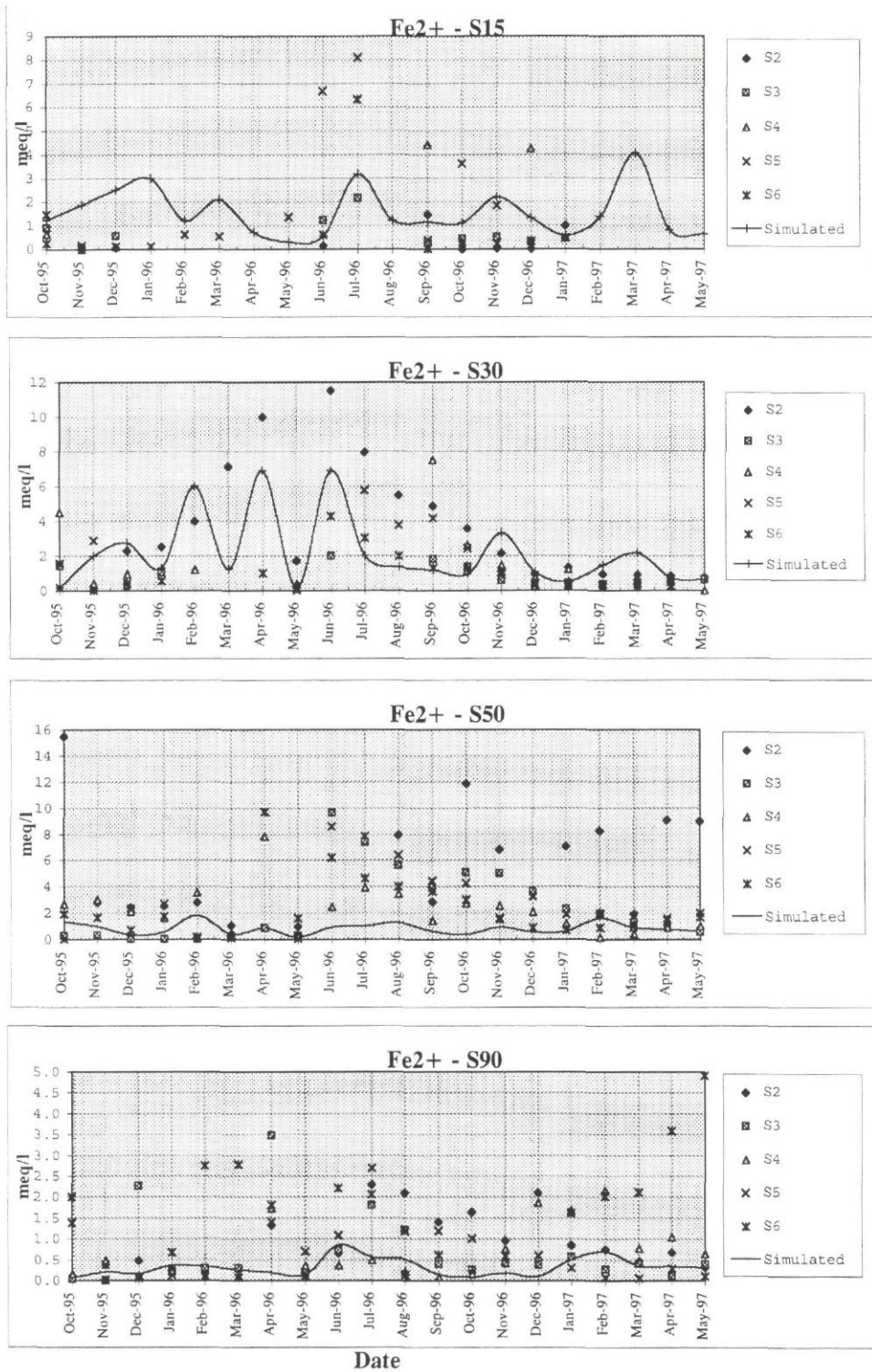

Fig. 6.8 Calibration result: Fe^{2+} concentration in the mound

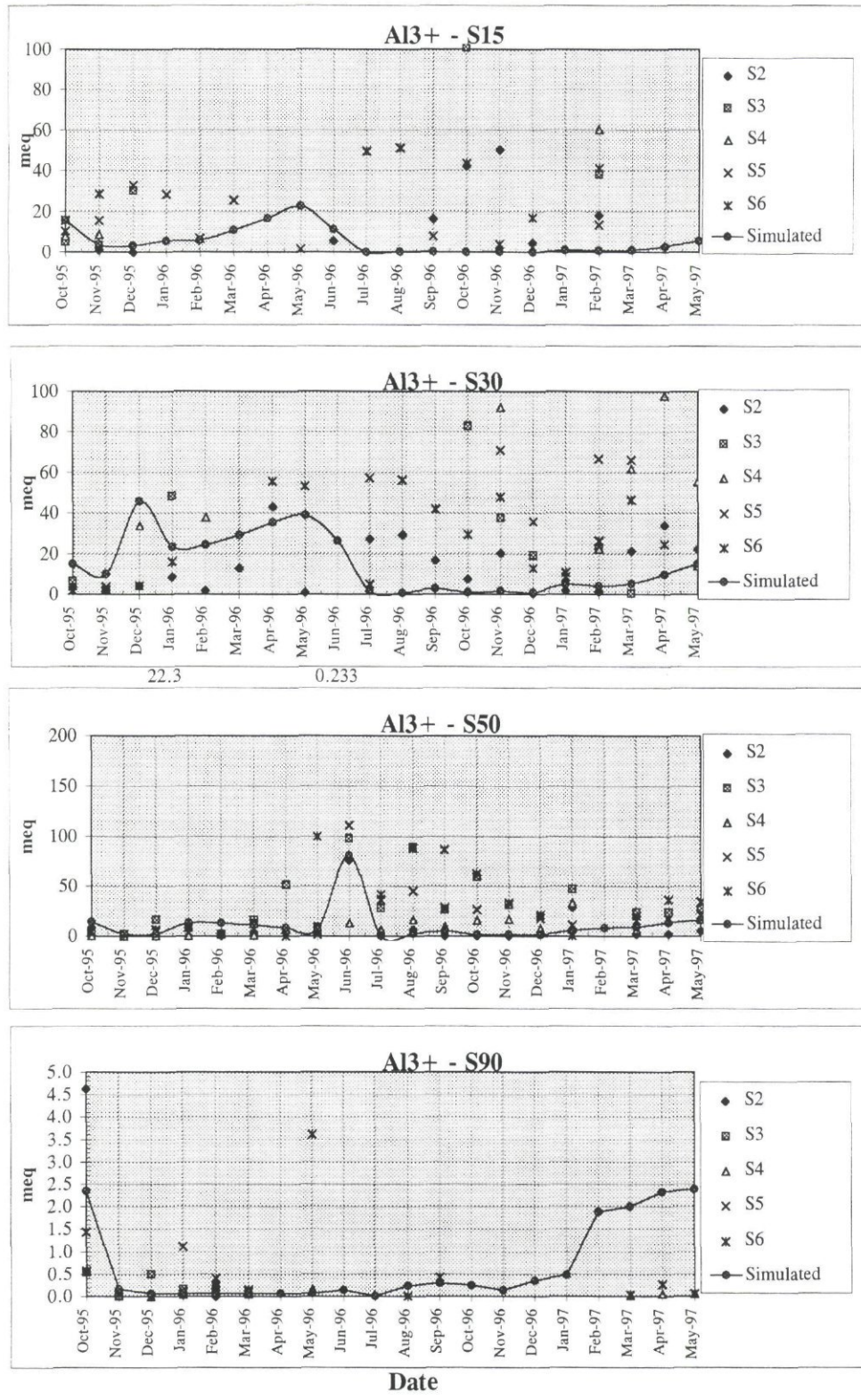

Fig. 6.9 Calibration result: Aluminium concentration in the mound

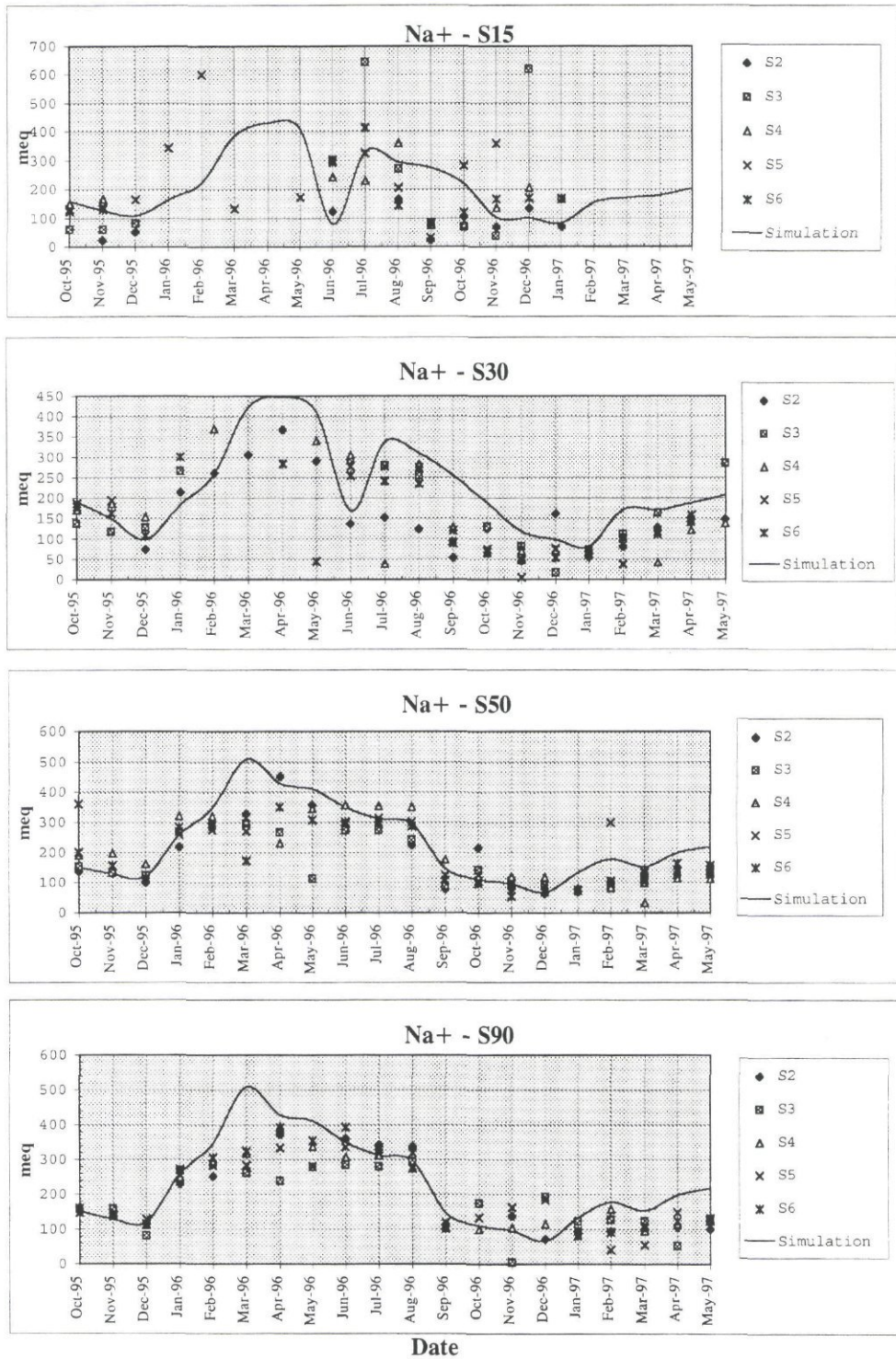

Fig. 6.10 Calibration result: Sodium concentration in the mound

6.2.3 Conclusions

The comparisons of measured and simulated data showed good results: the model can simulate the distinctive processes and their interactions occurring within a pyritic soil profile of a mound constructed in the saline area of Ly Nhon. However, some elements are still poor simulated like Mg^{2+}, Al^{3+}, and Fe^{2+}. Because many of the technical difficulties to get reliable data in the case of unsaturated soil of a mound, it is not easy to judge whether the differences between measured and calculated data are due to inaccuracy of measurements or of simulations. Generally, the major processes and elements in soil solution were good simulated.

7 Description of reference sites for Indonesia and Vietnam

7.1 Indonesia

7.1.1 General description

In the Soil map of the world (FAO/UNESCO, 1979), the distribution of the major soils in Indonesia was given. Most of the wetland areas were classified as Entisol, Histosol, and partly as Inceptisols. In some parts the soil is more developed, and gives more pronounced profiles. All soils originated from an unripe soil mineral material or organic material or a combination of both. The variability of soil characteristics in the humid tropics is well known, and the soils in Indonesian wetlands are a good example of this. Delineation of soil units is hard.

The acid sulphate soils cover more than 1% of Indonesia, and almost 10% of the Indonesian wetlands. The exact location and extent of Indonesian acid sulphate soils are not yet completely known. Generally they occur in young marine deposits along the coasts of Sumatra and Kalimantan and some places in Java (see Fig. 7.1).

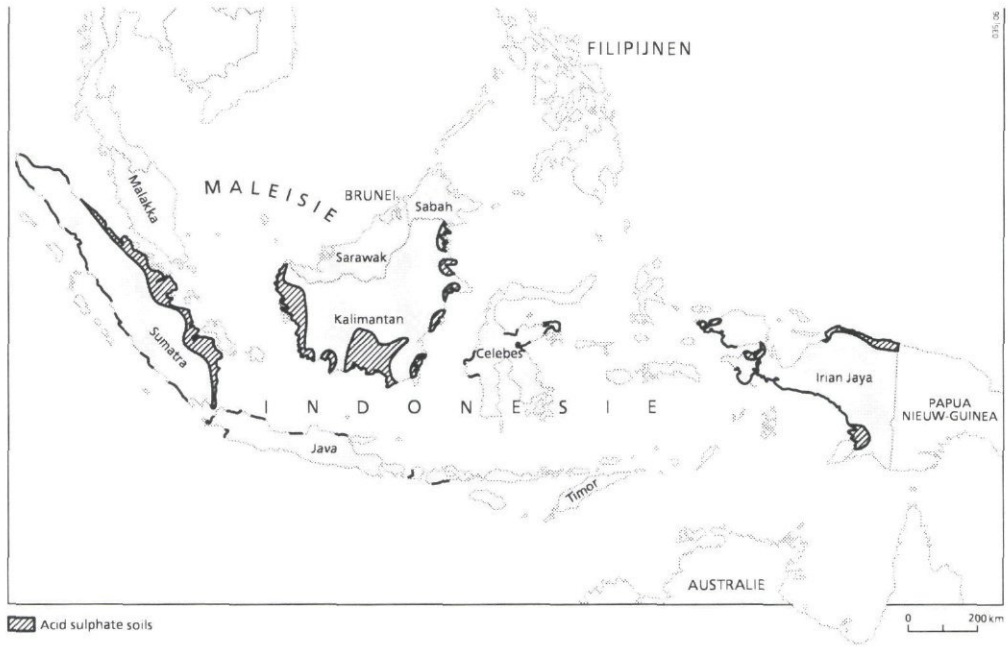

Fig. 7.1 General occurrence of acid sulphate soils in Indonesia

Acid sulphate soils in Indonesia can be classified as was done in Table 7.1.

Table 7.1 Classification of acid sulphate soil in Indonesia

Class	Description	Main geographical occurrence
Asa: Dominant Actual Acid Sulphate Soil	mineral soil, with pyrite concentration (0-6%) in the tops soil and higher in the sub-soils , mainly in reclaimed coastal areas, and back swamps, with artificial drainage	all area's indicated in map
Asp: Dominant Potential Acid Sulphate Soil	mineral soil, with pyrite concentration (2-6%) start from soil surface, mainly in unreclaimed coastal areas, and back swamps	all area's indicated in map
Asa/S: Dominant Actual Acid Sulphate Soil with Saline Soil	mineral soil, with pyrite concentration (0-6%) in the tops soil and higher in the sub-soils , mainly in reclaimed coastal areas, and back swamps, with artificial drainage, salt intrusion were l obvious	all area's indicated in map
Asa/P: Dominant Actual Acid Sulphate Soil with Peat Soil	mineral soil, with pyrite concentration (0-6%) in the tops soil and higher in the sub-soils , mainly in reclaimed coastal areas, and back swamps, with artificial drainage, have a high organic matter contents or peat soil in the top or some of sub-horizon.	all area's indicated in map
S/ASa: Dominant Saline Soil with Actual Acid Sulphate Soil	mineral soil, with high salt concentrations and having pyrite concentration (0-6%) in the tops soil and higher in the sub-soils , mainly in reclaimed coastal areas, and back swamps, with artificial drainage	all area's indicated in map
Asp/S: Dominant Potential Acid Sulphate Soil with Saline Soil	mineral soil, with pyrite concentration (2-6%) start from soil surface, mainly in unreclaimed coastal areas, and back swamps with salt intrusion	all area's indicated in map
Asp/P: Dominant Potential Acid Sulphate Soil with Peat Soil	mineral soil, with pyrite concentration (2-6%) start from soil surface, mainly in unreclaimed coastal areas, and back swamps with high organic matter or peat soil in the top	all area's indicated in map
S/ASp: Dominant Saline Soil with potential Acid Sulphate Soil	mineral soil, with high salt concentration and pyrite concentration (2-6%) start from soil surface, mainly in unreclaimed coastal areas, and back swamps	all area's indicated in map
P/AS: Dominant Peat Soil with Actual Acid Sulphate Soil	organic soil, with pyrite concentration (0-6%) in the tops soil and higher in the sub-soils , mainly in reclaimed coastal areas, and back swamps, with artificial drainage.	all area's indicated in map
P1: Shallow Peat soil which have pyrite (sulphidic material)	organic soil between 50- 100 cm thick, with pyrite concentration (2-6%) in the tops soil, mainly in unreclaimed coastal areas, and back swamps	all area's indicated in map
P2: Medium Peat soil which have pyrite (sulphidic material)	organic soil with peat thickness of 100-200 cm and pyrite concentration (2-6%) in the tops soil, mainly in unreclaimed coastal areas, and back swamps	all area's indicated in map
P3: Deep Peat soil which have pyrite (sulphidic material)	organic soil with peat thickness of more than 200 cm and pyrite concentration (2-6%) in the tops soil, mainly in unreclaimed coastal areas, and back swamps	all area's indicated in map
P: Soil with very deep pyritic layer (> 120 cm)	mineral or organic soil, with pyrite concentration (2-6%) in the sub soil, mainly in unreclaimed coastal areas, and back swamps	all area's indicated in map

7.1.2 Description of tidal land classes

Topography, tides, climate, and hydraulic properties of the soils are the most important factors that determine the hydrology. By combining these parameters into classes, areas with similar hydrological properties can be mapped. Using these hydrological maps in combination with soil maps, recommendations can be made for water management and land use.

In Indonesia, four tidal land classes (TLC) are distinguished in tidal swamp areas (Noorsyamsi, 1976) and later finetuned by AARD/LAWOO (1992). The classification mainly focuses on the possibilities for irrigation by flooding and drainage (see Fig 7.2). A brief description of the tidal land classes is given below.

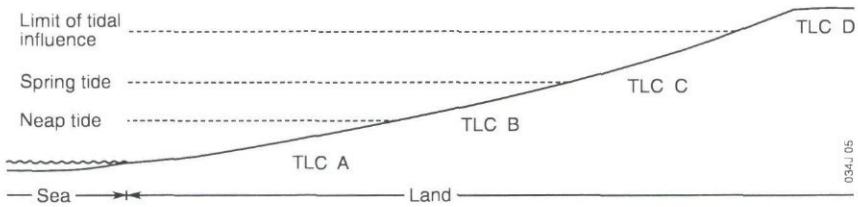

Fig. 7.2 Schematic cross section of Indonesian tidal swamps and its tidal land classes

Tidal land class A

Area between mean low tide and mean neap tide; daily flooding and shallow drainage occurs. TLC A occurs in almost all coastal areas in Indonesia. Almost everywhere in this TLC acid sulphate soils occur. Pyrite concentrations vary between 3 and 10%. In most cases the pyritic layer starts directly from the soil surface. In natural conditions the pyrite has not yet been exposed to drained conditions due to frequent flooding (potential acid sulphate soils). In long dry seasons, water tables can drop below the soil surface, immediately followed by severe acidification and the release of toxic elements. Salinity, especially in the dry season, is a major restriction for crop growth. Usually no fresh water is available.

In this tidal land class with potential acid sulphate soils, prevention of acidification is seen as the best option for land use. One-way flow water management is advised here. The system was applied in combination with the use of high tide water for irrigation. To handle the excess of water, the system was combined with surface drainage or intensive shallow drainage on field level, with a spacing of 12 m. The drainage canals should have a width of 40 cm and a depth of 20 cm.

Usually the land in TLC A the cropping pattern rice-rice is applied. Upland crops, such as coconut trees, pineapple or rambutan, are sometimes grown on raised beds, which have been leached from toxics by rainwater. This diversification usually increases farmers' income.

Tidal land class B

Area between mean neap tide and mean spring tide, with flooding during spring tide, and daily drainage. Irrigation water can only be brought to the field during springtide. TLC B occurs in almost all coastal areas in Indonesia. Almost everywhere in this TLC acid sulphate soils occur, both potential and actual. Pyrite concentrations vary between 3 and 10%. In natural situations, the area is flooded continuously during the wet season, whereas during the dry season fortnightly flooding during springtide occurs in combination with drainage between 50 and 100 cm depth.

One-way flow water management is advised here, reducing acidification by leaching, which was successfully tested in Pulau Petak, South Kalimantan. Good quality high tide water was used for irrigation, resulting in effective leaching of different toxic elements such as Al^{3+}, Fe^{2+} and SO_4^{2-}. To handle the excess of water, the system was combined with surface drainage or intensive shallow drainage at field level.

Since the area is inundated during high tide, rice-rice or rice-upland crop are common cropping patterns. Water availability is sufficient for two rice crops per year.

Tidal land class C

Area above spring tide, with no regular tidal flooding and permanent drainage. In TLC C predominantly actual acid sulphate soils occur, with pyrite starting at 40 cm below soil surface in moderate concentrations. However, the top soil is usually heavily acidified. Flooding is rare and drainage occurs up to a level of 100 cm.

Water management is aimed at leaching out the toxic elements from the top soil. Usually a one-way flow water management strategy is applied in combination with intensive shallow drainage (optimal spacing of 9 m). During low tide, drainage of the fields, by deliberately lowering the water in the canals, occurs, accelerating leaching. Precipitation water is used for leaching, since it is the best quality water available in the areas. Water conservation is applied during the growing season to prevent water stress in rice cultivation. Research showed that optimal water management increased rice yields with 40%. Puddling and liming is applied.

Rice-upland crop and continuous upland crop are common cropping patterns in TLC C. During the rainy season enough water is available for leaching and rice production, whereas in the dry season water availability is a constraint for rice production. Water control for upland crops is relatively easier than for rice. Shallow drainage helps to control the water supply for upland crop.

Tidal land class D

Area outside the tidal influences; no tidal flooding and limited drainage due to the absence of drainage infrastructure. Only during the dry season the water table drops below soil surface (to 50 cm), when evaporation exceeds rainfall. TLC D, when covered with primary or secondary forest, often serves as fresh water supply for acidified land in the surrounding area. For this reason, protection of the forest area has high priority. Mineral soils are usually covered with a peat layer, with low water retention. In saturated conditions water content is high and water is released from the soil very easily. The pyritic layer generally starts directly from the surface.

Drainage of the soil with subsequent subsidence immediately leads to severe oxidation. Leaching of toxics is difficult due to frequent waterlogged conditions. Water management is aimed at safeguarding the area's function of fresh water supply for the surroundings. The water is used for agricultural purposes as well as drinking water supply.

Rice cultivation is only possible in combination with pump irrigation, since no tidal flooding occurs. In some cases farmers have organised themselves to purchase and maintain pumps. But because of the limited fresh water availability and the importance of the area for fresh water generation, upland crops are preferred and recommended.

7.2 Mekong Delta, Vietnam

Land use in acid sulphate soil zones in the Mekong delta is diverse. The land use changed due to economic reason and irrigation water availability. Main crops in those areas are still wet land rice and some upland crops on raised bed such as pineapple, yam, cassava, sugar cane. Many successful trials are observed. However in some regions where favourable conditions are still remaining, malaleuca is dominant.

In most of areas where the farmers manage to develop profitable and sustainable land uses system, the common condition is fresh water availability. In remote zones with saline intrusion and without fresh water, it is still difficult to find a solution. The best economic land use for these regions is aqua farming, especially shrimp farming. There was a time when farmer expanded farming areas and tried to change from traditional farming method to intensive method. It resulted in hazardous water environment and repeated shrimp pests. Due to knowledge and experience lacking in such activity, it is still far to reach a sustainable situation for the region.

Referred to the map in Fig. 7.3 and the Tables 7.2 and 7.3, it can be recognised that major constraints in acid sulphate soil exploitation is fresh water unavailability. When irrigation canals systems are built, suitable water and land managements can help change the abandoned areas into multi-cropping lands in a few years. Impacts of pyrite horizon disturbance activities such as canal and pond construction on water quality and eco-systems are also well recognised. The fact is the basic reason leading to field studies described in Chapter 4 of this report.

Table 7.2 Description of hydrological conditions of areas with acid sulphate soil in the Mekong delta.

Zone	Flooding depth (cm)	Irrigation type	Drainage class	Acidity		
				severe (%)	moderate (%)	slight (%)
1	30 - 60 cm	Gravity	3	10	40	50
2	30 - 60 cm	Rainfed	2	15	55	30
3	30 - 60 cm	Rainfed	4	70	20	10
4	60 - 100 cm	Rainfed	3	80	15	5
5	Tidal flood	Rainfed	1	pAAS	pASS	pASS
6	100 - 150 cm	Power	5	20	50	30
7	60 - 100 cm	Power	5	70	25	5
8	30 - 60 cm	Rainfed	4	60	20	10
9	100 - 150 cm	Power	5	10	60	30
10	> 150 cm	Power	5	90	5	5
11	60 - 100 cm	Power	5	95	3	2
12	Tidal flood	Rainfed	4	pASS	pASS	pASS

Source: Tinh T.K. and Tri L.Q., (1991) Zoning acid sulphate lands for land uses, soil improvement and management. In: Collection of papers presented at the workshop on Management of Acid Sulphate Soil Project.

Notes: pASS= potential acid sulphate soil

Drainage classes:

1 can be drained when canals are available
2 good during dry season, difficult during wet season
3 good only during dry season (neap tide)
4 possible only when neap tide in both dry and wet season
5 good during dry season and earlier time of wet season

Table 7.3 Land uses of acid sulphate soil zones in the Mekong delta

Zone	Saline intrusion	Fresh water	Land use/vegetation
1	No	Yes	Rice, upland crops in raised bed
2	Yes	Yes	Rice, pineapple in raised bed
3	Yes	No	Shrimp farming, rice
4	Yes	No	Malaleuca, rice
5	Permanent	No	Mangrove forest, shrimp farming
6	No	Yes	High yield rice (2 crops)
7	No	No	Malaleuca, rice
8	Yes	No	Pineapple, rice
9	No	Yes	High yield rice (2 - 3 crops)
10	No	Yes	High yield rice (1 - 2 crops)
11	No	Some	Malaleuca, yam, cassava, sugar cane, rice
12	Yes	No	Rainfed rice

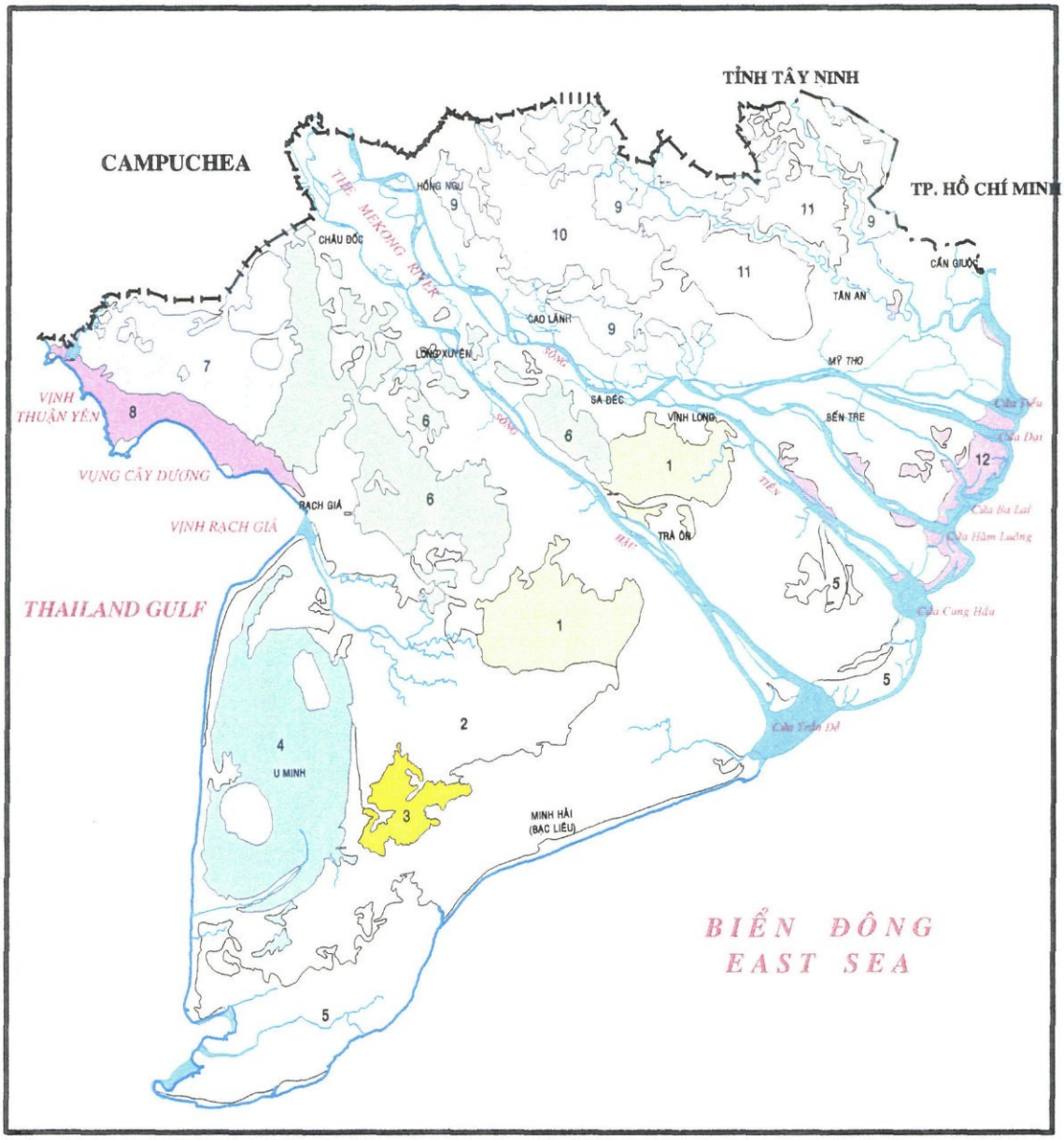

Sources: Phong T.A. et al, 1993. The soil map of the Mekong delta
Tri L.Q.and T.K. Tinh, 1990. Problem soils project report

Fig. 7.3 Acid sulphate soil zones in the Mekong Delta

8 Testing water management strategies for sustainable use of acid sulphate soils in coastal lands in the tropics

8.1 Scenarios Indonesia

8.1.1 Introduction

Scenarios were evaluated for TLC B, a land class under high reclamation pressure in Indonesia now and in the future. In this land class, CSAR conducted a lot of research projects aiming at optimising cropping patterns. One of the most frequently applied cropping pattern in acid sulphate soils is the so-called Sawitdupa system. Sawitdupa is an idiom for 'once planting and twice harvesting'. The technique is developed in view of Indonesia's wish to be self-sufficient in rice production. Two rice varieties (high yielding variety and local variety) are combined. During the growth of the short duration high yielding variety, the local variety is in nursery and in first transplanting stages, located at the outer fringes of the field. Harvest of the high yielding coincides with the last transplanting (to full field) of the local variety. The cropping pattern allows for efficient water use. Yields on yearly basis and economic returns are higher. Research carried out in Tarantang showed that rice yields increased from about 2 to 3 ton.ha^{-1}.a^{-1} under the SAWITDUPA system. The method has been recognized as the best system of rice cultivation in acid sulphate soils. Irawan (1995) stated that farmers' adoption of the technology is quite good. Further development and finetuning of Sawitdupa is high priority for CSAR and AARD (Agency for Agricultural Research and Development).

The scenarios tested in this chapter are all based on the water management strategy, required for implementing the Sawitdupa system (Fig. 8.1). The scenarios differ in soil type and climate (see Table 8.1). An actual and potential acid sulphate soils were used. The Sawitdupa system is currently predominantly applied in areas with actual acid sulphate soils and the effects of this system on the long run are tested in scenario 1. The Tarantang experimental field is a typical example of this. This land management is going to be applied in the very near future on large scale in areas with potential acid sulphate soils as well, with pyrite starting from the top of the soil profile (scenario 2). The Sawitdupa system is especially designed to leach out toxics from the soil profile. For the leaching efficiency of the system, the amount of rainfall surplus is important. The years 1996 and 1997 have been dry years, with average annual rainfall averaging 1100 mm. The effects of such a low rainfall on the leaching for Sawitdupa on both actual acid sulphate soils and potential acid sulphate soils is tested in scenarios S3 and S4.

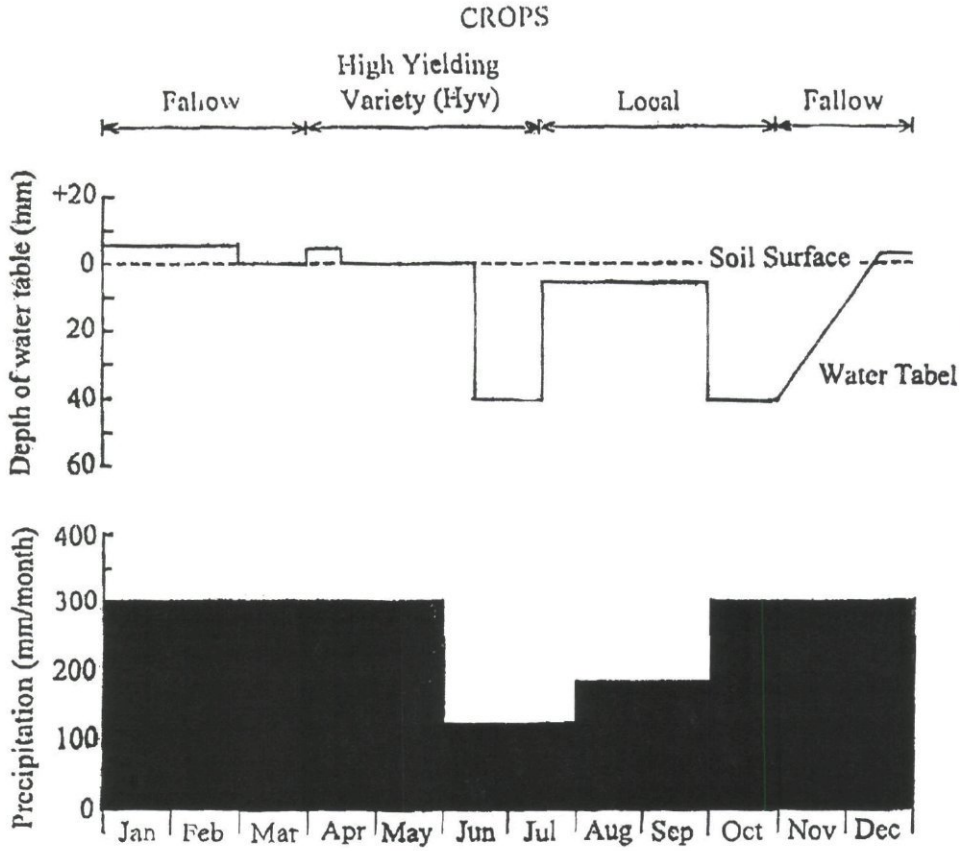

Fig. 8.1 Cropping pattern, water management and precipitation for all scenario's, based on SAWITDUPA system

Table 8.1 Scenarios tested for Indonesian reference sites

Scenario	Water/crop management	Soil	Climate
S1	Sawitdupa	actual ASS	average rainfall (2300 mm.a^{-1})
S2	Sawitdupa	potential ASS	average rainfall (2300 mm.a^{-1})
S3	Sawitdupa	actual ASS	typical dry year (1100 mm.a^{-1})
S4	Sawitdupa	potential ASS	typical dry year (1100 mm.a^{-1})

8.1.2 Evaluation of the scenarios

The results of the scenario evaluation are given in Fig. 8.2-8.5. Each figure gives the development of the concentrations of SO_4^{2-}, Cl^- and Fe^{2+} and the pH in soil solution.

Under scenario 1, i.e. Sawitdupa system on *actual* acid sulphate soils with normal climatic circumstances, the soil profile is reacidified every year due to in-situ oxidation of pyrite, in periods with a low water table (Fig. 8.2). This situation occurs during ripening and directly after harvest of the second crop. In these periods SO_4^{2-} and Fe^{2+} rapidly increase to levels of 6 and 4 meq.l^{-1}. The pH is rather well buffered,

but the values show a similar tendency. After 6 years the initially available pyrite is depleted, and a more or less stable situation develops, with a pH value of around 6. Conservative ions, such as chloride, are leached out effectively, with low concentration after one year.

Under scenario 2, i.e. Sawitdupa system on *potential* acid sulphate soils with normal climatic circumstances, acidification in periods with lower groundwater tables is much more severe as compared to scenario 1 (Fig. 8.3, note that the scale of the vertical concentration axis is different from Fig. 8.2). SO_4^{2-}, Fe^{2+} and Al^{3+} concentrations in the topsoil rapidly increase to levels of 60, 20 and 25 meq.l^{-1}. pH is buffering is not sufficient and on the long run it drops to values between 2 and 3.5. Similar patterns are observed for the subsoil.

Under scenario 3 (Sawitdupa system on *actual* acid sulphate soils with dry climatic circumstances) and under scenario 4 (Sawitdupa system on *potential* acid sulphate soils with dry climatic circumstances) the tendencies in the solute concentrations are to a large extend comparable to scenario 1 and 3 respectively. However, yearly re-acidification is slightly more severe than under average climatic conditions (scenario 1), due to dryer soil conditions. Leaching is also less effective, confirmed by the higher residual concentrations after 10 years, especially in the subsoil.

8.1.3 Conclusions

— Sawitdupa systems on a actual acid sulphate soil is effect to leach out toxic elements from the top soil. However, this only holds true if groundwater tables do not drop into the pyritic layer and therefore in-situ oxidation of pyrite does not occur.
— Sawitdupa systems on potential acid sulphate soils, with pyrite high in the profile, results in severe acidification and concentrations of Fe^{2+} and Al^{3+} far above their toxic levels. Also high loads of toxic elements to the environment were predicted.
— Typical dry circumstances have a limited impact on acidification: slightly more pyrite oxidation and slightly less leaching of toxic elements was predicted under these circumstances.

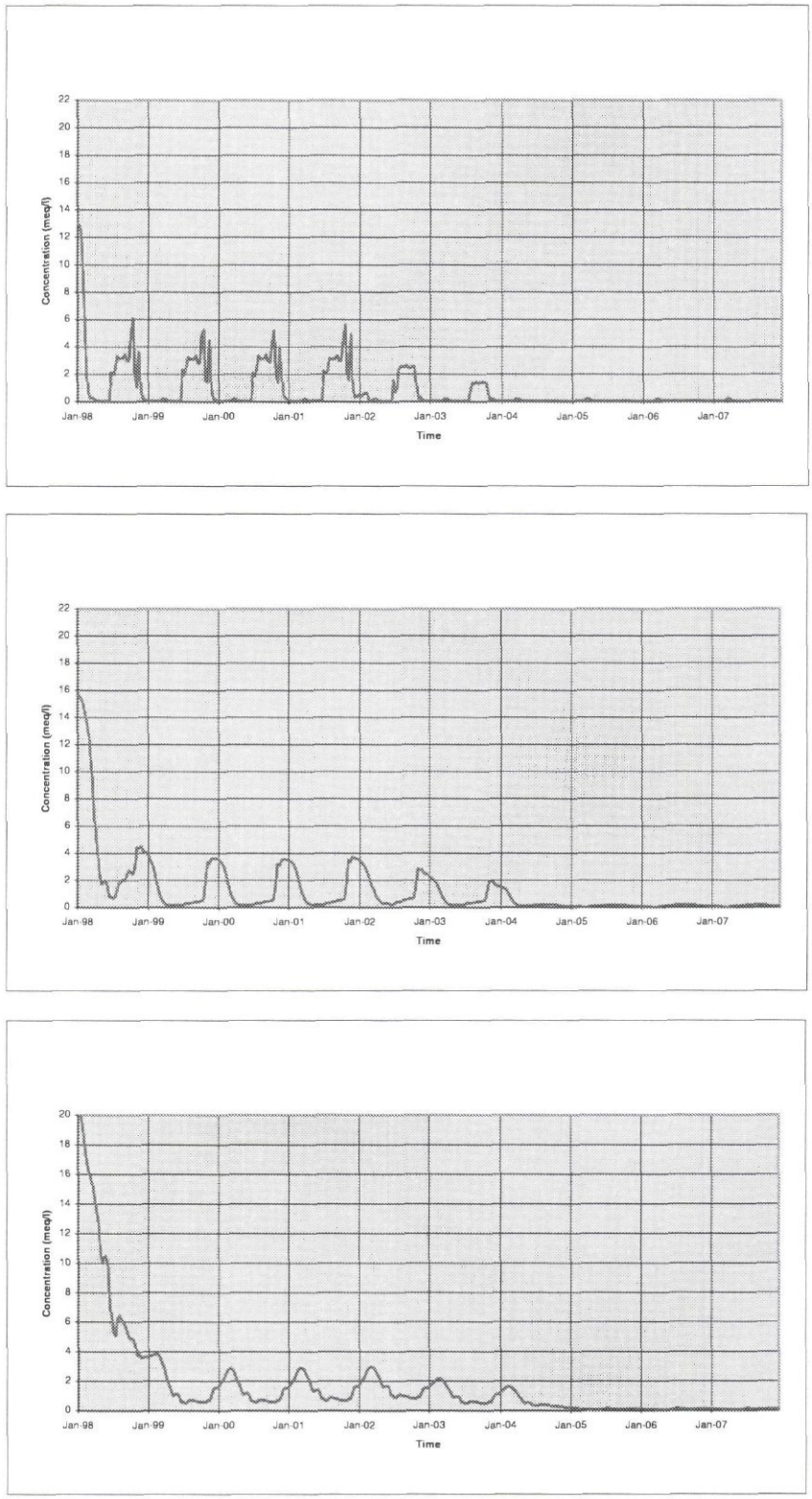

Fig. 8.2a Simulated SO_4^{2-}-concentrations (depths: 25, 65, 105 cm) under scenario 1

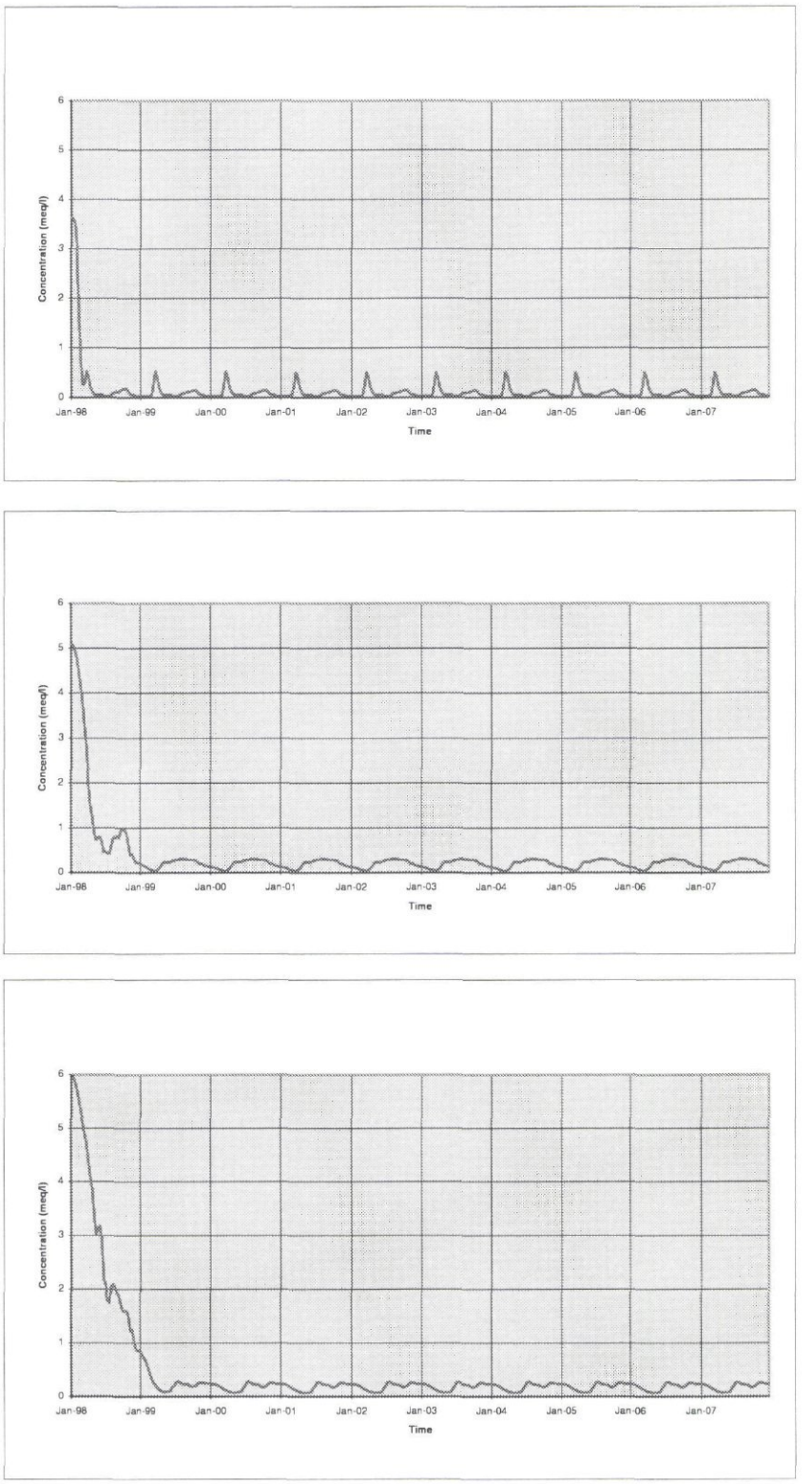

Fig. 8.2b Simulated Cl^--concentrations (depths: 25, 65, 105 cm) under scenario 1

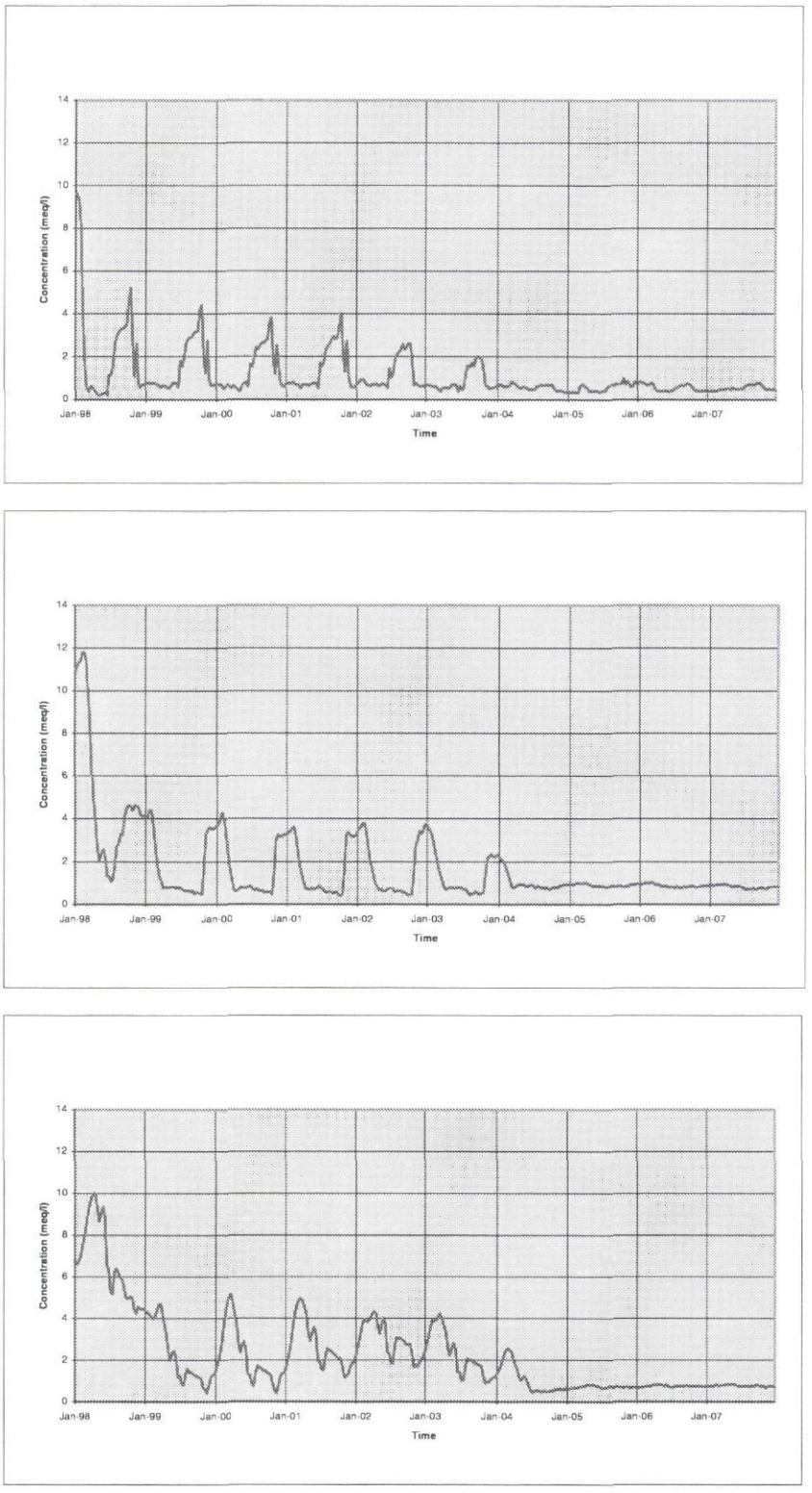

Fig. 8.2c Simulated Fe^{2+}-concentrations (depths: 25, 65, 105 cm) under scenario 1

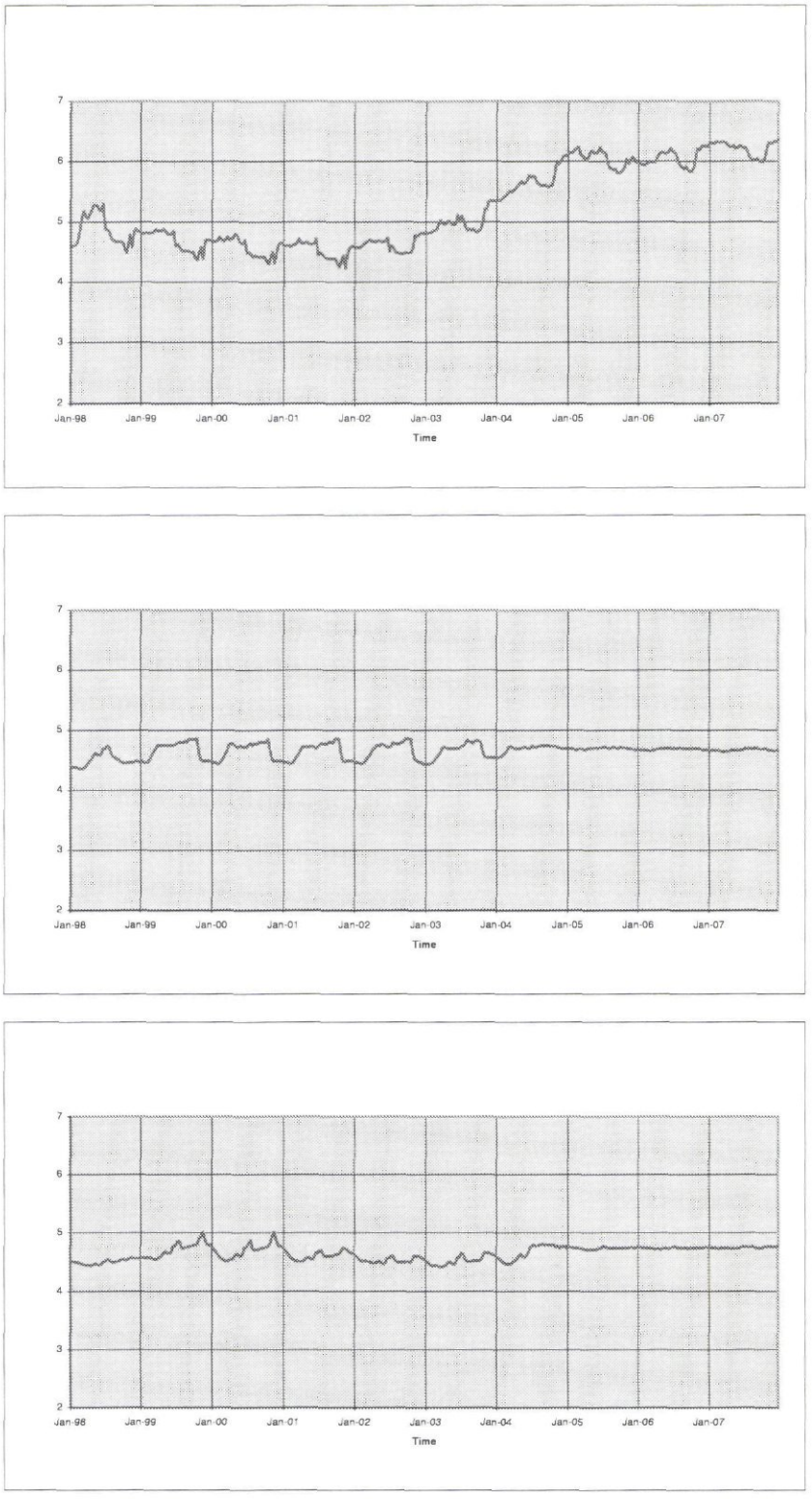

Fig. 8.2d Simulated pH values (depths: 25, 65, 105 cm) under scenario 1

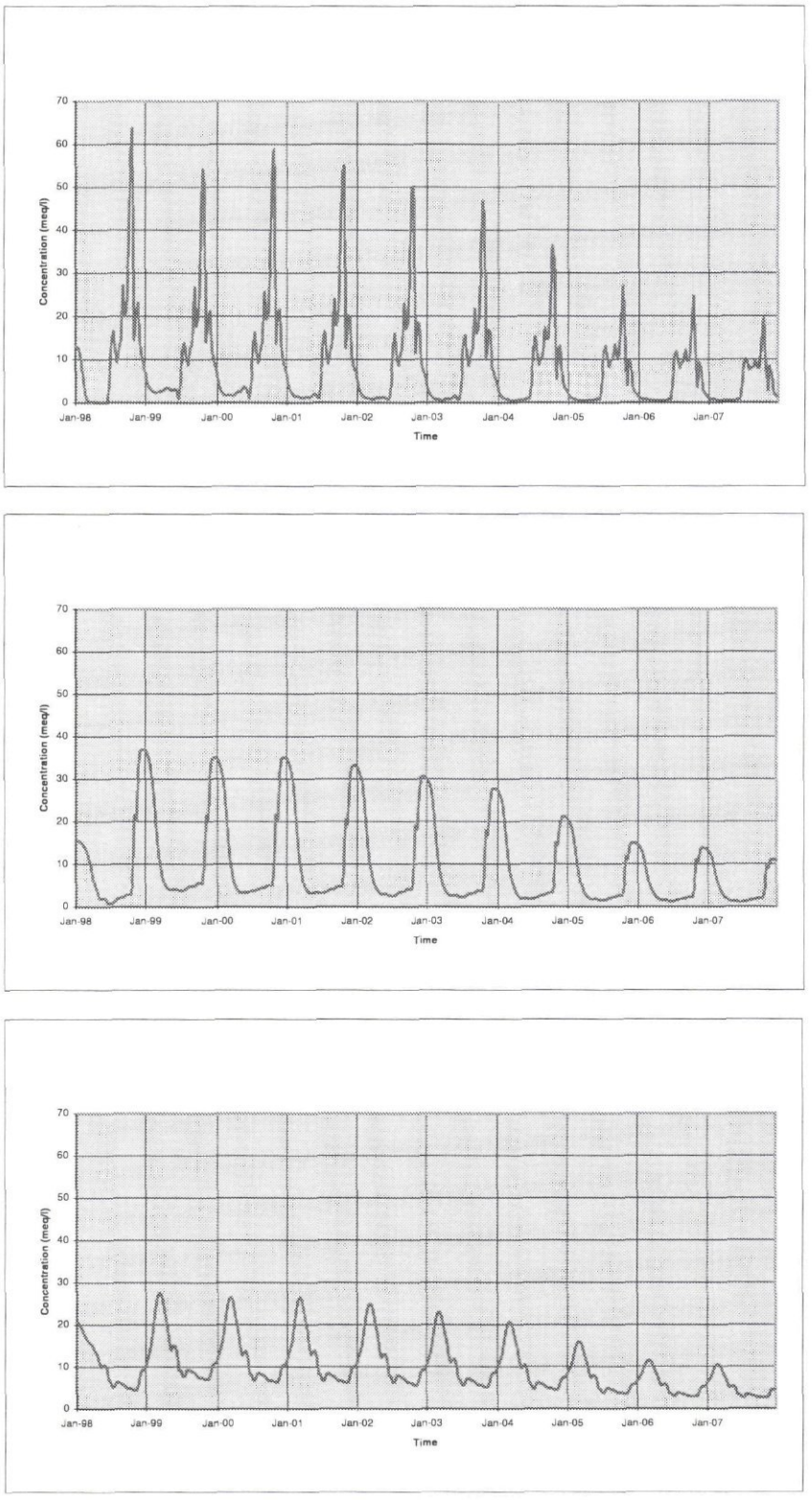

Fig. 8.3a Simulated SO_4^{2-}-concentrations (depths: 25, 65, 105 cm) under scenario 2

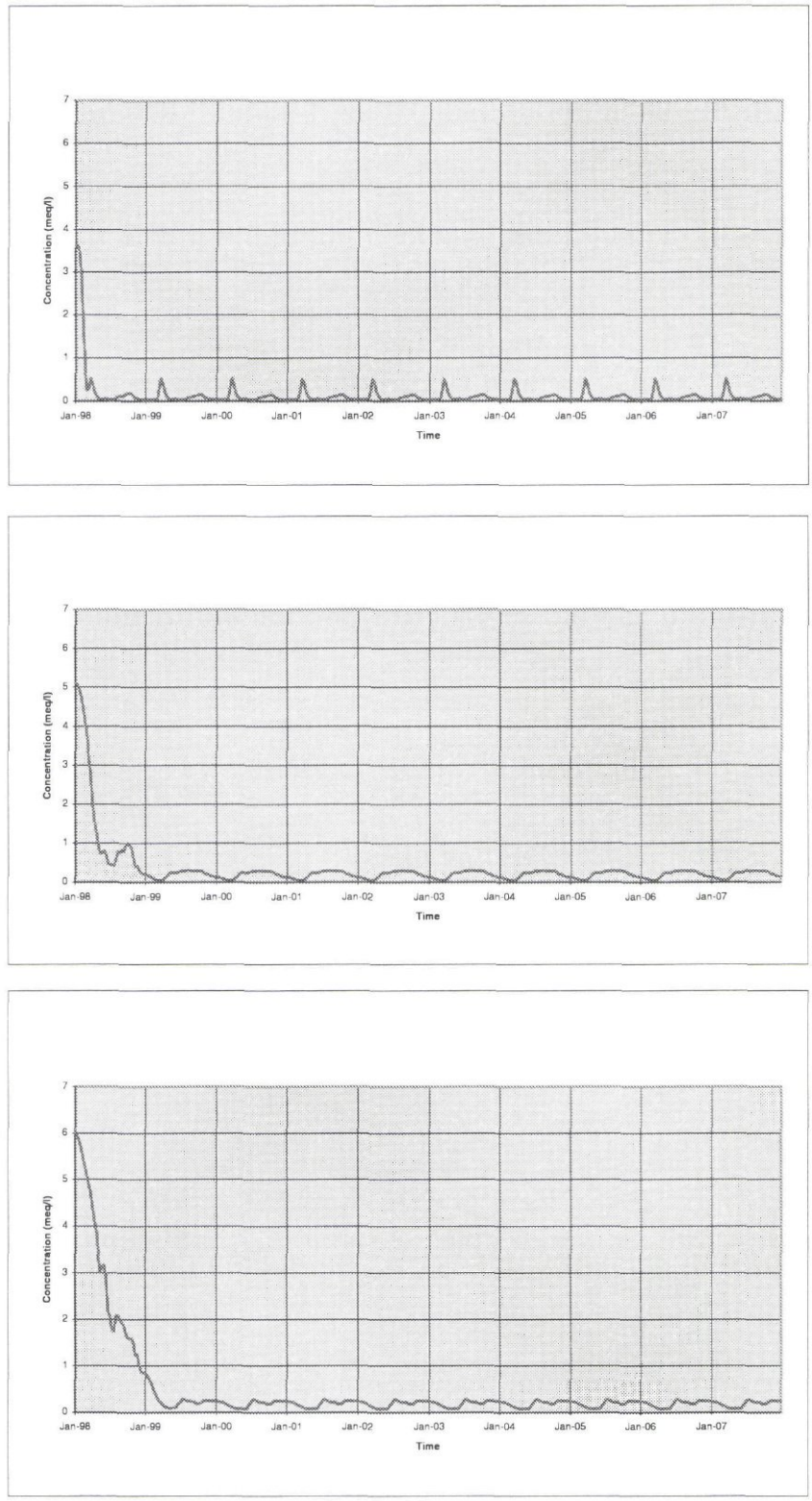

Fig. 8.3b Simulated Cl⁻-concentrations (depths: 25, 65, 105 cm) under scenario 2

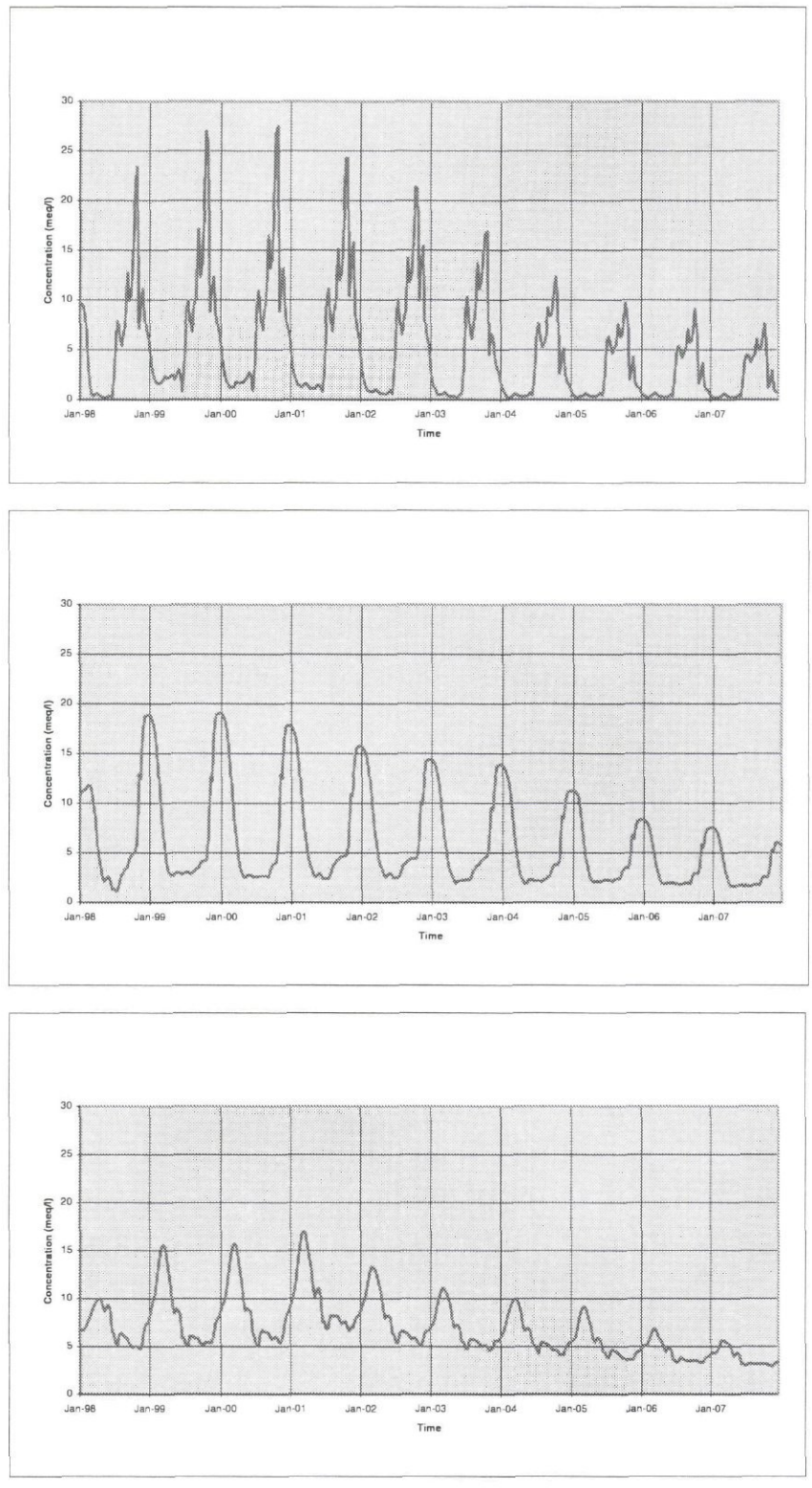

Fig. 8.3c Simulated Fe^{2+}-concentrations (depths: 25, 65, 105 cm) under scenario 2

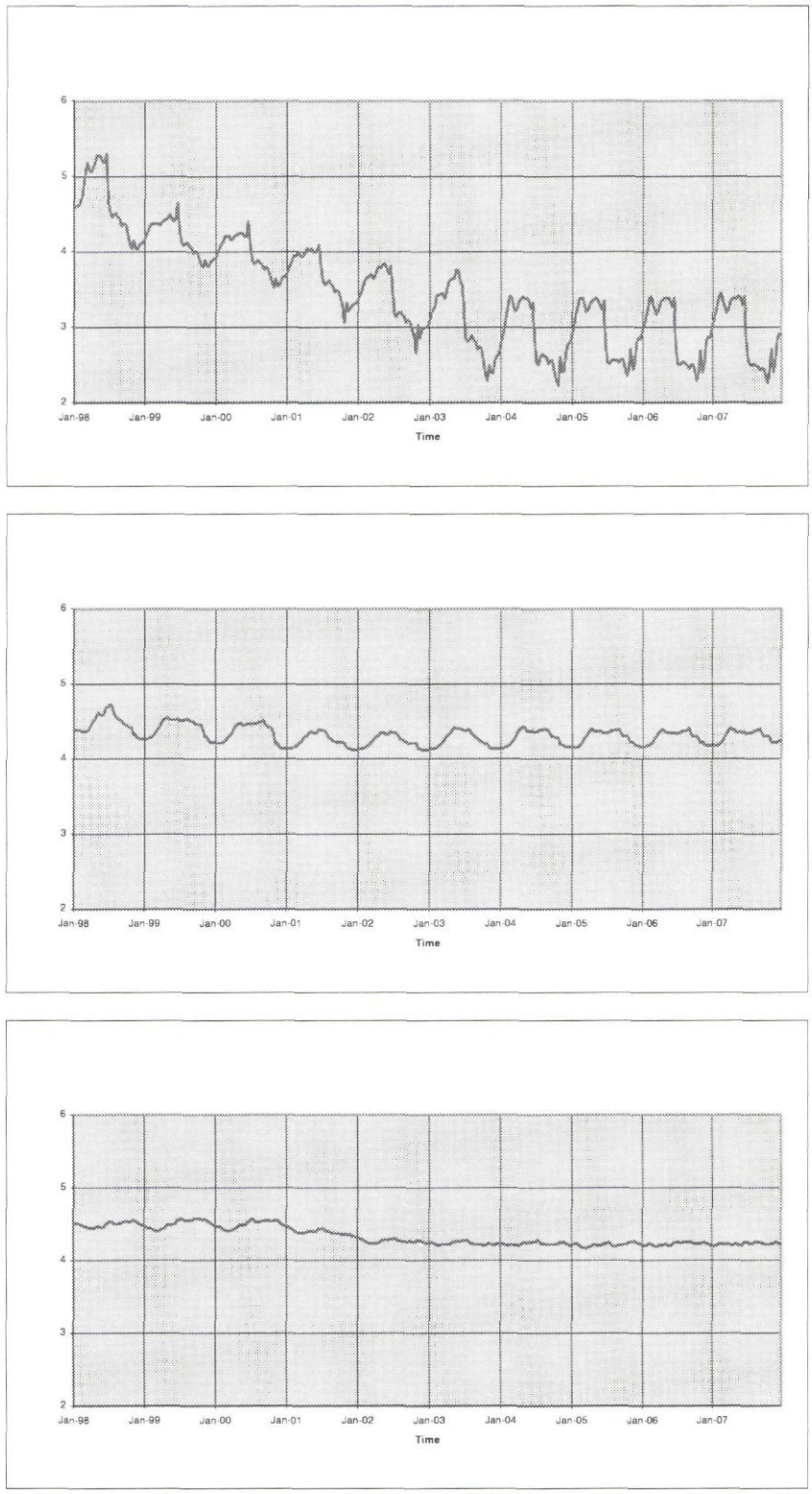

Fig. 8.3d Simulated pH values (depths: 25, 65, 105 cm) under scenario 2

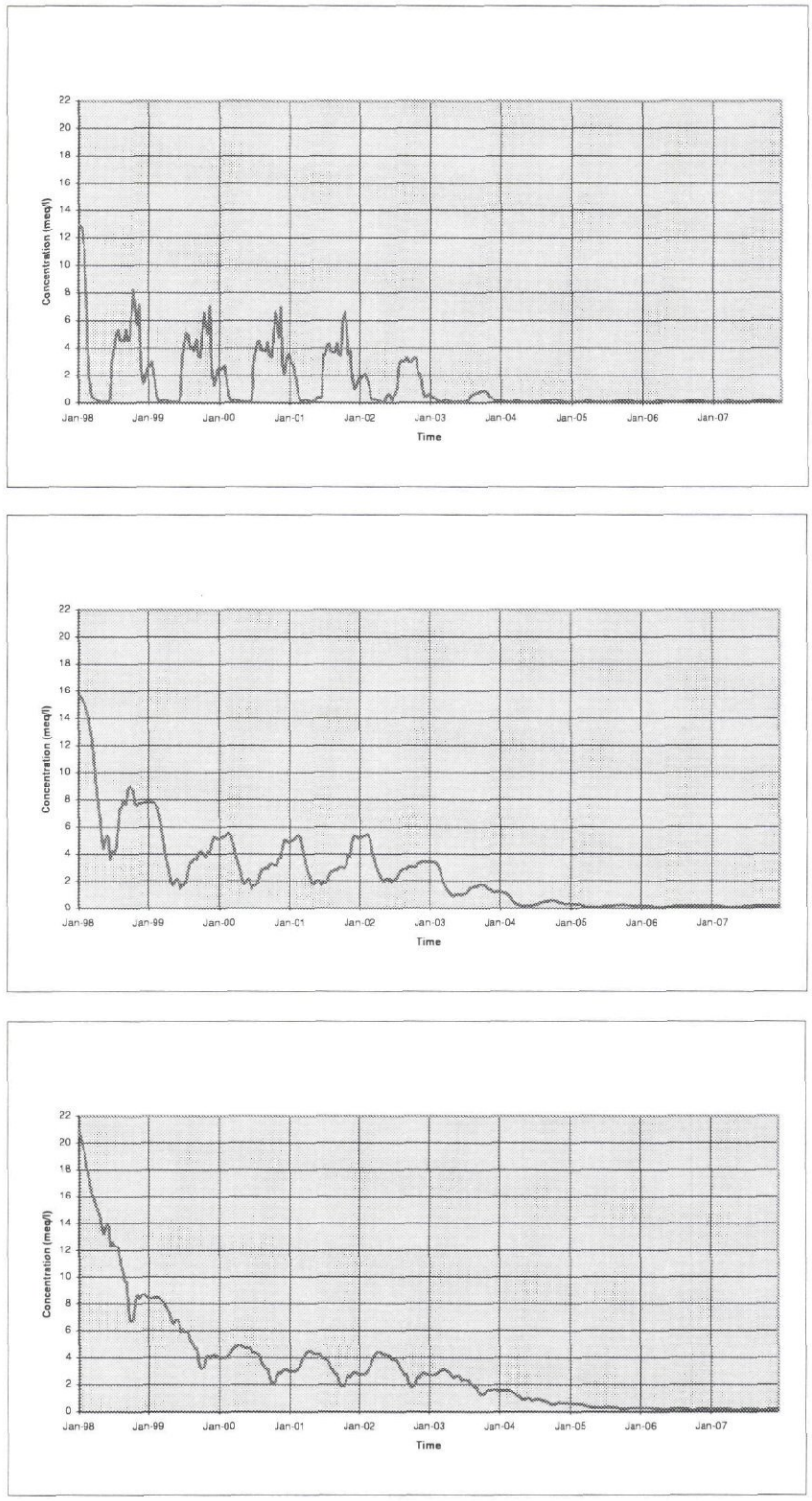

Fig. 8.4a Simulated SO_4^{2-}-concentrations (depths: 25, 65, 105 cm) under scenario 3

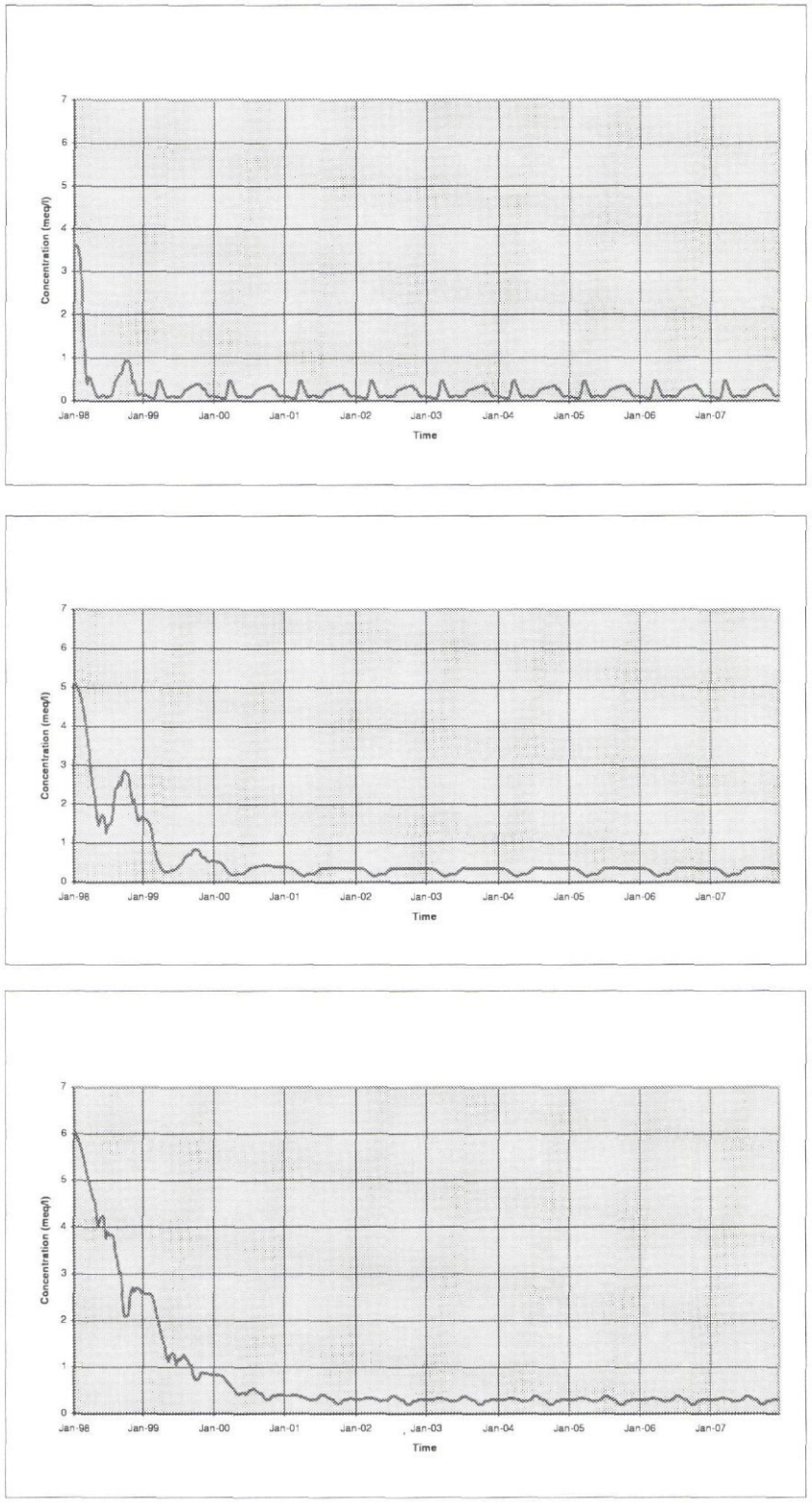

Fig. 8.4b Simulated Cl^--concentrations (depths: 25, 65, 105 cm) under scenario 3

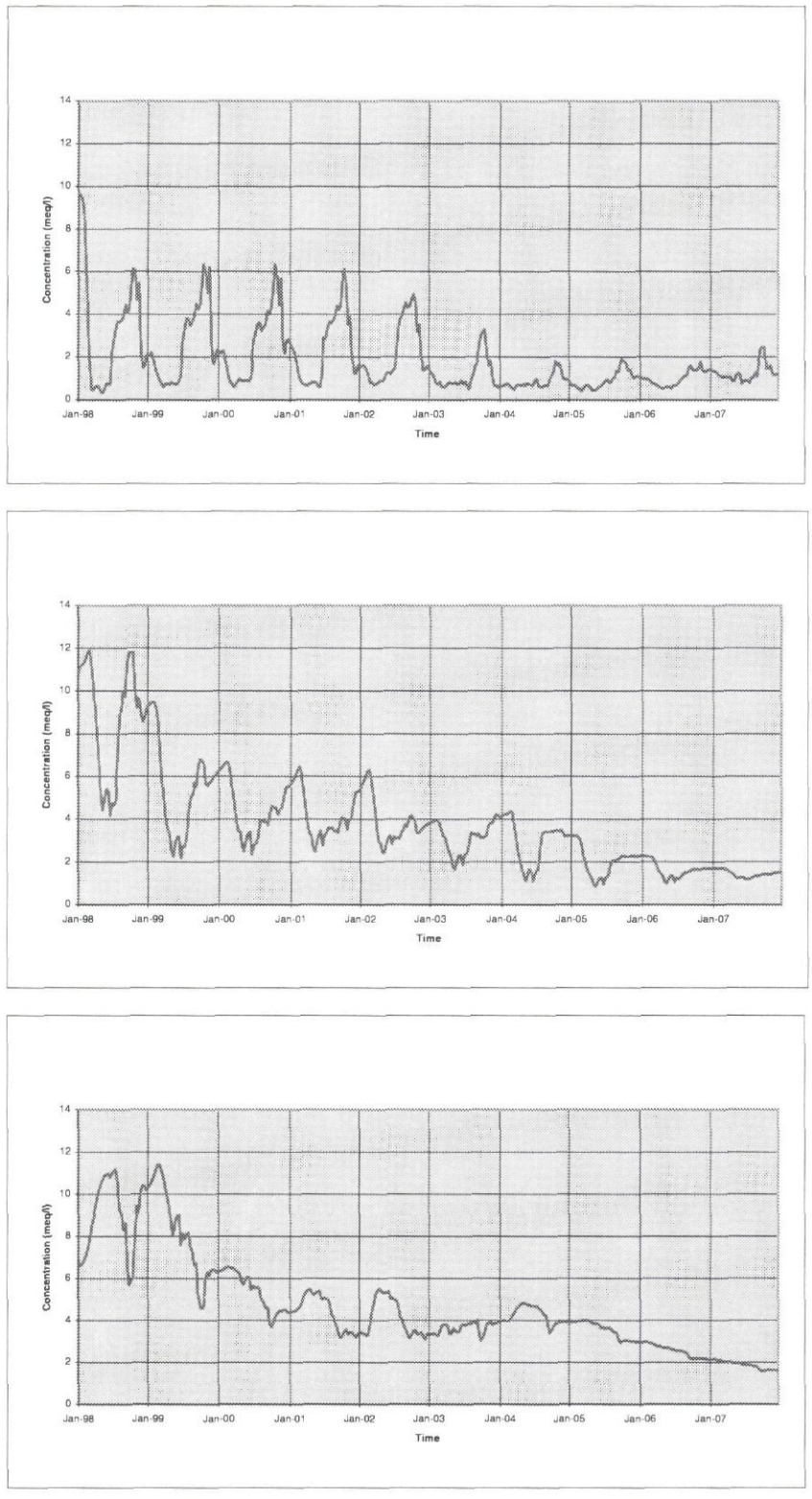

Fig. 8.4c Simulated Fe^{2+}-concentrations (depths: 25, 65, 105 cm) under scenario 3

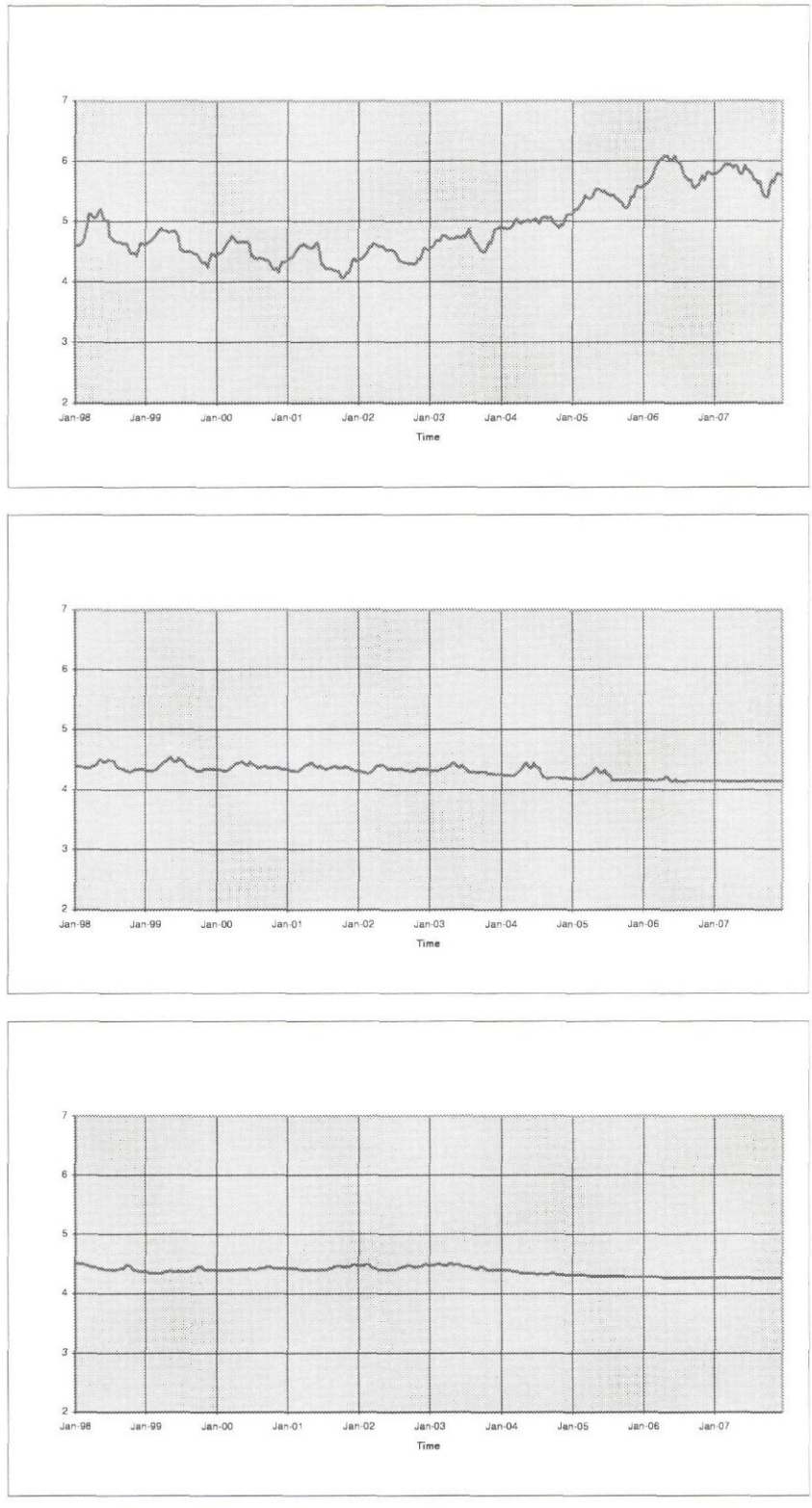

Fig. 8.4d Simulated pH values (depths: 25, 65, 105 cm) under scenario 3

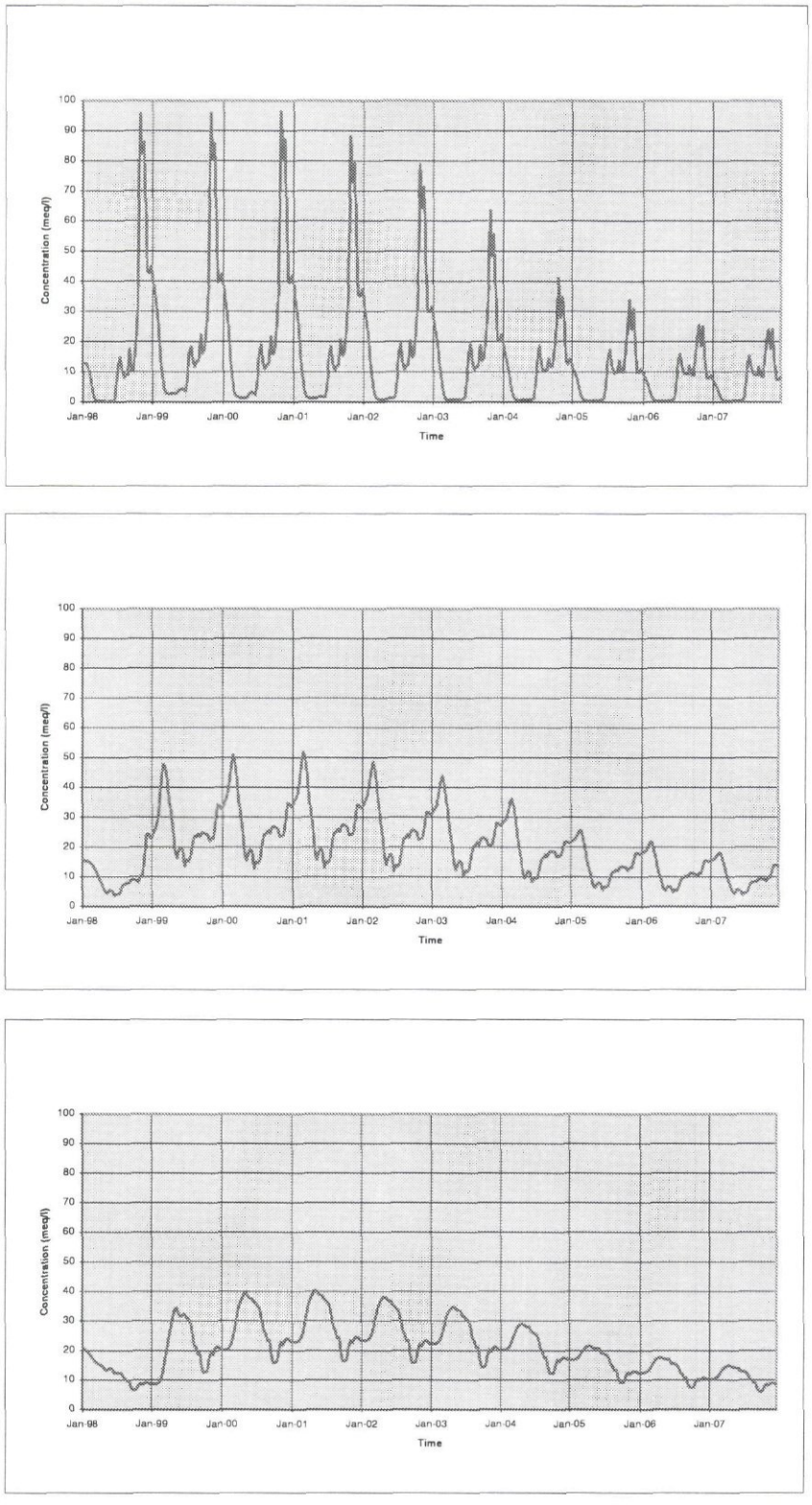

Fig. 8.5a Simulated SO_4^{2-}-concentrations (depths: 25, 65, 105 cm) under scenario 4

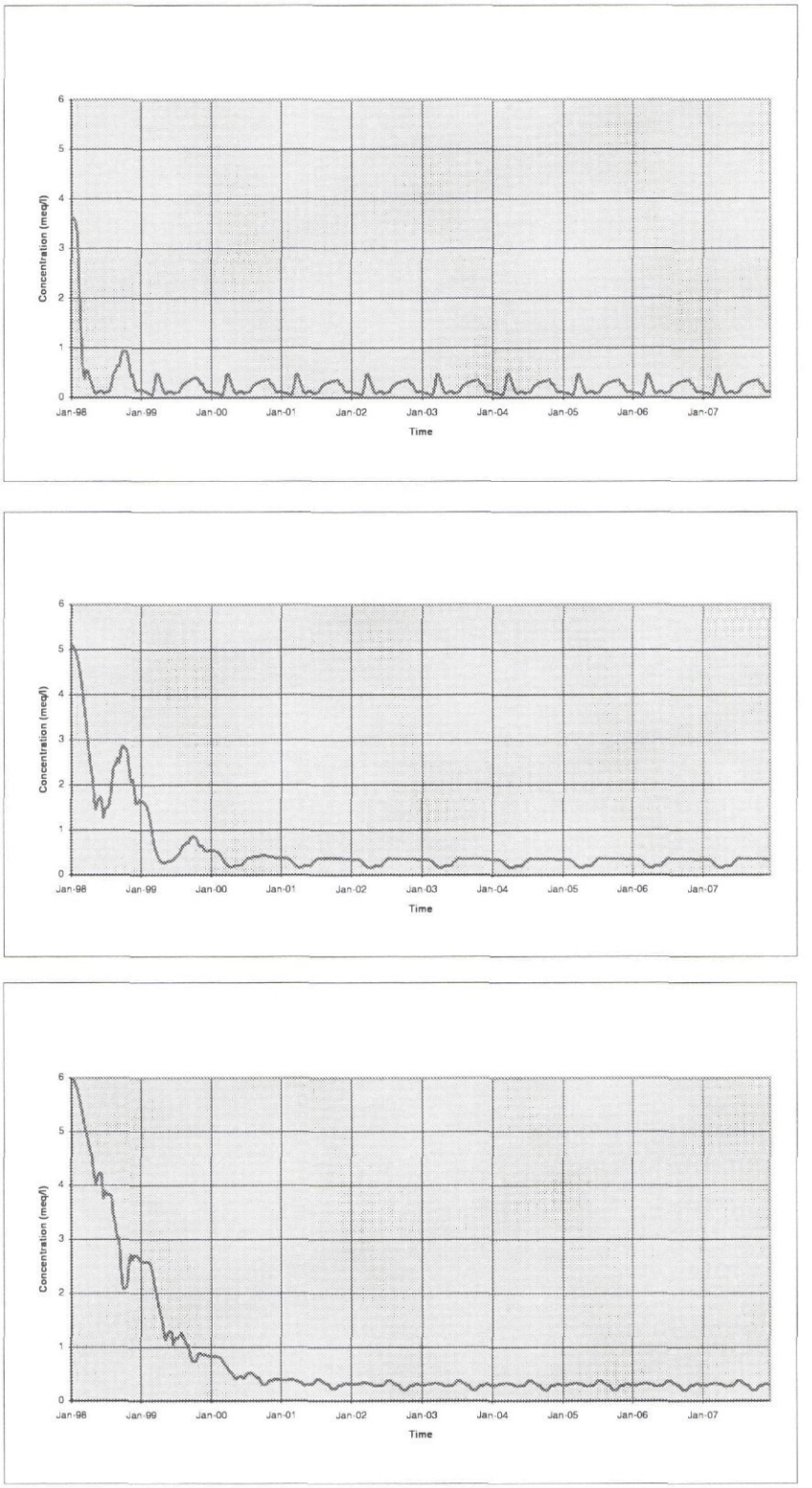

Fig. 8.5b Simulated Cl-concentrations (depths: 25, 65, 105 cm) under scenario 4

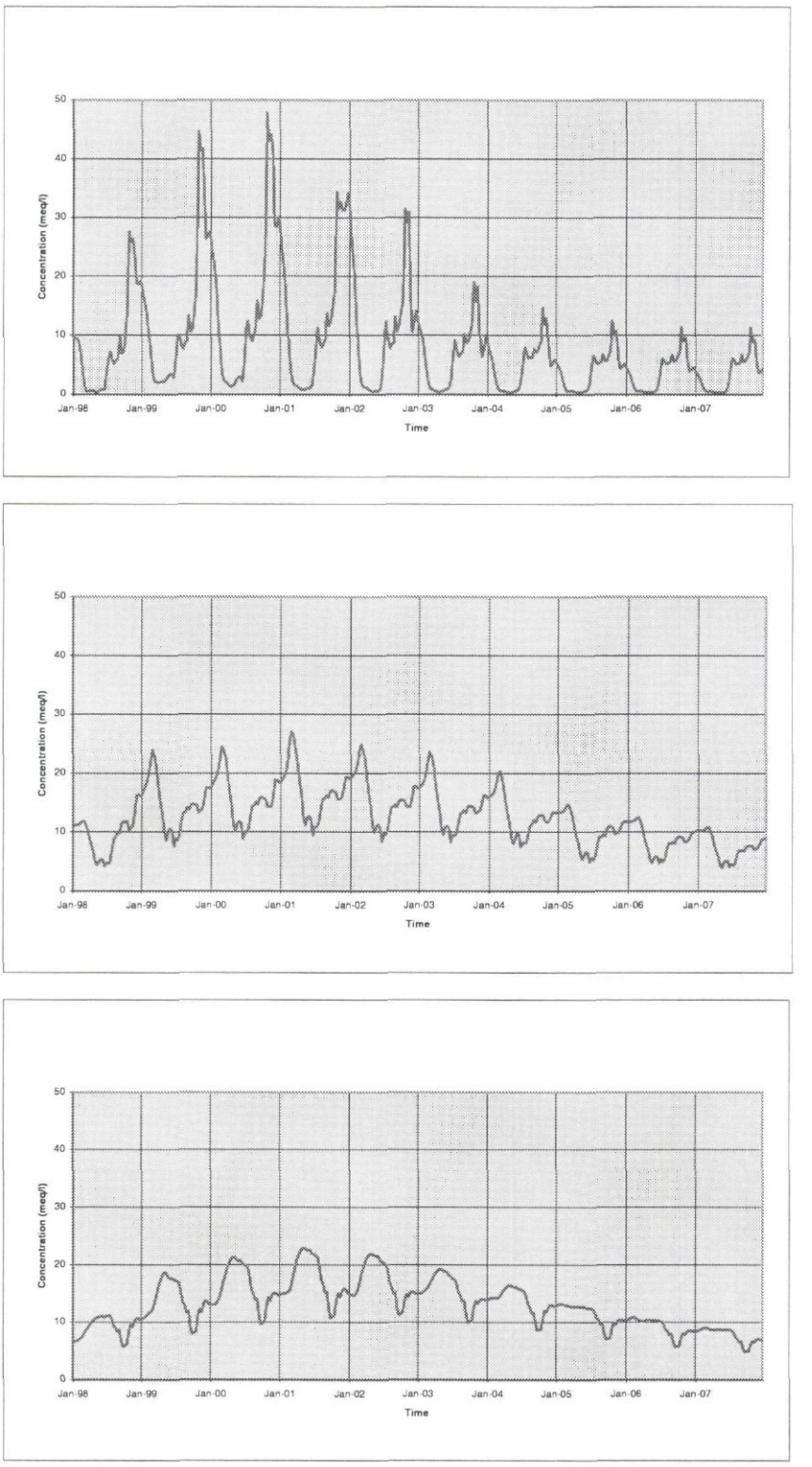

Fig. 8.5c Simulated Fe^{2+}-concentrations (depths: 25, 65, 105 cm) under scenario 4

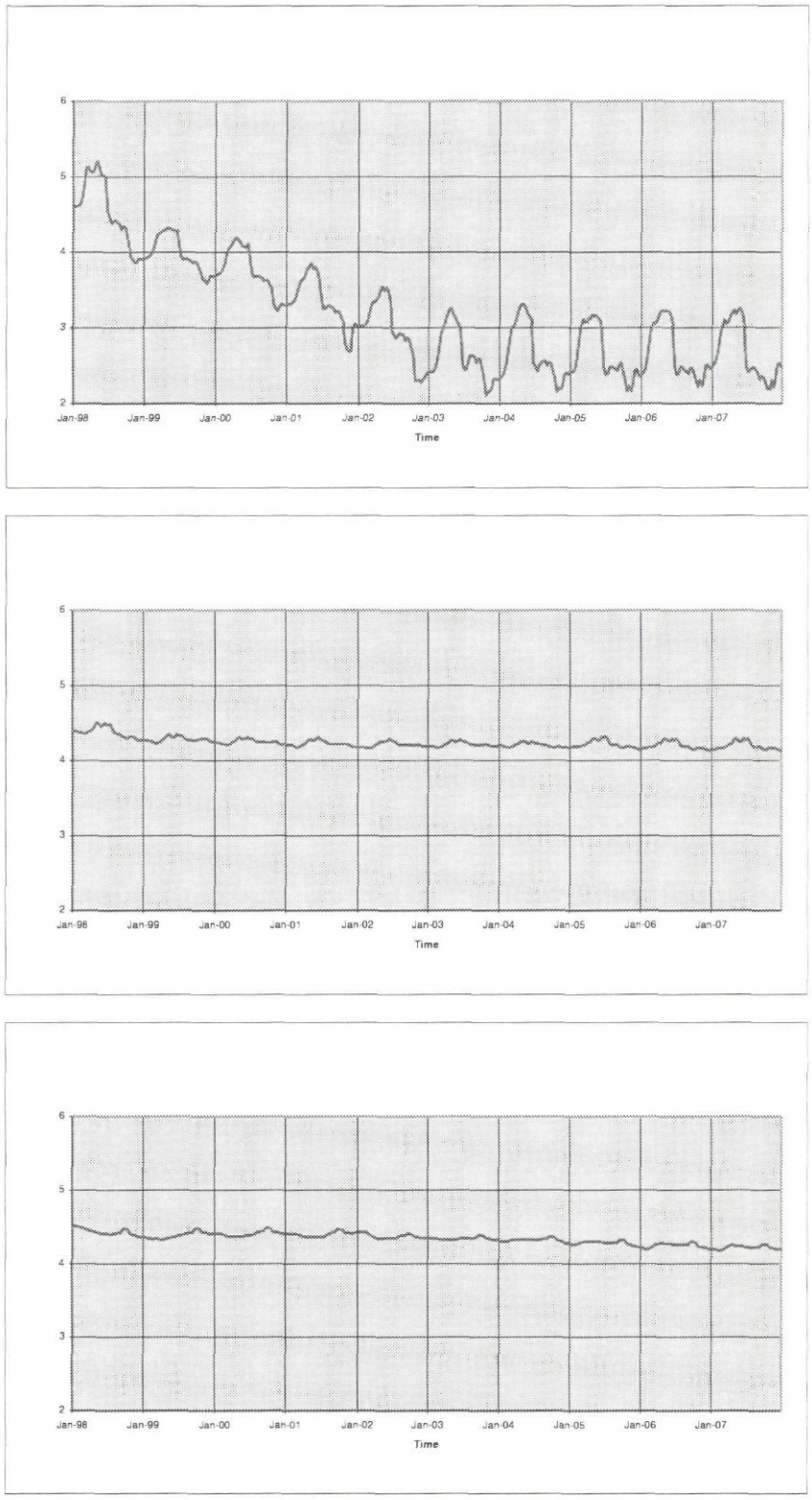

Fig. 8.5d Simulated pH values (depths: 25, 65, 105 cm) under scenario 4

8.2 Scenarios Vietnam

8.2.1 Scenarios description and simulation results

The simulations were done for four important scenarios in order to supply guidelines for land owners and region planners.

8.2.1.1 Normal scenario

The term 'normal' means normal construction and operation of a mound (or canal dike). In this case, earth material is excavated from upper horizon and mounded at bottom of the mound. The construction continues until the pond (or canal) reaches its designed depth. As a results, pyritic soil from the lower horizon is laid directly on the top of mound (or dike).

Simulation results predicts very slow processes of acidification and de-acidification in all soil horizons of a mound. Three years after construction, the topsoil (0-30 cm) will reach lowest pH values of 2. The pH does not vary much within a year during the first 3 years. During the last period of simulation, fluctuation of 1 unit or more between rain and dry season of a year (ranging from 2 to 4) is observed. The variation of pH increases with time from start. The products of pyrite oxidation, such as Fe^{2+}, SO_4^{2-}, show a different trend: large variation yearly during the first stage and smaller changes during the latter.

The pyrite disappearance calculated for various horizons is shown in Figure 8.6. These figures show that pyrite in the topsoil is almost oxidised totally after 3 years. However, the acidic elements such as H^+, Fe^{2+}, SO_4^{2-}, Al^{3+}, are still produced in lower horizon and transported to upper layers through capillary during the dry season. This process continues over a long period after construction. After 10 years, the acidification of the mounded soil still occurs. However, the concentration of acidic elements in the upper horizons reduces to under their toxic threshold after 5 year from the mounding.

For the case of pond construction in saline regions, the salinity of a mound is strongly determined by the saline water in the pond. The concentrations of exchangeable ions such as Na^+, Ca^{2+} and Mg^{2+}, vary in the same patterns as those in the surface water. These variations decrease their amplitudes upwards. This fact indicates that capillary flow plays a key role in the chemical processes occurring in a mound.

8.2.1.2 Ponding scenario

Farmers can build small dikes (height of 10-20 cm) on top of the mounds to minimize run-off and maximise infiltration. This accelerates leaching of acidic elements from the mounds and may reduce the minimum time span between pond preparation and the start of shrimp farming. A simulation was done with dikes of height of 20 cm, in order to predict the effect of this method.

Simulation results (Fig. 8.7) predict even slower processes of acidification, however the desalinisation in all soil horizons of a mound is accelerated strongly. The method increases the leaching effect remarkably, reduces oxidation duration and reduces also capillary flow of saline water from deeper horizon. As a result, the acidic elements are transported downwards to the subsoil resulting in higher concentration of H^+, Fe^{2+}, Al^{3+} and SO_4^{2-} in lower horizon (50 and 90 cm from soil surface). In this case, pyrite oxidation continues longer as compared to that in the normal case.

About 3 years after construction, the topsoil (0-30 cm) reached its lowest pH value of 2. Unlike the normal case, pH of the lower horizons decreases quickly within a year. After 7 years, when the pyrite of the upper soil horizons is oxidised totally, pH start to increase gradually. The acidic elements such as Fe^{2+}, SO_4^{2-} and Al^{3+} show very large variation yearly during the first stage (7 years), especially for the lower horizons. After 7 years Al^{3+} and SO_4^{2-} show almost negligible concentrations in upper horizons. However, high SO_4^{2-} concentration of the 50 cm horizon indicates that pyrite oxidation still occurs at this depth. In this scenario the total pyrite oxidation per year is less as composed to the normal case and therefore the total oxidation period is extended. After 10 years of oxidation, the acidification of the mounded soil still occurs within horizons below 50 cm.

Generally, the construction of dikes can accelerate leaching at upper depths and decreases oxidation possibility at deeper horizons, and therefore can extent disappearance duration of pyrite.

In saline region, salinity of mounded soil reduced sharply by leaching. It requires only 2 years to remove most of saline concentration of the mound.

8.2.1.3 Reversed construction scenario

Unlike the normal construction, in this construction farmers cover the pyritic material taken from subsoil by non-pyritic soil of top horizon. So they have to move aside the topsoil material before laying the pyritic soil in the bottom of the mound. The non-pyritic soil, then, will be laid in the top of mound. This method may reduce oxidation intensity since the pyritic soil is buried inside the mound. However, it will yield good result only if the pyrite horizon does not appear at shallow depth, and the soil cover is not deep enough to prevent oxygen entrance into the mound. In this scenario, pyritic soil is buried under 50 cm of non-pyritic soil.

During the first 5 years of simulation, the pH value of the top 30 cm horizon maintains around 3 to 4, which is about 1 unit higher than in the normal case. During the rainy seasons of the next 5 years, pH of topsoil can increase up to 5. The difference between the two case decreases gradually over time and reaches about 0.5 unit after 10 years. This method of soil manipulation can reduce the concentration of acidic elements such as Fe^{2+}, SO_4^{2-} and Al^{3+} in the topsoil during the first two years considerably. The concentration in soil solution of these elements is reduced from 100% to 1000% as compared to that in the normal case, and ranged in acceptable limits of toxicity. Generally, this treatment suggests a suitable method to keep the oxidation rate at a lower rate.

The salinity of the mounded soil remains influenced strongly by water quality in the pond. Exchangeable ions such as Na^+, Ca^{2+}, Cl^- show the same trend and range as compared to that in the normal situation.

8.2.1.4 Fresh water scenarios

In many region of coastal areas, irrigation systems were built to convey fresh water to rainfed areas. In these projects, canal systems for irrigation and drainage are excavated and pyritic soil was excavated to built dikes. Unlike the normal case, in this case the water environment around the dikes is not saline. This scenario aims to simulate chemical processes occurring in the dike in this fresh water condition. The characteristics of the soil profile applied in this scenario are the same with that in the normal case (initial saline soil, with pyritic material on the top), and the chemical quality of surface water is assumed to be normal quality of fresh river water.

During the first 5 years, for all simulated horizons, pH values are about 1 unit higher than that of the normal case. Whereas the pH values show the same behaviour as in the normal scenario.

Fe^{2+} concentrations simulated in this case are lower than that of the case normal during the first 2 years, and reaches the same range with that of the normal case after 5 years. SO_4^{2-}-concentration in all horizons were lower as compared to that of the normal case.

The fresh water quality applied can improve salinity in the mound significantly. It requires only one rainy season (about 1800 mm) to leach out all exchangeable ions such as Na^+, Ca^{2+} and Cl^-.

8.2.2 Conclusions

Some common scenarios are simulated in order to supply guidelines for building ponds or dikes in the coastal areas with acid sulphate soils. There are, however, two different aspects that must be considered:

8.2.2.1 Water environmental pollution aspect

For environmental reasons it is required to keep the quantities of bad quality leachate as low as possible. So the method applied has to result in low oxidation within the dike and slow leaching of toxic elements out of the dike. Using these criteria, the method of reverse construction of a dike will yield the best results. However, this method may require more labour and money. This method can be applied only if the pyritic soil is covered by at least 50 cm of the non-pyritic soil.

When farmers build ponds for shrimp/fish farming, they always want to leach the mound intensively before starting farming, otherwise the toxic leachate can damage the production. For this purpose, the method of ponding on the mound will meet their need. However the simulation indicates that this method can be applied if the pyrite

content in the soil is not too high, otherwise it will take long time to reach safe criteria of acidity in the mound. For the example in this chapter (with a maximum pyrite content in the mound of 5%) it takes about 7 years to reach reasonable quality of the whole soil profile.

For setting up irrigation systems to reclaim potential acid sulphate soil, numerous canals will be constructed that favour pyrite oxidation occurring in the dikes. The long term simulation predicts higher concentration of Fe^{2+} and Al^{3+} compared to that of the normal case. The method of reverse building of dike will help to reduce acidic water propagation in the surface water.

8.2.2.2 Soil quality of mounds

All scenarios predicted long term acidification of mounded soil construction of canals or ponds. The pyrite oxidation may continue at least 5 years after construction.

The mounding of the acid sulphate soil for orchards farming could be possible by applying the method of reverse construction of the mound. This treatment helps to keep oxidation intensity low. So the oxidation may still occur during very long time after mounding, but acidic productions will be kept within acceptable range.

Hence, this manipulation should be done if we have to do the soil disturbance at a large scale (in order to prevent acidic pollution). This method may be helpful for the case of building ponds or making raised bed for orchards in acid sulphate soil.

The method will be more effective if the pyritic soil is buried at deep horizon. A test run for the case in which pyritic soil is covered by 80 cm of non-pyritic soil shows that pyrite oxidation hardly occurs and toxic components such as Fe^{2+}, SO_4^{2-} and Al^{3+} become very low only after 2 years.

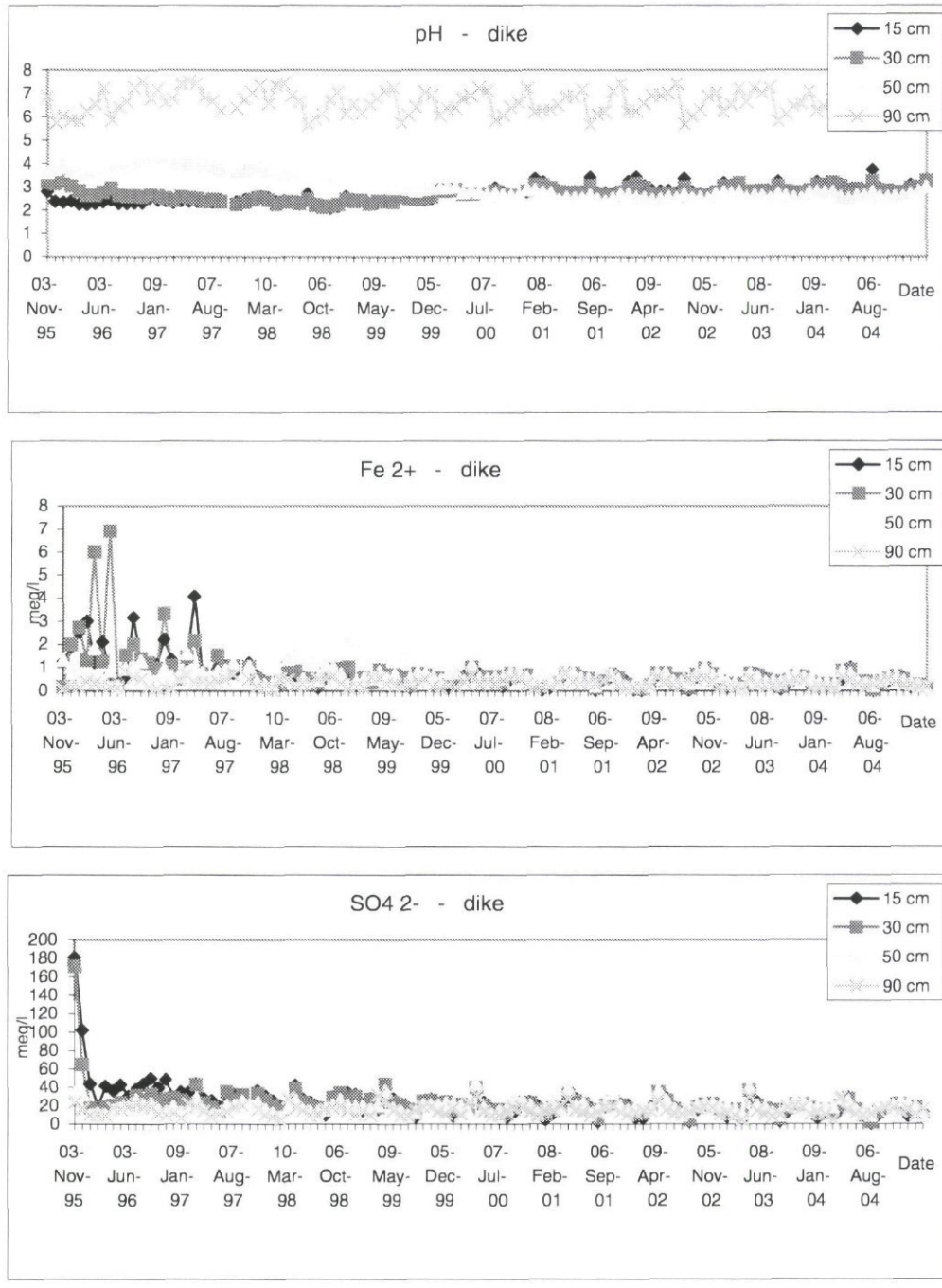

Fig. 8.6 Simulation results 'Normal scenario'

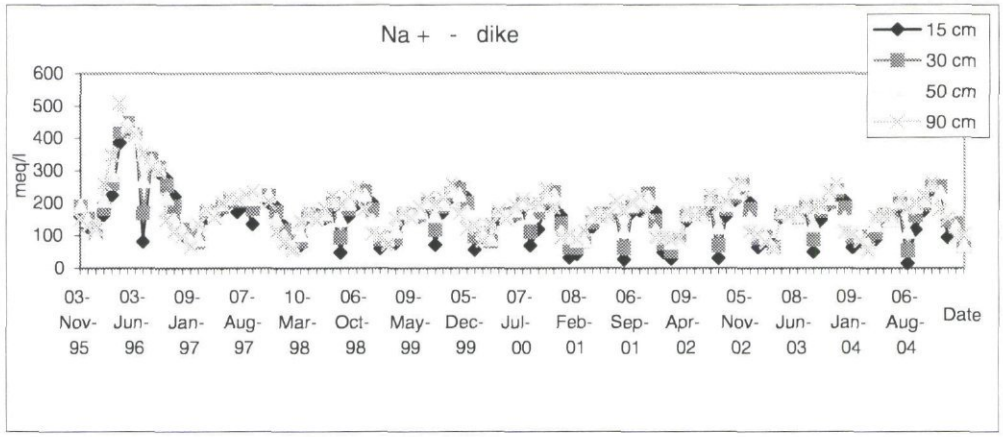

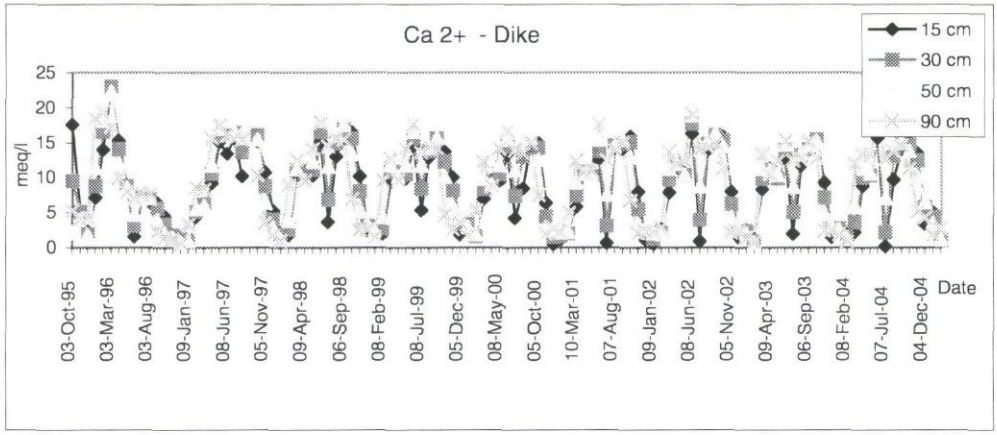

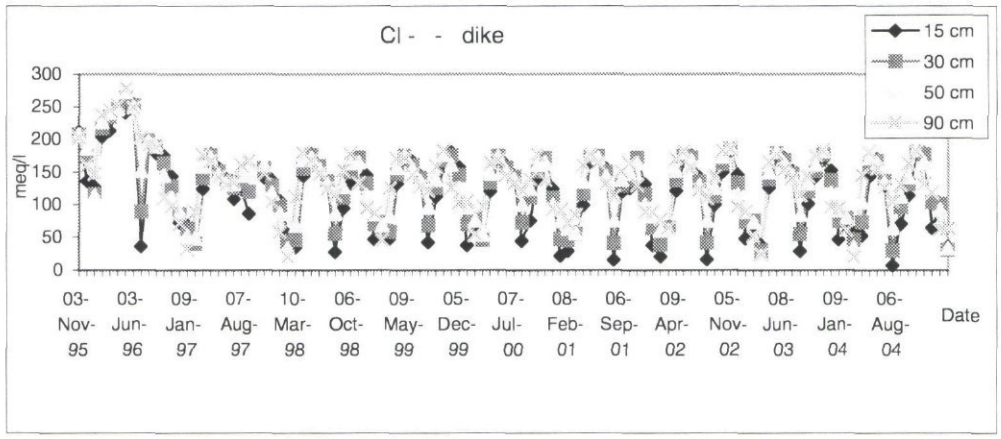

Fig. 8.6 Simulation results 'Normal scenario' (continued)

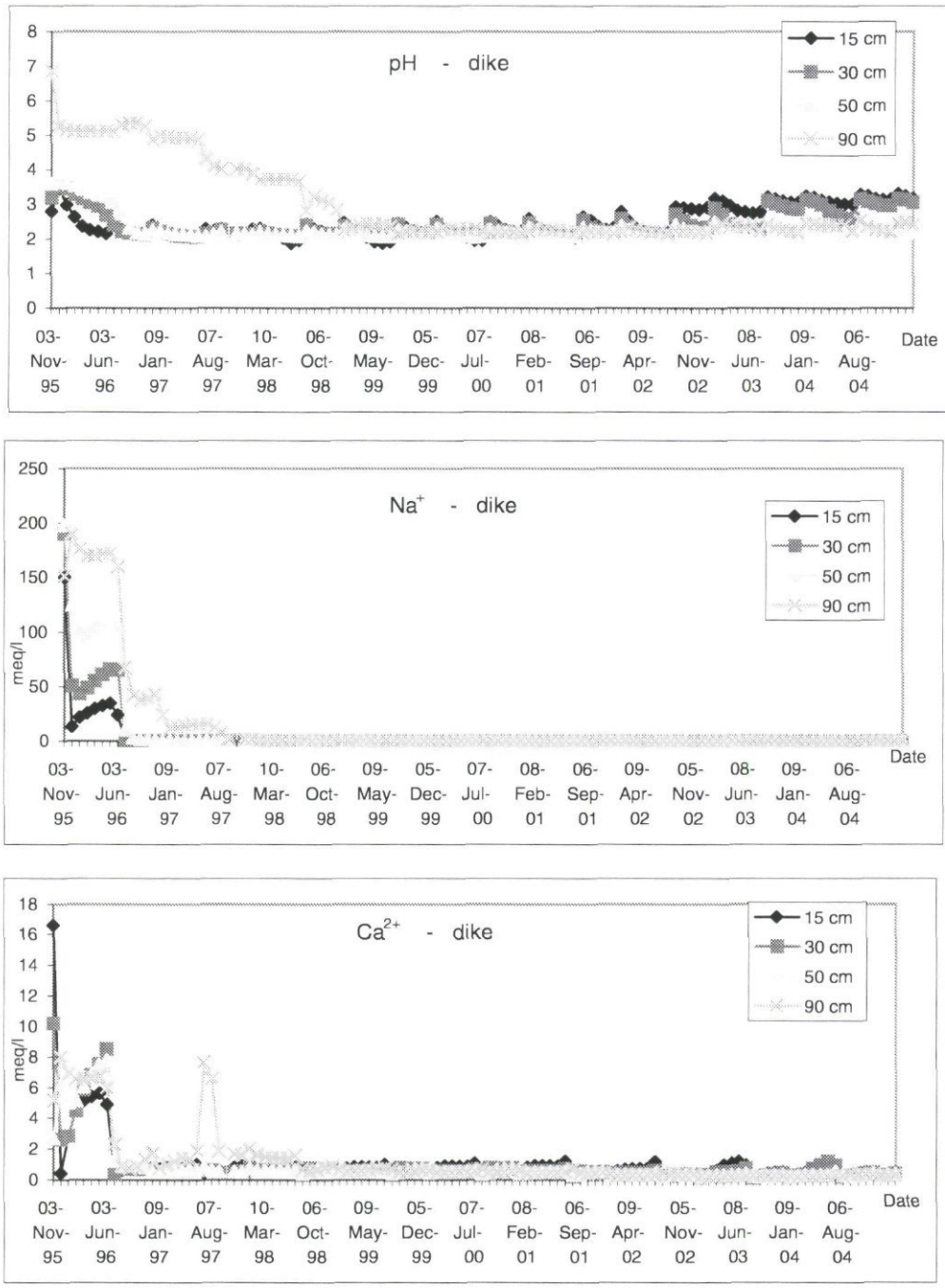

Fig. 8.7 Simulation results 'Ponding scenario'

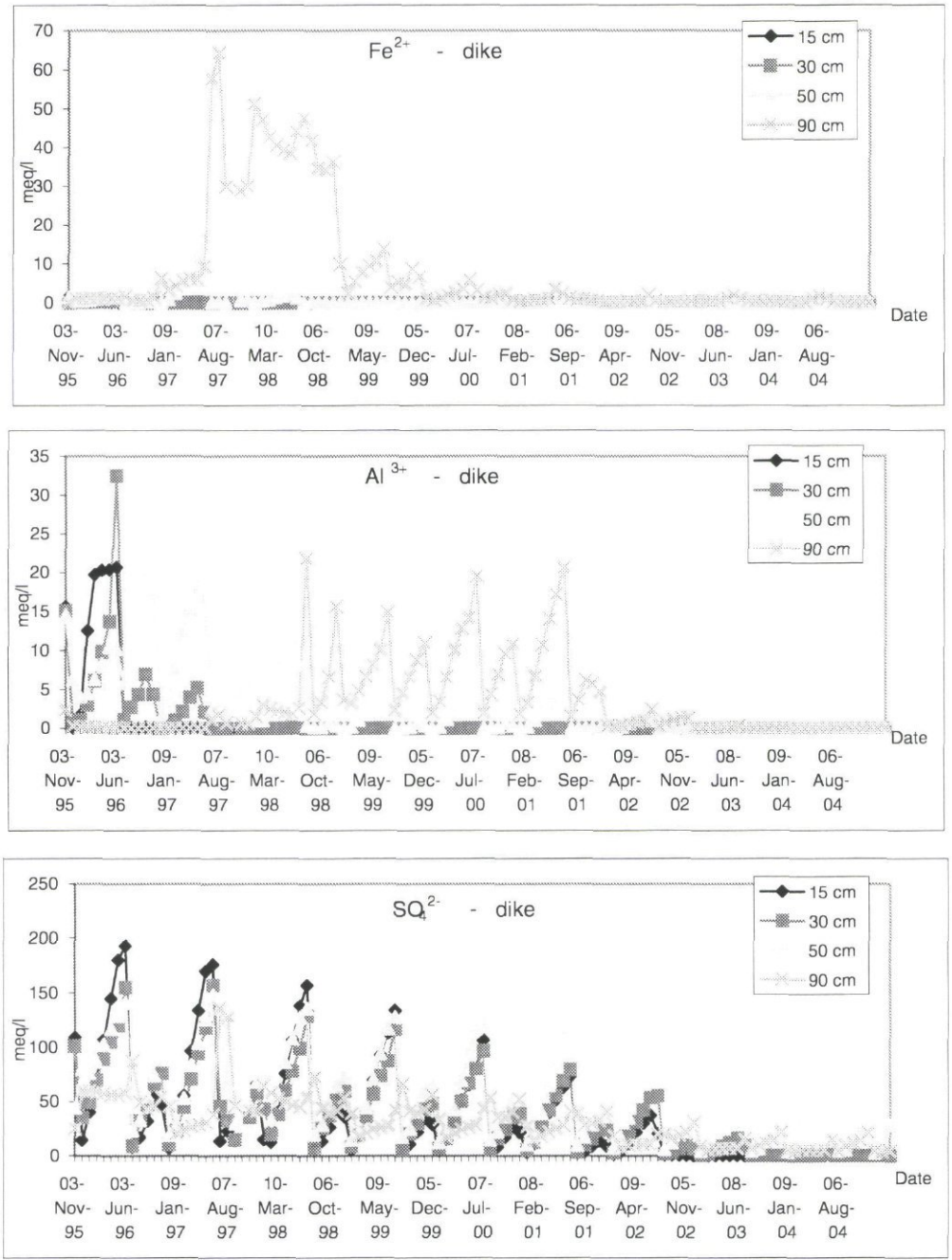

Fig. 8.7 Simulation results 'Ponding scenario' (continued)

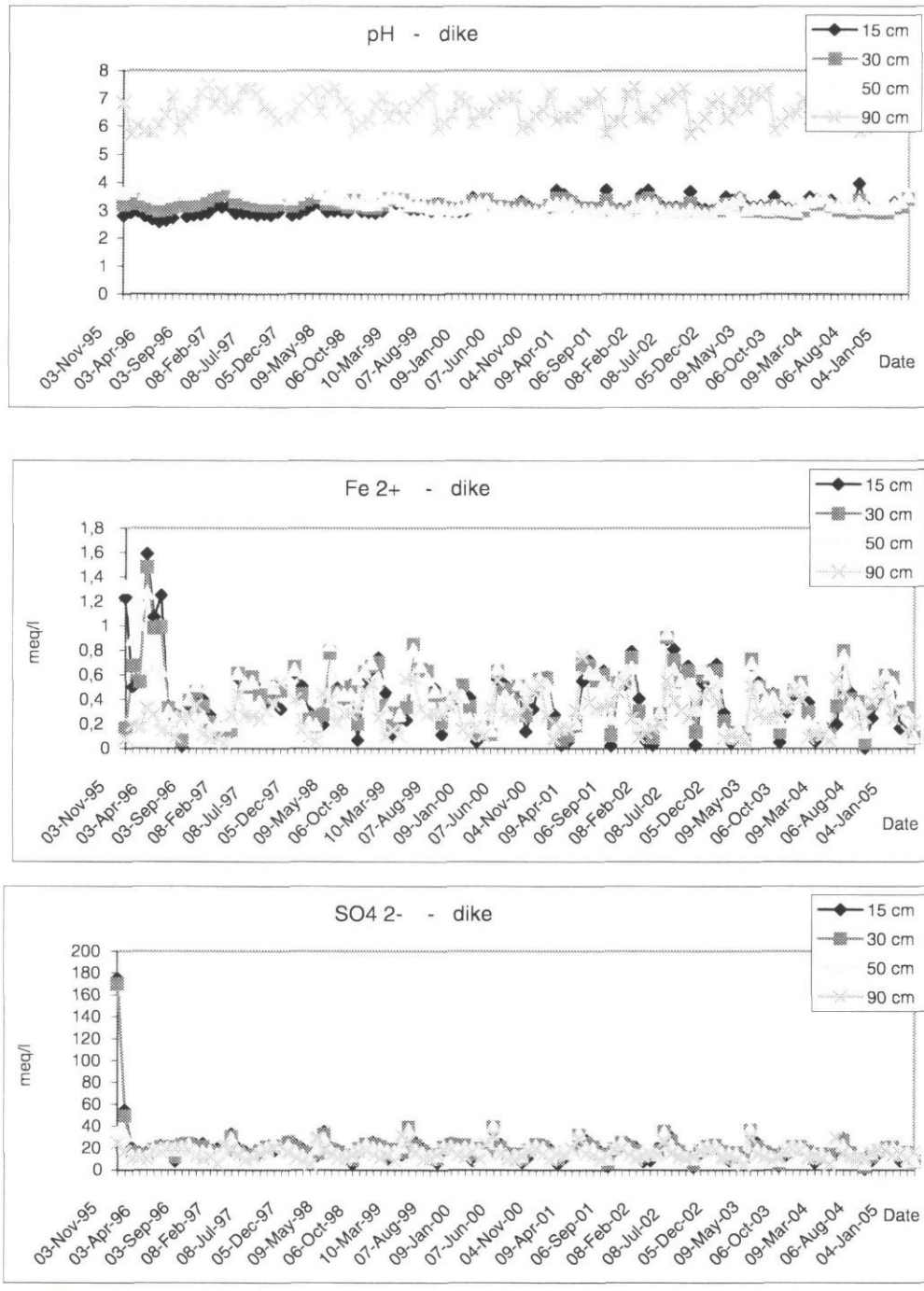

Fig. 8.8 Simulation results 'Reversed-construction scenario'

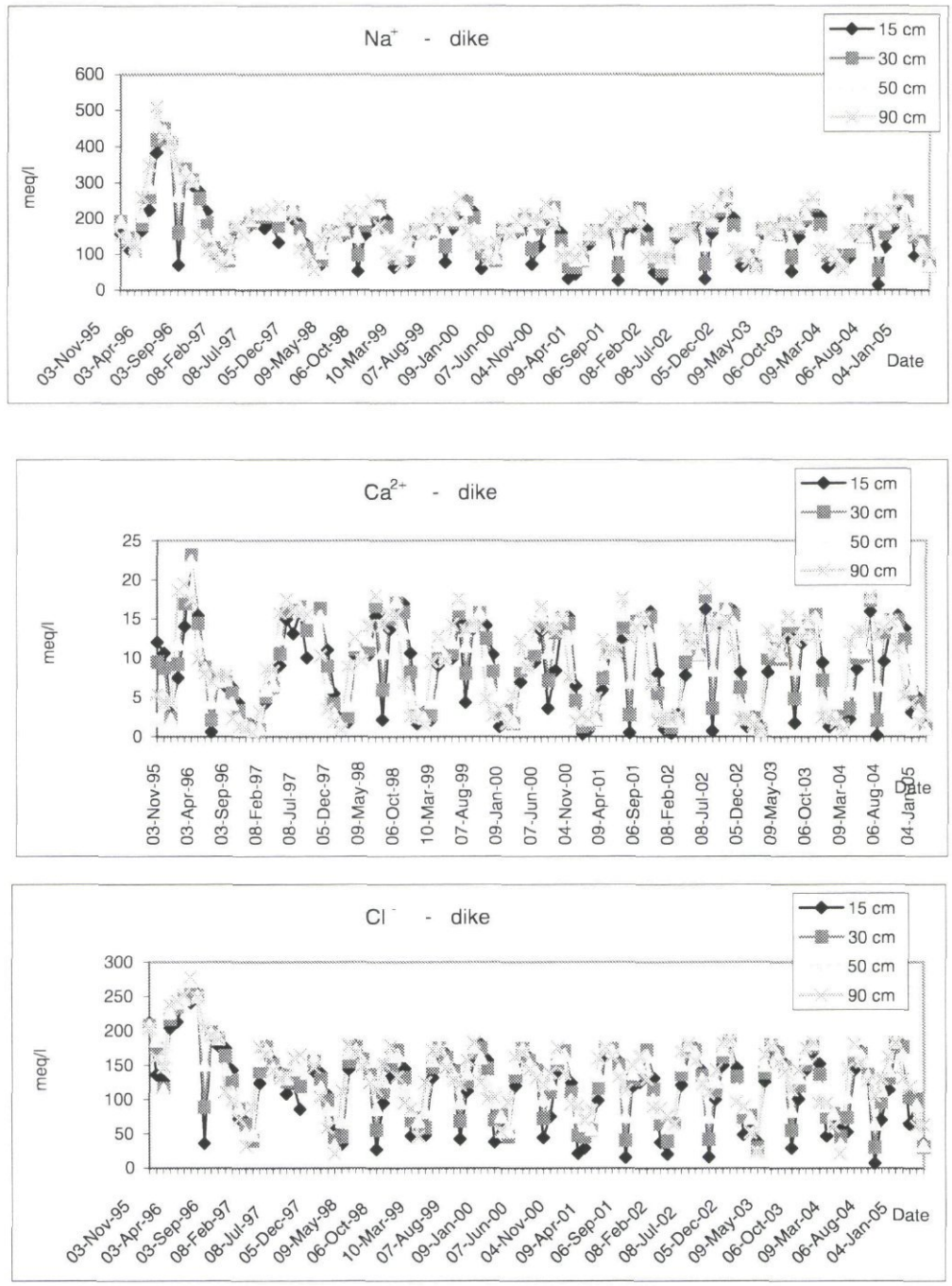

Fig. 8.8 Simulation results 'Reversed-construction scenario' (continued)

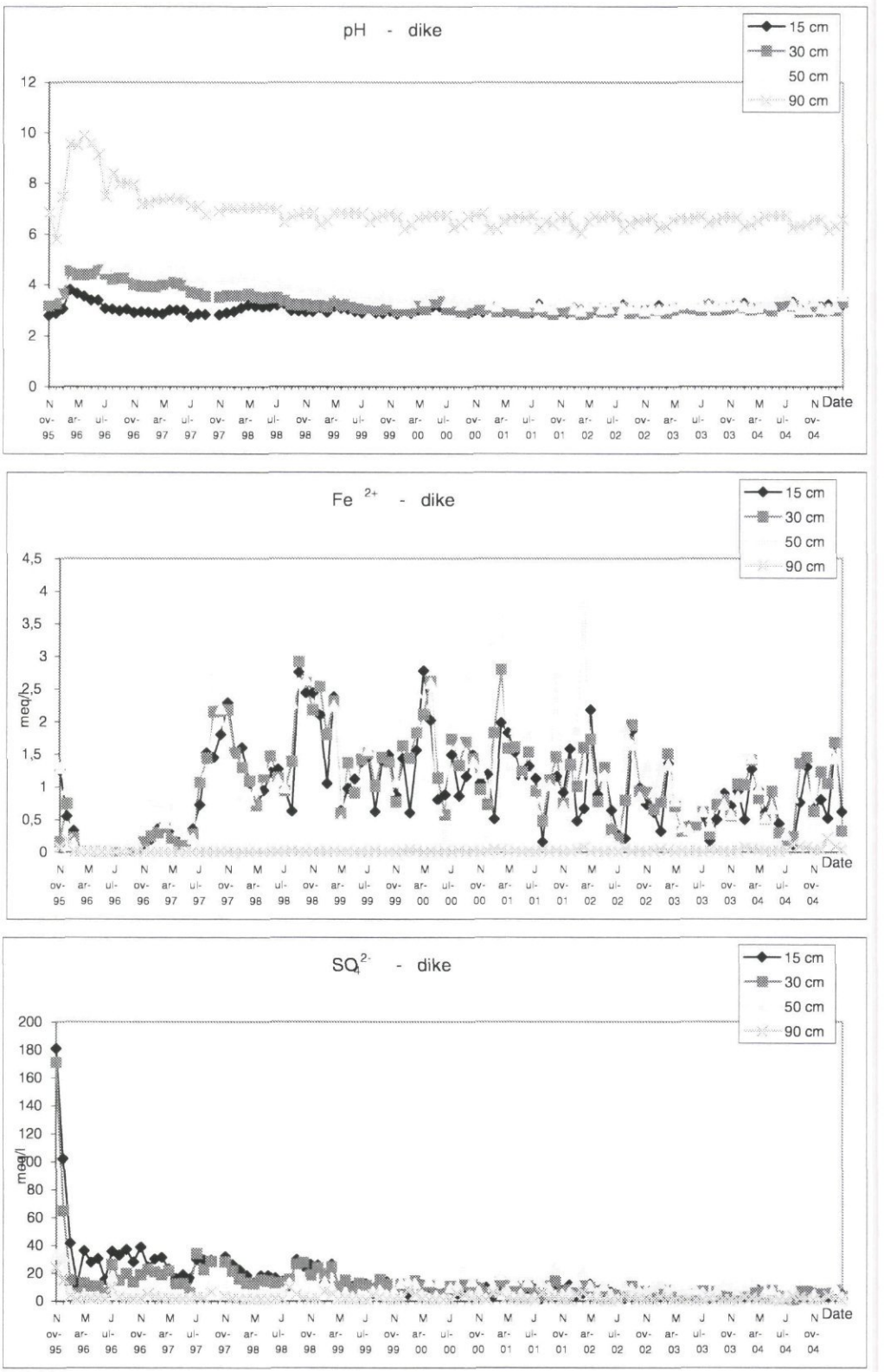

Fig. 8.9 Simulation results 'Fresh water scenario'

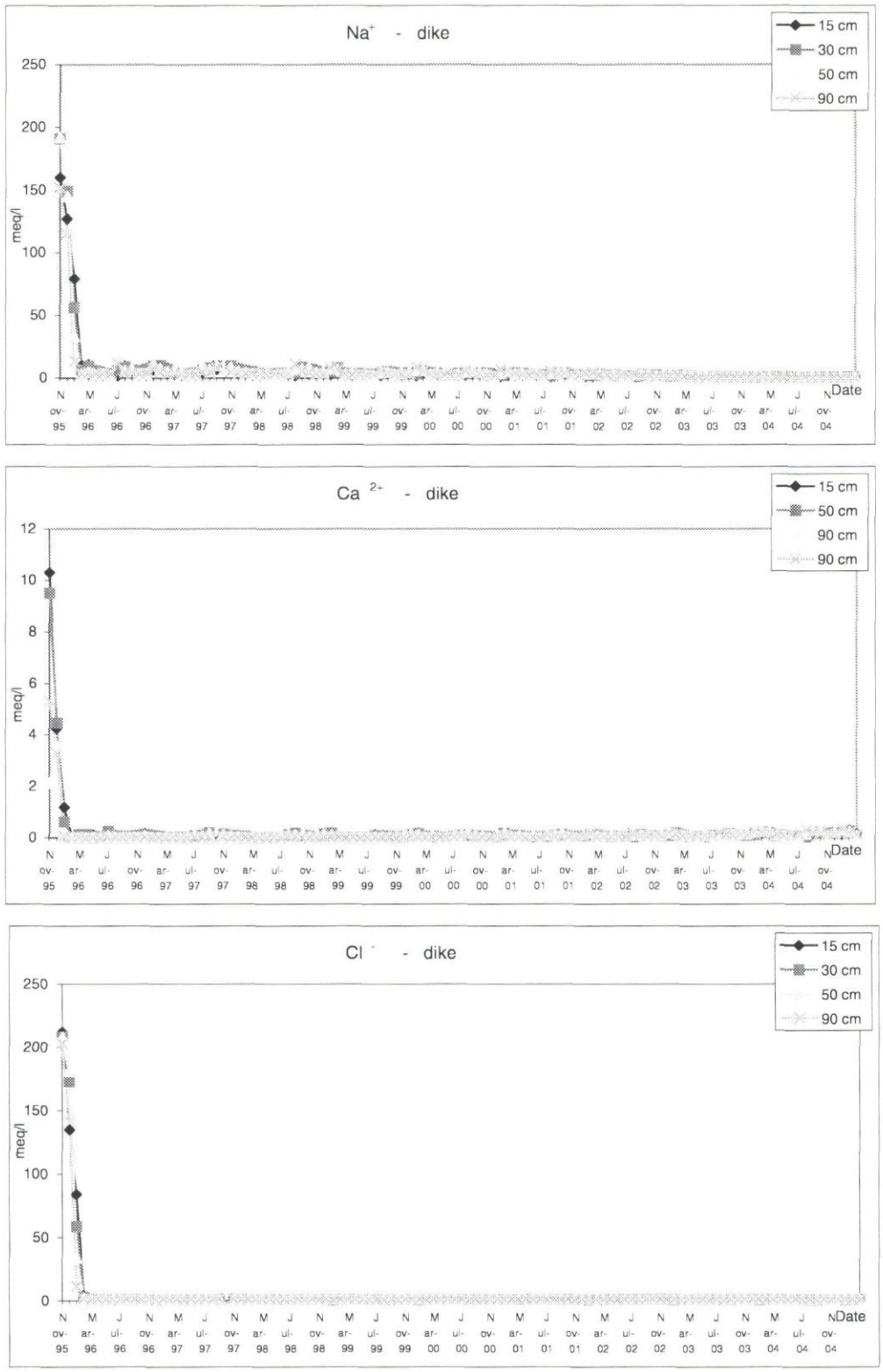

Fig. 8.9 Simulation results 'Fresh water scenario' (continued)

9. Conclusions and recommendations

The model

The computer simulation model SMASS consists of a number of mutually linked submodels in which the various physical and chemical processes occurring in acid sulphate soils are described with mathematical equations. To solve these equations, the soil profile is divided into compartments of variable size. The initial physical and chemical conditions in each compartment must be given as model input. For the complete simulation period, values for the boundary conditions are required as input. The physical and chemical conditions in each compartment, together with the water and solute fluxes at the boundary of the soil system are computed on a daily basis.

This model was extended from a one-dimensional to a two-dimensional approach to simulate water and solute flow from a field to and from surface water systems. This enables to simulate the effects of the surface water on the hydrology and chemistry of a field. With the two dimensional model water management strategies can be evaluated.

Model validation

The rapid leaching of conservative ions such as sulphate and chloride in the Indonesian was well simulated by the model. The development of Fe^{2+} concentrations in the top soil could be simulated reasonably well, whereas in deeper layers the model predicts considerably higher concentrations than was measured. Leaching of Fe^{2+}, produced in the topsoil during oxidation, caused these high concentrations in the subsoil. Al^{3+} concentrations showed similar patterns. The pH values (both measured and simulated) where relatively stable and could be simulated reasonably well.

Comparison of measured data and simulated data from the Vietnamese site showed good results. The model could simulate well the various processes and their interactions in a pyritic soil profile of a recently constructed dike bordering a fish pond. However, some elements are still poorly simulated like Mg^{2+}, Al^{3+}, and Fe^{2+}. Since there are many technical difficulties to get reliable measurements from oxidation processes in a newly constructed dike, it is not easy to judge whether the differences between measured data and calculated data are due to inaccuracy of measurements or due to poor simulations. In general, the major processes and elements in trends in concentrations were well simulated.

Water management strategies

Indonesian scenarios were evaluated for tidal land class B, a land class under high reclamation pressure in Indonesia now and in the future. In this land class, CSAR conducted a many research projects aiming at optimising cropping patterns. One of the most frequently applied cropping pattern in acid sulphate soils is the so-called Sawitdupa system. Sawitdupa is an idiom for 'once planting and twice harvesting'. The technique is developed in view of Indonesia's wish to be self sufficient in rice

production. The scenarios tested are all based on the water management strategy, required for implementing the Sawitdupa system. The scenarios differ in soil type and climate: an actual and potential acid sulphate soils were used, both in combination with average and dry meteorological conditions.

The Sawitdupa system on an actual acid sulphate soil is effective to leach out toxic elements from the top soil. However, this only holds true if groundwater tables do not drop into the pyritic layer and therefore in-situ oxidation of pyrite does not occur. Sawitdupa systems on potential acid sulphate soils, with pyrite high in the profile, results in severe acidification and concentrations of Fe^{2+} and Al^{3+} far above their toxic levels. Also high loads of toxic elements to the environment were predicted. Typical dry circumstances have a limited impact on acidification: slightly more pyrite oxidation and slightly less leaching of toxic elements was predicted under these circumstances.

All evaluated Vietnamese scenarios apply to the construction and exploitation of shrimp ponds. The "normal" scenario reflects the construction of a mound beside the shrimp pond (or a canal dike) in the traditional way. This means that the excavated soil from the upper layers is deposited at the bottom of the mound, whereas pyritic soil from the lower layers is deposited on the top. An alternative scenario was evaluated where farmers build small dikes (10-20 cm) on top of the mounds to maximise infiltration and minimize run-off. Increased infiltration will result in accelerated leaching of acidic elements from the mounds. As long as part of the toxics leach into the shrimp pond, shrimp farming is impossible. Accelerated leaching could therefore reduce the minimum time span between pond preparation and the start of shrimp farming. A second alternative was evaluated were farmers cover the pyritic material taken from the subsoil by non-pyritic soil of the topsoil (inverse construction).

All scenarios predicted long term acidification of mounded soil and of the shrimps ponds (or canals). The pyrite oxidation may continue at least 5 years after construction of the dikes. Small dikes on top of the mound did accelerates leaching from the mounds. This means that the minimum time span between pond preparation and the start of shrimp farming can be reduced with this technique. Simulations of the inverse mounds showed that oxidation still continues over a long time after construction, but acidification was moderate and within an acceptable range. It was found that the method will be more effective if the pyritic soil is buried deeper. To reduce environmental pollution, deep burial should be applied in situations where soil disturbance on large scale can not be avoided.

Recommendations

The Sawitdupa system on an actual acid sulphate soil is effective to leach out toxic elements from the top soil. However, this only holds true if groundwater tables do not drop into the pyritic layer and therefore in-situ oxidation of pyrite does not occur. Sawitdupa systems on potential acid sulphate soils, with pyrite high in the profile, results in severe acidification and concentrations of Fe^{2+} and Al^{3+} far above their toxic levels. Also high loads of toxic elements to the environment were predicted. Typical dry circumstances have a limited impact on acidification: slightly more pyrite

oxidation and slightly less leaching of toxic elements was predicted under these circumstances.

Construction of a dike or mound should be done by 'inverse construction'. This means that the pyritic material taken from the subsoil is covered by non-pyritic soil of the topsoil. However, this method is more labour and capital intensive. The pyritic soil should be covered by at least 50 cm of the non-pyritic soil. Construction of small dikes on top of the mounds to stimulate infiltration and leaching is effective and reduces the minimum time span between construction of the pond and the start of shrimp production. However, this method can only be applied if the pyrite content in the soil is less then 5%. For large scale irrigation systems in potential acid sulphate soil areas, the inverse construction of dikes will help to reduce surface water pollution.

References

AARD&LAWOO. 1992. *Water Management and Soil Fertility Research on Acid Sulphate Soils in Kalimantan, Indonesia.* Research on Acid Sulphate Soil in the Humid Tropics. AARD & LAWOO.

AARD/LAWOO. 1993a. *Acid Sulphate Soils in the Humid Tropics: simulation model of physical and chemical processes to evaluate water management strategies.* Final Report Res. Progr. Acid Sulphate Soils in the Humid Tropics, Vol. 3. International Institute for Land Reclamation and Improvement, Wageningen. 284 p.

AARD/LAWOO. 1993b. *Acid Sulphate Soils in the Humid Tropics: water management and soil fertility.* Final Report Res. Progr. Acid Sulphate Soils in the Humid Tropics, Vol. 4. International Institute for Land Reclamation and Improvement, Wageningen. 283 p.

Belmans, C., J.G. Wesseling and R.A. Feddes. 1983. Simulation of the water balance of a cropped soil: SWATRE. *J. Hydrol. 63*: 271-286.

Bennett, J.C. and H. Tributsch, 1978. Bacterial Leaching patterns on pyrite crystal surfaces. *Journal of Bacteriology, Vol.134,* No.1, P.310-317.

Berner, R.A., and R. Raiswell, 1983. Burial of organic carbon and pyrite sulphur in sediments over Phanerozoic time: a new theory. *Geochimica et Cosmochimica Acta, Vol.47,* P.855-862.

Berner, R.A., 1984. Sedimentary pyrite formation: An update. *Geochimica et Cosmochimica Acta, Vol.48*, P.605-615.

Bolt, G.H. 1967. Cation exchange equations in soil science. A review. *Neth. J. Agric. Sci.* 15: 81-103.

Bronswijk, J.J.B., K. Nugroho, I.B. Aribawa, J.E. Groenenberg and C.J. Ritsema. 1993. Modelling of oxygen transport and pyrite oxidation in acid sulphate soils. *J. of Environ. Qual. 22*: 544-554.

Bronswijk, J.J.B, H. van den Bosch, K. Nugroho, J.E. Groenenberg and C.J. Ritsema, 1995. SMASS - a simulation model of physical and chemical processes in acid sulphate soils, version 2.0. DLO Winand Staring Centre. Wageningen. Technical Document 21.

Bronswijk, J.J.B. and J.E. Groenenberg. 1993. *A simulation model for acid sulphate soils I: basic principles.* In: D.L. Dent and M.E. van Mensvoort (Eds). Selected papers of the Ho Chi Minh City Symposium on Acid Sulphate Soils. Ho Chi Minh City, Viet Nam, March 1992. ILRI Publ. 53: 341-355. International Institute for Land Reclamation and Improvement, Wageningen.

Callinan R.B., G.C. Frazer and M. Melville, 1993. Seasonally recurrent fish mortalities and ulcerative outbreaks associated with acid sulphate soils in Australian estuaries. P. 403-410. In: D.L. Dent and M.E.F. van Mensvoort (editors) Selected papers of the Ho Chi Minh City symposium on acid sulphate soils. Pub. 53, Int. Inst. Land Reclamation and Improvement, Wageningen

Christensen, T.H., B.L. Parker and J.C. Refsgaard. 1986. *A model for the unsaturated zone; oxygen transport and consumption model.* Report Danish Hydraulic Institute, Horsholm, Denmark.

Dent, D.L., 1986. *Acid sulphate soils: a baseline for research and development.* ILRI Publ. 39. International Institute for Land Reclamation and Improvement, Wageningen. 204 p.

Dost, H. and N. van Breemen (Eds.) 1982. Proceedings of the Bangkok Symp. on Acid Sulphate Soils. Jan. 1981. ILRI Publ. 31. International Institute for Land Reclamation and Improvement, Wageningen, 450 p.

Eriksson E. 1993. *Modelling flow of water and dissolved substances in acid sulphate soils.* In: Dent D.L. and Mensvoort M.E.F van (editors). Selected papers of the Ho Chi Minh city symposium on acid sulphate soils. International Institute for Land Reclamation and Improvement. Publication 53 p 369-380. Wageningen.

Ernst, L.F, 1973. *De bepaling van de transporttijd van het grondwater bij stroming in de verzadigde zone.* Nota 755. Instituut voor Waterhuishouding en Cultuurtechniek (at present: DLO Winand Staring Centre), Wageningen.

Euroconsult & Biec, 1991. *Special maintenance, efficient O & M and supervision of on-going swamp reclamation projects.* Draft Final O & M Manual. Volume IIe. Puntik Terantang, South Kalimantan. Ministry of Public Works. Directorate General of Water Resources Development. Directorate of Swamps. Jakarta.

FAO/UNESCO, 1979. *Legend of Soil of the world.* FAO/UNESCO. Rome.

Farina, M., D.M.S. Esquvel and H.G.P. Lins de Barros, 1990. Magnetic iron-sulphur crystals from a magnetotactic microorganism. *Nature, Vol. 343.*

Fassbinder, J.W.E., H. Stanjek and A.H. Vali, 1990. Occurrence of magnetic bacteria in soil. *Nature, Vol.343.*

Heywood, B.R., A. Garratt-Reed, S. Mann and R.B. Frankel, 1990. Controlled biosynthesis of greigite in magnetotactic bacteria. *Naturwissenschaften, Vol.77,* P.536-538.

Irawan. 1995. *Adopsi petani di lahan bertanah sulfat masam Kalimantan Selatan.* Unpublished report.

Kachanoski, R.G., K.K. Tanji, L.T. Rollins, L.D. Whittig and R. Fujii. 1992. Dissolution kinetics of CaCO3: CARKIN-1, a computer model. *Soil Sci. 153*: 13-24.

Kroes and Rijtema, 1996. *TRANSOL, a dynamic simulation model for transport and transformation of solutes in soil.* Report 103. DLO Winand Staring Centre. Wageningen.

Love, L.G., and G.C. Amstutz, 1963. Review of microscopic pyrite. *Fortschr. Miner. vol.43, No 2.*

Mann, S., N.H.C. Sparks, R.B. Frankel, D.A. Bazylinski and H.W. Jannasch, 1990. Biomineralisation of ferrimagnetic greigite and iron pyrite in a magnetotactic bacterium. *Nature, Vol.343.*

McKibben, M.A. and H.L. Barnes. 1986. Oxidation of pyrite in low temperature acidic solutions: rate laws and surface textures. *Geochim. Cosmochim. Acta 50:* 1509-1520.

Miller, S.D., 1980. *Sulphur and hydrogen ion buffering in pyritic strip-mine spoil: Proceedings of the fourth international symp. environ. biochemistry in relation to the mining industry and environ. pollution,* eds. P.A Tondinger and M.R. Walter. Publ. Springer.

Moore P.A. and W.H. Patrick Jr., 1993 Metal availability and uptake by rice in acid sulphate soils. p. 205-224. In: D.L. Dent and M.E.F. van Mensvoort (editors) *Selected papers of the Ho Chi Minh City symposium on acid sulphate soils.* Pub. 53, Int. Inst. Land Reclamation and Improvement, Wageningen

Noorsyamsi. H, H. Anwarhan, S. Soelaiman dan H.M.Beachell. 1984. *Rice Cultivation in The Tidal Swamps of Kalimantan.* (In) Workshop on Research Priorities in Tidal Swamps Rice. IRRI. Los Banos, Laguna. Philippines.

Nugroho K. 1991. *Penentuan areal potensial lahan pasang surut rawa dan pantai.* (Unpublished report) Centre for Soil and Agroclimate Research.

Pichtel, J.R., W.A. Dick and E.L. McCoy. 1989. Binding of iron from pyritic mine spoil by water soluble organic materials extracted from sewage sludge. *Soil Sci. 148:* 140-148.

Raiswell, 1982. Pyrite texture, isotopic composition and the availability of iron. *Am. J. of Science, Vol.282,* P.1244-1263.

Rodriguez-Leiva, M., H. Tributsch, 1988. Morphology of bacterial leaching patterns by Thiobacillus ferrooxidans on synthetic pyrite. *Arch. Microbiol., Vol.149*, P.401-405.

RV, 1987. *Der grosse Weltatlas.* Rv Reise und Verkehrsverlag, München

Sammut, J., R.B. Callinan and G.C. Fraser 1996. An overview of the ecological impacts of acid sulphate soils in Australia 140-143 in R.J. and H.J. Smith (editors) Proc. 2nd Nat. Conf. Acid Sulphate Soils. R.J. Smith & assoc. and ASSMAC, Australia

Schwertmann, U., and R.W. Fitzpatrick. 1992. *Iron minerals in surface environment: Biomineralization*, eds. H.G.W. Skinner and R.W. Fitzpatrick. Catena Supplement 21, 1992, Catena Cremlingen

Schwertmann, U., and E. Murad. 1983. Effect of pH on the formation of goethite and hematite from ferrihydrite. *Clays and clay minerals 31*: 277-284.

Subagyono K., I G.M. Subiksa, M. Sarwani, and K. Anwar. 1994. *Penelitian Pengelolaan Tanah dan air di tingkat Tersier pada lahan Pasang Surut Tipe B bertanah sulfat Masam di Tarantang, Kalimantan Selatan.* Proyek Pengembangan Penelitian Pertanian Nasional (ARMP II). Pusat Penelitian Tanah dan Agroklimat. Badan penelitian dan Pengembangan Pertanian

Sudjadi M., and M. Widjik. 1974. *Penuntun Analisa Kimia Tanah. Pusat Penelitian Tanah.* Bogor.

Tinh T.K. and Tri L.Q. 1991. *Zoning acid sulphate lands for land uses, soil improvement and management.* In: Collection of papers presented at the workshop on Management of Acid Sulphate Soil Project. HCMC 1991.

Tributsch, H., 1976. The oxidative disintegration of sulphite crystals by Thiobacillus ferrooxidans. *Naturwissenschaften Vol.63*, p 88.

USDA-NRCS, 1996. *Keys to Soil taxonomy.* Seventh Editions. United States Department of Agriculture. Natural Resources Conservation Service.

Van Breemen, N. 1976. Genesis and solution chemistry of acid sulphate soils in Thailand. *Agricultural research Reports* 848, PUDOC Centre for Agricultural Publishing and Documentation, Wageningen, the Netherlands

Van Dam, J.C., J. Huygen, J.G. Wesseling, R.A. Feddes, P. Kabat, P.E.V. van Walsum, P. Groenendijk and C.A. van Diepen, 1997. *Theory of SWAP version 2.0. Simulation of water, solute transport and plant growth in the soil-water-atmosphere-plant environment.* Report 71. DLO Winand Staring Centre. Wageningen.

Van den Bosch, H. and Kusumo Nugroho, 1996. *Set-up of a field experiment for the validation of SMASS, Tarantang, Pulau Petak, South Kalimantan, Indonesia.* DLO Winand Staring Centre. Wageningen. International Activities Report 61.

Van den Toorn, A., K. Nugroho and J. Harmsen. 1987. *Methods for determination of chemical composition of water samples from columns experiments.* Scientific Rep. No. 3. Research on Acid Sulphate Soil in the Humid Tropics. ILRI. Wageningen.

Van Mensvoort, M.E.F. and D.L. Dent 1997. Acid sulphate soils 301-333 in R. Lal et al. Methods for assessment of soil degradation. Advances in Soil Science CRC Boca Ratan, Flo.

Wakao, N., M. Mishina, Y. Sakurai and H. Shiota, 1984. Bacterial pyrite oxidation. III. Adsorption of Thiobacillus ferrooxidans cells on solid surfaces and its effect on iron release from pyrite. *J. Gen. Appl. Microbiol., Vol.30,* P.63-77.

Wilkin, R.T., H.I. Barnes and S.L. Brantley, 1996. Size distribution within pyrite framboids. *Geochimica et Cosmochimica Acta, Vol. 60*, No 20

Xuan, V.T. 1993. *Recent advances in integrated land uses on acid sulphate soil.* In: Dent D.L. and Mensvoort M.E.F van (editors). Selected papers of the Ho Chi Minh city symposium on acid sulphate soils. International Institute for Land Reclamation and Improvement. Publication 53 p 129-136. Wageningen.

Xuan, V.T. 1995. *An overview of coastal resource management situation of the Mekong delta.* Presented paper in the workshop on Integrated Management of Coastal Resources in the Mekong delta. 1-3 March 1995. University of Can Tho.

Unpublished sources

Groenendijk, P., 1991. *The calculation of complexation, adsorption, precipitation and dissolution reactions in a soil-water system with the geochemical model EPIDIM.* DLO Winand Staring Centre, Wageningen.

Oral presentations

Bui Dac Tuan and Tran Trong Luu, 1996. *Environmental characteristics of the new-built shrimp pond at Can Gio during the rainy season of 1995.* 2nd workshop 'Water management strategies for sustainable land use in coastal plains with Acid Sulphate Soils in the tropics' EC project, contract no.: ERBTS3*CT940338. April 1996. Ho Chi Minh City,Vietnam.

Trang, H.T.T., N.D. Nang and N.D. Phong, 1996. *The effect of dilution on the results of soil solution chemical analysis.* 2nd workshop 'Water management strategies for sustainable land use in coastal plains with Acid Sulphate Soils in the tropics' EC project, contract no.: ERBTS3*CT940338. April 15 to April 19, 1996. Ho Chi Minh City.Vietnam. April 1996. Ho Chi Minh City,Vietnam.

Trang, H.T.T., and N.D. Nang, 1996. *Determination of the suitable time for reading the redox potential of soil solutions.* 2nd workshop 'Water management strategies for sustainable land use in coastal plains with Acid Sulphate Soils in the tropics' EC project, contract no.: ERBTS3*CT940338. April 1996. Ho Chi Minh City,Vietnam.

Phi, H.L., N.D. Nang, N.D. Phong and H.T.T. Trang, 1996. *Spatial and temporal variation of toxicities in acid sulphate soils of Ly Nhon, Can Gio.* 2nd workshop 'Water management strategies for sustainable land use in coastal plains with Acid Sulphate Soils in the tropics' EC project, contract no.: ERBTS3*CT940338. April 1996. Ho Chi Minh City,Vietnam.

Phi, H.L., 1996. *Distinct features of field scale modelling of coastal acid sulphate soils.* 2nd workshop 'Water management strategies for sustainable land use in coastal plains with Acid Sulphate Soils in the tropics' EC project, contract no.: ERBTS3*CT940338. April 1996. Ho Chi Minh City,Vietnam.

Phi, H.L., and J. Michaelsen, 1996. *Instrumentation and installation of the new experimental sites at Ly Nhon, Can Gio.* 2nd workshop 'Water management strategies for sustainable land use in coastal plains with Acid Sulphate Soils in the tropics' EC project, contract no.: ERBTS3*CT940338. April 1996. Ho Chi Minh City,Vietnam.

Le Huy Tho and Le Huy Ba, 1996. *Activity and influence of the concentration of Al^{3+} and Fe^{2+} toxic ions in acid sulphate soil environment, Mekong Delta, on the rice plant growth.* 2nd workshop 'Water management strategies for sustainable land use in coastal plains with Acid Sulphate Soils in the tropics' EC project, contract no.: ERBTS3*CT940338. April 1996. Ho Chi Minh City,Vietnam.

Michaelsen, J., 1998. *Mineralogical and morphological aspects of pyrite from acid sulphate soil at Ly Nhon, Vietnam.* 3rd workshop 'Water management strategies for sustainable land use in coastal plains with Acid Sulphate Soils in the tropics' EC project, contract no.: ERBTS3*CT940338. January 1998. Bogor, Indonesia.

Michaelsen, J., 1995. *Investigations on water and solute movement in water saturated and unsaturated soil at IWL, Kiel.* 1st workshop 'Water management strategies for sustainable land use in coastal plains with Acid Sulphate Soils in the tropics' EC project, contract no.: ERBTS3*CT940338. March 1995. Kiel, Germany.

Nguyen van Thuong, 1996. *Aqua culture in coastal acid sulphate soils.* 2nd workshop 'Water management strategies for sustainable land use in coastal plains with Acid Sulphate Soils in the tropics' EC project, contract no.: ERBTS3*CT940338. April 1996. Ho Chi Minh City,Vietnam.

Phong, N.D., 1996. *A 2-D simulation of water movement in saturated soil: Case of study: groundwater at Ly Nhon experimental site.* Presented paper at the workshop on coastal acid sulphate soils. 4-1996. Ho Chi Minh city - Vietnam.

Van den Bosch, H., 1995. *Simulation Model for Acid Sulphate Soils (SMASS): Basic principles, validation, application.* 1st workshop 'Water management strategies for sustainable land use in coastal plains with Acid Sulphate Soils in the tropics' EC project, contract no.: ERBTS3*CT940338. March 1995. Kiel, Germany.

Van den Bosch, H., 1998. *Application of a simulation model for acid sulphate soils.* 3rd workshop 'Water management strategies for sustainable land use in coastal plains with Acid Sulphate Soils in the tropics' EC project, contract no.: ERBTS3*CT940338. January 1998. Bogor, Indonesia.

Publications resulting from this project

Kusumo Nugroho, 1996. *Set-up and results of column experiments and monitoring plots in the Indonesian/dutch acid soil project.* Center for Soil Research and Agroclimate. Bogor. Scientific Report CSAR 1.

Michaelsen, J. and Ho Long Phi, 1998. *Morphological investigations on pyrite crystals from acid sulphate soil, Ly Nhon Vietnam.* In prep.

Phi, H.L., 1995. *Simulation of pyrite oxidation in cracking acid sulphate soils: model PYROX.* In: presented papers of the international workshop of the project on Management of acid sulphate soils. The Mekong River Committee. 10 - 1995. Ho Chi Minh city. Vietnam

Phi, H.L., 1996. *Temporal variability of chemico-physical characteristics of a new-built shrimp pond in the coastal plain with acid sulphate soils and possible environmental impacts. The studied case: Cangio - Vietnam.* In: Selected papers presented at the International Symposium of Shrimp farming in mangroove areas: Reality and perspectives. ORSTOM - CRDMK. Ca Mau -Vietnam 9-1996.

Van den Bosch, H. and Kusumo Nugroho, 1996. *Set-up of a field experiment for the validation of SMASS, Tarantang, Pulau Petak, South Kalimantan, Indonesia.* DLO Winand Staring Centre. Wageningen. International Activities Report 61.

Van den Bosch, H. and A.L.M. Van Wijk, 1995. *Planning and inception of the Dutch-Indonesian collaborative work programme.* DLO Winand Staring Centre. Wageningen. International Activities Report 51.

Van den Bosch, H., J.J.B. Bronswijk, J.E. Groenenberg and C.J. Ritsema, 1998. SMASS - a simulation model of physical and chemical processes in acid sulphate soils. Version 2.1. Wageningen. DLO Winand Staring Centre. Technical Document 21.

Annex 1 An animation program to visualize the simulation results of the SMASS model

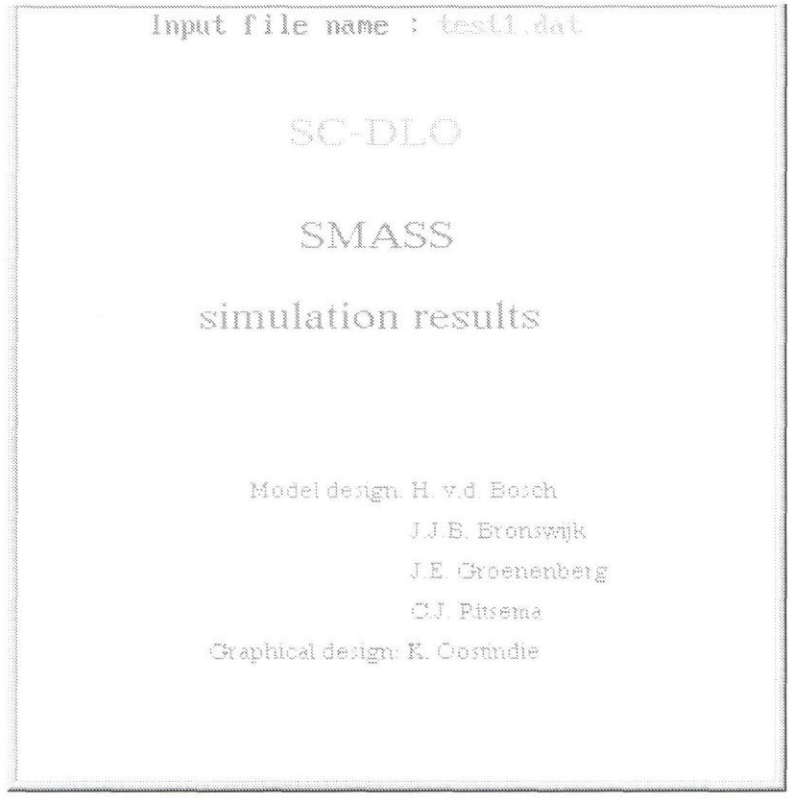

K. Oostindie & H. v.d. Bosch

Introduction

The Simulation model for Acid Sulphate Soils (SMASS) can be used to predict effects of water management strategies on acidification and de-acidification of potential and actual sulphate soils. The model computes the physical and chemical processes in acid sulphate soils. Starting with an initial profile, the model computes the physical and chemical conditions at each time step. At prescribed periods these conditions are written to file. When the total simulation period consists of several years, a lot of information is produced. This lot of information makes it difficult to check all the output.

For this purpose an animation program has been made. This program visualizes the results of the model simulations on the screen of a computer. It is just like a movie.
The animation program can also be helpful for demonstration purposes.

The animation

The program can produce two different animations. The first ones pictures the ground water level, the pyrite and pH profile and the initial and actual profile of the adsorption to the soil complex of different elements. The second one shows the fluxes of different elements to the surface water. At each time step these pictures are updated automatically.

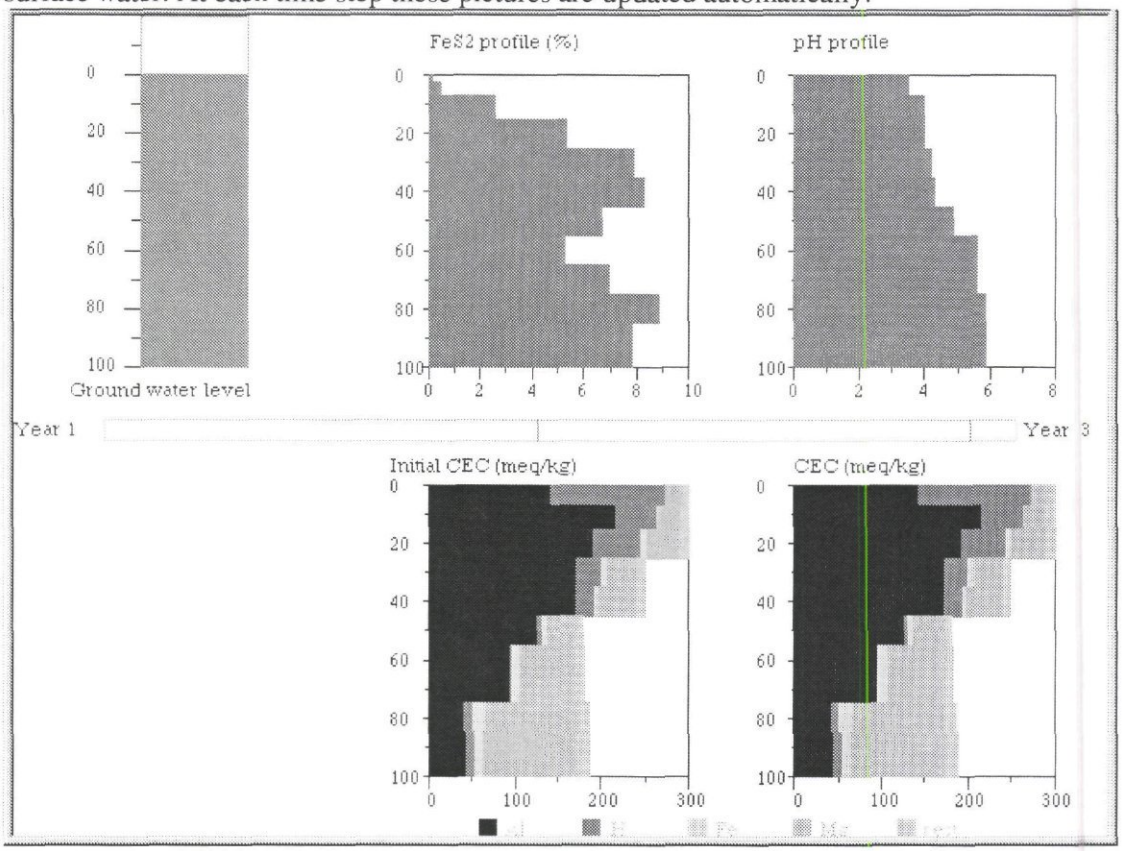

Figure 1. Screen layout at the start of the animation

In figure 1 the screen layout of the first animation is pictured at the start of the simulation. In the SMASS model, the profile is schematically divided into several compartments. Information about these compartments is written to file. This information is pictured to screen, up to depth of one meter. The ground water depth is shown at the upper left corner of the screen. Then, the pyrite- and the pH profile are

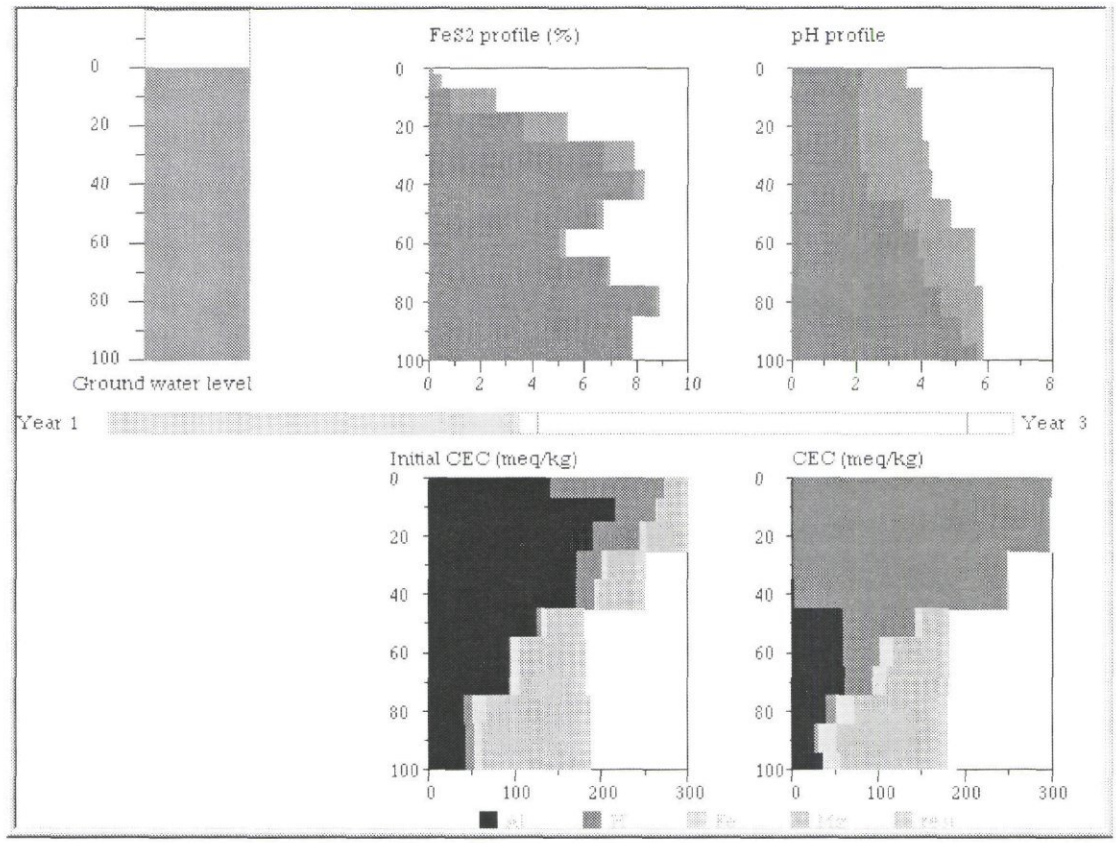

Figure 2. The animation after almost one simulated year

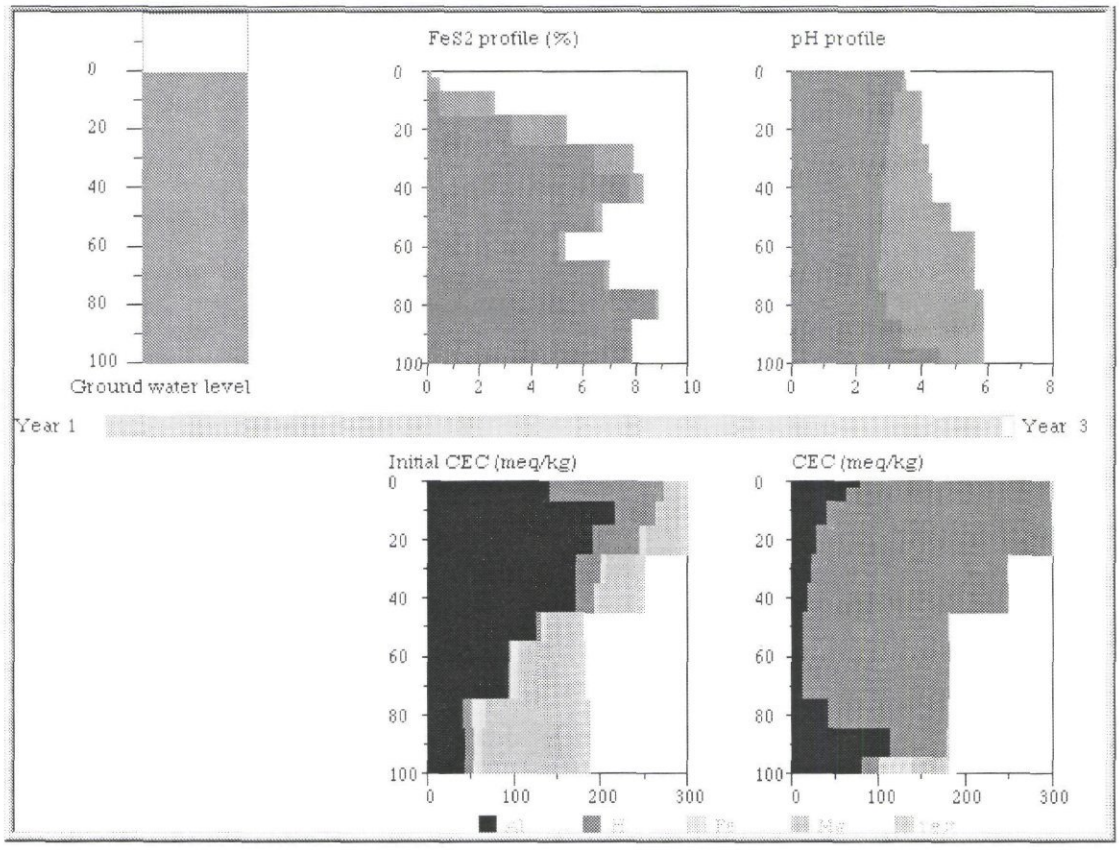

Figure 3. Layout of the screen at the end of the simulation period.

also pictured in the upper half of the screen. The actual as well as the initial profiles are displayed in these two figures. This is done using different colors for initial and actual profiles (figures 2 and 3). To read these graphs correctly, the user has to take notify of the following points:

- When the value of the actual profile is lower than the initial profile, the initial profile is displayed with the colors brown and blue. The actual profile is displayed in brown only.
- When the value of the actual profile is greater than the initial profile, the initial profile is in brown, while the actual profile is in brown and green.

Two charts are shown at the lower part of the screen, the first one is static and displays the adsorption to the soil complex at the beginning of the simulation. The second shows the same profile, but now it changes in time (Figures 1 to 3). In the middle of the screen a time bar is pictured. This bar shows the time passed after simulation start. This bar will be filled up with a green color during the animation. Figure 2 is a snapshot of the screen after almost one simulated year. Figure 3 shows the profile at the end of the simulation.
The second animation shows fluxes to the surface water of different elements. The user can choose 4 elements from a list of 11 elements. These elements are: H, NA+, K+, CA2+, Mg2+, Fe2+, Al3+, HCO3-, SO42-, CL- and Fe3+. The chosen elements are plotted to the screen cumulative. In figure 4, the animation is pictured after a simulation period of one year and a half.

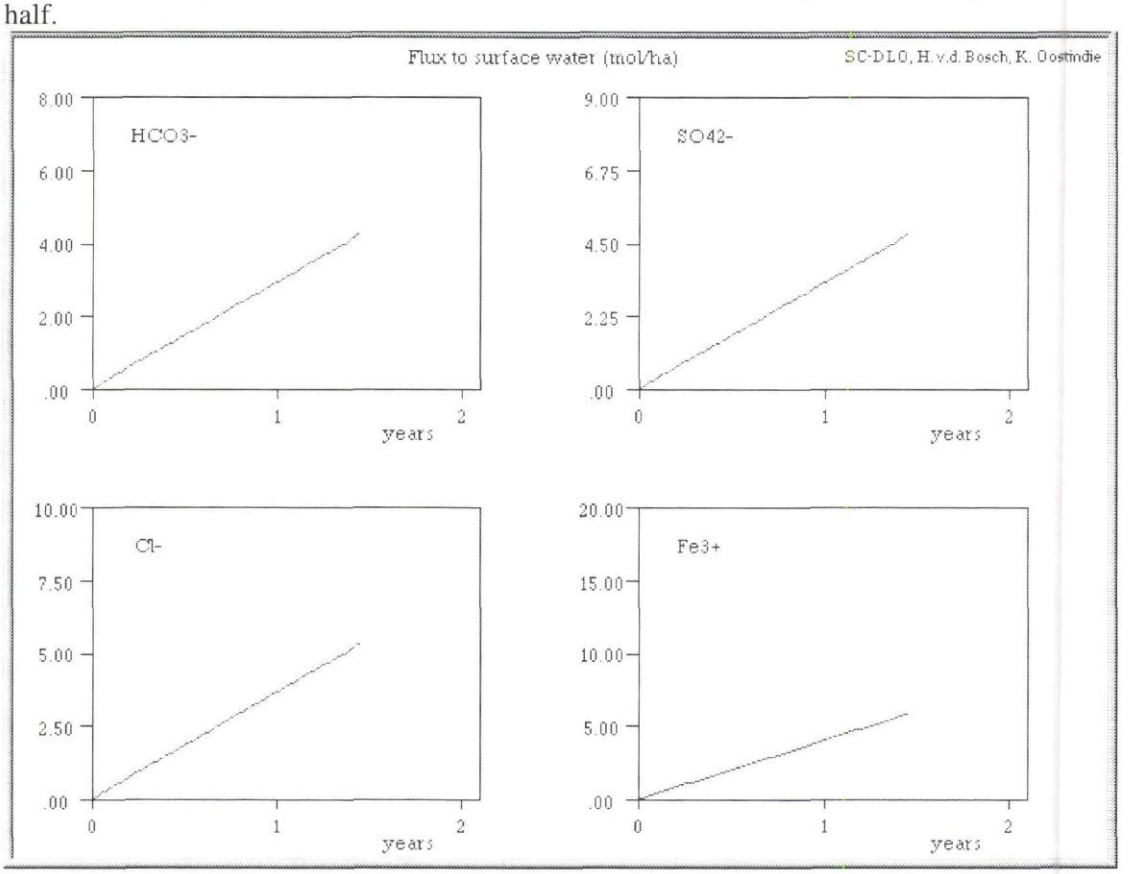

Figure 4. Layout of the screen when time series are animated.

The use of the program

The program is written in Fortran using the Microsoft Fortran Dos run-time graphics library functions. The program uses certain parameter settings and read these settings

from file. An example of the contents of a settings file is given in table 1. The following records have to be divined by the user:

- The name of the file which contains the oxygen data.
- An Y when the program has to read and show adsorption data, otherwise a N
- The name of the file with adsorption data when the previous record is Y otherwise a dummy value can be given.
- An Y when the pH data has to be shown and read or a N if not.
- The name of the file with pH data when the previous record is Y otherwise a dummy value can be given.
- Number of time steps to skip. The program can skip a certain number of time steps after it has plotted data to the screen. This option is useful when the total number of time steps is greater than 400, because this is the maximum number of data points.
- The number of compartments the profile consists of.
- The top of the first compartment in cm below soil surface
- The top of the second compartment. And so on.
- The bottom of the last compartment in cm below soil surface.
- The first day number
- The last day number
- Y or N. Have the adsorption elements H and Al to be displayed in different colors? This record should give the answer.
- Y or N. Has the background to be displayed in black? This record answers the question. When this question is answered with N, then the background will be displayed in white.
- Y or N. Do you want to plot the fluxes to the surface water? The user decides which kind of plot has to be displayed. If the answer is N, then profiles will be shown, otherwise (Y) the fluxes to the surface water are pictured. If answered with Y all the above settings are dummies, if answered with N all the rest of the settings are dummies.
- Three records with comments
- One record containing the label:'*ELEMENTS
- The name of the file with the fluxes to the surface water.
- Two records with comments
- The maximum values for the 11 elements (H, NA+, K+, CA2+, Mg2+, Fe2+, Al3+, HCO3-, SO42-, CL-, Fe3+)
- One comment record
- Eleven records with Y or N. These records give the answer if an element has to be plotted. Maximally 4 elements can be plotted at once. If the user answers more than 4 times with Y, then only the first four elements will be plotted.

One can start the program by activating the ANIMATE program. An introduction screen is displayed. (See title page of this document). The program will be continued after pressing the <ENTER> key. Then, the user is asked for the name of the settings file. After the user has given this information, the program starts reading the relevant files. The program shows a blinking star after each year that has been read. The color of this star is white when reading adsorption, oxygen and pH data and the color is yellow when the program reads fluxes. When all data has been read, the background

Table 1. Contents of the settings file.

```
oxygen.out          : Name of input file with oxygen data
Y                   : Show and read data related to adsorption to soil complex
adsorp.out          : File containing adsorption data
Y                   : Show and read pH ?
solutes.out         : File containing the pH data
0                   : Nr of time steps to skip
 12                 : Nr of nodes
  0
 -2.0
 -7.0
 -15.0
 -25.0
 -35.0
 -45.0
 -55.0
 -65.0
 -75.0
 -85.0
 -95.0
 -105.
1                   : Start day nr.
770                 : Last day nr.
Y                   : Display H and Al in different colors
N                   : Background color is black/blue when Y, otherwise it's white
N                   : Plot fluxes to surface water?
*************************************************************************
* Input data when plotting fluxes to surface water                      *
*************************************************************************
*ELEMENTS to plot from which file:
surface.out         : file with fluxes
* Give the maximum value for each element respectively
* H  NA+  K+  CA2+  Mg2+  Fe2+  Al3+  HCO3-  SO42-  CL-  Fe3+
  1.  10.  10.  10.    5.    10.    10.     8.      9.    10.  20.
* Choose the elements [Y/N] you want to display.( max. of 4 elements. If more, only the first four
elements are displayed!)
N          : H
N          : NA+
N          : K+
N          : CA2+
N          : MG2+
N          : FE2+
N          : AL3+
Y          : HCO3-
Y          : SO42-
Y          : CL-
Y          : Fe3+
```

will flicker for some time and in top of the screen the message "Press enter to start animation" will appear.
The animation will start when the user presses the <ENTER> key. When the animation ends, the program waits for the <ENTER> key again. The user has the possibility to start the same animation again, now without reading the files, or to stop the program.

The user can easily make hard-copies of the screen when working under Windows-95 or Windows-NT. The program then starts in a full-screen MSDOS box. While the

program runs, the user can press the <PAUSE> key at every moment. The program will be suspended and then it is possible to return to a window by holding down the <ALT> key and pressing the <ENTER> key. Then, hold down the <ALT> key again and press the <PRINT SCRN> key. A snap shot is then made of the active window and is placed on the clipboard. With a word processor or any other windows program it is possible to copy the contents of the clipboard into a document. Animations with a white background give the best results when making hard copies. The animation can be resumed by selecting the window and pressing the <ALT> and <ENTER> key simultaneously and then pressing any key.